PART I: THE SYNTHESIS OF CHENODEOXYCHOLIC ACID (CDCA) BASED MACROCYCLES AND CAGE COMPOUNDS.

PART II: SONOGASHIRA COUPLING FOR THE SYNTHESIS OF WELL-DEFINED π-CONJUGATED ARYLENE ETHYNYLENE OLIGOMERS

A DISSERTATION IN
Chemistry
and
Pharmaceutical Sciences

Presented to the Faculty of the University
of Missouri-Kansas City in partial fulfillment of
the requirements for the degree

DOCTOR OF PHILOSOPHY

by

XINYAN BAI

B.S., Qingdao University of Science and Technology 2000

M.S., East China Normal University 2003

Kansas City, Missouri

2011

PART I: THE SYNTHESIS OF CHENODEOXYCHOLIC ACID (CDCA) BASED MACROCYCLES AND CAGE COMPOUNDS.

PART II: SONOGASHIRA COUPLING FOR THE SYNTHESIS OF WELL-DEFINED π-CONJUGATED ARYLENE ETHYNYLENE OLIGOMERS

Xinyan Bai, Candidate for the Doctor of Philosophy Degree

University of Missouri-Kansas City, 2011

ABSTRACT

The design and development of novel chenodeoxychoic acid (CDCA) derivatives and its molecular architecture was accomplished. A novel CDCA derivative with an ambient CO_2 insertion to 7α-side chain has been serendipitously discovered. It is the first time that CO_2 has been directly introduced to the steroid molecules by organic synthetic method. It also provides a potential methodology to synthesize ^{14}C labeled bile acid derivatives to explore the transport mechanism of hASBT. Secondly, a series of CDCA based macrocycles with inner cavities have been synthesized and characterized. Particularly, the single crystal X-ray analysis has revealed an unequivocal structure of 4-pentenoate functionalized cyclodimer (**K**). The first CDCA based cage-type molecular architecture has been achieved by Grubb's reaction. Especially we have successfully synthesized and separated the first *cis*/*trans* isomers of the bridged CDCA cyclodimer. The most exciting thing is we have discovered the structure of *cis* bridged cyclodimer by

X-ray crystallography. The cavity size for cis-cyclodimer is about 1 nm x 1 nm x 0.6 nm dimension. The briged cyclodimer with well-defined small inner cavity could be used for gas adsorption such as hydrogen storage container. In addition, the *cis*/*trans* isomers of double handle basket-shaped cyclotetramer **O** could be used for drug delivery. Its inner cavity is suitable for encapsulating hydrophobic drug molecules.

In part II, it involved in the synthesis and characterization of well-defined π-conjugated arylene ethynylene oligomers. These oligomers have applications in the fabrication of potential organic photovoltaic cells and organic light-emitting diodes (OLEDs). Four series of arylene ethynylene oligomers: mono-terminated di-*tert*-butyl-substituted OPEs **4a-7a**, mono-terminated *tert*-butyl substituted mono-iodo-substituted OPEs **8-11**, unsymmetric phenylene-ethynylene trimers and tetramers **13a-d**, **16a-d** and unsymmetrical phenylene-ethynylene compounds with the terminal allyloxy group **18a-f**, **19a-b** and **23** have been successfully synthesized using oxygen-free Sonogashira reaction conditions. The structures of these oligomers have been confirmed by ^{1}H and ^{13}C NMR spectroscopy, HR-MS, MALDI-TOF spectroscopy. The detailed structure of oligomers **5a**, **5b** and homo**4** were revealed by single X-ray crystal diffraction measurements.

The electronic properties of these oligomers have been studied by UV-vis and fluorescence luminescence spectroscopy. It has been observed that both UV absorption and FL emission maxima have red shifts with either increasing conjugation length of oligomers or with more conjugated chromophores. The quantum yields of these oligomers are ranged from 0.2 to 1.0. In addition, the quantum yield for **5b**,**6a**, **7a**,

trimers **13a-d**, and tetramers **16a-d** are close to 1 which means these oligomers has very high emission efficiency.

The faculty listed below, appointed by the Dean of the School of Graduate Studies, have examined a dissertation titled "The Synthesis of Chenodeoxycholic Acid Derived Macrocyles and Cage Compounds, and Sonogashira Coupling for the Synthesis of Well-Defined π-conjugated Arylene Ethynylene Oligomers as Blue-Light-Emitting Materials," presented by Xinyan Bai, candidate for the Doctor of Philosophy degree, and certify that in their opinion it is worthy of acceptance.

Supervisory Committee

Jerry R. Dias, Ph.D., Committee Chairperson
Department of Chemistry

Tom Sandreczki, Ph.D.
Department of Chemistry

Nathan Oyler, Ph.D.
Department of Chemistry

William G. Gutheil, Ph.D.
Department of Pharmaceutical Sciences

Kun Cheng, Ph.D.
Department of Pharmaceutical Sciences

CONTENTS

ILLUSTRATIONS

SCHEMES

Scheme Page

ILLUSTRATIONS

TABLES

Table Page

PART II: Sonogashira Coupling for the Synthesis of Well-Defined π-Congugated Arylene Ethynylene Oligomers as Blue-Light-Emitting Material.

Chapter

ILLUSTRATIONS

SCHEMES

Scheme Page

ILLUSTRATIONS

TABLES

Table Page

ACKNOWLEDGEMENTS

I would like to deeply thank my research advisor Jerry Ray Dias, for his dedicated support, patience and encouragement during my Ph.D. study. My research work could not been done without his guidance and technical support. He has taught me how to be a real scientist on the working of academic research.

Secondly, I would like to express my gratitude to prof. Tom Sandreczki for his technical support and editorial advice on part II of my dissertation. He also supports me as research assistant during my summer and fall semester this year.

My thanks also go to the members of my committee, Drs. Nathan Oyler, William Gutheil and Kun Chen, for valuable comment and advice on my dissertation.

I also extend my thanks to my colleagues and technical staff at the Department of Chemistry at the University of Missouri-Kansas City.

Last, I would like to thank my husband Xueyi Chen for his help and support on my Ph.D. study during the past six years. I also would like to thank my parents and my mother-in law for their support and dedication.

Part I: The Synthesis of Chenodeoxycholic Acid Derived Macrocyles and Cage Compounds

1. INTRODUCTION

1.1 Bile Acid Derivatives: Preparation, Structure and Applications

The buildup of large macrocycles has been attractive in recent years due to the potential application of macrocycles in guest-host chemistry. Crown ethers are typical examples of two dimensional macrocycles that were successfully synthesized and used for encapsulating alkali metal cations in industry.[1] 18-crown-6 (Figure 1), the well-known crown ether specifically used to bind K^+, also forms stable complexs with protonated amino acids by hydrogen bonds.[2] Another fruitful synthesis of a variety of container-like calix[n]arenes (Figure 2), the condensation product of phenol and aldehyde, further- more expanded the structures of macrocycles to three dimensions.

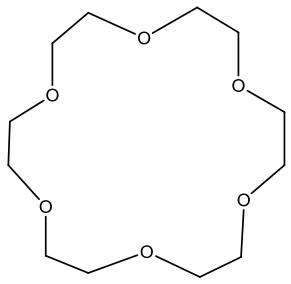

Figure 1. The chemical structure of 18-crown-6.

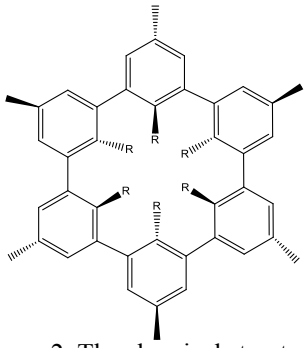

Figure 2. The chemical structure of calix [6]arene

Those synthesized calix[n]arenes based macrocycles with specific functional groups and large cavities have been used for various purposes. For example, C-alkyl

pyrogallol[4]arene, a macrocycle with OH groups, serves as a cation receptor to bind metal ions like Cu^{2+}, Cs^{+}, Ga^{3+}.[3] The calix[4]pyrrole is known to act as both anion species receptor for binding F^{-}, Cl^{-}, Br^{-} efficiently and contact ion pair receptor to bind CsX.[4] The Crown-6-calix[4]arene-capped calix[4]pyrrole with two binding sites, one of the most interesting macrocycles , has been proved to have the capability to bind the separated ion pair CsF.[5] The calix[n]arenes with relatively larger cavity were also used to encapsulate and separate fullerenes. The π-π stacking is believed to play a critical role in forming a complex between C_{60} fullerene and container like calixarenes. In addition, cone shaped β-cyclodextrins, produced from starch, are also well known using for drug delivery due to its unique property that the interior is relatively hydrophobic and capable of encapsulating drug molecules and the exterior is hydrophilic and water soluble [6] which meets the need as a delivery device for drug. Although a lot of effort has been dedicated to studying host-guest chemistry, there remains a need for synthesizing varying new macrocycles with characteristic properties. Therefore, the selecting moiety with specific structures favoring the formation of macrocycles and synthesis of macrocycles with controlled cavity size are very challenging. Members of our group have focused on the synthesis of novel bile acid derivatives for three decades. The synthesis of a variety of bile acid macrocycles is one of our goals.

The physiochemical properties of bile acid family have been extensively studied during the past three decades. Bile acids, biosynthesized from cholesterol in the liver, turn to water soluble salts by conjugating with amino acids such as taurine, glycine etc.

and are de-conjugated by bacteria in the terminal ileum and re-assimilated back into portal system.[7] The function of bile acids as bio-surfactants to emulsify and digest fat and Vitamins is well recognized. The discovery of unknown function of bile acid that controls gene expression and regulates metabolism by interaction with FXR (nuclear hormone receptor) brought BAs into a new stage. Therefore, BAs is not simply a bio-detergent, it plays more important roles in the process of metabolism. [8] The understanding of the mechanism of bile acid for controlling gene expression and regulating metabolism is critical to prevent or treat metabolism disease. Bile acids transportation by their active transporters through the luminal membrane of terminal ileum is actively being studied. Apical sodium-dependent bile acid transporter (ASBT) is believed to be the major and most important bile acid transporter. Tritium labeled taurocholic acids has been used to study the transportation mechanism of hASBT. [9] However, the fully understanding the interaction between bile acids and ASBT is still a challenge.

In recent years, pro-drug represents a new strategy for drug delivery, the circulation of bile acid in hepatic system with high efficiency and the active transportation of bile acids across membrane by bile acid transporters enlightened scientists to synthesize pro-drug delivered by bile acid transporters by conjugating the drug to a bile acid to improve drug's metabolic stability and membrane permeability.[10] It has been shown that peptide drug's oral absorption was greatly improved and its enzymatic hydrolysis in GI tract was decreased by conjugating the peptide drug to chenodeoxycholic acid (CDCA). [11]

(Figure 3) Attaching acyclovir, an anticancer drug, to CDCA which targets hASBT is another example that the intestinal permeability can be improved by conjugation. [12]

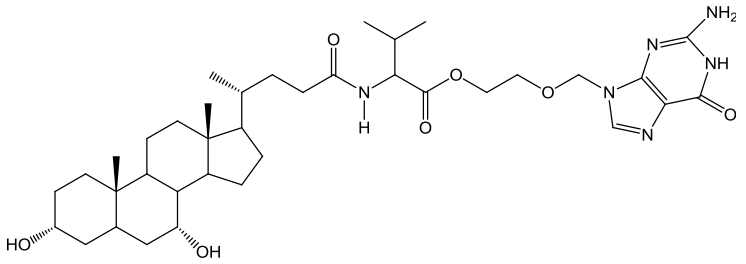

Figure 3. Structure of the prodrug acyclovir vaylchenodeoxycholate.

Cholic acid (CA) and CDCA(structures pictured in Figure 4) have been selected as good building blocks to construct supermolecular architectures due to three important and unique structural features of bile acids as following: (1) The bile acid has an extended and rigid steroid skeleton. (2) The curved α-face of bile acid steroid skeleton favors the formation of macrocyclic compounds with a cavity. (3) The functional groups on bile acid, hydroxyl group on the one end of the six member rings and the carboxylic acid group on the end of aliphatic chain, can undergo typical Yamaguchi macrolactonization.

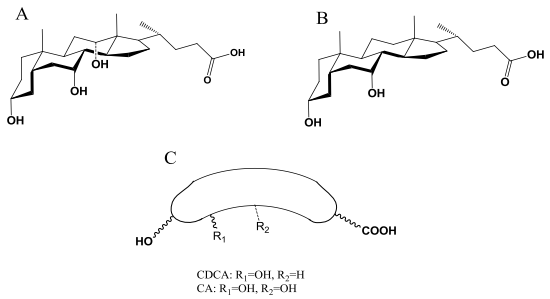

Figure 4: The structure of bile acid. A) Perspective structure of CA. B) Perspective structure of CDCA. C) Schematic description of CA and CDCA structures.

So far, two important types of bile acid derivatives were synthesized and proved to be potential host molecules for ions and small molecules for use in binding and recognition. One is known as cholaphane containing both steroids and aromatic rings in cyclic structure. The cholaphane normally has moderate cavity and polar functional groups, like OH^- groups, for enclosing polar substrates. For example, cholaphanes **A** and **B** (Figure 5) were found to be good receptors for selectively binding of monosaccharides in chloroform. [13]

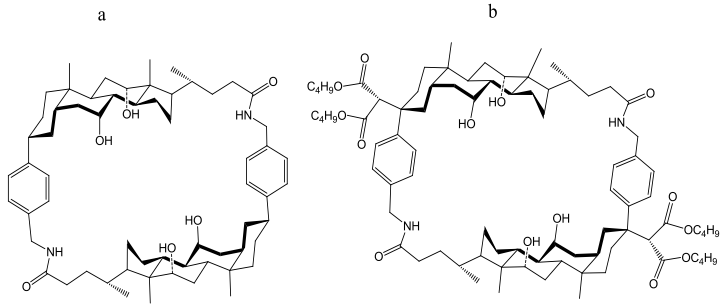

Figure 5. a) Structure of cholaphane **A**. b) Structure of cholaphane **B**.

Another useful application of cholaphane with special functional groups is to encapsulate halide anions. Cyclochoamide **C** (Figure 6) with a small cavity size compared to that of cholaphane **A** and **B** is suitable for enclosing Cl^-.[14] However, the synthesis of cholaphanes involves multiple steps and low yields. The other alternative approach was developed to make bile acid based anion receptors called "cholapod" with acyclic structures. "Cholapod" were synthesized by using one single bile acid unit and converting the hydroxyl groups at certain positions into useful functional groups such as diamino group which could be further converted into amide, sulfonamide, urea groups

with anion recognition properties. For example, the novel cholapods **D** and **E** with imidazolium groups as anion receptors (Figure 7) was successfully achieved by Pandy' group. [15]

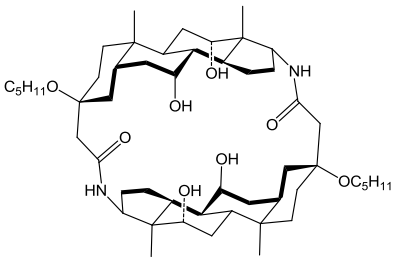

Figure 6. The structure of cyclochoamide **C**.

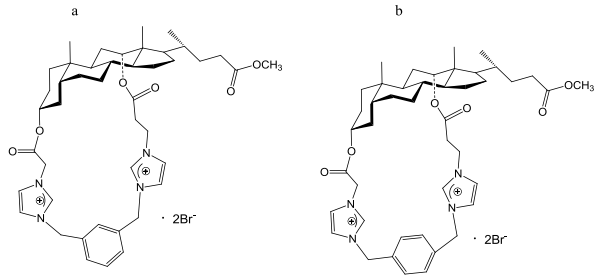

Figure 7. a) The chemical structure of cholapod **D**. b) The chemical structure of cholapod **E**.

The study has shown that cholapods **D** has the capability to bind halide anion, Br^-, Cl^-, F^- and I^-. In addition, the binding of F^- is favored by cholapod **D** with *m*-xylene while cholopod **E** with p-xylene has the priority to binding Cl^-. Both the NMR analysis and X-ray crystallography proved the mode of binding halides by cholapods **D** and **E**. The crystal structure is shown in Figure 8. The halide anion is centered in the cavity and bound with four hydrogen on cholapods **D** and **E**. Two of them are protons on imidazolium groups and the other two are methylene protons. Involvement of methylene protons in hydrogen bonding with halides is rarely observed.

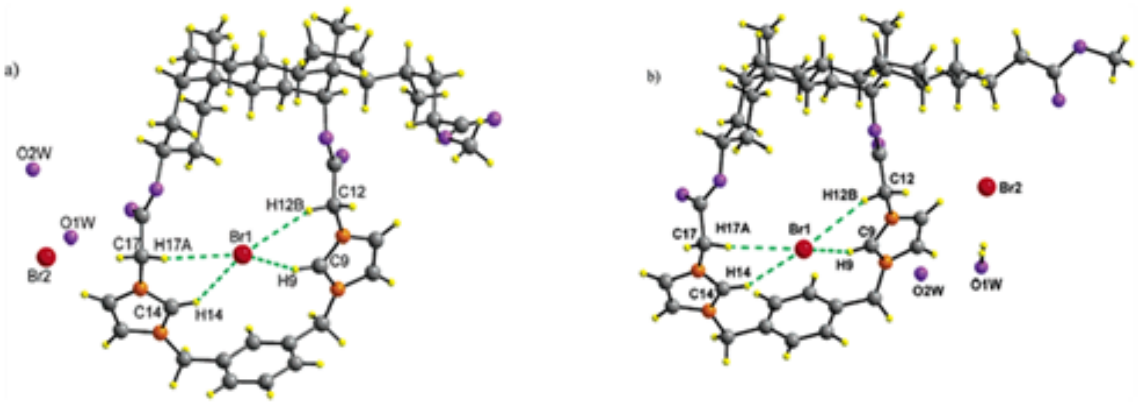

Figure 8. The single X-ray crystal structure of a) cholapod D-$(Br)_2$. $2CHCl_3$. $2H_2O$. B) Choapod E-$(Br)_2$. 1.5 H_2O.

Thus, chemists have made some remarkable progress on the synthesis of cholaphanes and cholapod and applying them for the molecules and ions recognition. The synthesis of cyclocholates involving three or more steroid units is rarely reported although these cyclocholates with large cavities could capable of encapsulating relatively large molecules and ions. Our group has been dedicated to constructing cyclocholates with only bile acid skeletons since 1990's. Hongwu Gao has synthesized and characterized various pure bile acid based cyclodimers, cyclotrimers and cyclotetramers with varied functional groups on 7α, 12α positions (Figure 9) prepared by Yamaguchi macrolactonization.[16]

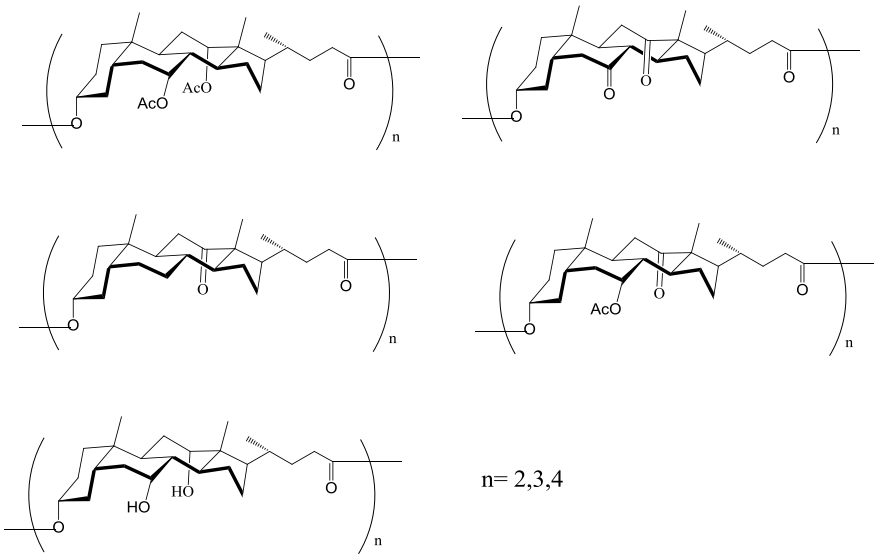

Figure 9. The pure bile acid based cyclocholates with various functional groups

This method was firstly developed and used for formation of esters by reacting carboxylic acid with alcohol in 1970's by Yamaguchi etal. Most esterification reaction can be carried out in THF solution at room temperature and use 2, 4, 6-trichlorobenzoyl chloride and DMAP as reagents. But the case of synthesizing cyclic esters by this method, THF as the solvent is not good enough to achieve the goal since the reaction to form cyclic compounds is favored at high temperature and dilution. Therefore, the typical Yamaguchi macrolactonization method was established by firstly using carboxylic acid to react with 2,4,6-trichlorobenzoyl chloride and Et_3N in small amount of THF to give the corresponding anhydrides, then, after removing the triethylammonium chloride by filtration and evaporating the THF, the anhydride mixture is added into refluxing DMAP toluene solution dropwise.[17]

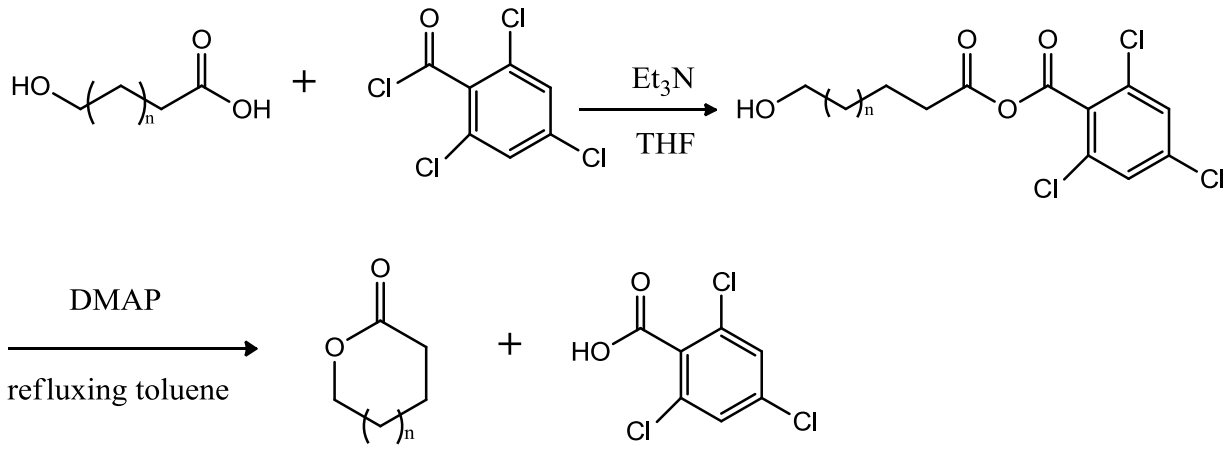

Scheme 1. The typical Yamaguchi marolactonization

In Hongwu Gao's work, The cylcocholates were synthesized by one step using 2, 4, 6-trichlorobenzoyl chloride, Et_3N and DMAP in toluene. The cyclic compounds are usually obtained as mixtures of cyclodimer, cyclotrimer and cyclotetramer even with some cyclopentamer. The major cyclic products obtained varied with the length of the 17-sode chain. For example, 12-acetyl-deoxycholic acid and 7,12-diacetylcholic acid gave the cyclotrimer as the major product with above 40% yield while the cyclotetramer as the major product was obtained by reacting 7, 12-diacetyl-24-norcholic acid with 2, 6-trichlorobenzoyl chloride and DMAP in toluene. However, the potential application of these cyclocholates in molecule or ion recognition has not been explored by so far. His previous work has led us to make more useful cyclocholates with CDCA moiety targeting to the potential drug delivery system. The polymers like PEG, biodegradable PLGA, naturally occurring chitosan, cyclodextrins and dendrimers such as PAMAM have been

widely used to transport drugs.[18] Among of various macrocycles, cyclodextrin is the only one used for drug delivery.

1.2. Goal of Research Project

The long term objective of this work is to synthesize novel tube-like bis-cyclocholates with moderate cavity size by majorly employing the Yamaguchi macrolactonization and Grubb's coupling reaction. The tube-like biscyclotricholates could act as a device to effectively deliver drug targeting for the liver and intestinal diseases. Based on this idea, the CDCA is selected as the starting material, and 7α-OH group is substituted by a functional group with terminal alkenes via multistep reactions. Then Yamaguchi marolactonization will be applied to give the cyclocholate which can be further converted to the tube-like bis-cyclocholate by Grubb's coupling reaction. The proposed construction of bis-cyclocholates is sketched in Figure 10.

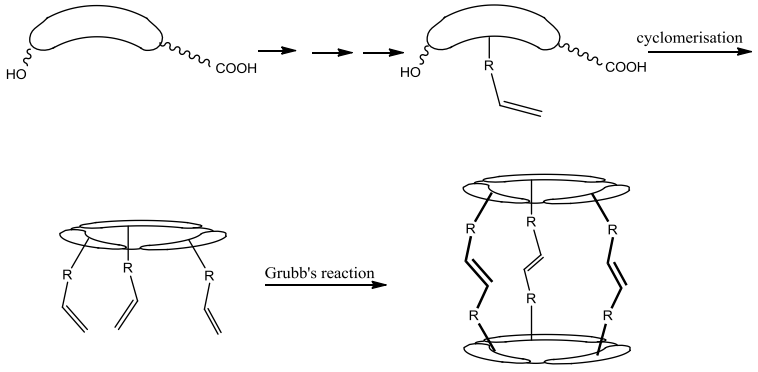

Figure 10. The designed scheme towards the synthesis of bis-cyclocholates.

The designed cyclotricholate could be well characterized by modern analytical techniques and meets the requirement to act as a practical drug delivery system by the following prevailing properties.

- The designed bis-cyclodicholate and bis-cyclotricholate as the drug carriers are biocompatible, biodegradable and non-toxic to the cells.
- It has a defined structure, moderate molecular weight (about 3000) to be exactly determined by MS compare to the polymers which are mixtures and not possible to be characterized precisely.
- It has three dimensional structures with a single and suitable cavity for encapsulating hydrophobic drugs.
- It could form a stable 1:1 ratio complex with hydrophobic drugs. Drugs with poor bioavailability such as peptides can be delivered safely through the GI tract without enzymatic hydrolysis. It also avoids the unnecessary loss of oral drug through the passage to the target site and decreases the toxicity to the normal cell by enclosing the drug in the cavity.
- When the bis-cyclocholate is circulated into the terminal ileum. The ester bond of cyclocholates can be hydrolyzed by bacteria. The cyclotricholate breaks into parts and therefore, the encapsulated drug can be slowly released.
- The major metabolized product of the bis-cyclocholate by bacteria is CDCA which either circulates in hepatic system or secreted into feces.

The following part will give the synthetic routes toward the bis-cyclocholates. The syntheses of CDCA derivatives by substituting hydroxyl group with functional group containing the terminal alkenes and the formation of cyclocholates by Yamaguchi macrolactonization will be described in a detailed way as well as the Grubb's reaction to couple the terminal alkenes.

2. RESULTS AND DISCUSSION

2.1. Synthesis and characterization of novel CDCA derivatives

2.1.1. Synthesis and characterization of methyl 3α-(ethoxycarbonyloxy)-7α-(allyloxycarbonyloxy)-5β-cholanoate (C)

The approach toward the synthesis of **C** is shown in Scheme 2. The selective synthesis of **A** (3α-(ethoxycarbonyloxy)-7α-(hydroxyl)-5β-cholanoate) from CDCA by two steps was reported previously. Firstly, the carboxylic acid on CDCA was methyl esterified, then, the hydroxyl group on 3α position was selectively protected by reacting with ethyl chloroformate in dried pyridine at -20 °C to form **A** with 91% yield. [19] The initial purpose is to synthesize **1** from **A** by reacting with NaH and allyl bromide in THF. [20] However, there is no reaction at all under this condition. The dipolar-aprotic solvent DMSO was also used instead of THF to improve the reaction conditions, but resulted in the product like polymers. The alternative method was adopted by silylation of 7α-OH on compound **A** with TMCS and imidazole in THF[21], followed by dried TBAF desilylation of **B** to produce unstable alkoxide intermediate, which is supposed to afford **1** with allyl group in the presence of allyl bromide.

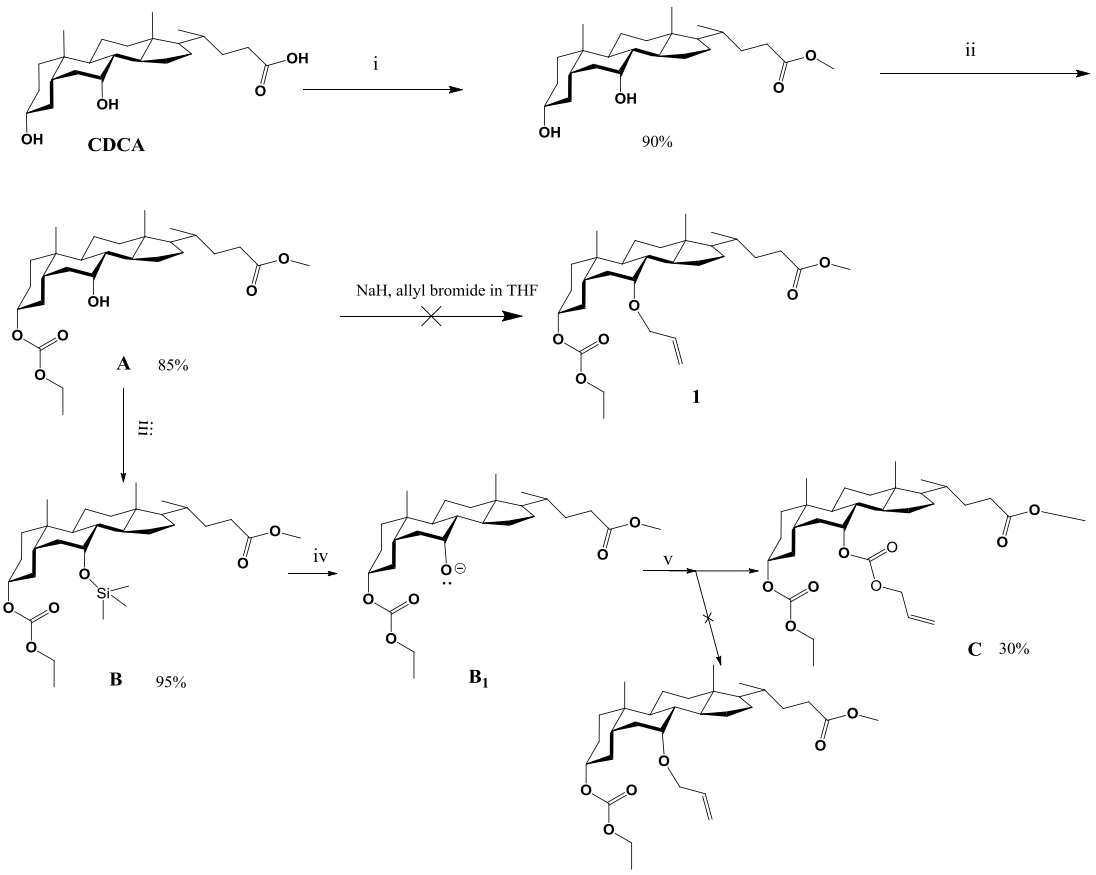

Scheme 2. The synthesis of compound **C**. i) Acetyl chloride, methanol, at 0 °C. ii) Ethyl chloroformate, pyridine, at 0 °C. iii) TMCS, imidazole, THF. iv) Anhydrous TBAF, THF, 24 h. v) Anhydrous allyl bromide.

To our surprise, by this protocol, instead of producing **1**, it afforded a novel compound **C** and accompanied by **A** as the side product. The obtained product **C** has shown that there is a CO_2 molecule inserting between the alkoxide anion and allyl group. Though it is hard to imagine that the ambient CO_2 could participate in such a reaction, we proposed the mechanism for the formation of **C** shown in Scheme 3 that prior to

attacking allyl bromide, the bulky and sterically hindered $\mathbf{B_1}$ intermediate with 7α-O^- favorably reacted with small and acidic CO_2 to form a new intermediate with a more extended and less sterically hindered carbonate anion (7α-$OCOO^-$) which facilitates the reaction with allyl group via S_N^2 mechanism.

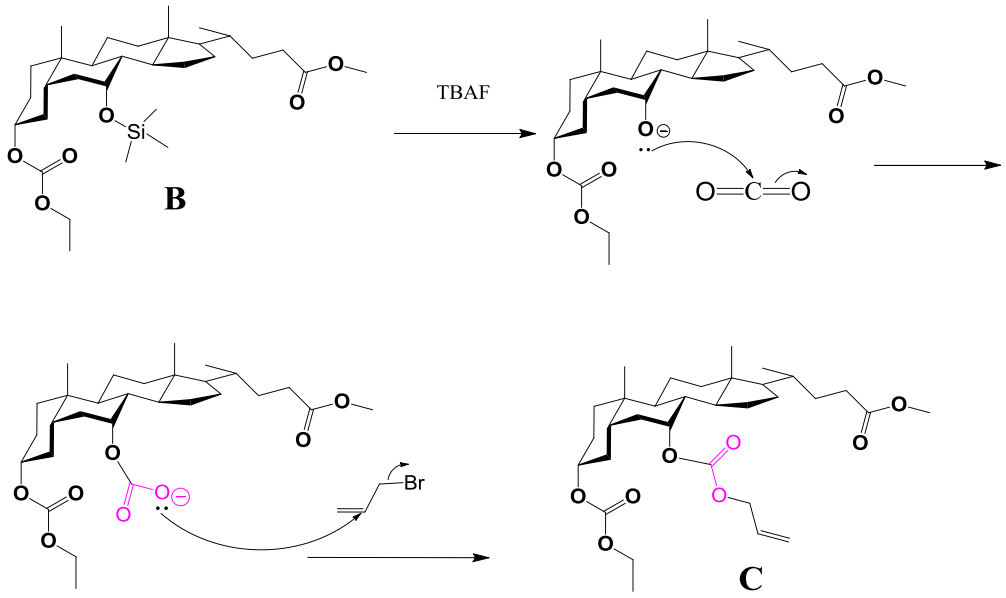

Scheme 3. The proposed mechanism for the formation of **C**.

The attempt has been made to synthesize **1** by rigorously exclusion of atmospheric CO_2. When the reaction was carried out in either under N_2 gas or in a sealed glass chamber with degassed reaction mixture, it failed to give even a little **1**. It is indicated that the direct attack of allyl bromide to give **1** was not possibly accomplished by unstable alkoxide anion $\mathbf{B_1}$ with 7α-O^- because the following two reasons have greatly decreased the reactivity of $\mathbf{B_1}$ intermediate toward SN^2 reaction. First, it is too bulky and 7α-O^- anion is sterically hindered since it is located in the concave face and shielded by

steroid skeleton. Second, the 7α-O^- anion has high priority to react with water compared to the allyl bromide when even trace amount of water was brought into reaction mixture by TBAF. The commercially available TBAF as trihydrate is highly hygroscopic. It has been difficult to remove water molecules completely from TBAF. The highest yield of **C** is only 30%. Due to the presence of even trace amount of water, **A** as the side product was obtained. Thus the synthesis of **C** has to be proceeded with freshly distilled THF from sodium and potassium alloy and anhydrous TBAF. The removal of water from TBAF can be carried out under vacuum with the presence of P_2O_5 below 40ºC for extended periods.[22] During this process, TBAF is partially decomposed and form stable difluoride ion upon the removal of water. The use of tetrabutylammonium triphenyldifluosilicate readily soluble in organic solvents (TBAT) and cesium fluoride which are available in anhydrous form failed to deprotect silyl group on **B** , probably, due to the steric bulk of TBAT and the insolubility of CsF in THF although TBAT and CsF are good alternatives of TBAF to provide a source of naked F^-.

As mentioned above, this methodology provides a pathway to make ^{14}C labeled CDCA derivatives by fusing $^{14}CO_2$ onto 7α-position of steroid skeleton. This could be the most economical and efficient way because $^{14}CO_2$ is produced for the commercial available $Ba^{14}CO_3$ which is the cheapest source containing ^{14}C element. In addition, the ^{14}C labeling CDCA derivatives by this method would be a very useful source for studying the transport mechanism of hASBT, monitoring the BA loss and determining bile acid synthesis rate etc.

The structure of **C** has been confirmed by ^{1}H and ^{13}C NMR studies. The partial ^{1}H-NMR spectra of **A** and **C** are shown in Figure 11. In comparison with partial ^{1}H NMR spectrum of **A**, 7β-H in **C** has a chemical shift at 4.68 due to the strong deshielding effect of the neighboring 7α-allyloxycarbonyloxy group, While 7β-H next to the OH group in **A** gives a singlet at 3.75. The chemical shifts of protons on 7α-allyloxycarbonyloxy group (–OCOOC$\underline{H}_2$C$\underline{H}$=C$\underline{H}_2$) are assigned in the bottom spectrum of Figure 11 which appeared as a doublet at 4.57, a doublet of a doublet at 5.19-5.32 and multiple peaks from 5.84 to 5.94 respectively.

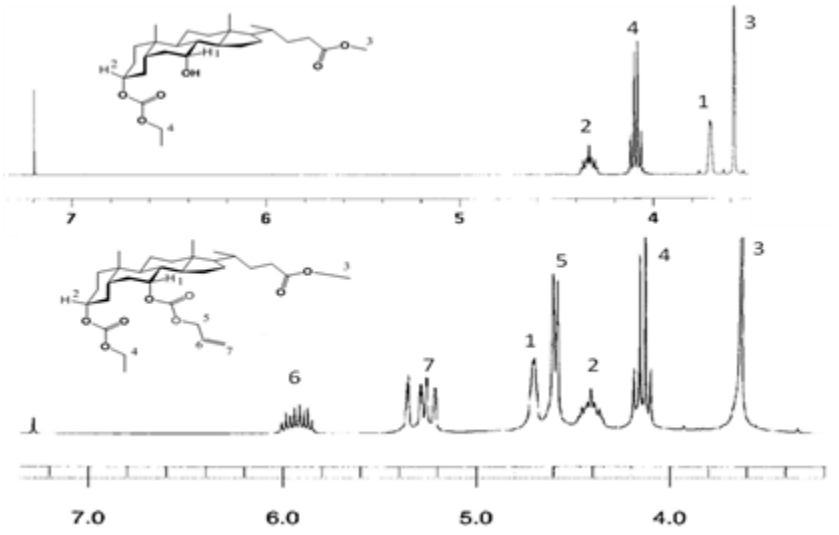

Figure 11. Partial H NMR of **A** and **C** in downfield region.
a) Decoupled ^{13}C-NMR of **A**

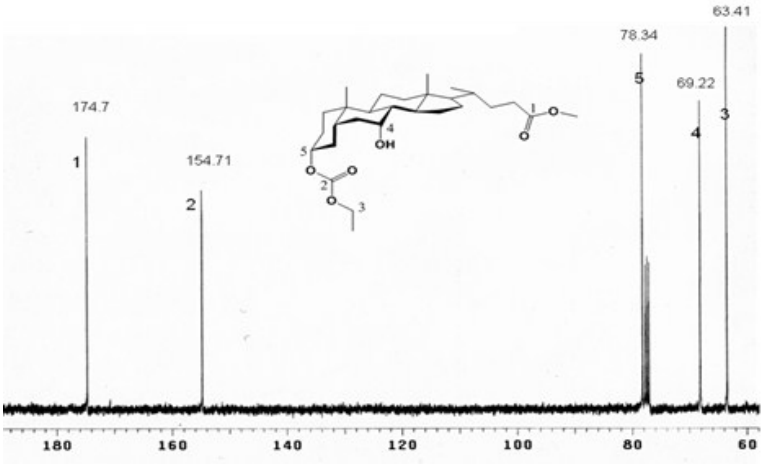

b) Coupling ^{13}C-NMR of **C**

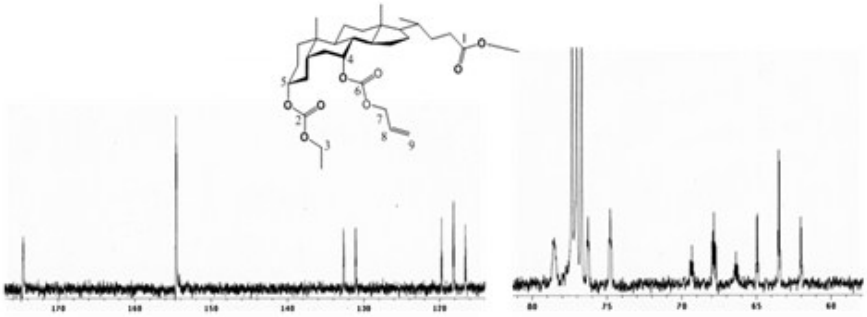

c) Decoupled ^{13}C-NMR of **C**

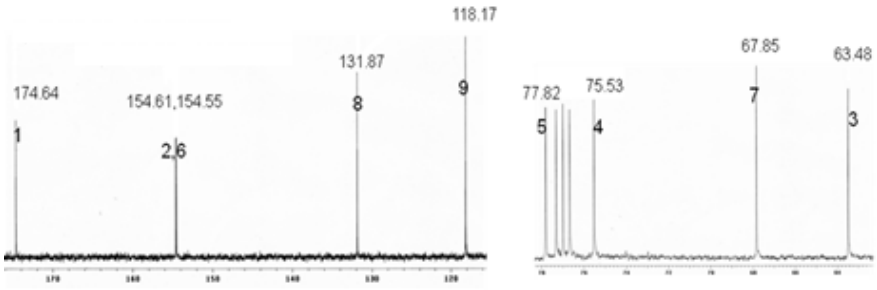

Figure 12. Assignment and comparison of the partial ^{13}C-NMR of **A** and **C** in the down field.

The partial ^{13}C-NMR spectrum of **A** was shown in Figure 12 a) for comparison. The peaks at 174.7, 154.71 are assigned to the carbonyl carbons of methyl ester group (–

COOCH$_3$) and ethoxycarbonyloxy group (–OCOOCH$_2$CH$_3$) respectively. For compound **C**, the peak for carbonyl carbon on 7α–OCOOCH$_2$CH=CH$_2$ appeared at 154 ppm which is overlapped with the peak of carbonyl carbon on 3α–OCOOCH$_2$CH$_3$. The signal of 7α-**C** which was 69.22 on **A** has shifted to 75.53 with the formation of 7α-allyloxycarbonyloxy group. The assignment of peaks for 3α-C, 7α-C and CH$_2$ on –OCOOCH$_2$CH$_3$ is confirmed by the information provided by partial coupling ^{13}C-NMR spectra of **C** and the comparison of decoupled ^{13}C-NMR spectra of **A** with **C.** The peak at 63.4 shown as a triplet split by two protons in Figure 12b is assigned to CH$_2$ on OCOOCH$_2$CH$_3$ group. The peaks for 3α-C and 7α-C appeared at 77.82, 75.53 correspondingly in Figure 12c which both split as a doublet in coupling ^{13}C-NMR spectrum. However, one single peak of the doublet for 3α-C is not observed because it is buried by the solvent peaks (CDCl$_3$).The signals at 67.85, 131.87, 118.17 are assigned to carbons on alloxy group (–CH$_2$CH=CH$_2$) and confirmed by coupling ^{13}C-NMR spectrum shown as a triplet, doublet and triplet accordingly. The structure of **C** was also confirmed by both LRFAB (low resolution fast atom bombardment) and HRFAB (high resolution fast atom bombardment) mass spectroscopy. FAB is a relatively soft ionization technique and usually produces positive molecular ion peaks like $[M+H]^+$ and $[M+Na]^+$. In this experiment, the 3-NBA (3-nitrobezyl alcohol) is used as the matrix. The HRFAB of **C** was shown in Figure 13. The calculated exact molar mass of $[M+H]^+$ is 563.3584 (100%) while it is found at 563.3592 (100%) which is the highest peak in Figure 13. The difference of exact mass between found and calculated is only 1.5 ppm. The isotopic

intensity peaks are M+1 at 564.3649 (37.4%), M+2 at 565.3702 (7.8%). The calculated intensities are m/z at 562.3506 (100.0%), 563.3539 (34.6%), 564.3573 (5.8%), 564.3548 (1.6%).

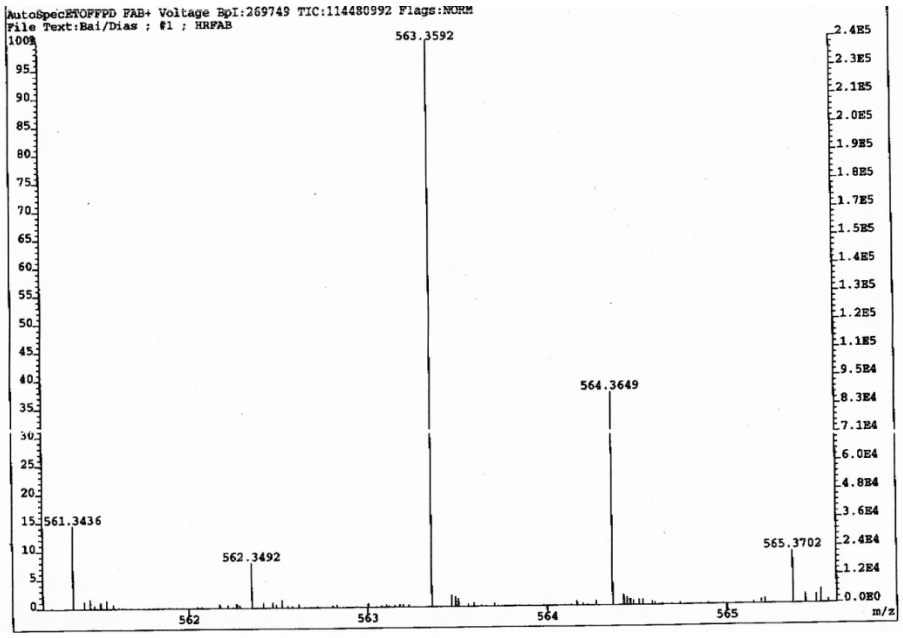

Figure 13. HRFAB mass spectrum of **C**

The structure of **C** was finally confirmed by single-crystal X-ray diffraction. The single crystals of **C** were obtained by slowly evaporating the solution of ethyl acetate and hexanes. The authentic structure shown in Figure 14 gives the solid evidence that there is CO_2 insertion between 7α-O^- and allyloxy to form allyloxycarbonyloxy. The crystal structure of C is monoclinic (C_2) and tightly compacted and arrayed by extensive intermolecular van der Waals interaction shown in Figure 15. The driving force for the formation of single crystal structure of **C** is hydrophobic interaction. The distances of

H4…..H_{19A}, O_6…..H_{6A}, O_1……H_{19} and H_{31C}…..O_7 are 2.36 Å, 2.36 Å, 2.54 Å, and 2.64 Å, respectively shown in Figure 16.

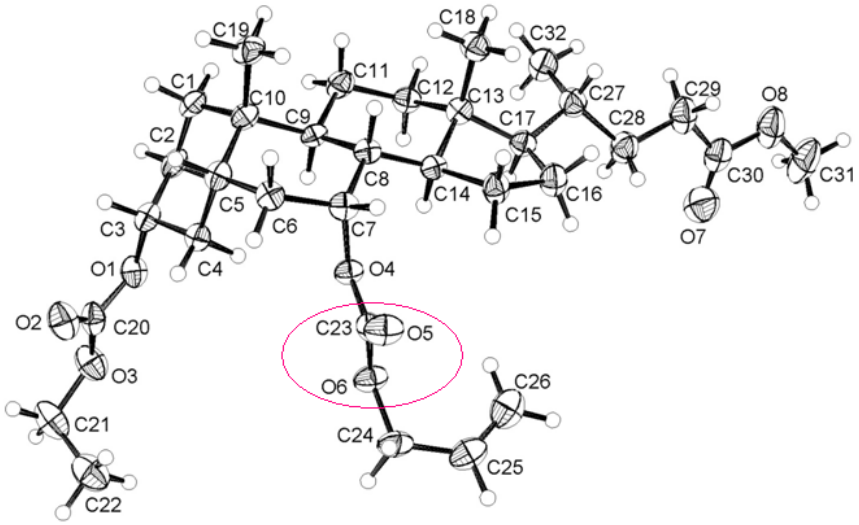

Figure 14.The ORTEP drawing of compound **C**. The displacement ellipsoids were drawn at the 50% probability level.

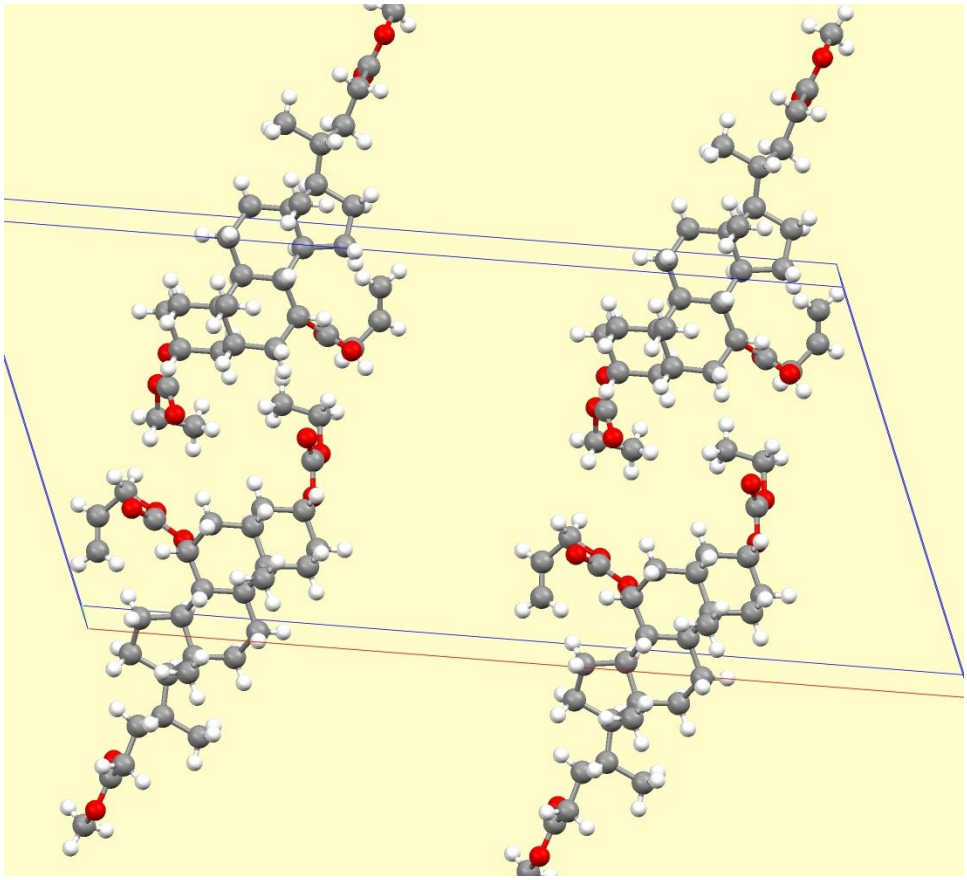

Figure 15**.** The unit cell of compound **C.**

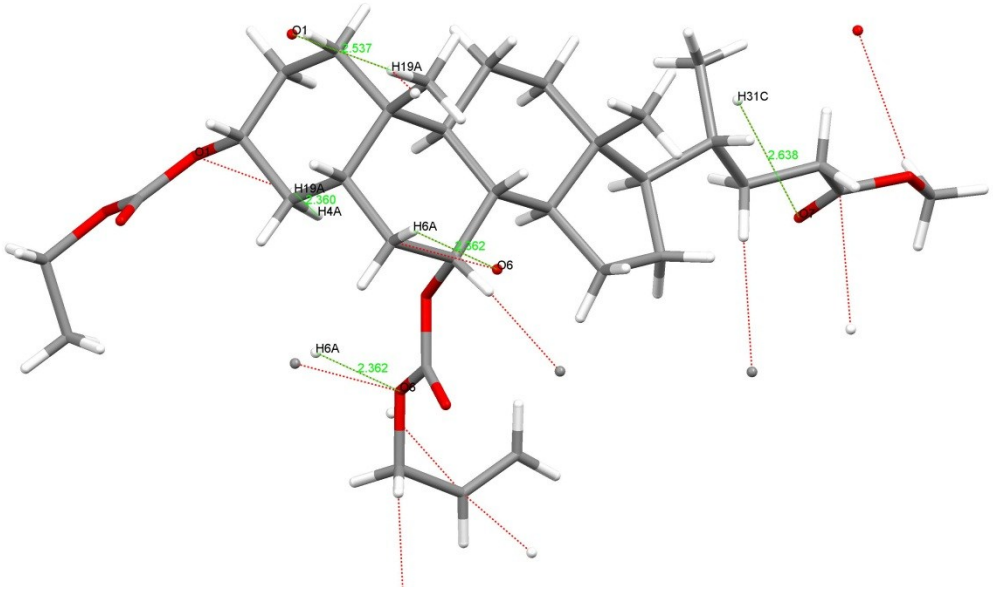

Figure 16**.** The distances (in Å) of intermolecular interaction observed in X-ray crystal structure of **C.**

Table 1. Crystallographic data for Compound **C**

	C
T , K	173(2)
Space group	C_2
a , Å	32.329(3)
b, Å	6.4576(5)
c, Å	15.8329(13)
α , deg	90
β , deg	111.8830
γ , deg	90
V, $Å^3$	3067.2(4)
Z	4
Calculated density(Mg/m^3)	1.219
Absorption coefficient(mm^{-1})	0.086
F(000)	1224
θ range ,deg	1.7-27.15
Limiting indices	-41<=h<=37 -7<=k<=8 -20<=l<=20
Reflections collected	10950 / 3665
Data / restraints / parameters	3665 / 1 / 366
Goodness-of-fit on F^2	1.037
Final R indices [I>2sigma(I)]	R1 = 0.0520 wR2 = 0.1035
R indices (all data)	R1 = 0.0795 wR2 = 0.1130
Largest diffraction. peak (eA^{-3}) hole (eA^{-3})	0.229 -0.195

2.1.2. The synthesis and characterization of allyl 3α-(ethoxycarbonyloxy)-7α-hydroxy-5β-cholanoate.

In this procedure shown in Scheme 4, our targeted compound is methyl 3α-(ethoxycarbonyloxy)-7α-(allyloxy)-5β-cholanoate (**D**). In the first step, TBAF was used to remove the silyl group and give the naked alkoxide anion, and then, NaH was added prior to allyl bromide to get rid of water brought by TBAF in reaction system. By adding NaH, we supposed that the produced alkoxide anion would not be destroyed by water and survive to react with allyl bromide to give **D**. However, we've found that the obtained product was allyl 3α-(ethoxycarbonyloxy)-7α-hydroxy-5β-cholanoate (**E**) instead of **D.** From partial ^{1}H-NMR spectra, two possible structures are contrasted shown in Figure 17.

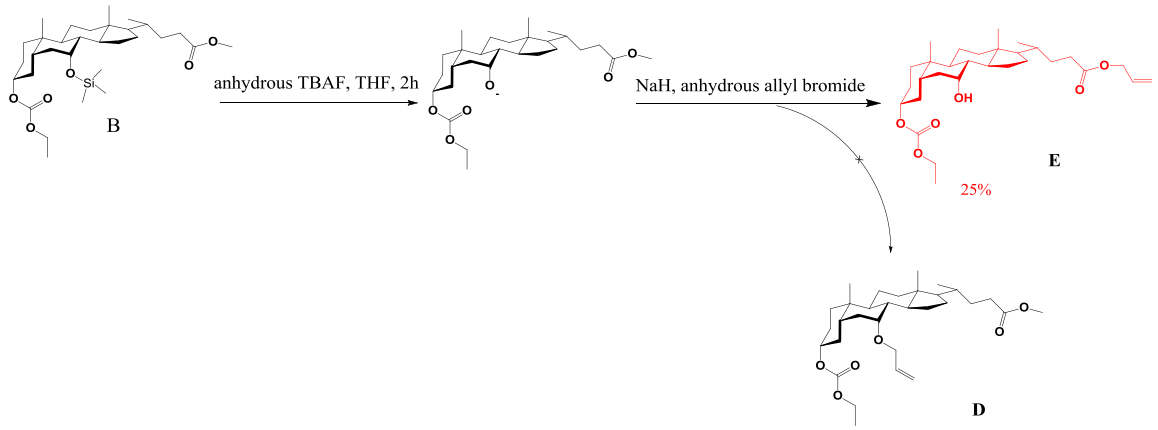

Scheme 4. The synthesis of compound **E**.

a)

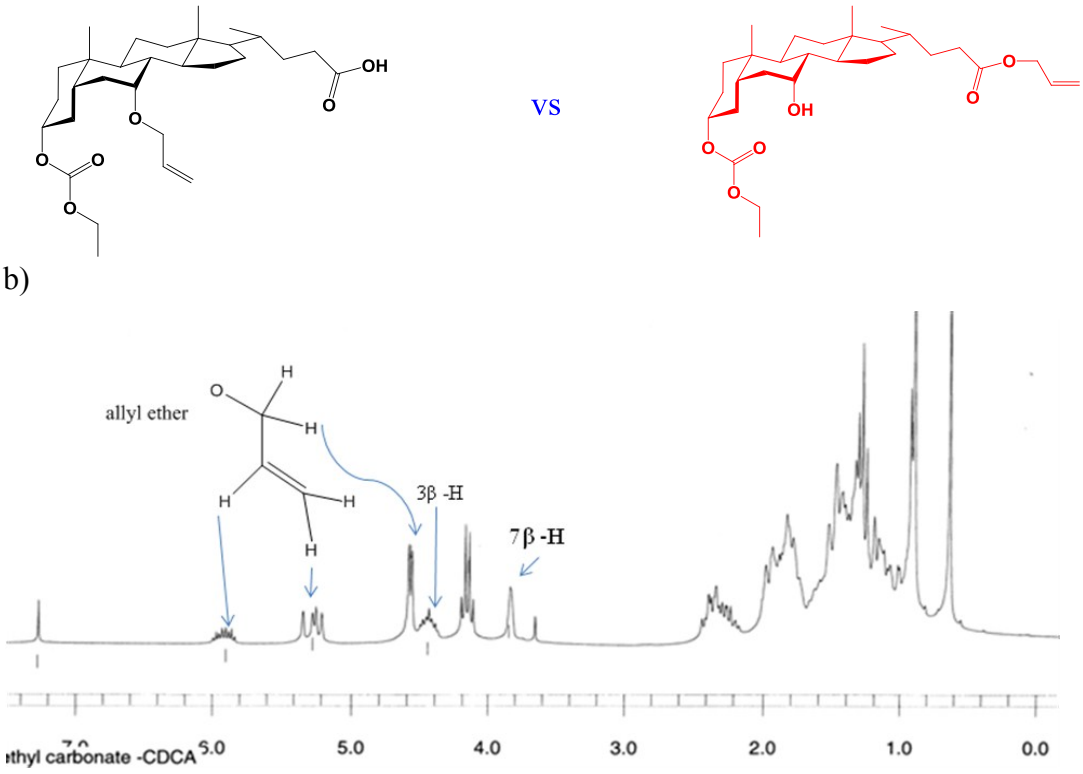

Figure 17. a) Two possible structure predicted from ^{1}H-NMR data. b) The partial ^{1}H-NMR spectrum of compound **E**

The ^{1}H-NMR spectra showed that the singlet peak for three protons on $-OCH_3$ group next to C24 disappeared. It means that the ester group is probably hydrolyzed by basic TBAF or NaH during the reaction. Three new signals occurred at downfield are assigned to protons on allyl ether group. The two protons on the carbon next to double bond and deshielded by the neighboring oxygen appear as a doublet at 4.55 and 4.57. One proton on double bond next to $-OCH_2$ group split into multiple peaks resonances from 5.87 to 5.94. The two protons at terminal alkene have the signal as a quartet at 5.21, 5.23, 5.28 and 5.32. Since the disappearance of the $-CH_3$ group from C_{24}, there is two possible

positions to attach allyl group. If allyl group was attached on 7α position, it would give 3α-(ethoxycarbonyloxy)-7α-allyloxy-5β-cholanoic acid described on the left of Figure 17. Otherwise, under basic condition, it forms the $-C_{24}OO^-$ anion which attacked allyl bromide to give allyl 3α-(ethoxycarbonyloxy)-7α-hydroxy-5β-cholanoate as pictured on the right of Figure 17 a). However, the 7β-H in Figure 17 b) has the signal at 3.79 and is almost the same as the chemical shift of 7β-H on compound **A**. It is indicated that the neighboring 7α position is probably the un-functionalized OH group. The hydrolysis of ester group on the obtained compound by using K_2CO_3 in methanol and THF solution under reflux resulted in CDCA and the disappearance of peak for allyl group which confirmed that the allyl group was attached on C24 by forming ester instead of C7 position to give ether. The HRFAB mass spectrum of compound **E** is shown in Figure 18. The matrix is 3-NBA+Na, The exact mass of $(M+Na)^+$ is found at 527.3347 (100%) which is the molecular ion peak, while the calculated is 527.3349. The difference between the found and the calculated mass is only 0.2 ppm. The isotope peaks of M+1, M+2 appeared at 526.3388 with the intensity of 32.3% and 529.3427 with the intensity of 8.4%. The calculated m/z of ($M+Na)^+$ are 527.3349 (100.0%), 528.3382 (32.4%), 529.3416 (5.1%), 529.3391 (1.2%).

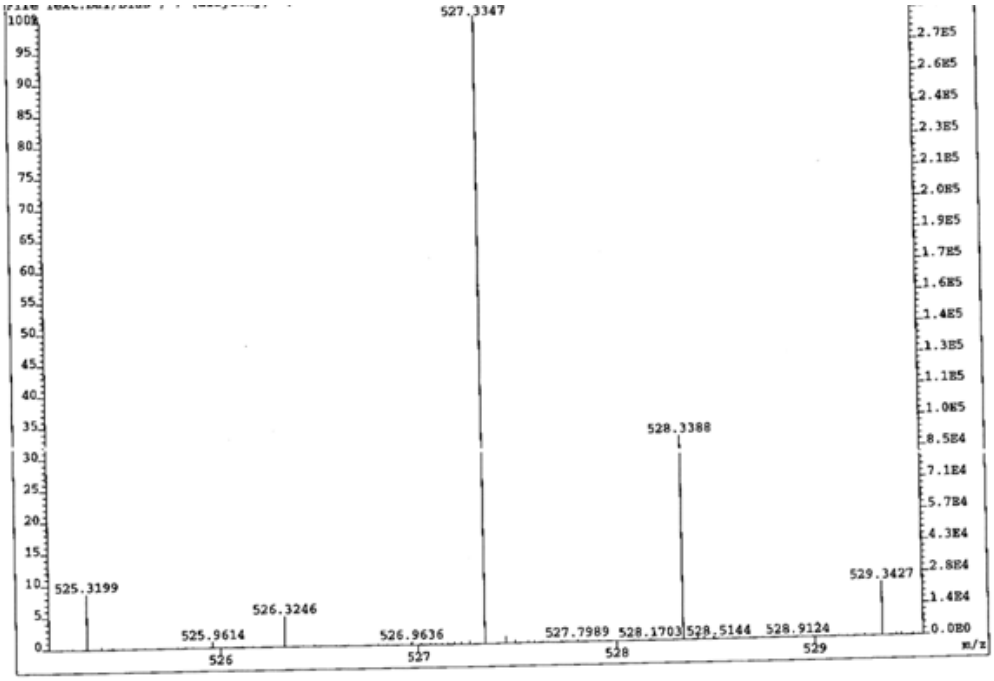

Figure18. The HRFAB mass spectrum of allyl 3α-(ethoxycarbonyloxy)-7α-hydroxy-5β-cholanoate (**E**)

2.1.3 Synthesis and characterization of 3α-hydroxy-7α-(4-pentenoyloxy)-5β-cholanoic acid (H).

The synthesis of compound **H** is shown on Scheme 1. The carboxylic acid on CDCA was methyl etherified to give the methyl cholanoate, and the hydroxyl group on 3α-position of the methyl cholanoate was selectively protected by reacting with ethyl chloroformate in dried pyridine at -20 °C to form 7α-monohydroxyl cholanoate **A** (91%).

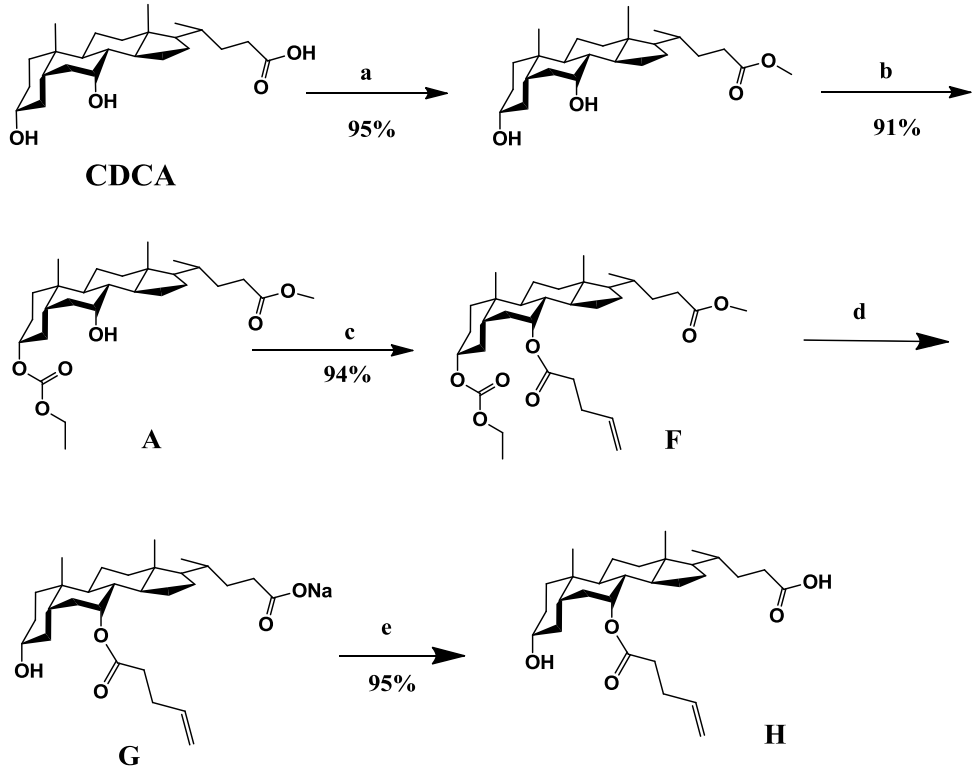

Scheme 5. Synthesis of **H**. a) AcCl, CH_3OH, at 0 °C , 1 h ; b) ClCOOEt, py -20 °C, 1 h ; c) 2,6-dichlorobenzoyl chloride,4-pentenoic acid, Et_3N, DMAP, rt. 24 h; d) K_2CO_3, CH_3OH, THF, reflux,12 h. e) 3M HCl.

Ester **F** was produced by reacting 7α-hydroxyl group of **A** with 4-pentenoic acid, 2, 6-dichlorobenzoyl chloride and DMAP via Yamaguchi reaction. Since the 3α position of

CDCA is less sterically hindered than 7α-position, under basic condition, the 3α-ethoxycarbonyloxy and 5β-methyl ester can be selectively hydrolyzed to give compound **G** by using saturated potassium carbonate solution mixing with THF and methanol under reflux. By this way, the obtained compound **G** is a sodium salt which remains in the basic aqueous layer. **H** is precipitated out from the aqueous layer by slow addition of 3M HCl. The compound **H** has a 3α-hydroxyl group and a 5β-carboxylic acid functional group available to form macrocycles by Yamaguchi macrolactonization, in addition, the 7α-pentenoate group with a terminal alkene group could have coupling reaction by Grubb's catalyst.

As shown in Figure 19, the peaks 5 and 6 (5.7 and 4.9 ppm) appearing at relatively upfield are signals for protons on terminal alkene group. The peak for 7β-H is a singlet (4.8 pm) and next to peak 6 (4.9 pm). Comparing to the spectrum of b, after hydrolysis, the disappearance of a singlet peak 3 (3.6 pm) which is the signal for three protons on methyl ester group ($-C_{24}OOC\underline{H}_3$) indicated that methyl ester has converted into carboxylic acid. In addition, a quartet peak 4 (4.1 pm) which is assigned to two protons on 3α-ethoxycarbonyloxy ($OC_3OOC\underline{H}_2CH_3$) also disappeared confirmed the removal of ethoxycarbonyloxy group. The peak 2 of a multiplet for 3β-H which is 4.35 for compound **F** has shifted to 3.48 due to the shielding effect of hydroxyl group.

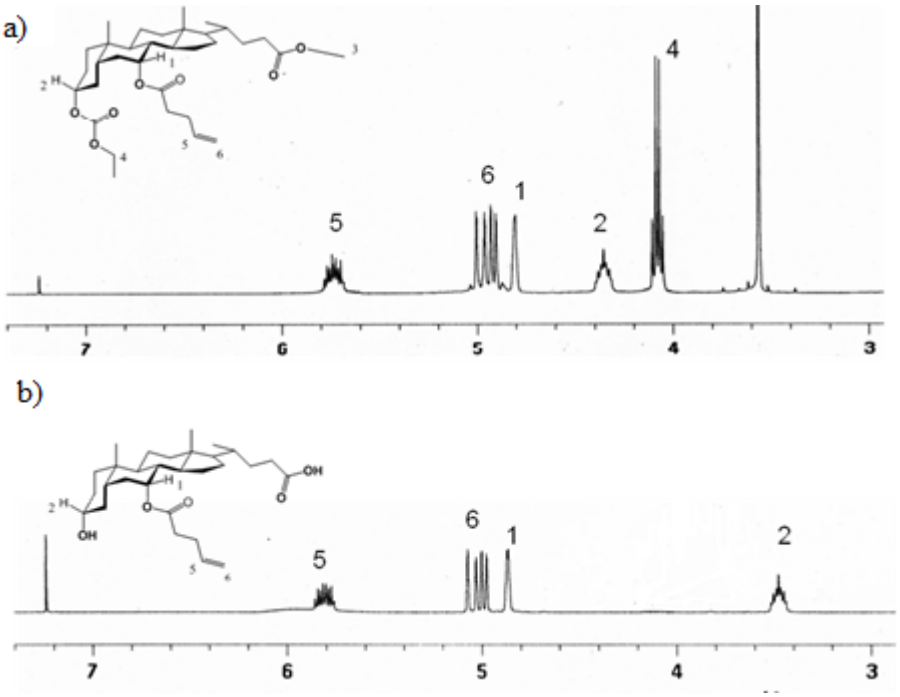

Figure 19. a) Partial ^{1}H-NMR spectrum of compound **H**. b) Partial ^{1}H-NMR spectrum of compound **F**.

Comound **F** and **C** have a closely related 7α moieties. The protons of $CH=CH_2$ for the compound **F** with 7α-4-pentenoate group shift to the high field (5.73 ppm, 4.97-5.07 ppm), but 7β proton shifts to the low field(4.88 ppm) in comparison with corresponding protons (5.91 ppm, 5.34-5.22 ppm for the alkene and 4.70 ppm for 7β-H) on compound **C** with an 7α-(allyloxycarbon-yloxy) group. In addition, the chemical shift for C25 on compound **F** is 172.1 ppm; it is 154.6 ppm for compound **C**.

The structure of **H** is also confirmed by single X-ray diffraction. The single crystals of **H** were obtained by slow evaporation of chloroform and crystallized in orthorhombic (P 21 21 21) space group. Compound **H** has a typical curved structure. The convex face is

hydrophobic with two methyl group extruding out. The concave face has 3α-hydroxyl group in the one end and carboxylic acid in the other end which are typical hydrogen bonding functional group for the formation of single crystals. The 7α-(4-pentenoyloxy) group is exactly docked in the center of the concave face. Those features observed from Figure 20 indicated that compound **H** could be an ideal moiety for macrocyclization.

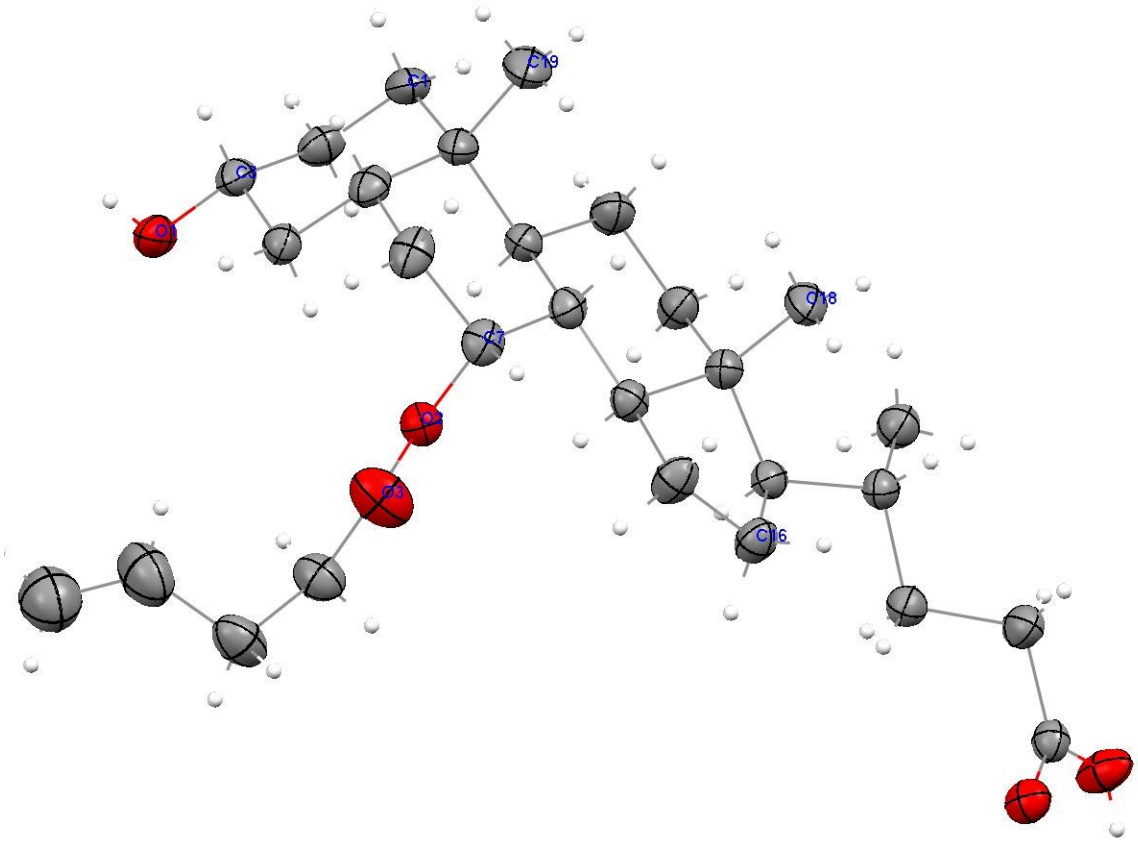

Figure 20. Structure of **H**; the ellipsoids are drawn at the 50% probability level.

Compared to the structure of CDCA, the 7α-OH has been replaced by the 4-pentenoyloxy group in structure of **H**, no hydrogen bond is involved in 7α position, which makes the hydrogen bonding network of **H** less complex than that of CDCA single crystal structure. The 3α-hydroxyl and 24-carboxylic acid groups of **H** provide two hydrogen bonding sites and each site forms two hydrogen bonds with other two molecules. As shown in Figure 21, the O5 on carboxylic acid group is hydrogen bond acceptor and O5-H of carboxylic acid is hydrogen bond donor, but O1 on 3α-OH group acts as both hydrogen bond donor and acceptor.

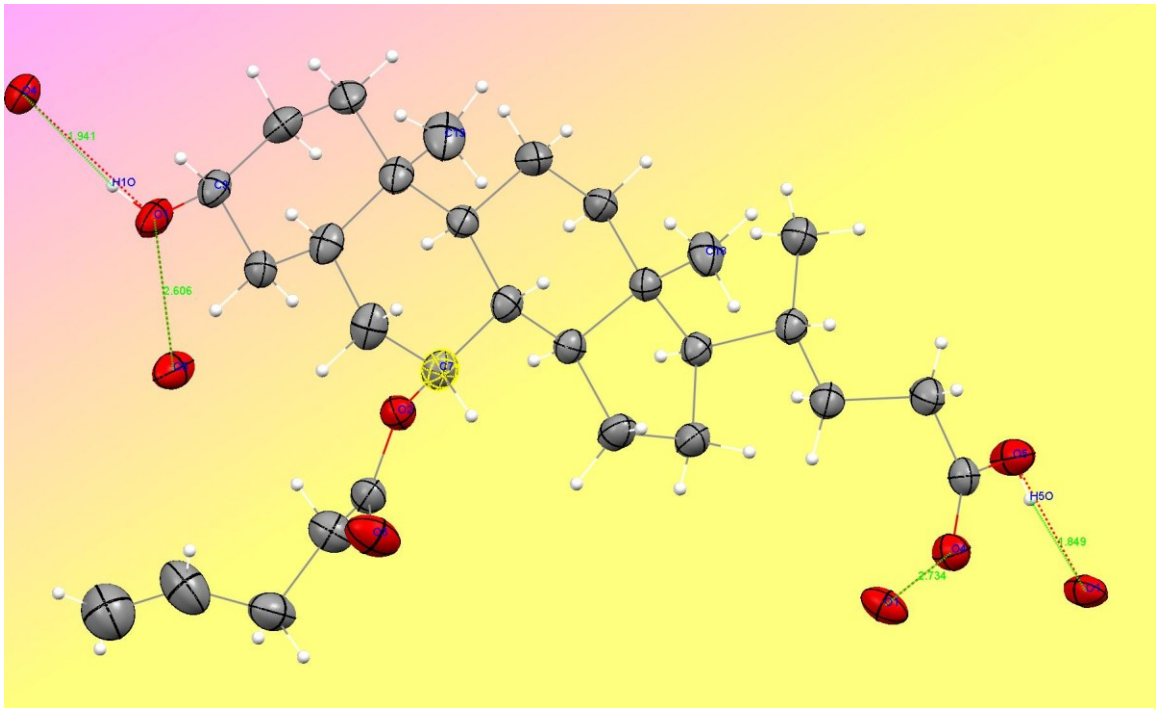

Figure 21. Distances (in Å) of the hydrogen bonds observed in **H**.

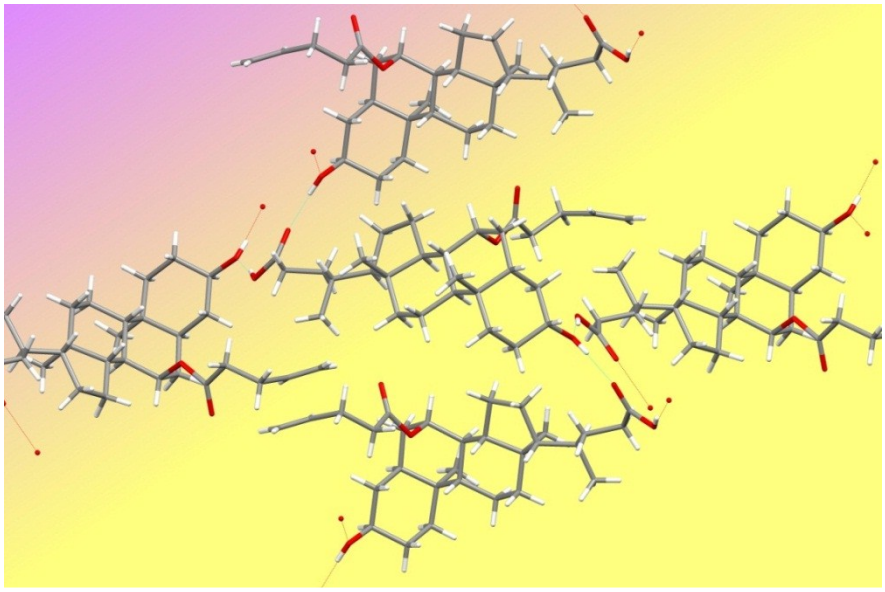

Figure 22. Top view of hydrogen bond network formed by five molecules of **H.**

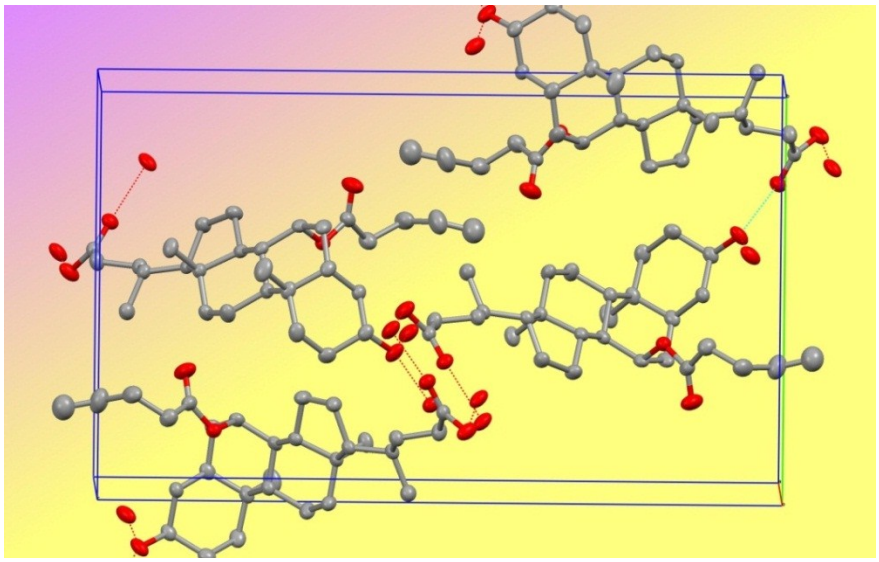

Figure 23. The unit cell of compound **H**.

The distance of hydrogen bond between H_{10} and O4 is 1.94Å, and between H_{50} and O1 is 1.85. The distances of O1→O4, O5→O1 are 2.73 Å and 2.61Å respectively. The

expanded hydrogen network is shown in Figure 22, each molecule **H** is interconnected with four molecules via two different hydrogen bonds.

Table 2. Crystallographic data for Compound **H**

	H
T , K	173(2)
Space group	P 2_1 2_1 2_1
a , Å	8.4713(4)
b, Å	13.9207(6)
c, Å	23.3039(10)
α , deg	90
β , deg	90
γ , deg	90
V, $Å^3$	2748.1(2)
Z	4
Calculated density(Mg/m^3)	1.147
Absorption coefficient(mm^{-1})	0.076
F(000)	1040
θ range ,deg	1.36-27.12
Limiting indices	10<=h<=10 -17<=k<=17 -29<=l<=21
Reflections collected	19726
Data / restraints / parameters	3431 / 0 / 318
Goodness-of-fit on F^2	1.046
Final R indices [I>2 sigma(I)]	R1 = 0.0408 wR2 = 0.1029
R indices (all data)	R1 = 0.0498 wR2 = 0.1098
Largest diffraction. peak (eA^{-3}) hole (eA^{-3})	0.411 -0.194

2.2 Macrolactonization

The syntheses of macrocyclic lactones have been greatly attractive since investigators have found the uses of natural macrocyclic lactones in perfumery, medicinal and insecticide industries. [23] During the past several decades, a wide variety of macrolactones has been either isolated or synthesized. Their potential applications were also extensively studied.

One of the typical example of macrolactones is the natural product exaltolide (musk) firstly isolated in 1930's and used as perfume fixative later. [24] Another class of representative macrolactones has the function as antibiotics, such as erythromycin, which was isolated in 1950's and has been widely used in the treatment of bacterial infections.[25] In addition, depsipeptides, one class of macrolatones with biological activities, are more promising. For example, FK228 has been identified as a potencial anticancer drug in phase II clinical trials. [26] Due to the biological significance of cyclic structure of macrolides, various methods have been established to form lactones with large rings. The lactonization of the hydroxy acid is the mostly used and predominant approach to synthesize the macrolides although some other new methods such as RCM, HWE,etc. have been developed to make macrocyclization efficiently. For macrolactonization, the cyclization of hydroxy alkynoic acid can not be proceeded without activation of the terminal group of alcohol or carboxylic acid. The formation of lactones by intramolecular reaction usually requires high dilution technique to avoid forming diolides and oligomers by intermolecular reaction no matter whether it

undergoes acid activation or alcohol activation.[27] Due to the diversity of hydroxy alkanoic acids, the influence of conformation and the impact of the substituents, no single and universal method can be applied to all macrolactonization reactions. Therefore, various reagents and solvents has been employed to improve and optimize the macrolactonization of hydroxy alkanoic acids. Hitherto, there is more than a dozen of approaches has been developed for macrolatonization through acid activation. Among these methods, Yamaguchi conditions through the formation of mixed anhydrides and basic activation is probably the most popular method used for the syntheses of more than 200 macrolactones. The classic Yamaguchi macrolactonization is one pot, two step reactions. The mechanism of Yamaguchi macrolactonization by acid activation is shown in Scheme 6. The typical Yamaguchi reagent 2,4,6-trichlorobenzoyl chloride or 2,6-dichlorobenzoyl chloride is employed to initiate the reaction by forming anhydrides with hydroxy alkanoic acids in the presence of Et_3N in THF, then the Et_3N-HCl precipitate is filtered and THF is evaporated by rotvap, finally, the anhydride intermediate is diluted in toluene and added into highly diluted DMAP toluene solution under reflux.[28] However, this condition cannot fulfill some macrolactonizations because of the complexity of some hydroxyl acids by its advanced substrates. For example, during the synthesis of leucascandrolide, the macrolactonization of seco acid **A** under the classic Yamaguchi conditions only gave the oligomers owing to the possibly undesirable hydrogen bonding in seco acid.

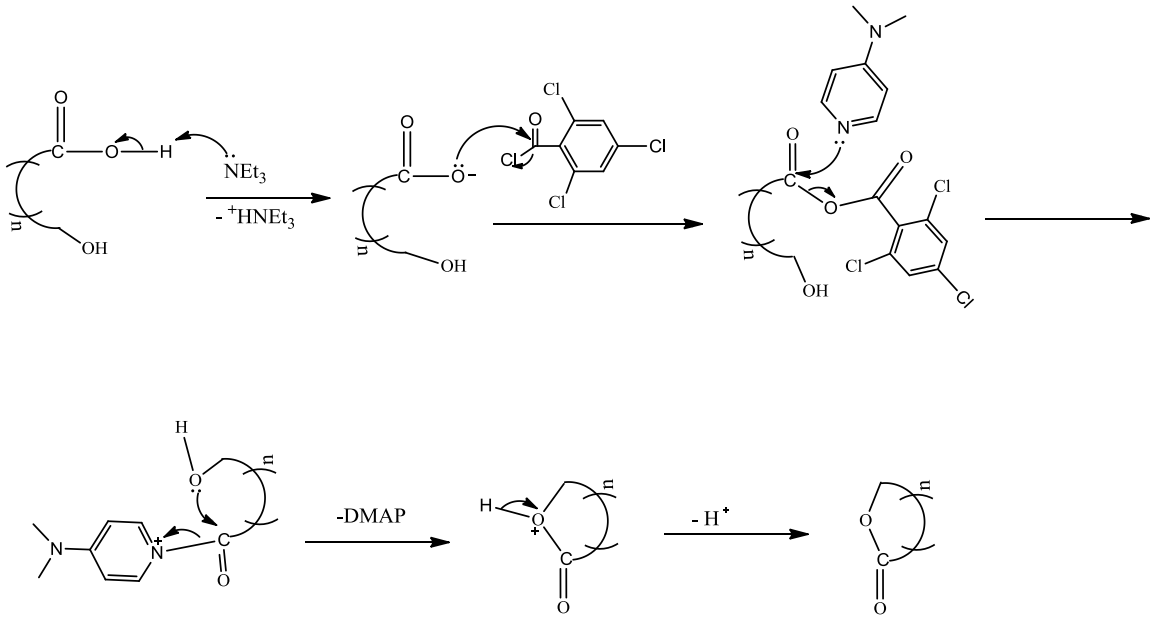

Scheme 6. The mechanism of Yamaguchi macrolactonization

Finally, this lactonization was realized by using DMF as the solvent instead of toluene, THF or xylene Shown in Scheme 7.[28] However, the seco acid **B** with methoxy replacing hydroxyl group at 9 position can be conveniently cyclized with 80% yield via Yamaguchi method by adding the preformed anhydride intermediate to DMAP in THF solution (Scheme 8). The two macrolactonizations of seco acids for the synthesis of leucascandrolides mentioned above indicated that the reactivity of seco acid A and B toward Yamaguchi macrolactonization is significantly affected by their substrates or stereochemical modifications. Therefore, the Yamaguchi method has been modified to cyclize some hydroxyl acid with particular substrates. Yonemitsu has made two important modifications on this method. One is called "modified Yamaguchi conditions" which is the direct addition of large amount of DMAP into the preformed anhydride

intermediate without slow addition at room temperature. The other one is known as "Yonemitsu conditions" that the DMAP is added into the reaction mixture of Et_3N, hydroxyl acid, Yamaguchi reagent at the beginning without pre-forming the anhydride intermediate at room temperature. [29] Generally, the synthesis of lactones with large rings usually adopts Yonemitsu conditions, and classic Yamaguchi method is used to form medium ring lactones. However, there is no absolute rule for realization of lactones. The reaction conditions have to be adjusted according to the types of moieties and the functional groups attached on the moieties for macrolactonization.

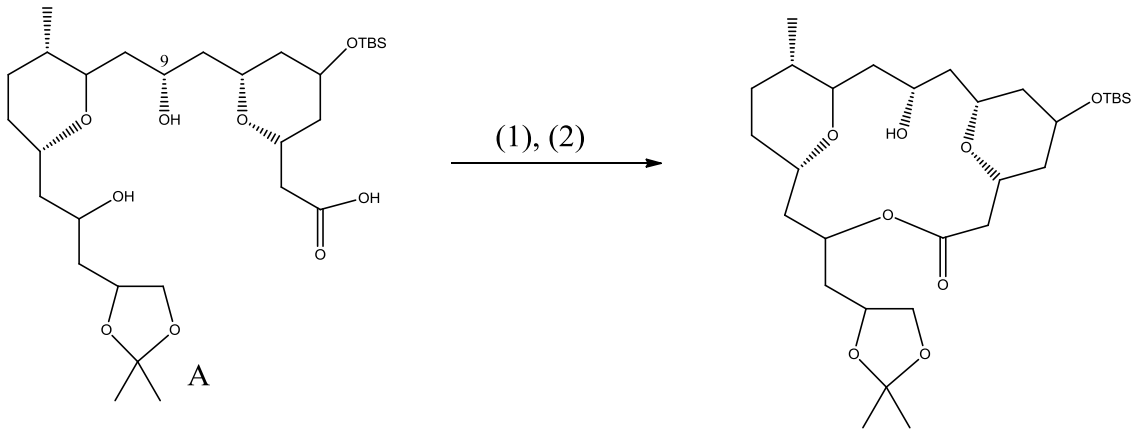

Scheme 7. The synthesis of macrocycles by using DMF as solvent. (1) 2, 4, 6-trichlorobenzoyl chloride, Et_3N, rt, 1 h, then dilution with DMF. (2) Slow addition of anhydride intermediate to DMAP in DMF solution, rt, 2 h.

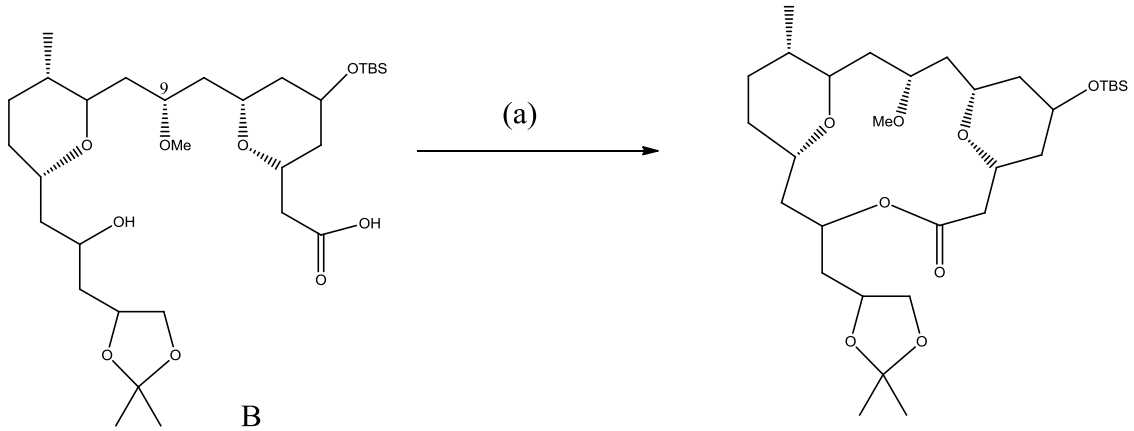

B

Scheme 8. (a) 2, 4, 6-trichlorobenzoyl chloride, Et3N, THF, rt, 1 h; then addition to DMAP in THF, 80%.

In addition, the use of PS-bound DMAP as catalyst for Yamaguchi macrolactonization is another strategy which allows the formation of lactones without high dilution. Recently, a wide variety of polymer supported reagents and catalysts have been developed and applied in solution phase synthesis for macrolides. To date, the PS-bound phosphonium salt, polymer-bound carbodiimide, a commercial available PS-bound DMAP have been extensively used in the synthesis of large ring lactones. [30] It has been shown that polymer supported reagents and catalysts are capable of improving the yield of lactones and realizing some macrolactonizations which cannot perform under conventional reagents and catalysts. While the use of polymer supported reagents and catalysts also avoids the need to have highly diluted solution. Only few methods through alcohol activation were developed and also far less useful compare to those acid activation methods.

The protocol of Yamaguchi macrolactonization has also been used to make natural diolides successfully. [31] The macrolactonization of bile acid derivatives by Yamaguchi Yonemitsu conditions was firstly synthesized in our group. The bile acids with various functional groups have been used as the motif to construct macrocycles with different cavity size by Yamaguchi etherification. So far, very few bile acid macrocyles have been successfully synthesized and well characterized.

2.2.1. Synthesis of cycloid (chenodeoxycholate)-dipentenoate conformational isomers by two Yamaguchi macrolactonization sequences and their characterizations.

The synthesis of cyclodimer **J** by Yamaguchi method is shown in Scheme 9. It is one pot, two steps reaction. The first step is targeted to cyclodimerize CDCA itself by adding CDCA, excess of 2,6-dichlorobenzoyl chloride, Et_3N, DMAP in THF and reacting for 12h at room temperature. And then 4-pentenoic acid is added into reaction mixture to esterify the 7α-hydroxyl group on preformed CDCA cyclodimer to give 7α-4-pentenoate substituted cyclodimer **J** with a 15% yield. Cyclodimer **J** is easily dissolved in acetone, ethyl acetate, or DCM. The compound **I** with two pentenoate groups at 3α- and 7α-positions was also obtained as a major product from this reaction.

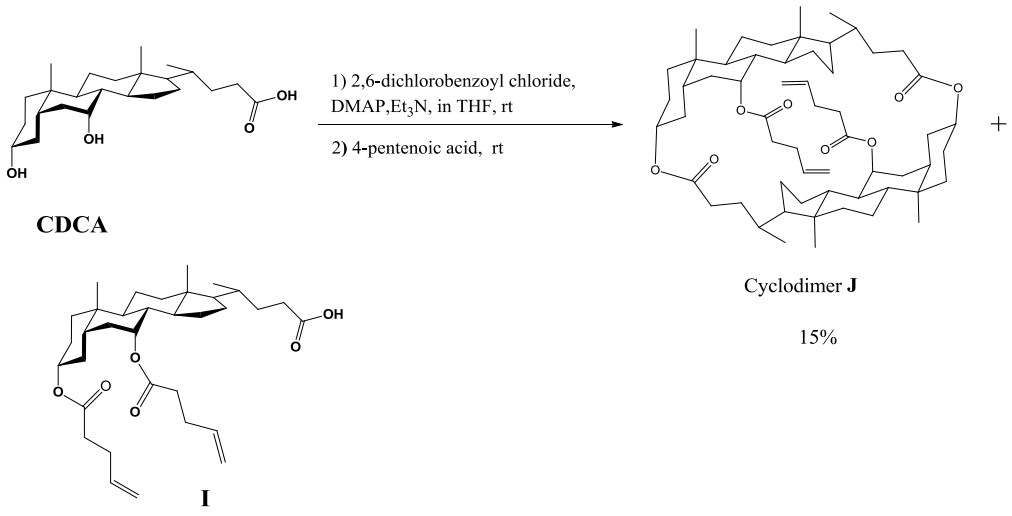

Scheme 9. The synthesis of cyclodimer **J** by Yamaguchi protocol.

In an alternative synthetic sequence designed to make CDCA based cyclodimer (Scheme 10). The 4-pentenoate group substituted CDCA (**H**) can be easily cyclized in an appreciable yield (60%) via stepwise adding the anhydride intermediate residue pre-formed by reacting 3 with 2, 6-dichlorobenzoyl chloride in the presence of Et_3N in THF into highly diluted DMAP in toluene solution under reflux. The resulting product was proved to be another conformational dipentenoate cyclodimer (cyclodimer **K**) by comparison of NMR spectra and mass spectroscopy with cyclodimer **J**.

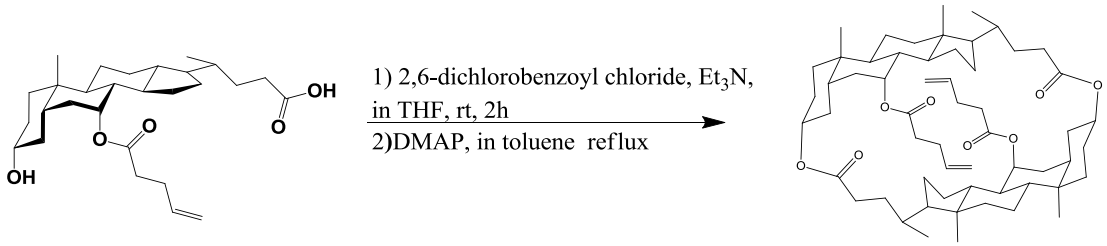

H

Cyclodimer **K**

60%

Scheme 10. The synthesis of cyclodimer **K** by classic Yamaguchi macrolactonization

The evidence obtained from NMR and mass spectroscopy indicates that two conformational isomers of di-pentenoate cyclodimer have been obtained. The FABMS showed ions at m/z 913.6 $(M+H)^+$ for both cylcodimer **J** and **K** in agreement with the calculated exact molecular mass of 912.65.

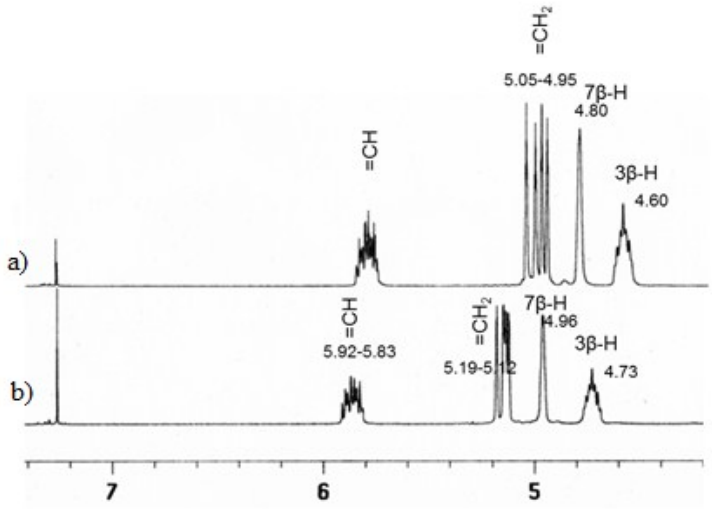

Figure 24.Comparison of partial ^{1}H NMR spectra of conformational isomers. a) cyclodimer **J** b) cyclodimer **K**.

Comparison of NMR spectra of cyclodimer **J** and **K** (Figure 24), it exhibited that the proton peaks of 7α-$OCOCH_2CH_2C\underline{H}=CH_2$, 7α-$OCOCH_2CH_2CH=C\underline{H}_2$, 7β-H and 3β-H on cyclodimer **J** down-shifted 0.06 ppm, 0.13ppm, 0.16 ppm, and 0.13 ppm, respectively, comparing with corresponding peaks on cyclodimer **K**.

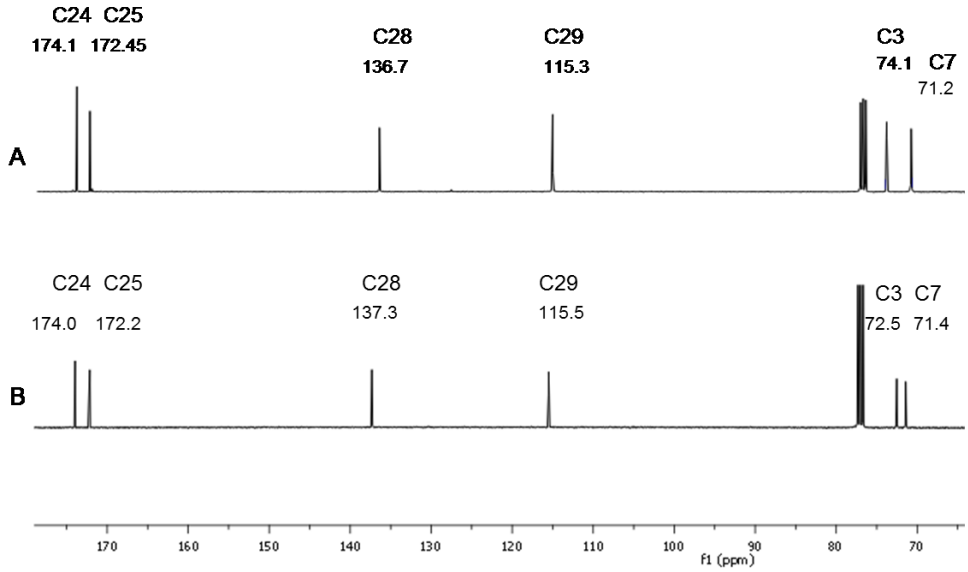

Figure 25.Comparison of partial ^{13}C NMR spectra of conformational isomers. A) cyclodimer **J** B) cyclodimer **K**

The chemical shift of C3 on cyclodimer **J** is 74.0 ppm and 72.5 ppm for cyclodimer **K**. These discrepancies indicate that there is significant conformational difference between the cyclodimer **J** and **K**. In addition, the evidences based on R_f value and solubility also give positive support for obtaining two conformational cyclodimers. The R_f value of cyclodimer **J** (0.33) is much higher than that of cyclodimer **K** (0.21) by applying 4:1 ratio of hexanes: ethyl acetate as the eluent. The cyclodimer **J** has

considerable solubility in acetone while cyclodimer **K** is completely insoluble. The existence of these two different conformers is probably the result of steric-hindrance which prevents the facile conformational conversion of one to the other.

The structure of cyclodimer **K** is also confirmed by single crystal X-ray diffraction. Cyclodimer crystallized in the space group of C 2 2 21. With 4-pentenoate side chain, the cyclodimer **K** exhibits the unusual conformation in its solid state structure: one of 4-pentenoate is inwardly directed to the cavity, while the other is excluded out as shown in Figure 26 and 27. Although a few examples of inward-pointing side chains in cyclodextrins and macrocyclic phenols have been reported in the past, [10] the solid state structure of cyclodimer **K** featured with inwardly directed side chain presented here is the first example in a cyclic steroid. It is believed that the curved α face of CDCA acts as a dock for accommodating one of the flexible 4-pentenoate chains while the other was excluded due to the limited space of the cavity and the hydrophobic interaction between two 4-pentenoate groups.

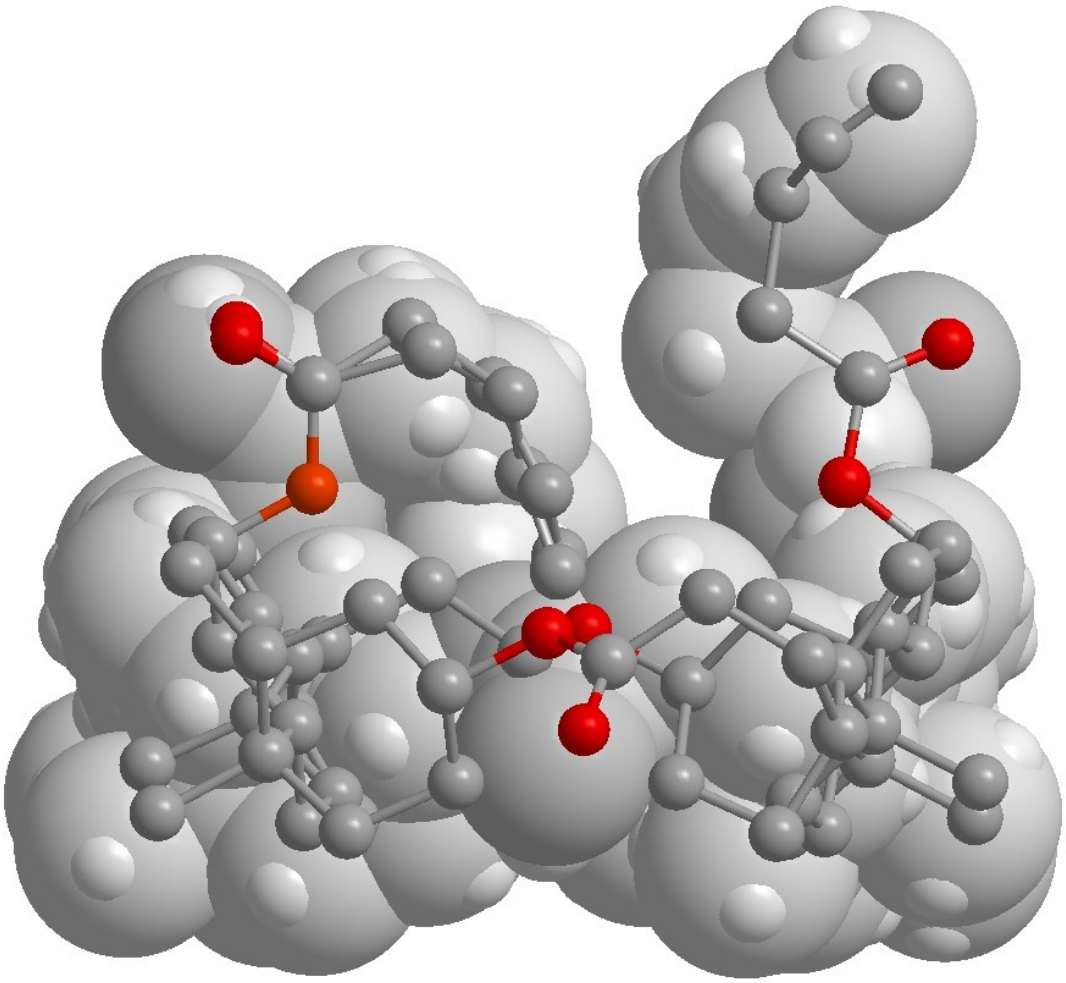

Figure 26. X-ray structure of cyclodimer **K**. Side view of molecular structure showing one of the pentenoates folded into the cavity and the other excluded out.

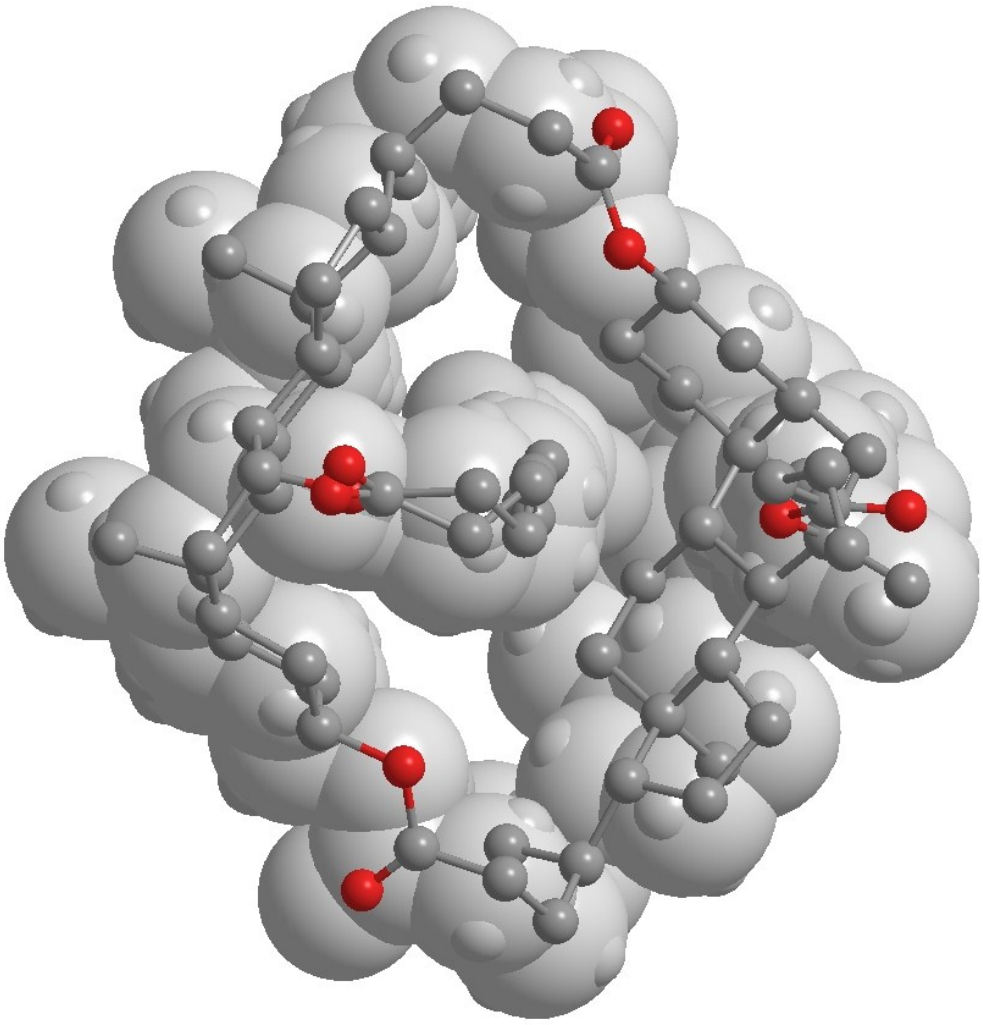

Figure 27. X-ray structure of cyclodimer **K**. Top view of molecular structure showing inwardly directed side chain pointing to the cavity.

In this crystal lattice, the two sites disorder model is applied for solving the inwardly directed side chain, but that there is a large amount of genuine thermal motion as well that causes the laterally elongated ellipsoids. In many respects, the inwardly-directed side chain is just a proxy for more solvent that would otherwise occupy this void in the crystal. As for the solvent, there appears also to be ocupational

disorder; that is, a given site is occupied by two different molecules. In this case, some of the solvent sites contain chloroform, and others contain acetone, but the overall electron density measured by the diffraction experiment is the sum of both. Although the solvent molecules are disordered in the crystal lattice, the halogen bonding interaction between the two chlorine atoms on the solvent molecule and oxygens on two cyclodimers is observed. The distance between C-Cl (1)⋯⋯O5 is 2.89 Å. Another one betwwen C-Cl (3)⋯⋯O3* is 2.90 Å. There are eight bowl-shaped cyclodimers inside each crystal cell and the space inside each cavity partially occupied by a pentenoate ester is larger than the space outside the cavity (Figure 28 a). The cyclodimer **K** molecules assembled head to tail into supermolecular nanotubular motif along c axis (Figure 28 c). The big voids between the two adjacent nanotubes in the same layer are filled by another layer of identical nanotube network and therefore stabilize the crystal pattern. Overall, the adjacent nanotube motif layers are oriented in opposite direction and mutually interpenetrated and interlocked to form a 2-fold interpenetrating 3-D network (Figure 28 b).

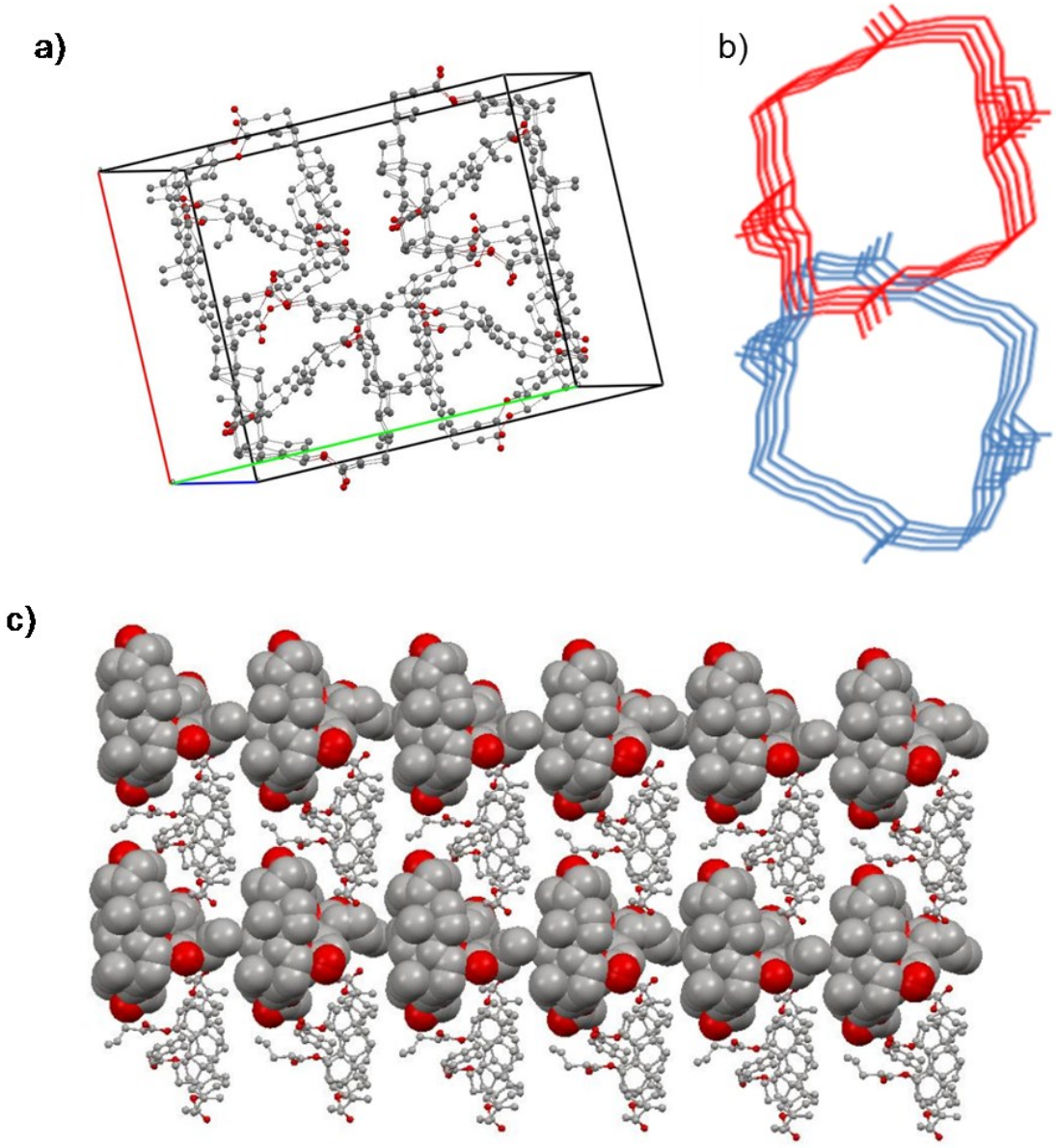

Figure.28 a) Unit cell packing of the cyclodimer **K** along c axis. Solvent are omitted for clarity **b**) Schematic view of the 2-fold interpenetrating framework of the cyclodimer **K** from top view. **c**) The extended packing of cyclodimer structure assembled into naotubes along c axis. Solvents are omitted for clarity.

As shown in Figure 26-28, the conformation isomer **K** has been achieved by X-ray crystallography. In the crystal structure of the cyclodimer **K**, both bile acid units are conformationally oriented α-face to α-face, by this way, which maximizes the cavity size. For evaluating the structure of the other cyclodimer **J**, A molecular structure simulation of MMFF 94 and MM2 minimization were used. The simulated 3-D structure of cyclodimer **J** is shown in Figure 29. In this case, it featured the α-face to β-face orientation in the inner cavity of cyclodimer ring instead of the α-face to α-face conformation described from the crystal structure of cyclodimer **K**. Therefore, this connection leads to one of 4-pentenoate groups being on the upper rim and the other being on the lower rim cyclodimer plane in opposing direction, but for cyclodimer **K**, both 4-pentenoate groups are on the upper rim (same side) of cyclodimer ring. These two

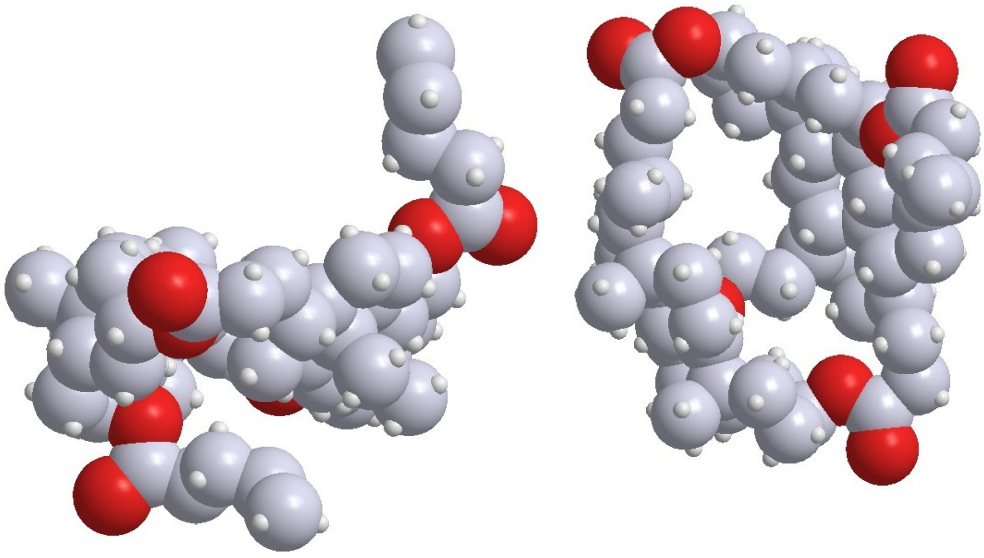

Figure 29. The simulated structure of cyclodimer **J** . Side view (left) and top view (right)

different conformers are sterically prevented from interconverting from one to the other. In addition, the grubb's coupling of two 4-pentenoates of cyclodimer **J** failed to give intramolecular metathesis product which indicates two 4-pentenoate groups are not on the same side of cyclodimer ring. This agrees with the MM2 and MMFF 94 simulation result. Why the two different reaction conditions lead to different conformers of the cyclodimers remains an open question.

2.2.2. Synthesis and characterization of cyclotri (chenodeoxycholate)-tripentenoate (L) and cyclotetra (chenodeoxycholate)-tetrapentenoate(M).

The synthesis of cyclotrimer **L** (Scheme 11) was achieved via modified Yamaguchi macrolactonization method by reflux of 7α-4-petenoate substituted CDCA **H**, 2,6-dichlorobenzoyl chloride and DMAP in toluene for 24 hr. This reaction gives only cyclotrimer **L** as the product with rather low yield (5-10%) and leaves large amount of starting material **H** unreacted in the reaction mixture.

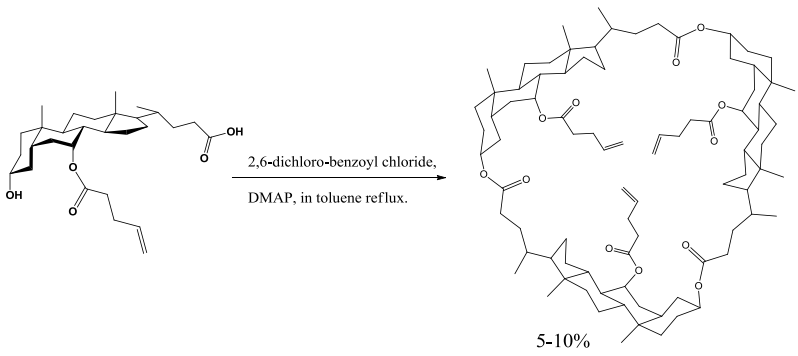

Scheme 11. The synthesis of cyclotri (chenodeoxycholate)-tripentenoate (cyclotrimer **L**) from **H**.

The cyclotetramer **M** was synthesized by following the same method as the synthesis of cyclodimer **K** but with a relatively high 7α-4-petenoate substituted CDCA concentration. For this method, highly diluted bile acid solution favors the formation of small ring, while less diluted bile acid solution tends to form large ring and even various linear oliogomers. For synthesis of cyclotetramer **M**, the anhydride intermediate residue formed by reacting **H** with 2, 6-dichlorobenzoyl chloride in the presence of Et_3N in THF was added into DMAP toluene solution directly and reflux for 24h, which gives cyclotetramer **M** as the major product, accompanied by small amount of cyclodimer **K**, cyclotrimer **L** and some amount of linear oligomers. The cyclotetramer **M** crystallized in 1:1 hexanes/EtOAC solution as rectangle shaped single crystals, however, the crystal structure of cyclotetramer **M** can't be fully resolved due to the complexity of cyclotetramer **M** with a large cavity. The crystals are like jello in which the four flexible side chains are extremely disorder and the solvent is all over the place.

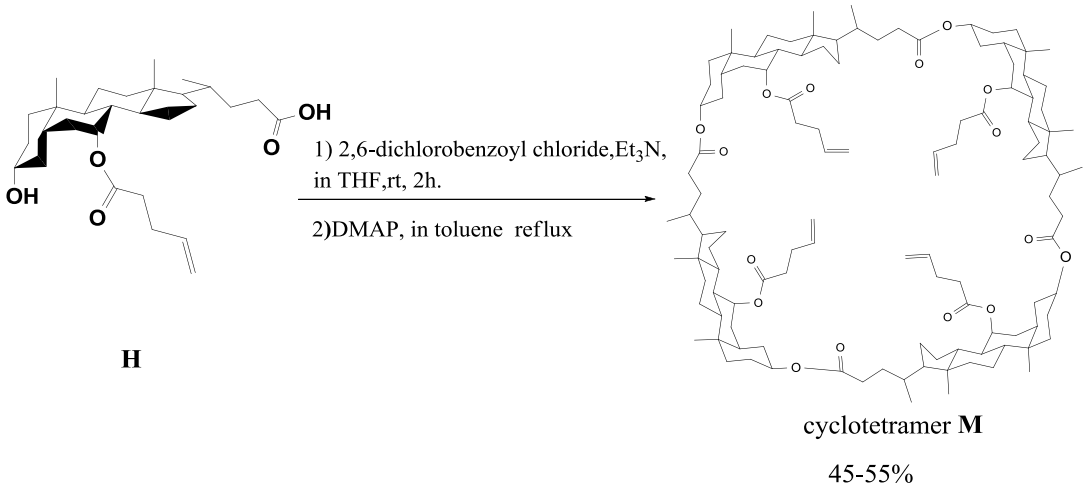

Scheme 12. The synthesis of cyclotetramer **M.**

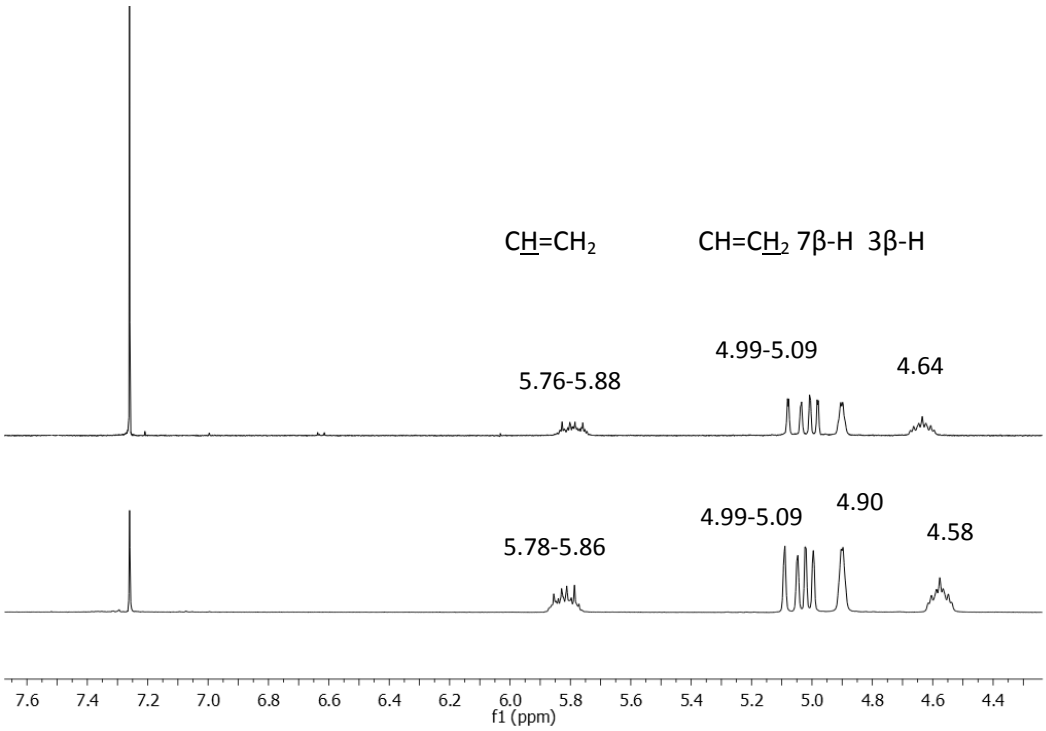

Figure 30. Partial ^{1}H NMR spectra of cyclotrimer **L** (top) and cyclotetramer **M** (bottom).

The proton NMR spectra of the cyclotrimer **L** and cyclotetramer **M** are shown in Figure 30. Basically, there is no difference on proton NMR spectra for these two cyclomers. The FAB MS showed ions at m/z 1370.00 $(M+H)^+$ for cyclotrimer **L**, 1369.98 for the calculated exact molar mass $(M+H)^+$. For the cyclotetramer **M**, the HRFAB MS showed ions at m/z 1848.2915 $(M+Na)^+$, the calculated one is 1848.2856, the discrepancy is 3.2 ppm. The isotopic intensity peaks are: $(M+Na)^+$ at 1848.2915 (79.7%), 1849.3003 (100%), 1850.3087 (62.2 %), 1851.3027 (25.6 %), 1852.3038 (7.8 %). The calculated intensities are 1849.2890 (100.0%), 1848.2856 (79.7%), 1850.2923 (62.2%), 1851.2957 (25.6%), 1852.2990 (7.8%).

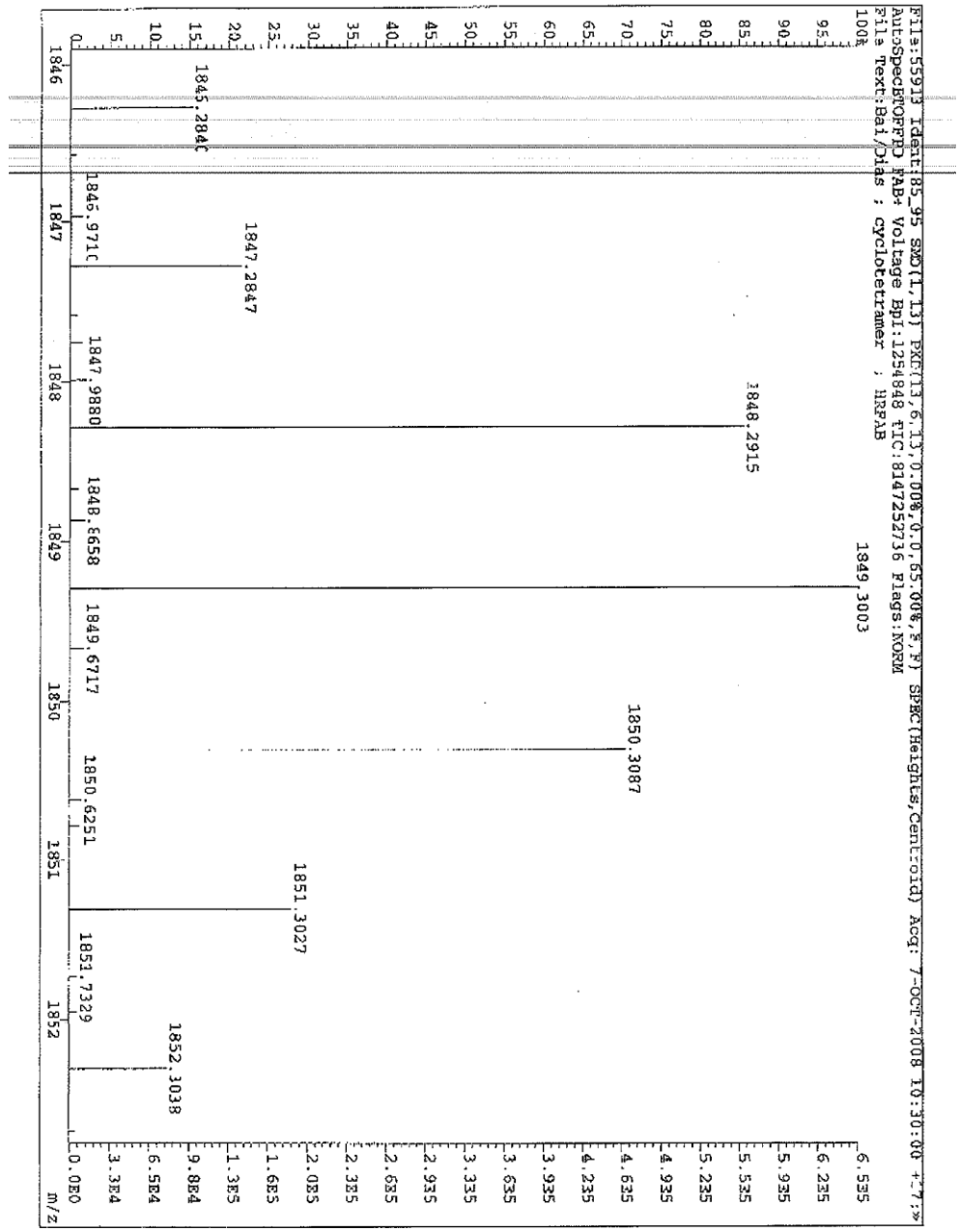

Figure 31. HRFAB mass spectrum of cyclotetramer **M**.

2.3. Ruthenium-catalyzed metathesis reaction of bridged 7*α*-4-pentenoate substituted CDCA based macrocycles.

Ruthenium catalyst has been useful to synthesize various alkene related organic compounds and polymers via Grubb's reaction. Ruthenium-catalyzed olefin metathesis includes intramolecular metathesis such as ring closure between two terminal vinyl groups, intermolecular metathesis between two alkene molecules and ring opening metathesis of strained alkenes to give polymers.[32] The most successful and versatile catalysts for olefin metathesis are 1st and 2nd generation Grubb's catalysts which tolerate a variety of functional groups. Especially 2nd generation catalyst has a higher activity and been more stable than the 1st generation catalyst. [33] The Grubb's reaction normally gives the products as *cis*/*trans* isomeric mixture. For ring closing metathesis, the formation of *cis*-double bond is favored with small membered rings like six or eight membered rings due to the significant ring strain, while the formation of trans-double bond becomes possible with larger rings. Numerous novel organic compounds has been synthesized via the formation of carbon-carbon double bond by RCM, however, the synthesis of alkylidene bridged macrocycles using RCM is rare, particularly, the construction of novel cage-type, alkylidene bridged bile acid macrocycles has never been reported. With defined cavity, this type of organic compounds is capable of encapsulating organic molecules in use as drug delivery system.

2.3.1. The synthesis and characterization of chenodeoxycholic acid (CDCA) based bridged cyclodimers by olefin metathesis.

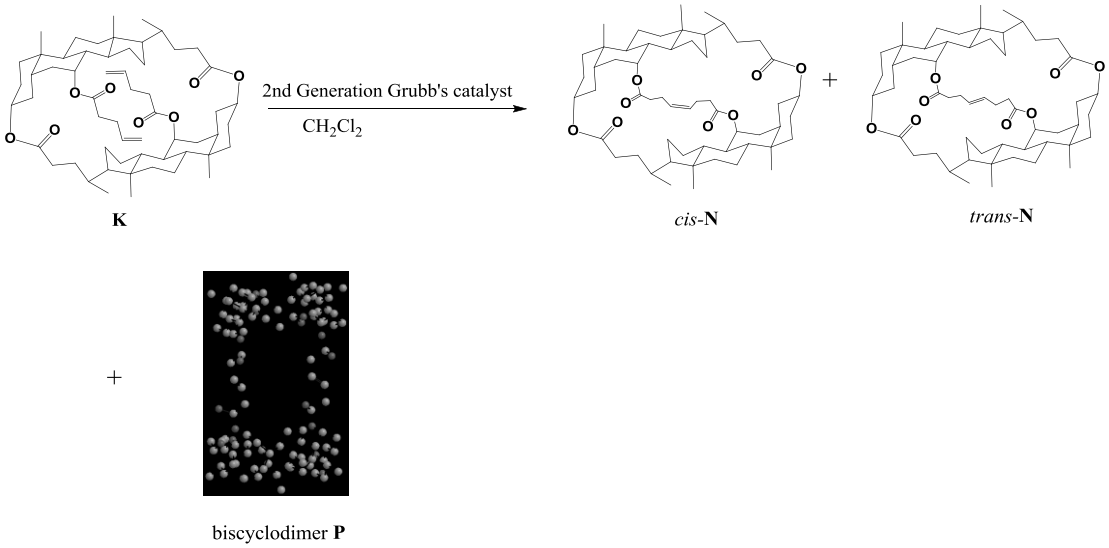

Scheme 13. The synthesis of bridged cyclodimer *cis*-**N** and *trans*-**N**.

We intended to synthesize a cylindrical like super molecule (biscyclodimer **P**) with a structure shown in Scheme 13 by coupling terminal vinyl groups of two 4-pentenoates between a pair of cyclodimer **K** by intermolecular metathesis. The expected product biscyclodimer **P** featured with a hollow cylinder structure could be an ideal candidate for encapsulating organic molecules, therefore, which has the potential application for biomedical studies. For example, this type of molecules could be an ideal candidate for drug delivery system. It is also a very interesting structure as a reactive site to

encapsulate, insulate and stabilize the reaction intermediate for characterization. The Grubb's reaction was carried out in (0.2M) CH_2Cl_2 solutions with 2% of 2nd generation grubb's catalyst for 24 h followed by literature method [12]. However, it gives the major intramolecular products *cis*-**N** and *trans*-**N** by coupling two terminal alkenes of 4-pentenoate groups on a single molecule of cyclodimer **K**. In addition, the trace presence of an intermolecular metathesis product (a bis-cyclodimer) was evident in the HRFAB mass spectrum. The precise mass observed was 1771.2489, in excellent agreement with that calculated for the bis-cyclodimer, 1771.2514 ($C_{112}H_{170}O_{16}$).

Although having very close R_f value, the *cis* and *trans* isomers were separated by ordinary column chromatography. After passing through a flash column, the crude product, a mixture of *cis* and *trans* isomers in 90% total yield, was obtained. A 3:1 ratio of the *cis* and *trans* isomers was determined by integration of the two triplets at δ 5.61 and δ 5.55 in its ^{1}H NMR spectrum (Figure 32b). The *cis* and *trans* isomers were then separated on a second column. Both isomers were obtained in pure form and were characterized by ^{1}H NMR, ^{13}C NMR and HRMS. Large prisms of cis-5 were obtained by slow evaporation of a CH2Cl2-acetone solution and proved suitable for X-ray analysis. In addition, the trace presence of an intermolecular metathesis product (a bis-cyclodimer) was evident in the HRFAB mass spectrum. The precise mass observed was 1771.2489, in excellent agreement with that calculated for the bis-cyclodimer, 1771.2514 ($C_{112}H_{170}O_{16}$).Since 3:1 *cis-trans* ratio was observed, which indicated the formation of

cis-**N** is favored than *trans*-**N** with medium length 4-pentenoate groups on cyclodimer **K**. No matter what reaction condition has been adjusted, the intermolecular metathesis product is not favored. Although the two 7α-4-pentenoates group with medium length are not only in nonadjacent positions but also far separated by cyclodimer ring which seems to favor the formation of intermolecular metathesis product. Probably, the bulky steroid ring shields alkenyl groups and causes great steric hindrance for intermolecular metathesis reaction.

As illustrated in Figure 31 a) and b) for convertion of cyclodimer **K** to cis-**N** and trans-**N** in ^{1}H NMR spectra, the olefin resonances of protons for cyclodimer **K** at 5.92-5.82 ppm (multiplet) and 5.18, 5.15, 5.14 and 5.13 ppm (quartet) had been replaced by two triplet olefin resonated at 5.61 and 5.54 ppm. By comparison of ^{1}H and ^{13}C NMR spectra of cyclodimer **K** with *cis*-**N** and *tran*-**N** isomers, the chemical shifts for all corresponding protons and carbons on *cis*-**N** and *trans*-**N** are different. It indicated that the shielding and deshielding effects of cis/trans double bond extends to the whole cyclodimer ring. For instances, the protons of double bond for *cis*-**N** have an triplet olefin resonance at δ 5.61, about 0.06 ppm downfield from the olefin resonance of *trans*-**N** (δ 5.55).While the chemical shifts of 7β-H and 3β-H are 5.00, 4.61 for *trans*-**N**, 4.97, 4.70 for *cis*-**N** and 4.97,4.73 ppm for cyclodimer-**K** respectively. In addition, there is siginificant chemical difference for C17 which is 58.68 ppm for *trans*-**N** and 54.07 ppm

for *cis*-**N**, about 6 ppm and 1.5 ppm downfield from the cyclodimer-**K** (δ 52.66 ppm) respectively.

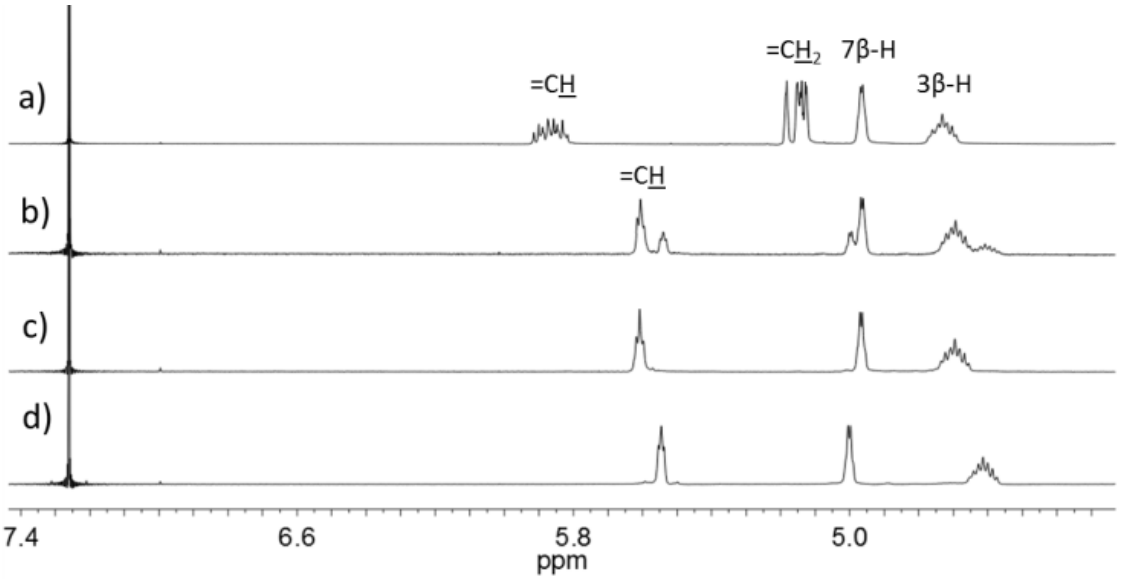

Figure 32. a) Partial ^{1}H NMR of cyclodimer **K.** b) Partial ^{1}H NMR of 3:1 ratio of *cis*-**N** to *trans*-**N** mixture. c) Partial ^{1}H NMR of *cis*-**N**. d) Partial ^{1}H NMR of *trans*-**N**.

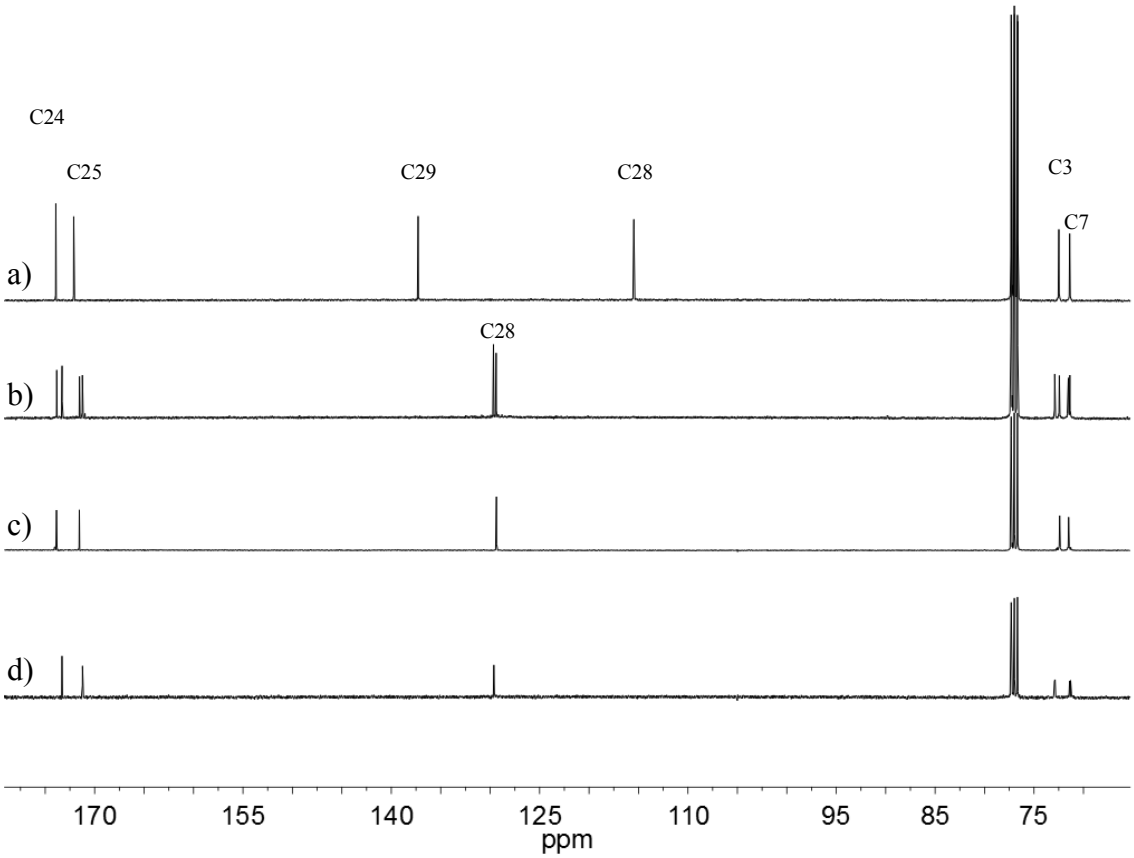

Figure 33 a) Partial ^{13}C NMR of cyclodimer **K.** b) Partial ^{13}C NMR of 3:1 ratio of *cis*-**N** to *trans*-**N** mixture. c) Partial ^{13}C NMR of *cis*-**N**. d) Partial ^{13}C NMR of *trans*-**N**.

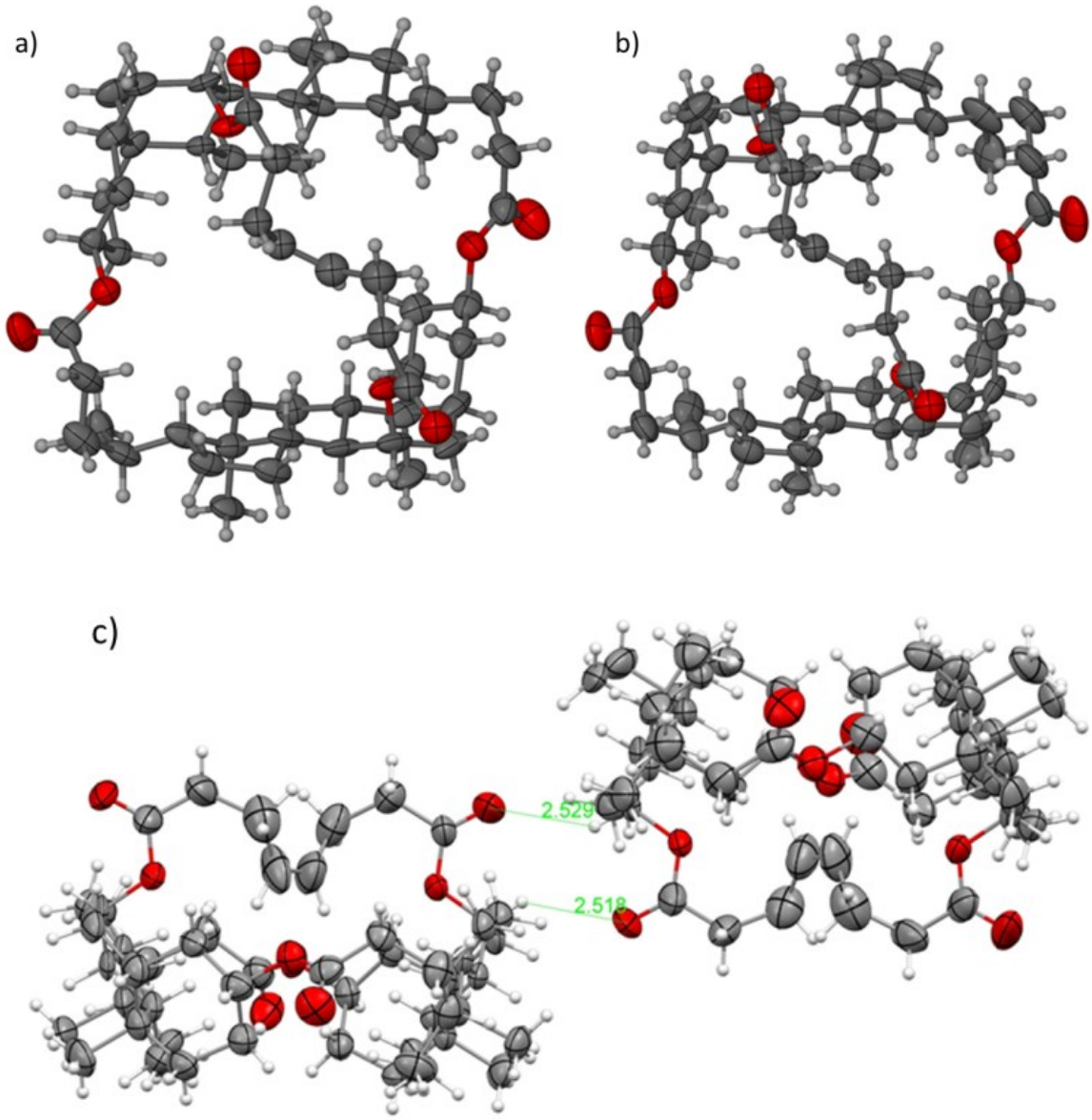

Figure 34. X-ray structure of cyclodimer *cis*-**N**. a) Independent molecule A. b) Independent molecule B. c) View of two independent molecules facing up and down in the crystal structure. Dashed line shows the tight C-H---O contacts between two independent molecules which possibly direct the packing. Thermal ellipsoids have been drawn at the 50% level.

The molecular structure of *cis*-**N** as revealed by X-ray crystallography is shown in Figure 34. Compound *cis*-**N** crystallized in the space group *P*1. The included solvent molecules in this structure were severely disordered and were removed by the SQUEEZE/BYPASS procedure.[10] The structure contains two independent molecules of *cis*-**N** orientated facing in opposite directions in the crystal. The two independent molecules I and II make tight interactions with themselves. For instance, the molecule I composed of subunits A and B contacts its symmetry generated self, the other molecule composed of C and D plays in the same way and forms wrinkled layers composed of only AB molecules or CD molecules. The solvent resides in the spaces between the layers. In the crystal structure, all the carbonyl O atoms have fairly tight contacts.

Two types of short contacts are observed. Short contacts between two independent molecules [d(C(25)=O(3)---H(7β)-C) = 2.529 Å and 2.518 Å, as shown in Figure 34c, and d(H(27)---O(4)=C(23)) = 2.513 Å and 2.717 Å] seem to direct the crystal packing. The flexible oct-4-enedioate side chains form an "m"-shaped linkage connecting two 7α-positions of the steroid skeleton. Additionally, the *cis* double bond on the oct-4-enedioate chain adopts the "in conformation" being oriented toward the ring centroid to fill the voids of the cavity. The shortest distances from the two hydrogen atoms on the *cis* double bond to hydrogen atoms on cyclodimer upper rim are 2.563 Å and 2.631 Å, indicating that *cis*-**N** has a sterically crowded conformation. It also suggests that the flexible oct-4-enedioate chain must be stretched away from the cavity in order to form a *trans* C=C double bond to avoid steric hindrance from the upper rim of cyclodimer ring. In contrast

to the X-ray structure of cyclodimer **N** , with the *cis*-C=C as the linker, a halve of flexible chain on *cis*-**N** still keep the same conformation as the 'toward-in' pentenoate group of cyclodimer **N** except the ending $=CH_2$ is removed, while the other halve is also pointing toward to the cyclodimer ring instead of directing away the cavity after coupling reaction.

A molecular structure simulation (MM2) shows that *cis* and *trans* isomers of **N** have essentially the same energy. The *cis* geometry is not thermodynamically favored; however, the bridge of *cis*-**N** in its crystal structure resembles the inwardly directed side chain of the precursor compound **K**. Furthermore, the chemical shifts observed in the ^{1}H and ^{13}C NMR spectra for *cis*-**N**, for example, the chemical shifts of 3β-H, 7β-H and C17, are much closer to the corresponding chemical shifts of cyclodimer **K** than those of *trans*-**K**. This suggests a lower energy for the transition state when forming the cis conformation; therefore, *cis*-**N** is a kinetic product.The *cis*-**N**, with well defined cavity size of 5.5 x 4.4 x 4.0 in dimention, is suggested to be an ideal candidate for CH_4 and CO_2 gas adsorption.

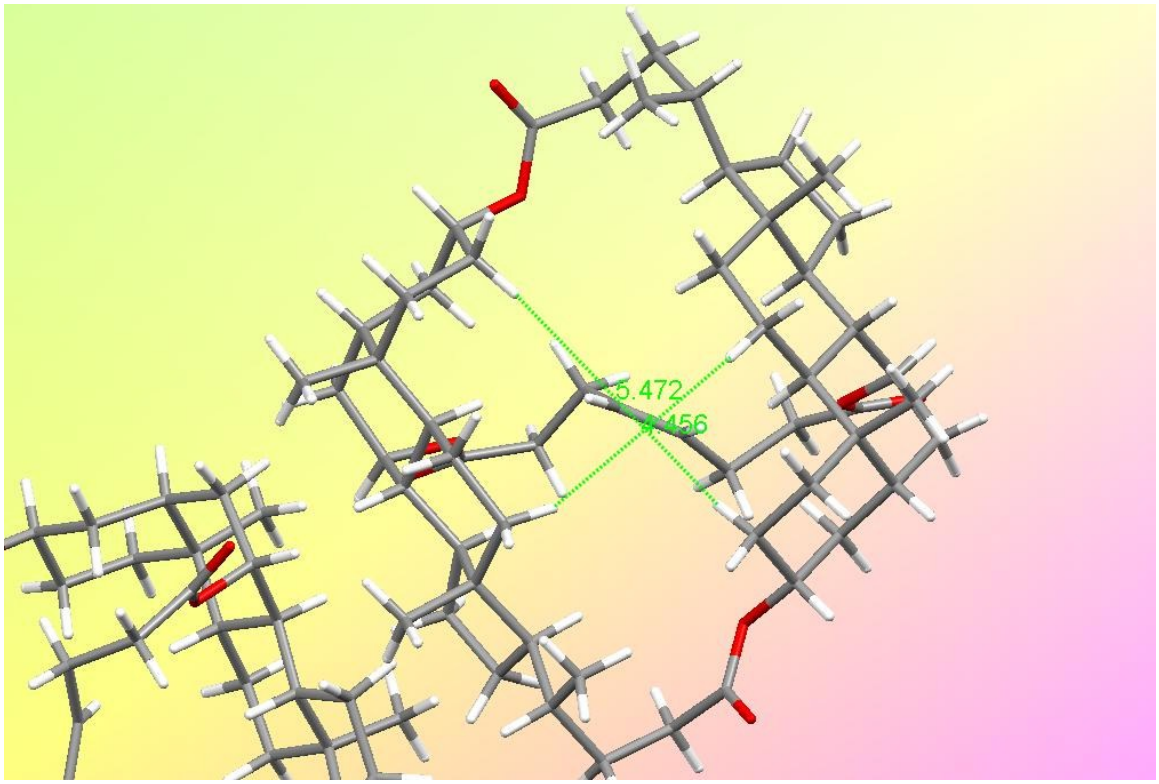

Figure 35. The crystal strucutre of *cis*-**N** with a lower rim cavity size of 5.5 Å in length, 4.4 Å in length and appromixately 4.0 Å in depth from the double bond to the plane of lower rim.

2.3.2 The synthesis and characterization of chenodeoxycholic acid (CDCA) based bridged cyclotetramers by intramolecular metathesis.

By treatment of cyclotetramer **M** with 2nd generation Grubb's catalyst in CH_2Cl_2 for 24 h, the double bridged cyclotetramers were achieved and shown in scheme 14. The TLC plate showed that these two isomeric compounds have very close R_f value in 4: 1 ratio of hexanes to ethyl acetate eluent. The resulted products are inseparable *cis*-**O** and *trans*-**O** isomeric mixture which were indicated by ^1H and ^{13}C NMR and mass spectroscopy.

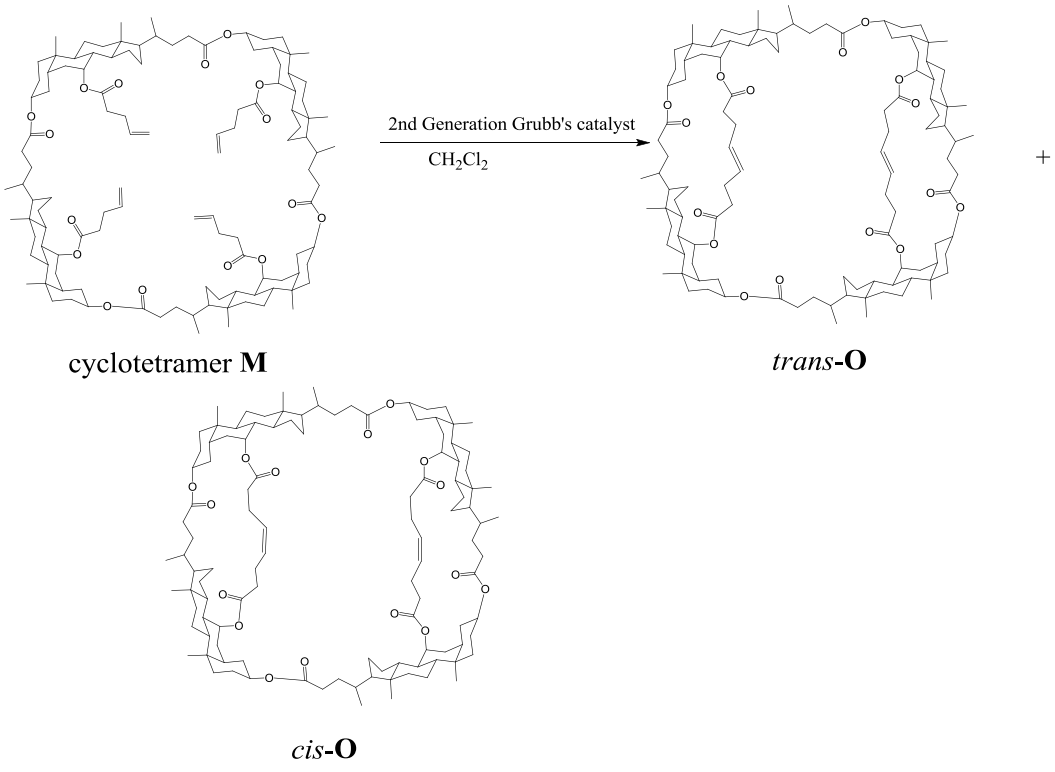

cyclotetramer **M**

trans-**O**

cis-**O**

Scheme 14. The synthesis of bridged cyclotetramer *cis*-**O** and *trans*-**O**.

The *cis*/*trans* isomers of compound **O**, with two flexible oct-4-enedioates crossed over the cyclotetramer ring, is predicted to be a double handle basket shaped structure. In addition, the head-capped cyclotetramer **O** with a defined large inner cavity could be an ideal biocompatible drug delivery system with the capability of storing and releasing hydrophobic drug molecules.

3. CONCLUSION

A novel method has developed to attach allyloxycarbonyloxy group to 7α position of chenodeoxycholic acid with an ambient CO_2 inserted between the 7α-O^- and ally group. A reaction mechanism was proposed, that sterically hindered 7α-O^- is favored to react with small and acidic CO_2 to form a more extended carbonate anion (7α-$OCOO^-$), which can react with allyl group. This route offers a pathway to make ^{14}C-labeled bile acid derivatives, which could be used to explore the transport mechanism of hASBT through labeling with $^{14}CO_2$. In addition, we have demonstrated that the bowl-shaped bile acid based cyclodimers (**J** & **K**), cyclotrimer (**H**) and cyclotetramer(**M**) can be selectively synthesized from 7α-4-pentenoate functionalized chenodeoxycholic acid in good yield and with high purity by using Yamaguchi macrolactonization method. The cage compounds *cis*-**N**, *trans*-**N**, *cis*-**O** and *trans*-**O** have been successfully synthesized by the subsequent closure of these macrocycles by fusion of the terminal vinyl groups on their two side chains of compound **K** and **M** respectively via Grubbs' olefin

metathesis. The structures of these chenodeoxycholic acid derivatives have been confirmed by ^{1}H and ^{13}C NMR, HRMS and X-ray crystallography.

4. EXPERIMENTAL

4.1 General methods

^{1}H NMR and ^{13}C NMR spectra were recorded at Varian 400 MHz and 100 MHz, respectively. The HRFAB and LRFAB Mass spectroscopy was performed at University of Nebraska-Lincoln Mass Spectrometry center. The high resolution ESI-MS was performed in chemistry department of University of Kansas. The single X-ray crystal analysis was performed by Bruker SMART 1K CCD area detector system in University of Missouri-Columbia. Reagent grade tetrahydrofuran (THF) was distilled from sodium potassium alloy. Triethylamine (Et_3N) was distilled from CaH_2 under N_2 atmosphere. Toluene was distilled from P_4O_{10}. Column chromatography was performed on silica gel (MERCK C60).

4.2 Experiment Procedures

Methyl 3α-(ethoxycarbonyloxy)-7α-(hydroxyl)-5β-cholanoate (**A**): Methyl cholanoic acid (0.8 g, 1.92 mmol) was treated by ethyl chloroformate (0.94 mL) in pyridine (3 mL) at -20 ˚C for 30 min, then the reaction mixture was poured into ice and extracted with EtOAc, dried with Na_2SO_4. The crude product was purified by flash column and dried in vacuum oven to afford **A**. 1H NMR in CDCl3 (400 Hz), δ 0.59 (s, 3H, 18-CH_3), 0.86 (d, 3H, 21-CH_3), 0.89 (s, 3H, 19-CH_3), 3.63 (s,3H, 24-OCH_3), 4.13 (q, J = 8 Hz, 3α-$OCOOCH_2CH_3$), 1.26 (t, J = 8Hz, 3α-$OCOOCH_2CH_3$), 3.75 (s, 7α-H), 4.41 (m, 3α-H); 13C NMR δ 11.9 (C18), 14.0 (3α-$OCOOCH_2CH_3$), 17.9 (C19), 20.2, 22.4, 23.3, 26.3,

27.8, 30.6, 32.4, 34.2, 34.6, 35.0, 39.1, 39.3, 40.9, 51.1 (24-OCH_3), 50.0 (C14), 55.4 (C17), 42.3 (C13), 40.9 (C5), 63.1 (3α-$OCOOCH_2CH_3$), 67.69 (C7), 77.8 (C3), 154.4 (3α-$OCOOCH_2CH_3$), 174.3 (C24).

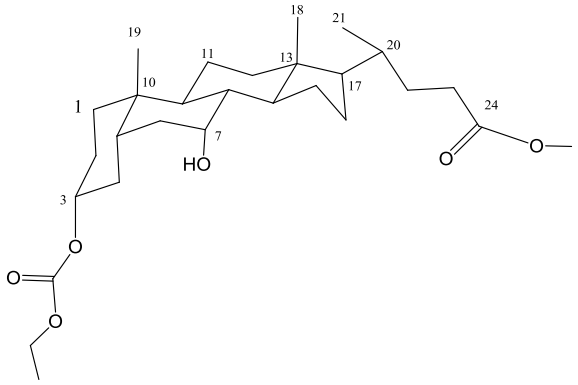

Figure 1. The labeling of compound **A.**

3α-(ethoxycarbonyloxy)-7α-(trimethylsilyl)-5β-cholanoate (**B**): A soln of 3 (1.00 g, 2.1 mmol) in THF (4 mL) was treated with TMCS (0.27 g, 2.5 mmol) and imidazole (0.36 g, 5 mmol). After the soln was stirred at rt for 24 h, and then poured into ice water, extracted with EtOAc, dried over anhydrous Na_2SO_4, the solvent evaporated by rotary vaporization. The pure product was obtained by a flash column. ^{1}H NMR δ 0.05 (s, 0.05 , 7α-SiH_3), 0.59 (s, 3H, 18-CH_3), 0.86 (s, 3H, 19-CH_3), 0.883 (d, *J* =3.2 Hz , 3H, 21-CH_3), 3.63 (s, 3H, 24-OCH_3), 3.75 (s, 1H, 7α-H), 4.11 (q, J = 8Hz , 2H, 3α-$OCOOCH_2CH_3$), 4.30-4.42 (m, 1H, 3α-H). 13C NMR, 0.62 (7α-OSi($\underline{C}H_3)_3$), 11.9 (C18), 14.3 (3α-$OCOOCH_2\underline{C}H_3$), 18.3 (C21), 20.5(C11), 22.6(C19), 23.7(C15), 26.6(C2), 28.0(C6), 31.0(C22), 32.4(C20), 34.8(C9), 35.0(C10), 35.2(C1), 35.4(C4), 39.5(C8), 40.0(C12),

41.5(C5), 42.3(C13), 50.0 (C14), 51.4 (C24OO$\underline{C}H_3$), 55.6 (C17), 63.4 (3α-OCOO$\underline{C}H_2CH_3$), 69.2 (C7), 78.3 (C3), 154.7 (3α-O$\underline{C}OOCH_2CH_3$),174.7 (C24).

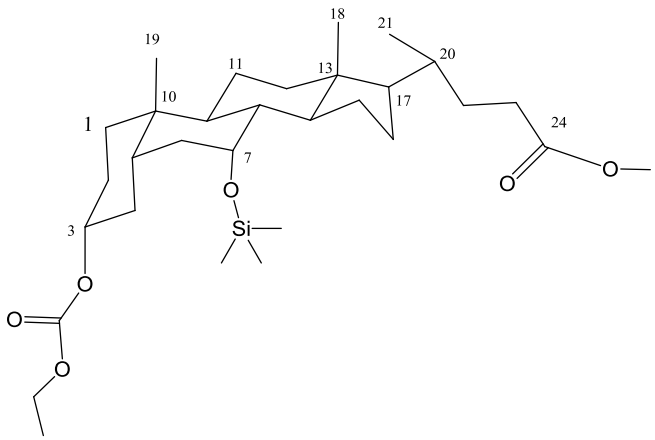

Figure 2. The labeling of compound **B**.

Methyl 3α-(ethoxycarbonyloxy)-7α-(allyloxycarbonyloxy)-5β-cholanoate (**C**): To solution of **B (**1.0 g, 1.8 mmol**)** in anhydrous THF (4 ml), anhydrous TBAF (0.60 g, 2.3 mmol) was added. The solution was stirred for 24 h at rt, and then treated with freshly distilled allyl bromide (1.2 g, 9.2 mmol) for another 10 h, the reaction mixture was diluted with ice water and extracted by EtOAC. The organic layer was dried over anhydrous Na_2SO_4. The solvent evaporated by rotary evaporation. The crude product was purified by column chromatography to give **C** with 30% yield.^{1}H NMR δ 0.60 (s, 3H, 18-C$\underline{H}_3$), 0.871 (d, *J* = 3.2 Hz, 3H, 21-C$\underline{H}_3$), 0.89 (s, 1H, 19-CH_2), 3.62 (s, 3H, 24-C-OCH_3), 4.12 (q, *J* = 8Hz, 2H, 3α-OCOOC$\underline{H}_2CH_3$), 4.35-4.42 (m, 1H, 3α-H), 4.571 (d, *J*=

9.6 Hz, 2H, 7α-OCOOC$\underline{H}_2$CH=CH_2), 4.68 (s, 1H, 7α-H), 5.19-5.32 (m, 2H, 7α-OCOOCH_2CH=C$\underline{H}_2$), 5.84-5.94 (m, 1H, 7α-OCOOCH_2C$\underline{H}$=CH_2), ^{13}C NMR, 11.6 (C18), 14.2 (3α-OCOOC$H_2\underline{C}H_3$), 18.2 (C21), 20.53(C11), 23.5(C19), 26.58(C2), 27.94(C6), 30.84(C22), 30.87(C23), 31.1(C16), 33.7(C20), 34.2(C9), 34.65(C10), 34.70(C1), 35.2(C4), 38.0(C8), 39.2(C12), 40.7(C5), 42.6(C13), 49.9 (C14), 51.4 (24-O$\underline{C}H_3$), 55.4 (C17), 63.5 (3α-OCOO$\underline{C}H_2CH_3$), 67.9 (7α-OCOO$\underline{C}H_2$CH=CH_2), 75.5 (C_7), 77.8 (C_3), 118.2 (7α-OCOOCH_2CH=$\underline{C}H_2$), 131.9 (7α-OCOOC$H_2\underline{C}$H=CH_2), 154.55 (3α-O$\underline{C}$OOCH_2CH_3), 154.62 (7α-O$\underline{C}$OOCH_2CH=CH_2), 174.6 (C24). HRFABMS calcd for $C_{32}H_{51}O_8$ (MH^+): 562.35, found 563.3592.

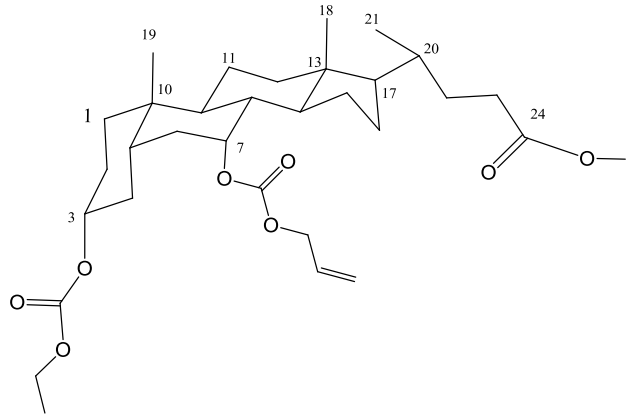

Figure 3. The labeling of compound **C**.

Allyl 3α-(ethoxycarbonyloxy)-7α-hydroxy-5β-cholanoate (**E**): To solution of **B** (1.0g, 1.8 mmol) in anhydrous THF(5 mL), anhydrous TBAF (0.6g, 2.3 mmol) was added. The solution was stirred for 1 h at rt to deprotect the silyl group, and then treated by NaH (0.08g, 3.6mmol) and freshly distilled allyl bromide (0.6g, 4.6 mmol) for 24 h, the reaction mixture was poured into ice water and extracted by EtOAC. The organic layer

was dried by anhydrous Na_2SO_4. The crude product was purified by column chromatography to give **E** with 50% yield. ^{1}H NMR in $CDCl_3$ (400 MHz), δ 0.65(s, 3H, 18-CH_3), 0.91(d, *J* = 3.2 Hz, 3H, 21-CH_3), 0.93(s, 3H, 19-CH_3), 3.83(s, 1H, 7β-H), 4.14(q, *J* = 8Hz, 2H, 3α-OCOOC$\underline{H}_2CH_3$), 4.55(d, 2H, 25-CH_2),4.42(m, 1H, 3β-H)5.21-5.33(m, 2H, 27-CH_2), 5.90(m, 1H, 26-CH). ^{13}C NMR in $CDCl_3$ (100 MHZ) 173.90(C24), 154.67(3α-O$\underline{C}$OOCH_2CH_3), 132.28(C26), 118.28(C27), 78.06(C3), 68.32(C7), 64.94(C25), 63.48(3α-OCOO$\underline{C}H_2CH_3$), 55.68(C17), 50.35(C14), 42.65(C13), 41.13(C5), 39.55(C12), 39.36(C8), 35.29(C4),35.13(C1), 35.00(C10),34.87(C9), 32.70(C16), 31.12(C23),30.89(C22), 28.10(C6), 26.61(C2), 23.66(C15), 22.64(C19), 20.52(C11), 18.17(C21), 14.26(3α-OCOOC$H_2\underline{C}H_3$), 11.74(C18).

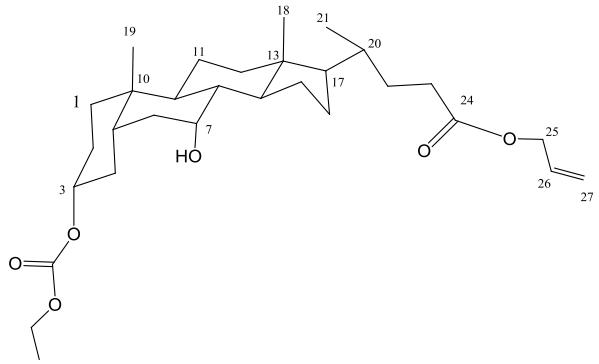

Figure 4. The labeling of compound **E.**

Methyl 3α-ethoxycarbonyloxy-7α-(4-pentenoyloxy)-5β-cholanoate (**F**): Et_3N (2 mL) was added to a mixture of 4-pentenoic acid (0.25 g, 2.5 mmol) and 2,6-dichlorobenzoyl chloride (0.525 g, 2.5 mmol) in THF for 1 h, then compound **A** (1.00 g, 2.09 mmol) and 5% DMAP (0.03 g) were added to reaction mixture which was stirred for 24 h. Then, the

mixture was extracted by EtOAc, dried by Na_2SO_4, and purified by chromatographic column. ^{1}H NMR in $CDCl_3$ (400 MHz), δ 0.55 (s, 3H, 18-CH_3), 0.83 (d, J = 3.2 Hz, 3H, 21-CH_3), 0.85 (s, 3H, 19-CH_3), 3.565 (s,3H, 24-OC$\underline{H}_3$), 4.08 (q, J = 8 Hz, 2H, 3α-OCOOC$\underline{H}_2$CH$_3$), 4.35 (m, 1H, 3β-H), 4.81(s, 1H, 7β-H), 4.90-5.00 (m, 2H, 7α-OCOCH$_2$CH$_2$CH=C$\underline{H}_2$), 5.66 (m, 1H, 7α-OCOCH$_2$CH$_2$C$\underline{H}$=CH$_2$); ^{13}C NMR in $CDCl_3$(100 MHZ) δ 174.4(C24), 172.1(C25), 154.4(3α-O$\underline{C}$OOCH$_2$CH$_3$), 136.5(C28), 115.2(C29), 77.6(C3), 70.9(C7), 63.4(3α-OCOO$\underline{C}$H$_2$CH$_3$), 55.5(C17), 51.3(24-O$\underline{C}$H$_3$), 50.2(C14), 42.4(C13),40.7(C5), 39.3(C12), 37.7(C8), 35.1(C4), 34.6(C1), 34.5(C10), 34.4(C9), 33.9(C26), 33.8(C20), 31.2(C16), 30.8(C23), 30.7(C22), 28.6(C27), 27.8(C6), 26.5(C2), 23.4(C15), 22.4(C19), 20.4(C11), 18.1(C21), 14.1(3α-OCOOCH$_2\underline{C}$H$_3$), 11.5(C18).

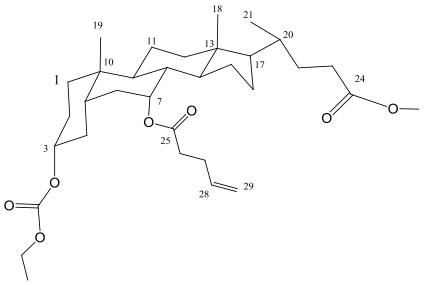

Figure 5. The labeling of compound **F.**

3α-hydroxy-7α-(4-pentenoyloxy)-5β-cholanoic acid (**H**): To a solution of **F** (1.0 g, 2.1 mmol) in CH_3OH (10 mL) and THF (10 mL), K_2CO_3 (satd, 20 mL) was added. The solution was refluxed for 5h. The extra base was neutralized by 3*M* HCl, extracted with EtOAc. The organic layer was dried by Na_2SO_4 and solvent was evaporated by rotary vaporization. The crude product was crystallized from acetone to give pure compound

H.^{1}H NMR δ 0.62 (s, 3H, 18-CH_3), 0.89 (s, 3H, 19-CH_3), 0.91 (d, 3H, 21-CH_3), 2.33(d, *J* = 8 Hz 7α-$OCOCH_2C\underline{H}_2CH{=}CH_2$), 3.48 (m, 3α-H), 4.87 (s, 7α-H), 4.97-5.07 (m, 7α-$OCOCH_2CH_2CH{=}C\underline{H}_2$), 5.80 (m, 7α-$OCOCH_2CH_2C\underline{H}{=}CH_2$). ^{13}C NMR δ 11.7 (C18), 18.2 (C21), 20.6 (C11), 22.7 (C19), 23.5 (C15), 28.0 (C2), 28.7 (C6), 30.5 (C27), 30.7 (C22), 31.0 (C23), 31.5 (C16), 34.0 (C20), 34.1(C26), 34.7 (C9), 35.1 (C10), 35.3 (C1), 37.9 (C4), 38.9 (C8), 39.5 (C12), 41.0 (C5), 42.7 (C13), 50.3(C14), 55.7 (C17), 71.3 (C7), 71.8 (C3), 115.4 (C29), 136.7 (C28), 172.5 (C25), 179.684 (C24).

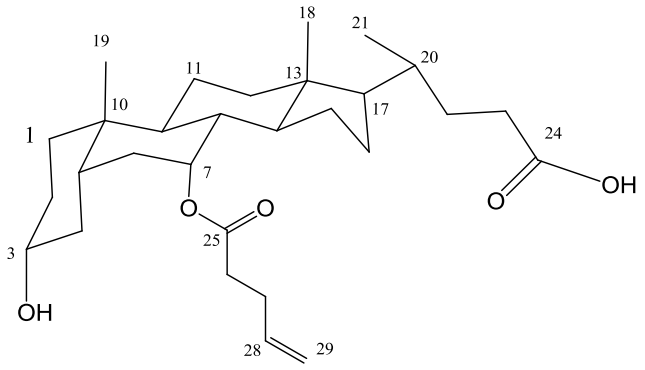

Figure 6. The labeling of compound **H.**

3α-(4-pentenoyloxy)-7α-(4-pentenoyloxy)-5β-cholanoic acid (**I**): 2, 6-dichlorobenzoyl chloride (10 mmol, 2.10 g) and 4-pentenoic acid (10 mmol, 1.00 g) were dissolved in 30 mL anhydrous THF, 1.8 mL Et_3N was added. The soln was stirred for 30 min, and then CDCA (2.54 mmol, 0.98 g) was added with another 1.8 mL Et_3N while stirring. After 1h, 5% equivalent DMAP (0.061g) was added. After stirring for 12 hr at rt, the solution was

heated to reflux for 1h, then diluted with water, extracted by CH_2Cl_2, dried in a vacuum oven, and purified by column chromatography. It gave compound **I** 0.72 g (60% yield).^{1}H NMR in $CDCl_3$ (400 MHz), δ 0.65(s, 3H, 18-CH_3), 0.93 (d,2H,21-CH_3),0.94(s,3H, 19-CH_3), 4.61(m, 1H, 3β-H), 4.91(d, 1H, 7β-H), 5.03 (m, 4H, 7α-$OCOCH_2CH_2CH=C\underline{H}_2$), 5.83 (m, 2H, 7α-$OCOCH_2CH_2C\underline{H}=CH_2$). ^{13}C NMR (100 MHz), 180.28 (C24), 172.76 (7α-$O\underline{C}OCH_2CH_2CH=CH_2$), 136.81 (7α-$OCOCH_2CH_2C\underline{H}=CH_2$), 115.54 (7α-OCOC $H_2CH_2CH=\underline{C}H_2$), 74.2 (C7), 71.41 (C3), 55.92 (C17), 50.45 (C14), 42.72 (), 39.62(), 18.35 (C21), 11.82 (C18).

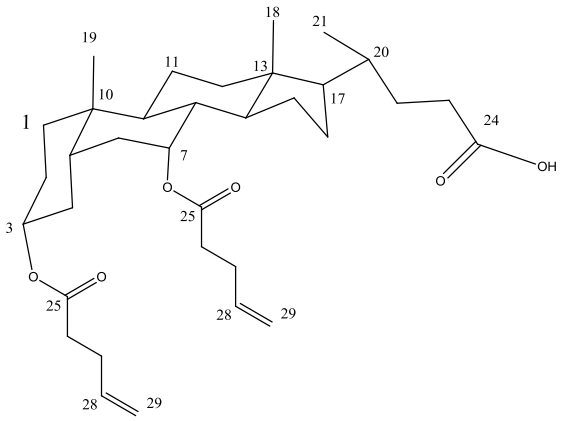

Figure 7. The labeling of compound **I.**

Cyclodimer **J**: 2, 6-dichlorobenzoyl chloride (10mmol, 2.10 g) and 4-pentenoic acid (10 mmol, 1.00 g) were dissolved in 30mL anhydrous THF, 1.8 mL Et_3N was added. The soln was stirred for 30 min, and then CDCA (2.54 mmol, 0.98 g) was added with another 1.8 mL Et_3N while stirring. After 1h, 5% equivalent DMAP (0.061g) was added. After stirring for 12 hr at rt, the solution was heated to reflux for 1h, then diluted with water,

extracted by CH_2Cl_2, dried in a vacuum oven, and purified by column chromatography. It gave compound **J** 0.20g (16% yield). 5.82 (m, 2H, 7α-$OCOCH_2CH_2C\underline{H}=CH_2$), 5.02 (m, 4H, 7α-$OCOCH_2CH_2CH=C\underline{H}_2$), 4.85 (s, 2H, 7β-H), 4.63 (m, 2H, 3β-H), 0.92 (s, 6H, 19-CH_3), 0.90 (d, 4H, 21-CH_3), 0.67 (s, 6H, 18-CH_3). ^{13}C NMR: 174.1 (C24), 172.5 (C25), 136.7 (C28), 115.3 (C29), 74.1 (C3), 71.1 (C7), 53.1 (C17), 51.3 (C14), 42.3 (C13), 40.9 (C5), 20.7 (C11), 18.4 (C21), 11.7 (C18).

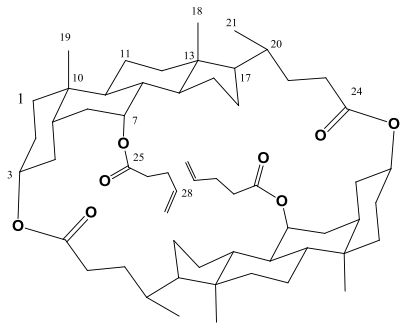

Figure 8. The labeling of cyclodimer **J**

Cyclodimer **K**: To a soln of **H** (0.20mmol, 0.1g) in THF (2 mL), Et_3N (0.5 mL) and 2, 6-dichlorobenzoyl chloride (0.1 mL) were added. The reaction mixture was stirred for 2 h at r.t. The solvent was removed in vacuum, and the residue was dissolved in 20 mL toluene. The solution was added stepwise over 10 h to a refluxed solution of DMAP (0.06g) in toluene (100 mL). The reaction mixture was stirred for an additional 5 h and then diluted with EtOAc and poured into ice water. The organic layer was dried with Na_2SO_4 and solvent was removed by under vacuum. The resulting product was further purified by column chromatography on silica gel (5:1 hexanes: ethyl acetate) affords the

cyclodimer as a white solid (0.08 g). The cubic single crystals of cyclodimer grown by slow evaporation of 1:1 ratio of chloroform/acetone solution were submitted for X-ray crystallography. ^{1}H NMR in $CDCl_3$ (400 MHz), δ 5.82-5.91 (m, 7α-$OCOCH_2CH_2C\underline{H}=CH_2$), 5.12-5.18 (m, 7α-$OCOCH_2CH_2CH=C\underline{H_2}$), 4.97, 4.96 (d, 7β-H), 4.73 (m, 3β-H). ^{13}C NMR (100 MHz), 174.03 (C24), 172.21 (C25),137.28 (C28), 115.47 (C29), 72.51 (C3),71.40 (C7), 52.66 (C17), 50.34 (C14), 42.61 (C13), 40.62 (C5), 39.60 (C12), 37.63 (C8), 34.81 (C4), 34.77 (C1), 34.60 (C10), 34.30 (C9), 34.20 (C26), 33.80 (C20), 31.3 (C16), 30.84 (C23), 29.85 (C22), 28.60 (C27), 27.30 (C6), 26.30 (C2), 23.35 (C15), 22.40 (C19), 20.66 (C11), 20.34 (C21), 11.55 (C18).

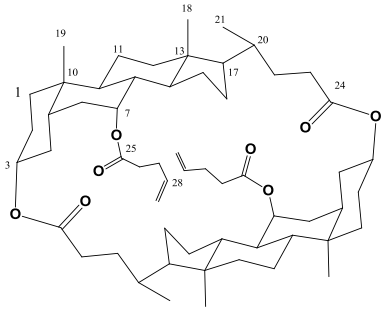

Figure 9. The labeling of cyclodimer **K**

Cyclotrimer **L**: 0.656 (s, 9H, 18-CH_3), 0.94 (d, 6H, 21-CH_3), 0.95 (s, 9H, 19-CH_3), 4.64 (m, 3H, 3β-H), 4.91 (s, 3H, 7β-H), 4.99-5.09 (m, 6H, 7α-$OCOCH_2CH_2CH=C\underline{H_2}$), 5.76-5.88 (m, 3H, 7α-$OCOCH_2CH_2C\underline{H}=CH_2$), ^{13}C NMR (100 MHz), 11.57 (C18), 18.26 (C21), 20.62 (C11), 22.61 (C19), 23.51 (C15), 26.73 (C2), 28.05 (C6), 28.69 (C27), 30.56 (C22), 30.67 (C23), 31.22 (C16), 33.94 (C26), 34.25 (C9), 34.68 (C10), 34.83

(C1), 34.97 (C4), 37.80 (C8), 39.69 (C12), 40.71 (C5), 42.65 (C13), 50.62 (C14), 54.86 (C17), 71.35 (C7), 73.60 (C3), 115.42 (C28), 136.67 (C29), 171.83 (C25), 173.60 (C24).

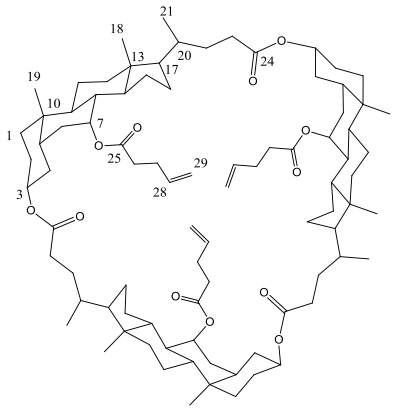

Figure 10. The labeling of cyclotrimer **L.**

Cyclotetramer (**M**): 0.64(s, 12H, 18-CH_3), 0.91 (d, 8H, 21-CH_3), 0.93(s, 12H, 19-CH_3), 4.58 (m, 4H, 3β-H), 4.90 (s, 4H, 7β-H), 4.99-5.09 (m, 8H, 7α-$OCOCH_2CH_2CH=C\underline{H}_2$), 5.78-5.86 (m, 4H, 7α-$OCOCH_2CH_2C\underline{H}=CH_2$). ^{13}C NMR (100 MHz), 11.70 (C18), 18.43 (C21), 20.60 (C19), 22.62 (), 23.51 (), 26.78 (), 27.78 (), 28.75 (), 31.37 (C16), 33.98 (C26), 34.03 (C9), 34.78 (C10), 34.85 (C1), 34.95 (C4), 37.94 (C8), 39.48 (C12), 40.85 (C5), 42.63 (C13), 50.33 (C14), 55.26 (C17), 71.22 (C7), 73.86 (C3), 115.37 (C28), 136.78 (C29), 172.02 (C25), 173.78 (C24).

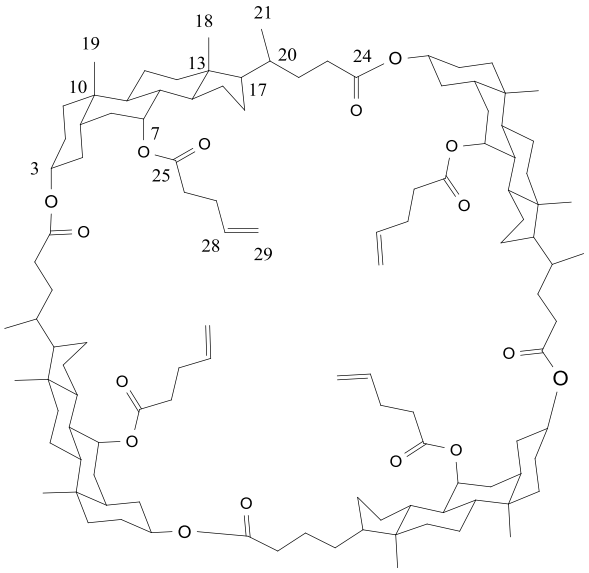

Figure 11. The labeling of cyclotetramer **M**

***cis*-N & *trans*-N**. To a solution of cyclodimer **4** in CH_2Cl_2, 10 mol % of 2nd generation Grubb's ruthenium catalyst were added. The reaction mixture was stirred under reflux and N_2 flow. After completion of the reaction, the grubb's catalyst was removed by passing through a flash column. The mixture of ***cis*-5** and ***trans*-5** was separated and purified by column chromatography (5:1 hexanes-ethyl acetate).The ***cis*-5** with a higher R_f value was eluted out as the first component, and the ***trans*-5** washed out as the second component .

***cis*-N:** ^{1}H NMR in $CDCl_3$ (400 MHz), δ 5.61 (t, *J* = 4.0Hz, 2H, C<u>H</u>=C<u>H</u>), 4.97 (s, 2H, 7β-H), 4.70 (m, 2H, 3β-H), 0.94 (s, 6H, 19-CH_3), 0.91 (d, *J* = 8.0Hz, 6H, 21-CH_3) 0.65(s, 6H, 18-CH_3) ^{13}C NMR (101 MHz), 173.88 (C24), 171.57 (C25), 129.39 (C28), 72.42 (C3), 71.52 (C7), 54.07 (C17), 50.37 (C14), 42.53 (C13), 40.56 (C5), 40.08 (C12), 37.89 (C8), 35.54 (C4), 34.94 (C1), 34.52 (C10), 34.48 (C9), 34.46 (C26), 31.16 (C16), 30.92 (C23), 30.76(C20), 29.69 (C22), 27.32 (C6), 26.31 (C2), 23.63 (C15), 22.53 (C27), 22.26 (C19), 20.53 (C11), 19.85 (C21), 11.47 (C18). HRMS (ESI) Calcd for $C_{56}H_{84}O_8Na$ [M+Na^+] 907.6064, found 907.6088.

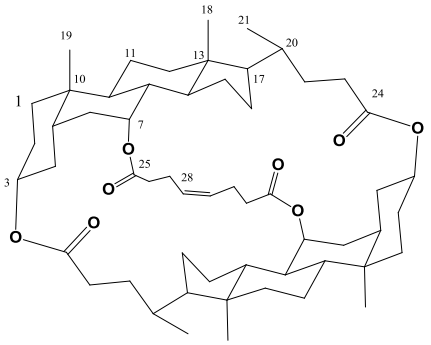

Figure 2. The labeling of *cis*-**N**

***trans*-N**. ^{1}H NMR in $CDCl_3$ (400 MHz), δ 5.55 (t, *J* = 4.0Hz, 2H, C<u>H</u>=C<u>H</u>), 5.01 (s, 2H, 7β-H), 4.61 (m, 2H, 3β-H), 0.94 (s, 6H, 19-CH_3), 0.89 (d, 6H, 21-CH_3), 0.66 (s, 6H, 18-CH_3). ^{13}C NMR (101 MHz), 173.32 (C24), 171.24 (C25), 129.64 (C28), 72.91 (C3), 71.36 (C7), 58.68 (C17) 50.41 (C14), 42.60 (C13), 40.41 (C5), 40.26 (C12), 37.80 (C8), 35.69 (C4), 35.63 (C9), 34.84 (C1), 34.38 (C10), 34.00 (C26), 32.71 (C23), 31.14 (C16), 30.11 (C20), 27.47 (C6), 26.90 (C22), 26.03 (C2), 23.31 (C15), 22.39 (C27), 22.39 (C19), 20.49 (C11), 17.65 (C21), 11.63 (C18). HRMS (ESI) Calcd for $C_{56}H_{84}O_8NH_4$ [M+NH_4^+] 902.6510, found 902.6514. Calcd for $C_{56}H_{84}O_8Na$ [M+Na^+] 907.6064, found 907.6087.

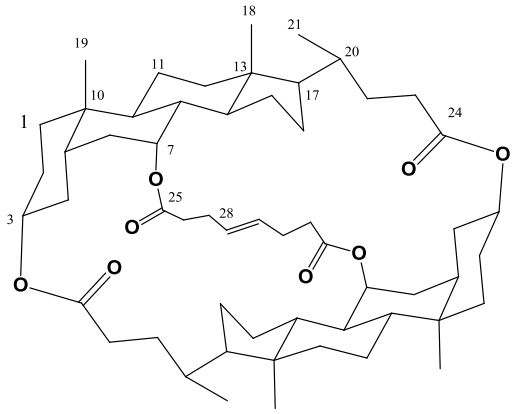

Figure 2. The labeling of *trans*-**N**

4.3 Supporting spectra

^{1}H NMR spectrum of Methyl 3α-ethoxycarbonyloxy-7α-hydroxyl-5β-cholanoate **(A)**

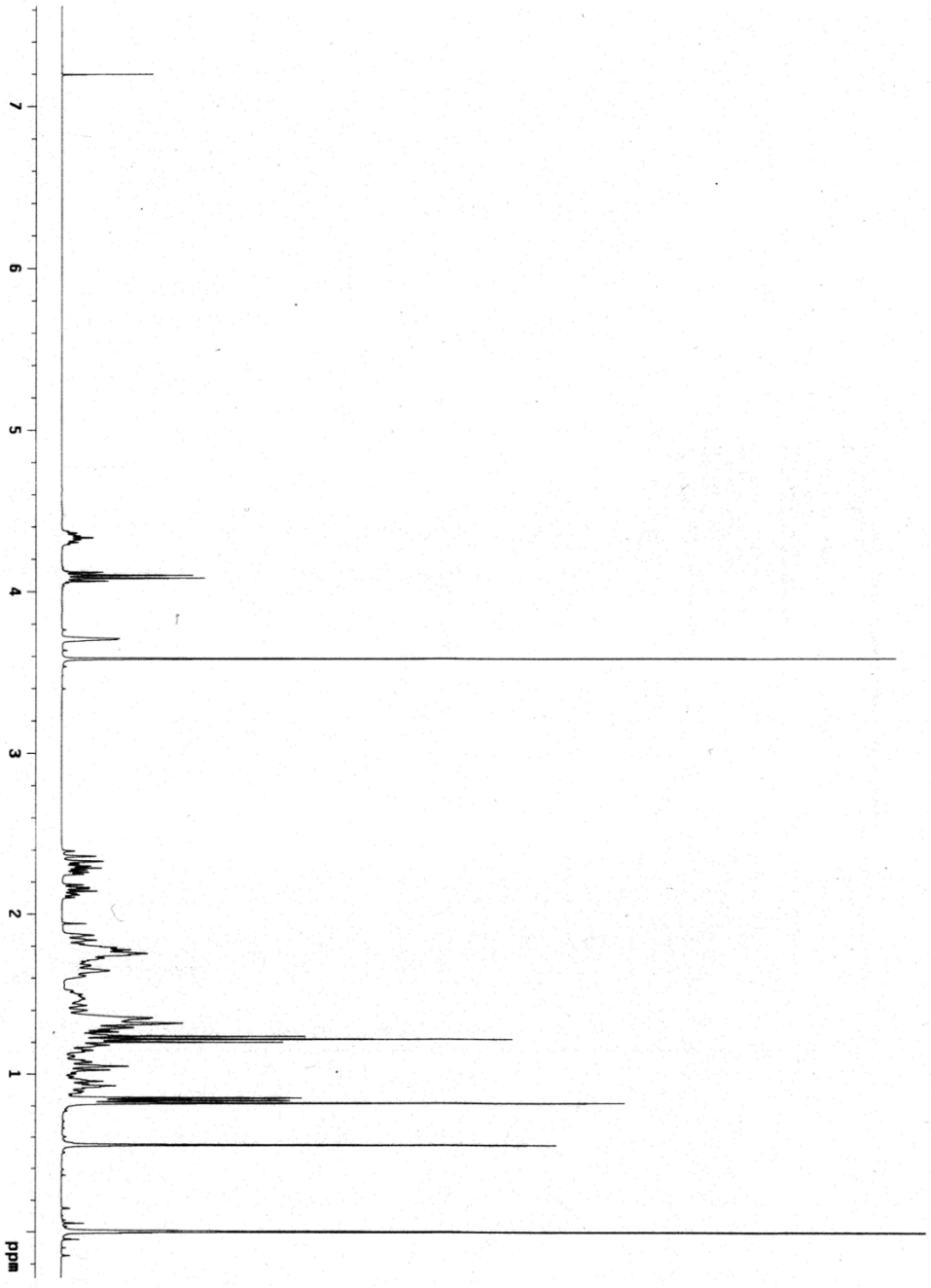

^{13}C NMR spectrum of Methyl 3α-ethoxycarbonyloxy-7α-hydroxyl-5β-cholanoate (**A**)

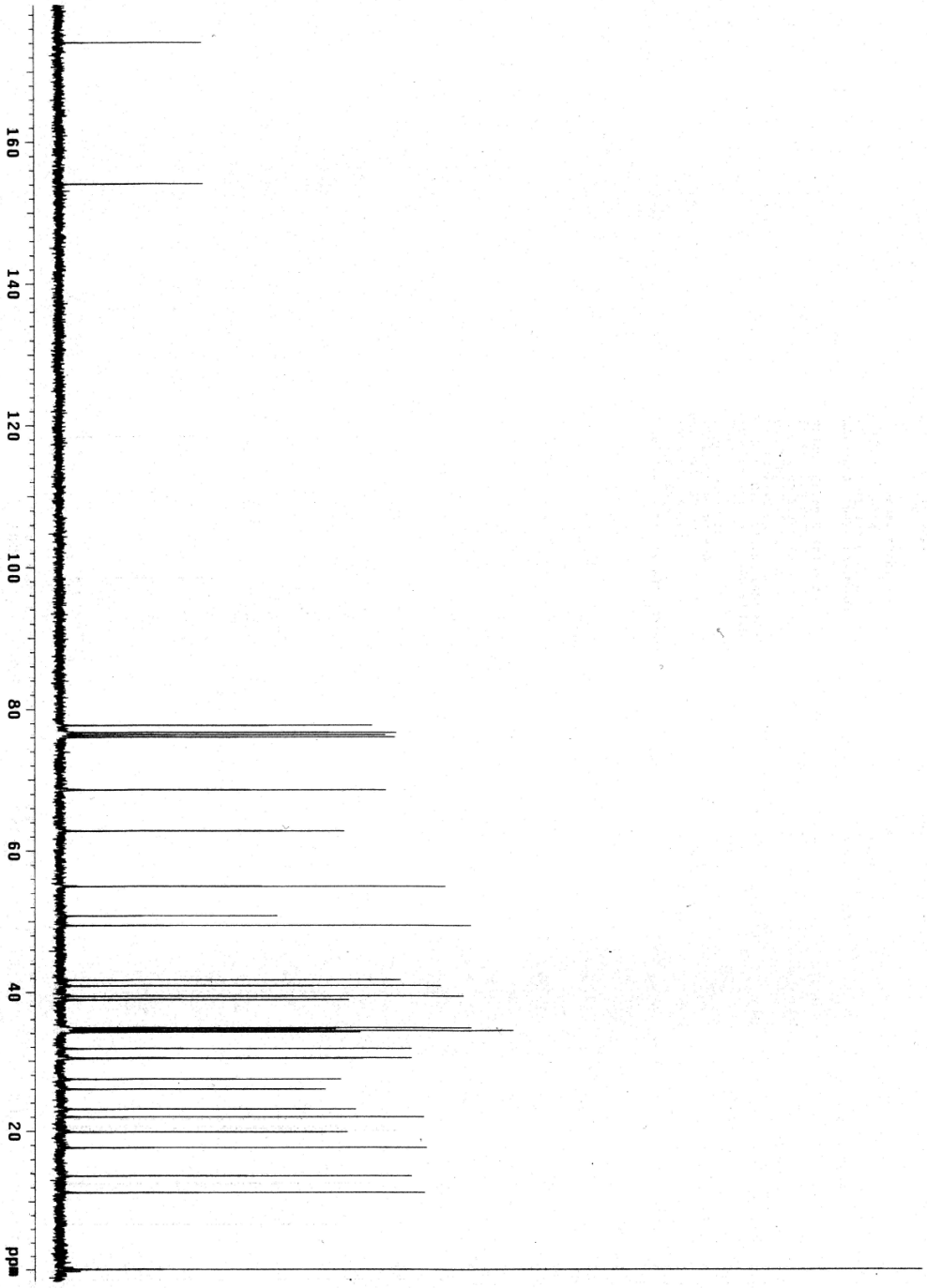

^{1}H NMR spectrum of Methyl 3α-(ethoxycarbonyloxy)-7α-(allyloxycarbonyloxy)-5β-cholanoate (**C**)

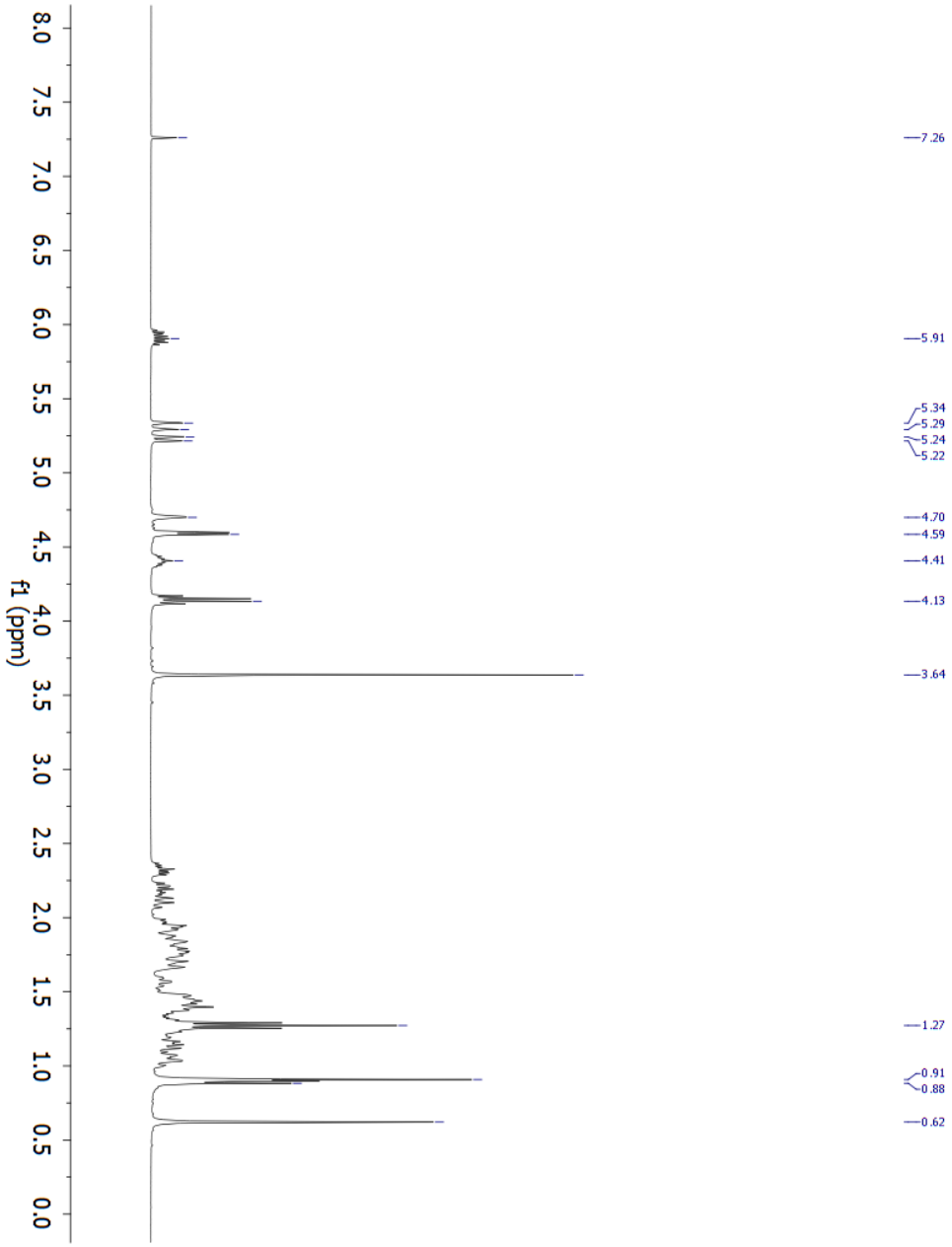

^{13}C NMR spectrum of Methyl 3α-(ethoxycarbonyloxy)-7α-(allyloxycarbonyloxy)-5β-cholanoate (**C**)

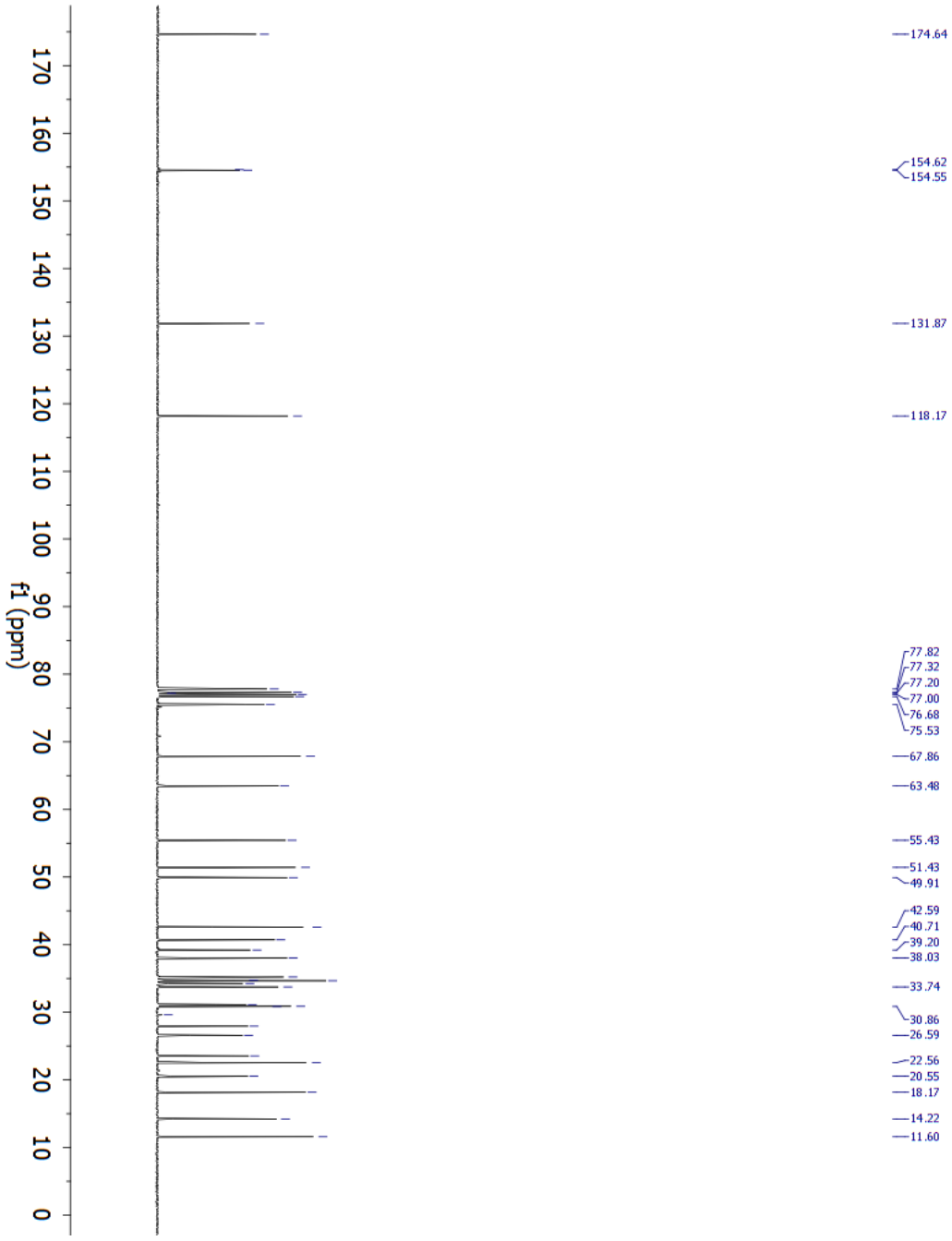

^{1}H NMR spectrum of allyl 3α-(ethoxycarbonyloxy)-7α-hydroxy-5β-cholanoate (**E**)

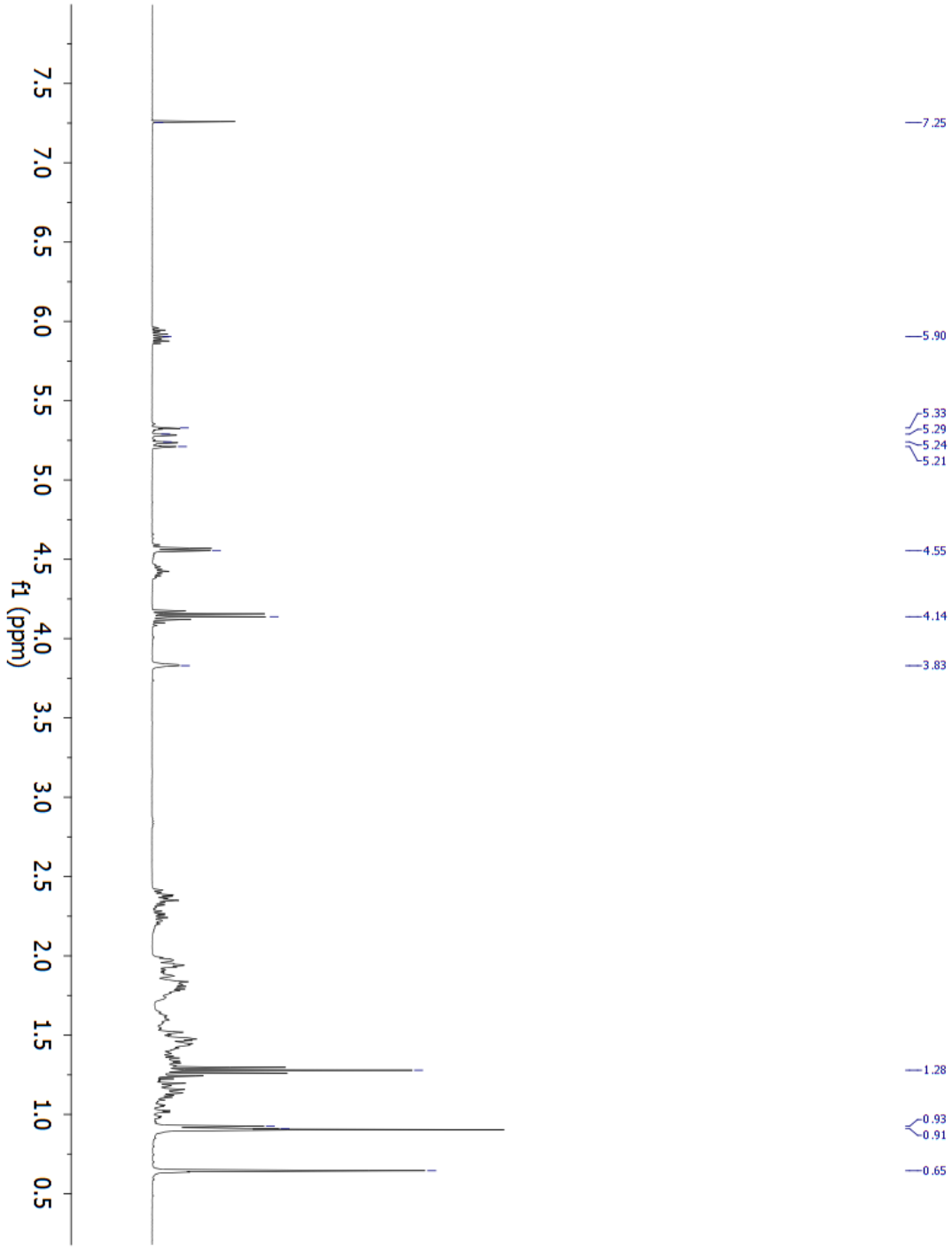

^{13}C NMR spectrum of allyl 3α-(ethoxycarbonyloxy)-7α-hydroxy-5β-cholanoate (**E**)

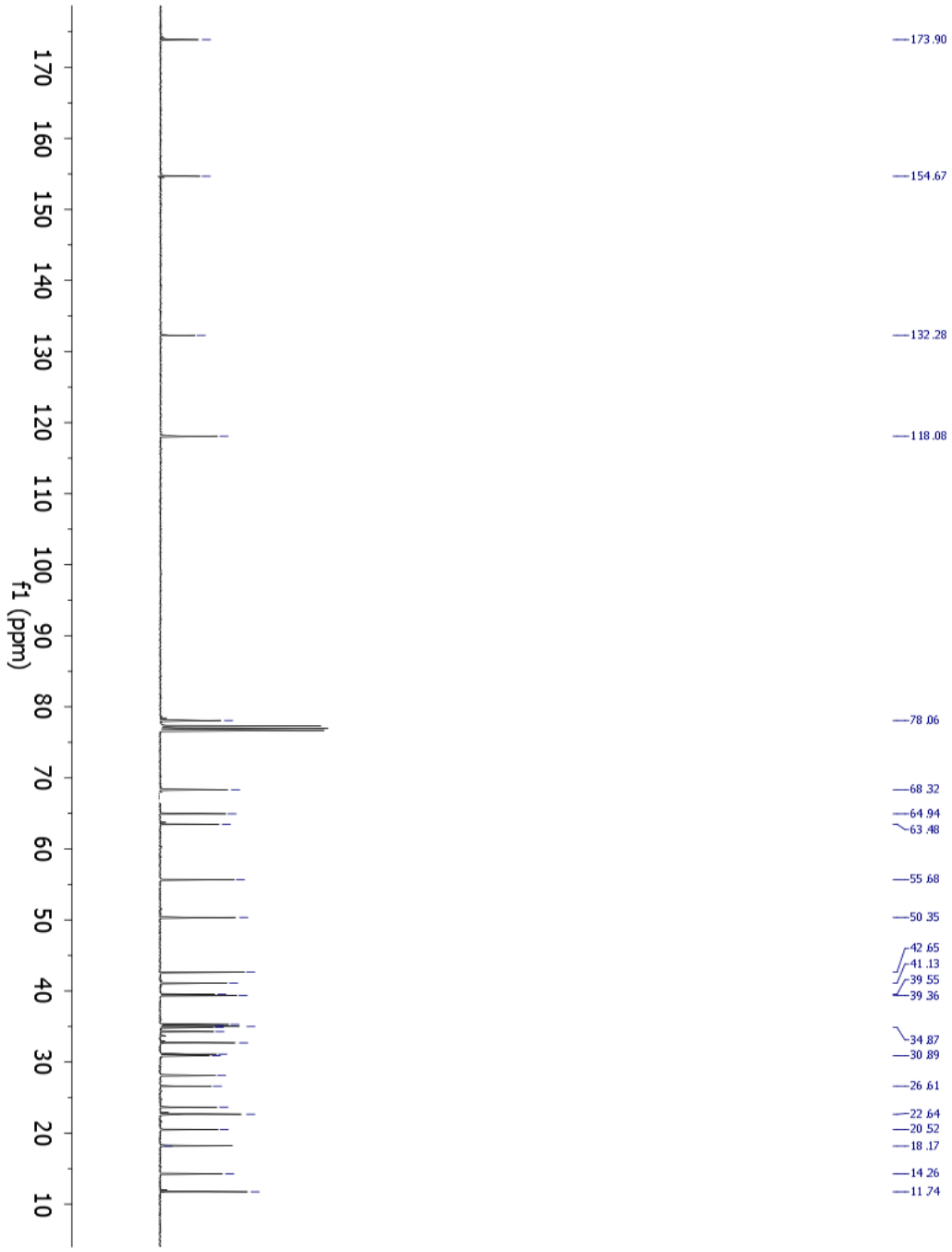

^{1}H NMR spectrum of methyl 3α-ethoxycarbonyloxy-7α-(4-pentenoyloxy)-5β-cholanoate (**F**)

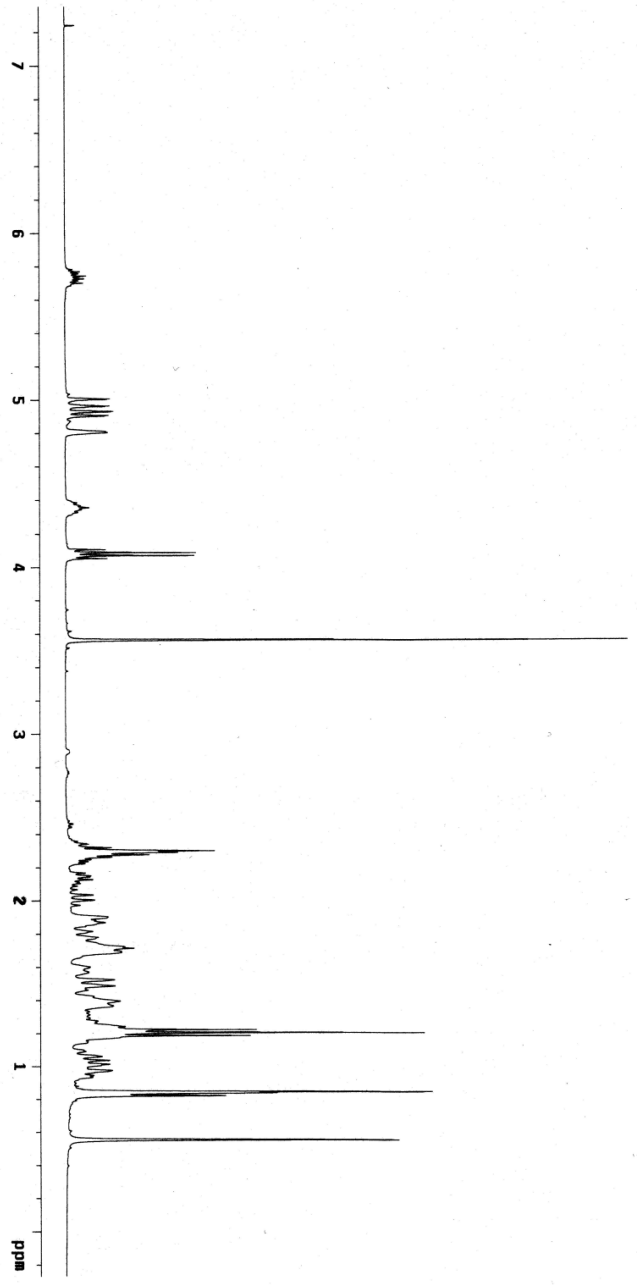

^{13}C NMR spectrum of methyl 3α-ethoxycarbonyloxy-7α-(4-pentenoyloxy)-5β-cholanoate (**F**)

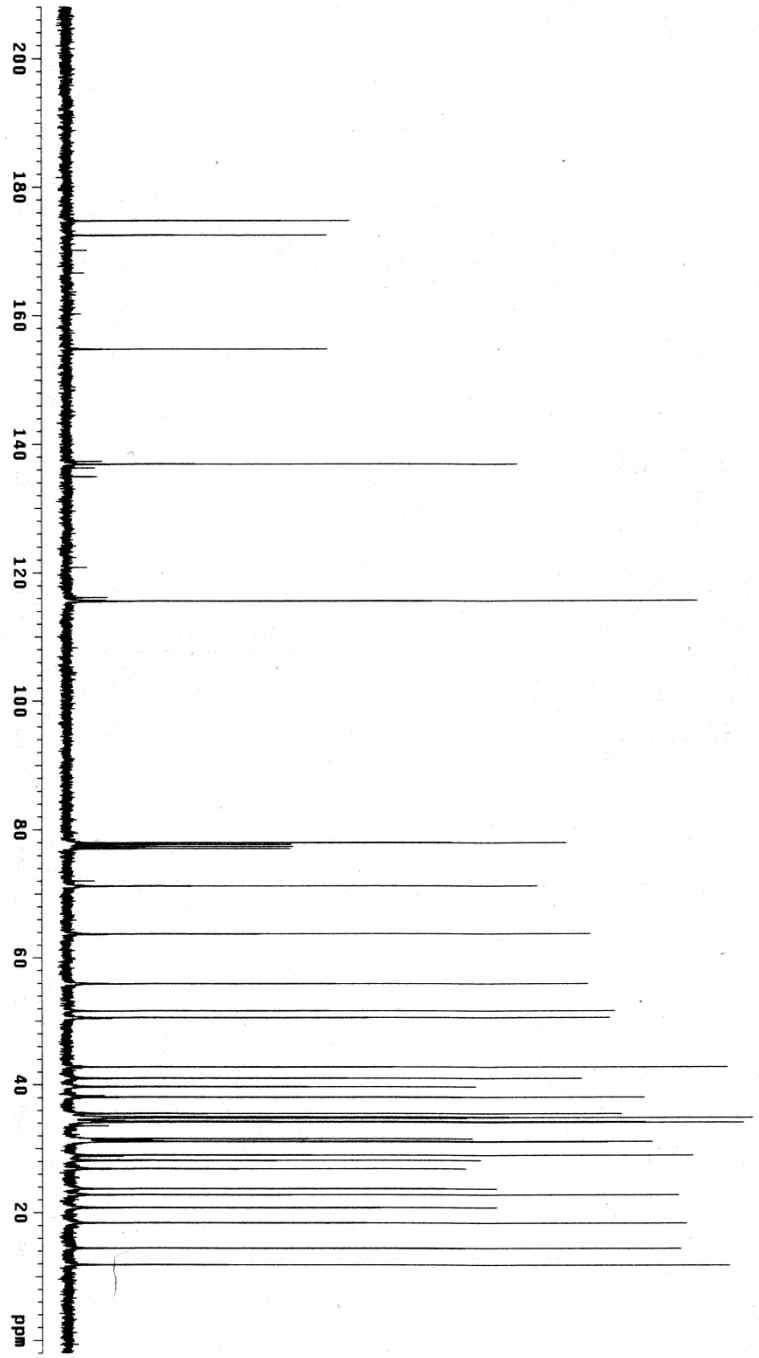

^{1}H NMR spectrum of 3α-hydroxy-7α-(4-pentenoyloxy)-5β-cholanoic acid (**H**)

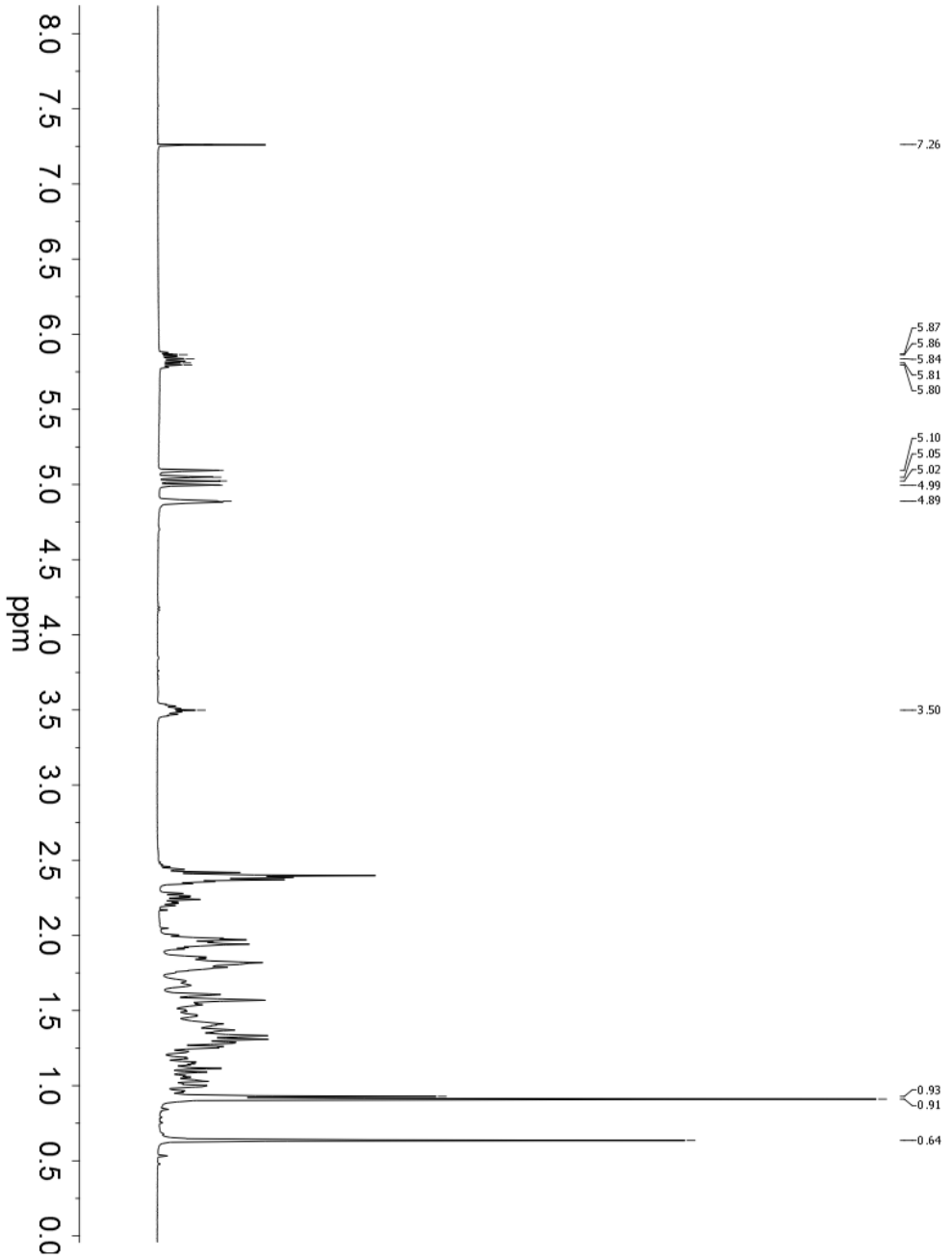

^{13}C NMR spectrum of 3α-hydroxy-7α-(4-pentenoyloxy)-5β-cholanoic acid (**H**)

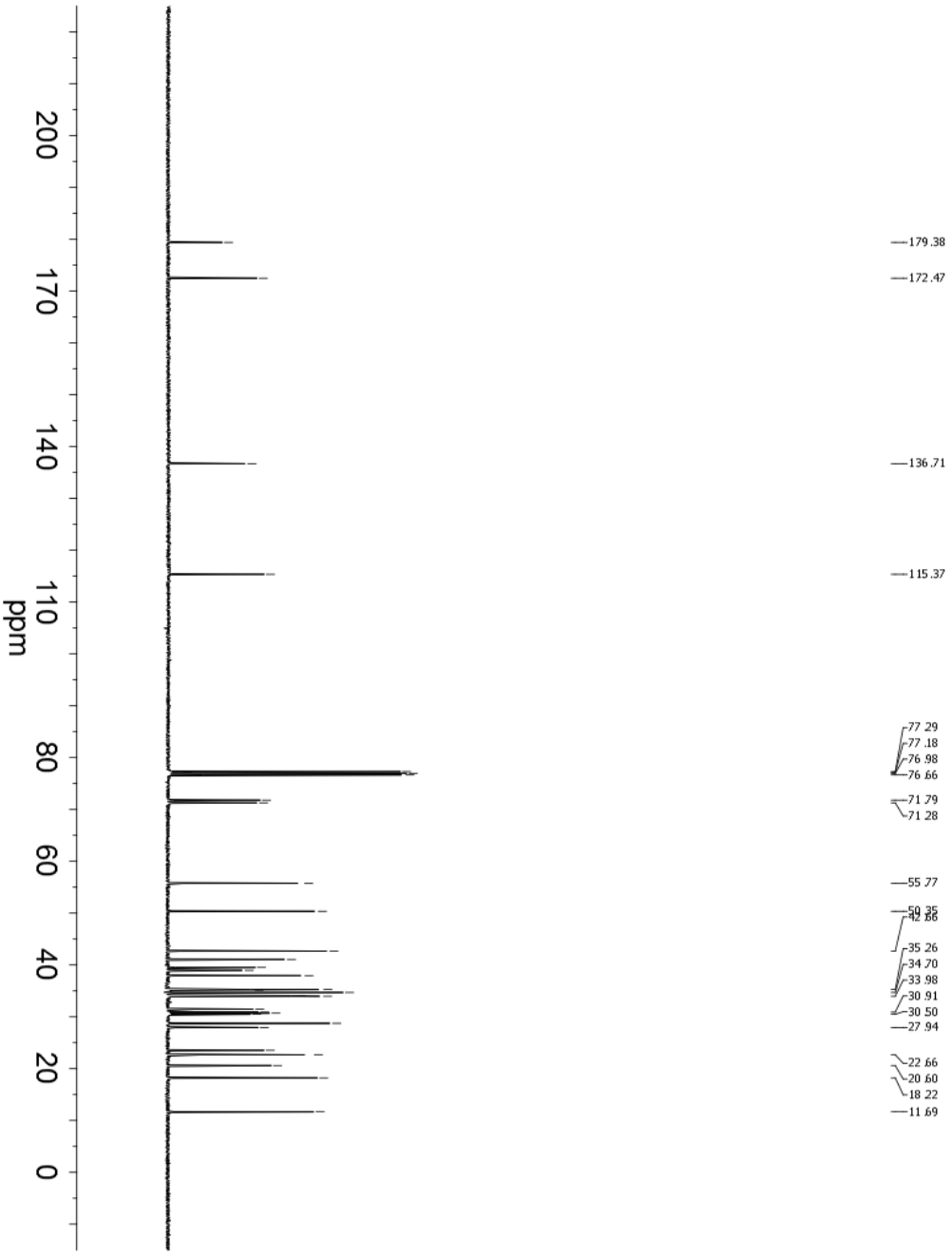

^{1}H NMR spectrum of cyclodimer **J**

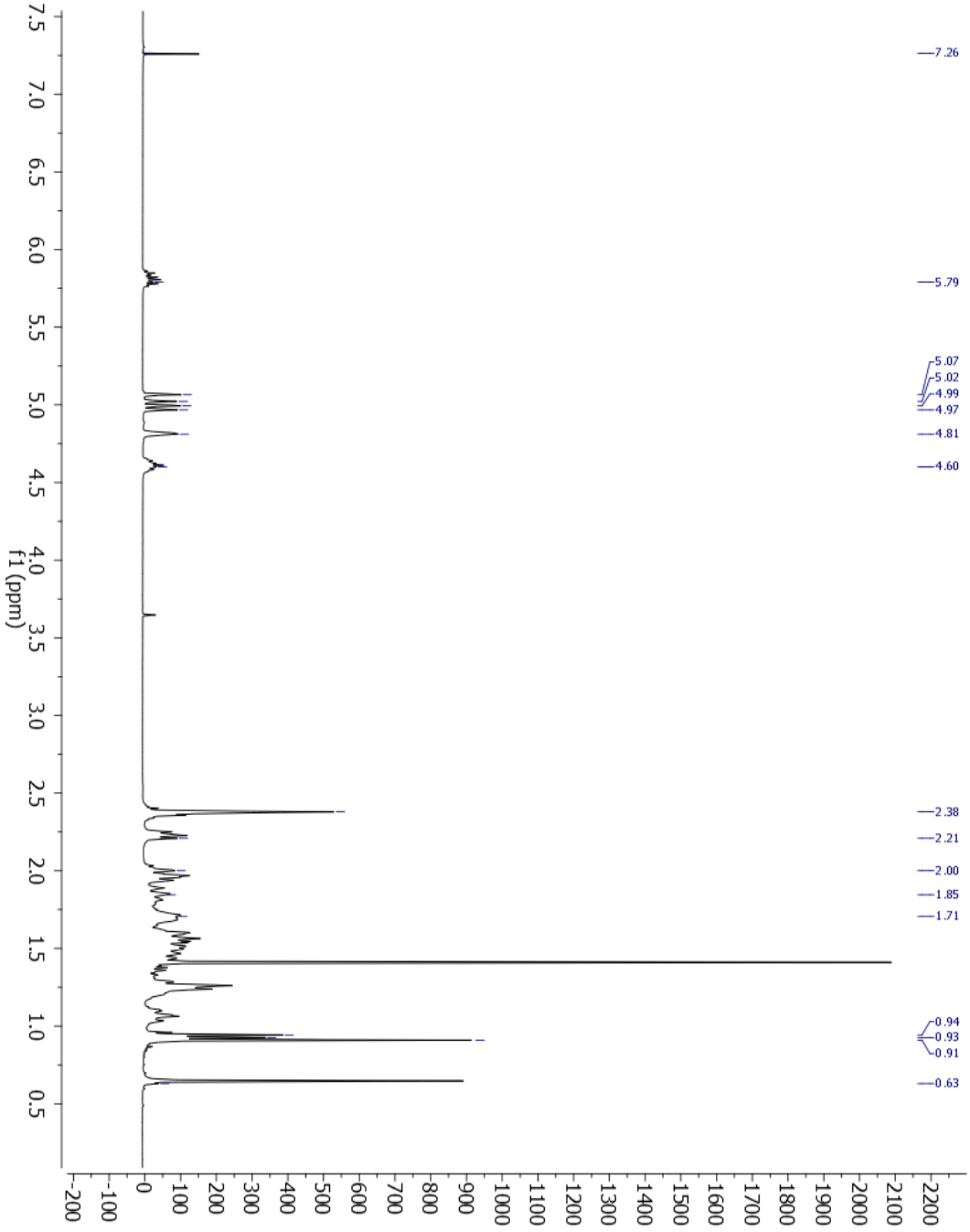

^{13}C NMR spectrum of cyclodimer **J**

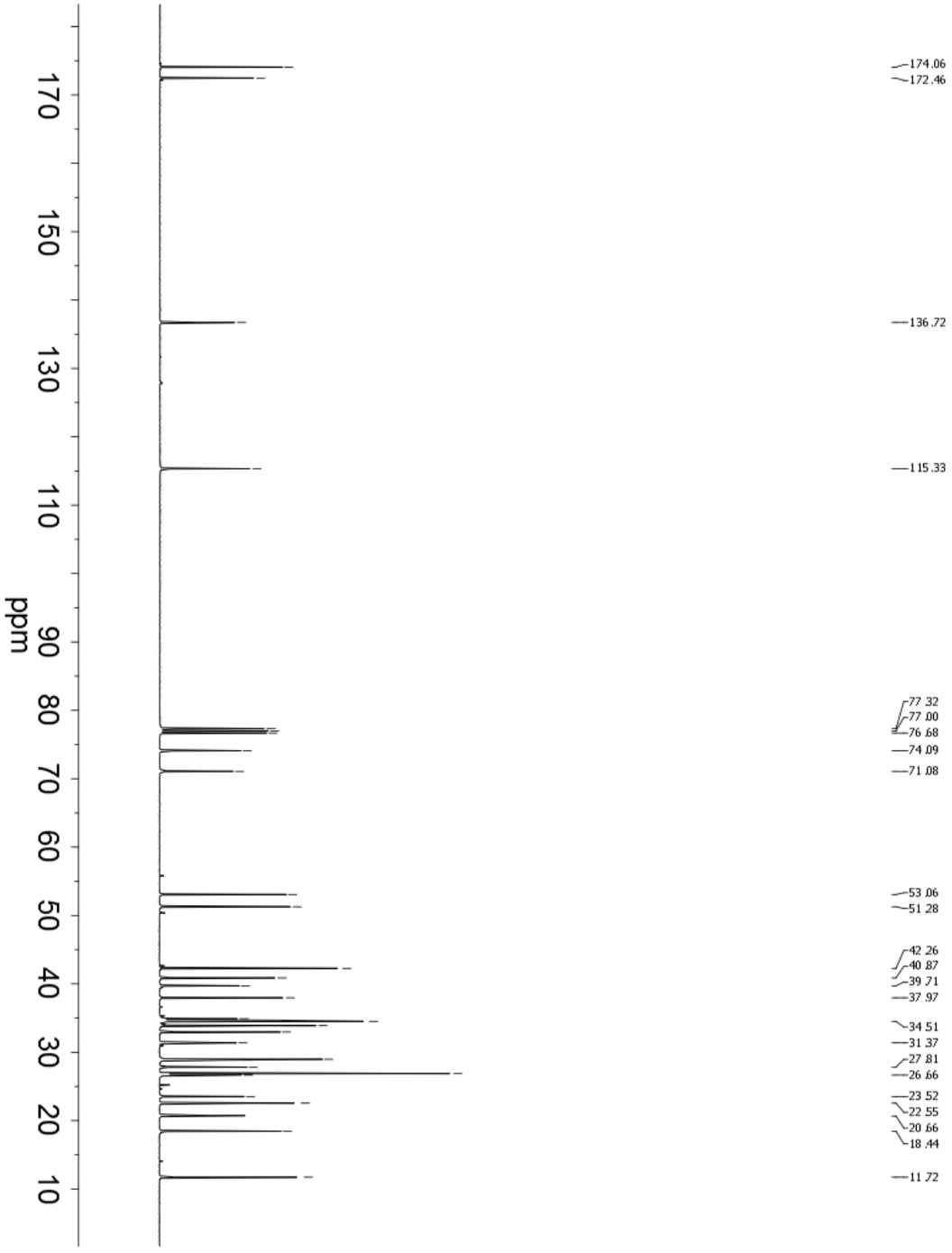

^{1}H NMR spectrum of cyclodimer **K**

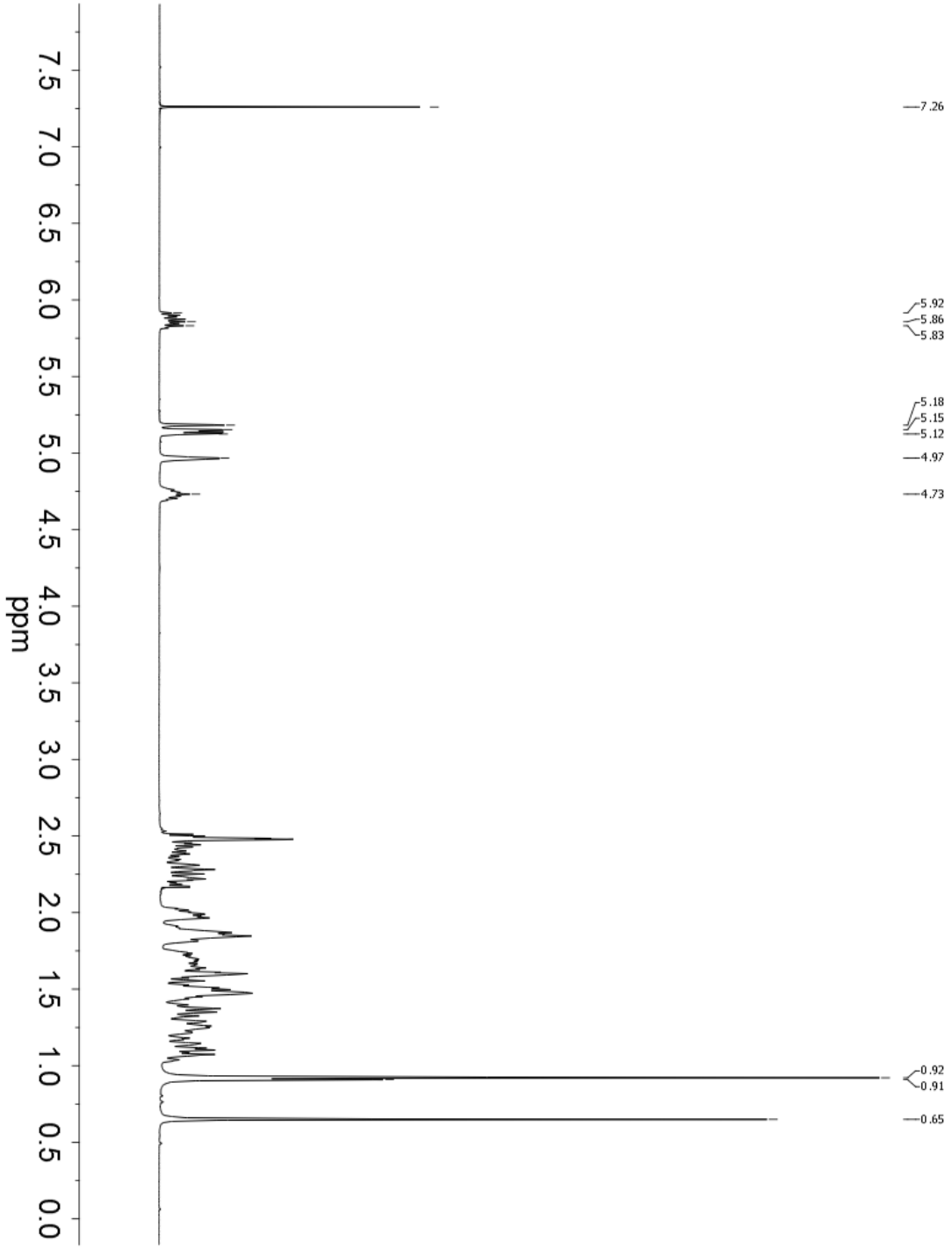

^{13}C NMR spectrum of cyclodimer **K**

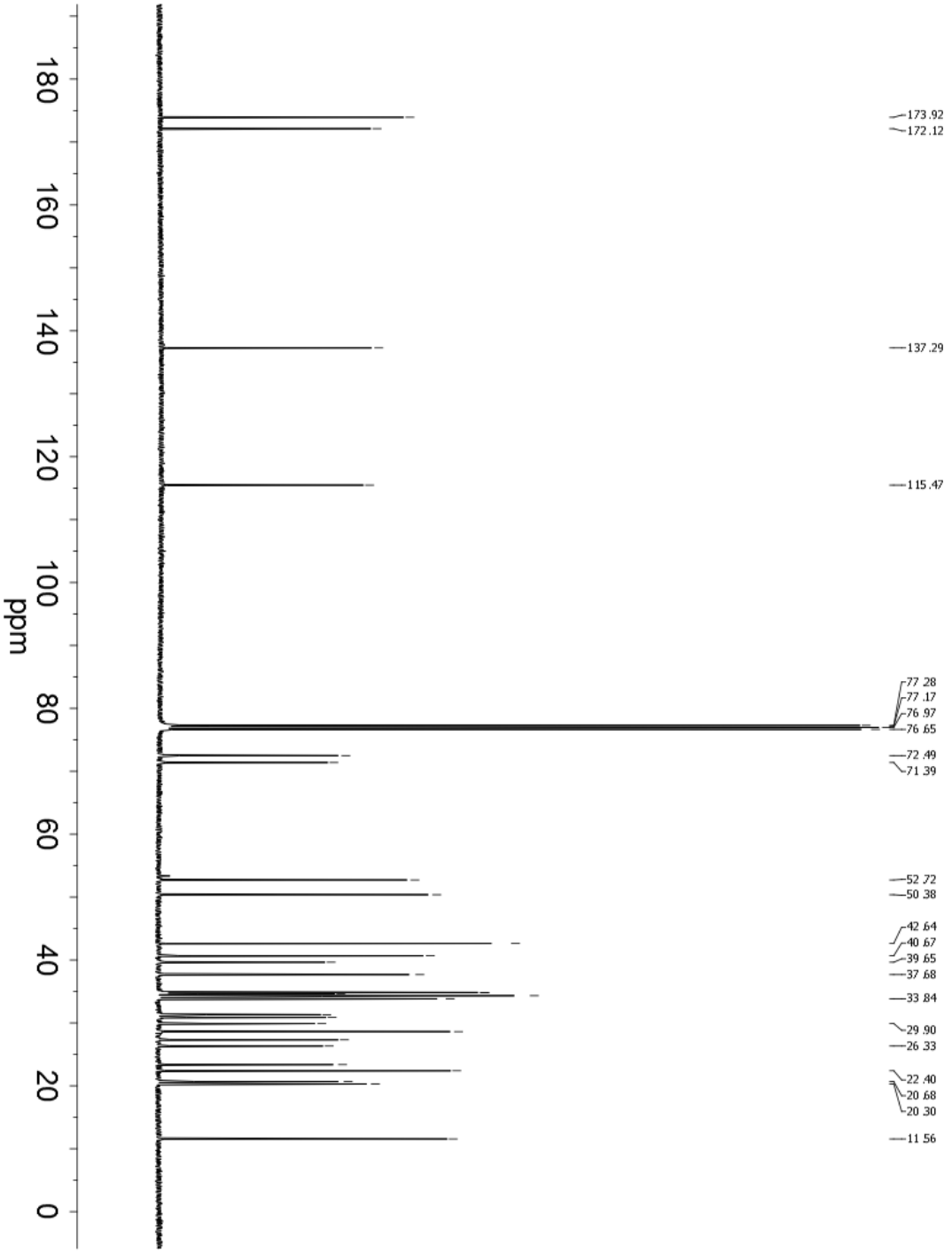

^{1}H NMR spectrum of cyclotrimer **L**

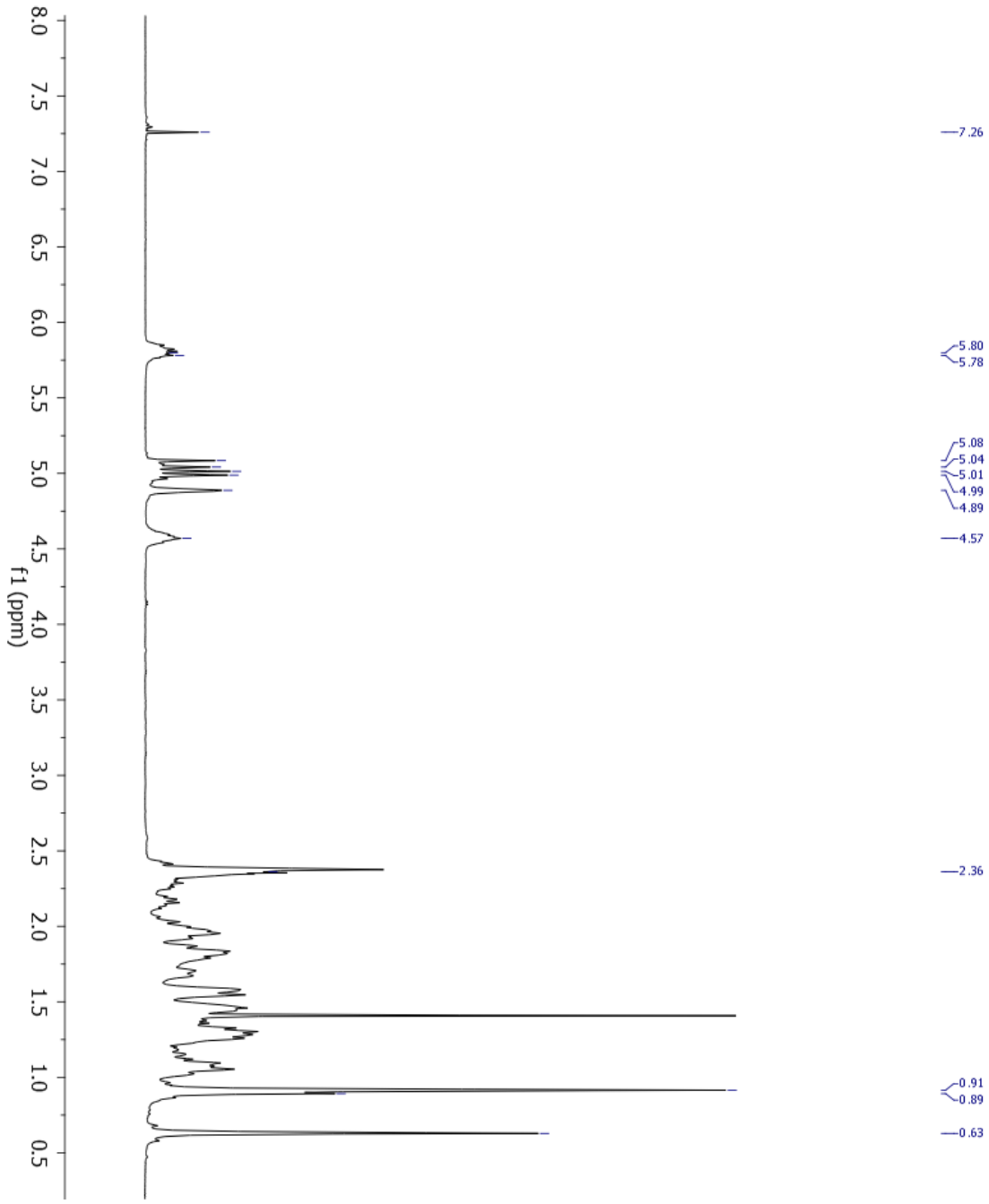

^{13}C NMR spectrum of cyclotrimer **L**

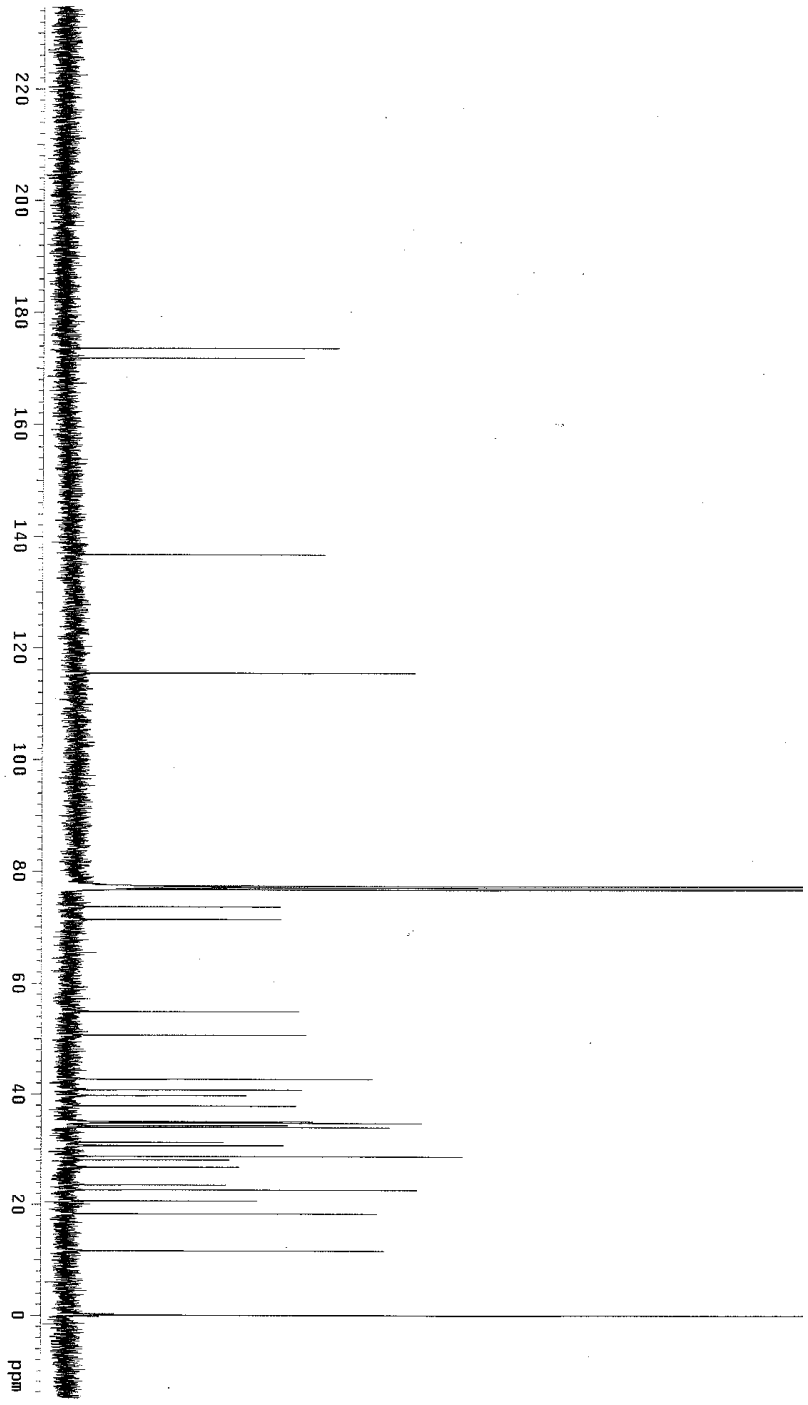

^{1}H NMR spectrum of cyclotetramer **M**

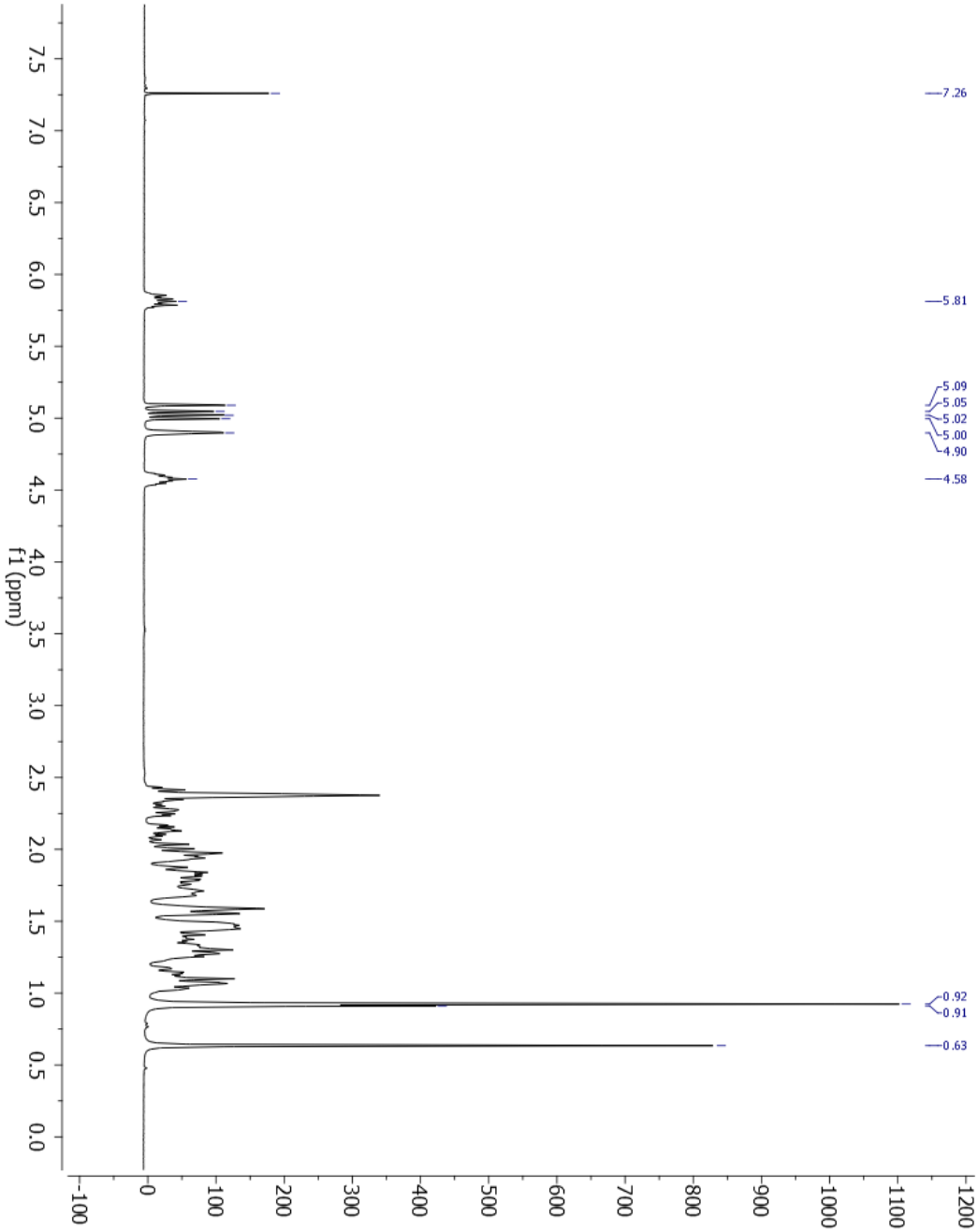

^{13}C NMR spectrum of cyclotetramer **M**

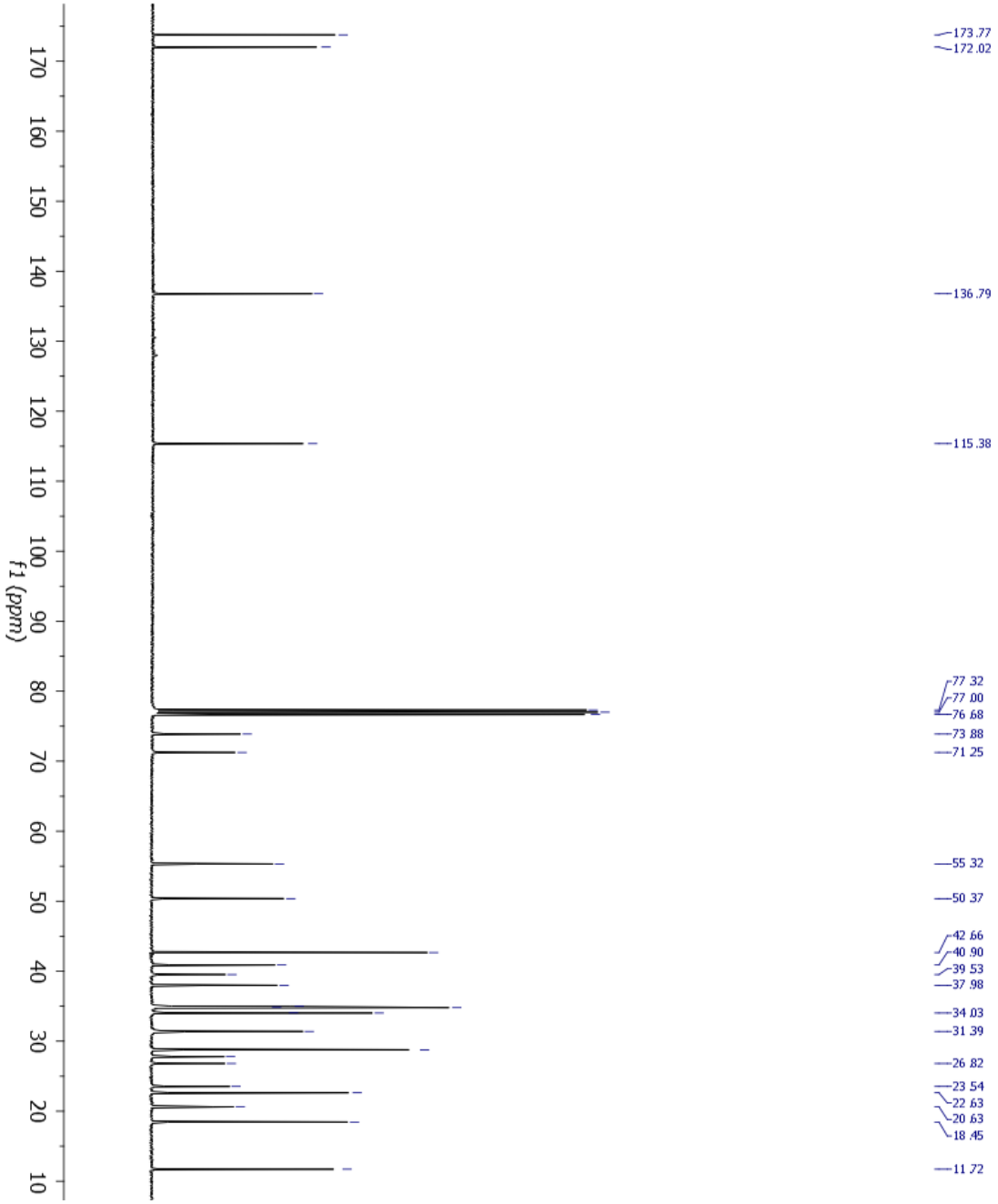

^{1}H NMR spectrum of *cis*-**N**

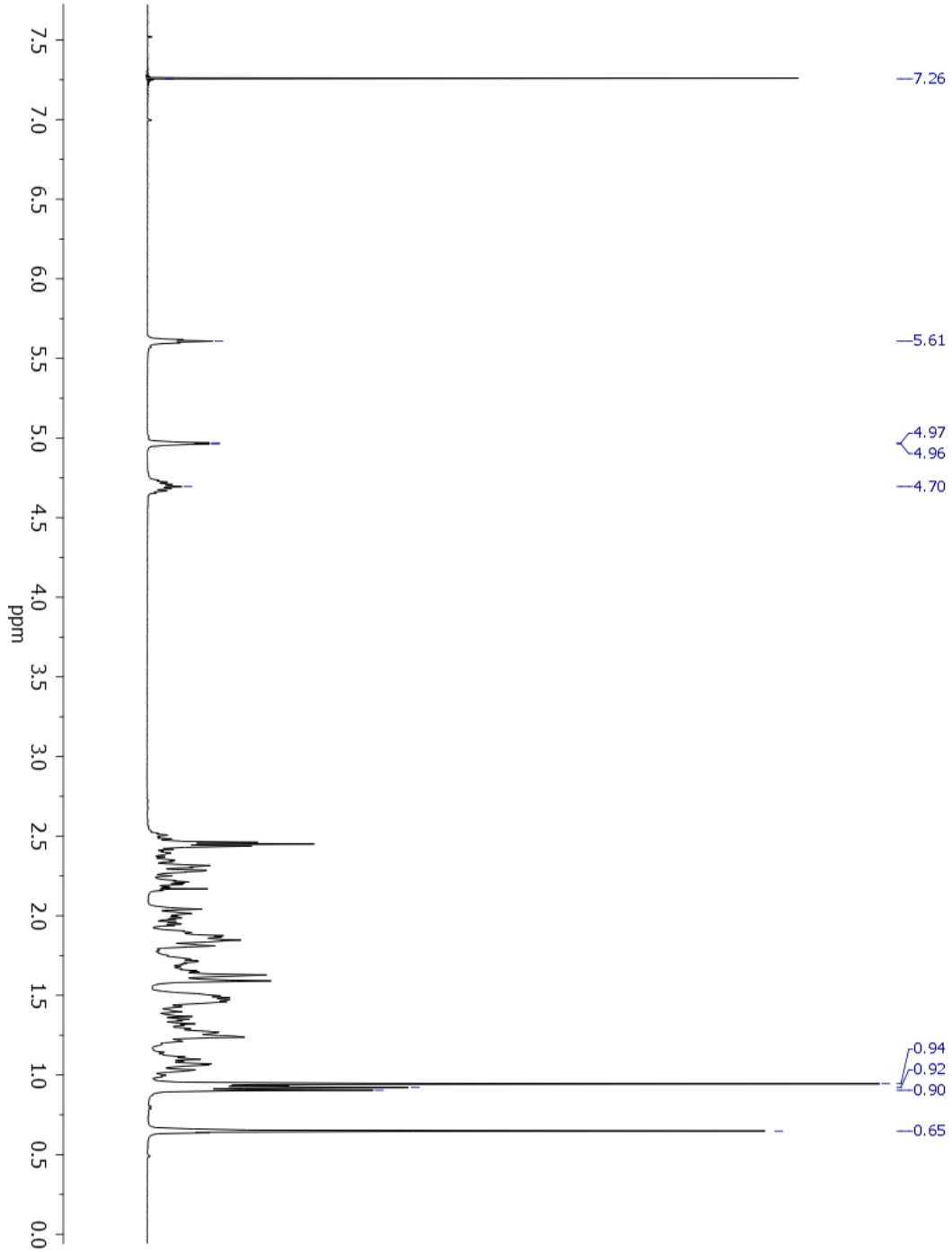

^{13}C NMR spectrum of *cis*-**N**

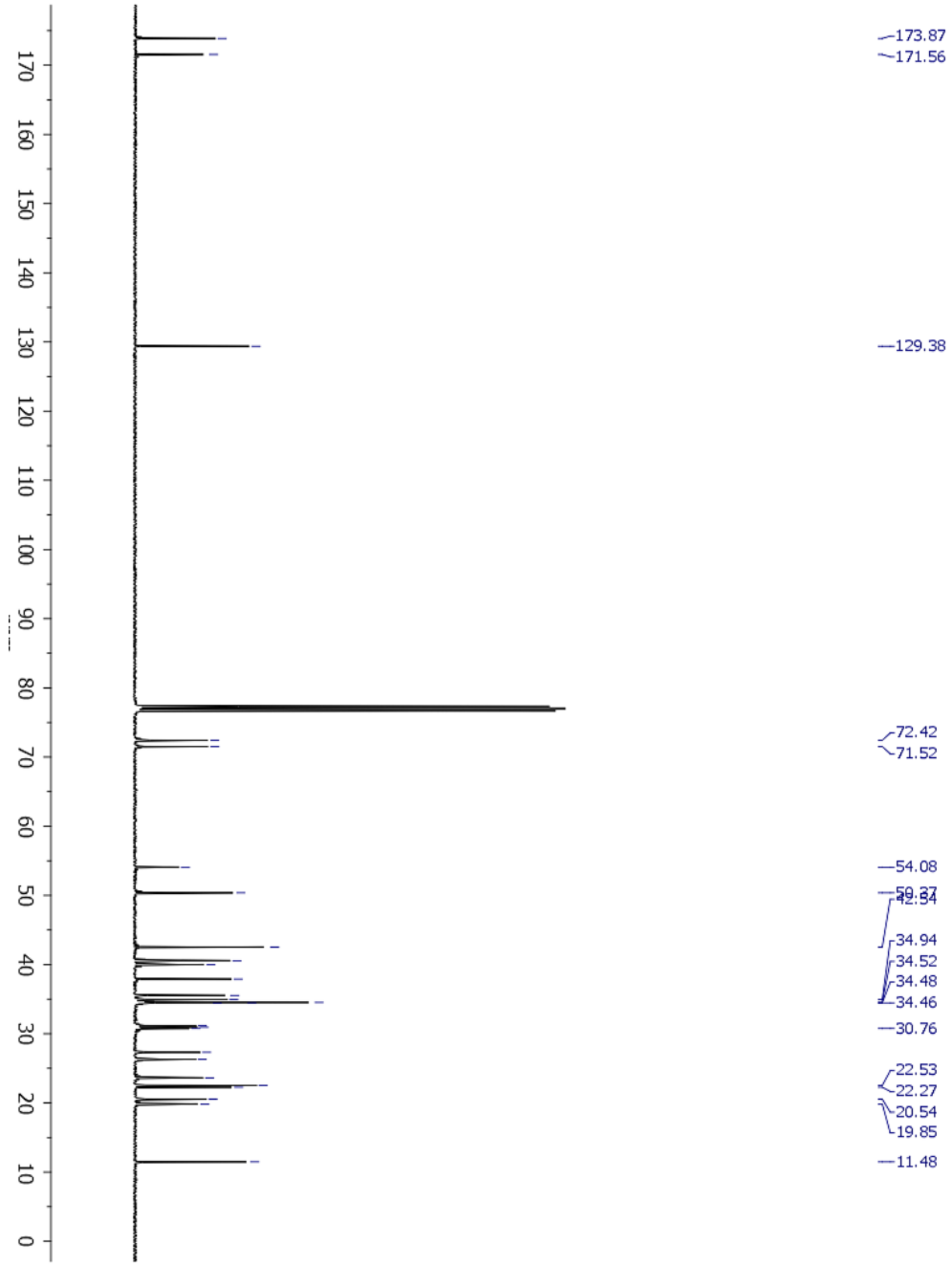

^{1}H NMR spectrum of *trans*-**N**

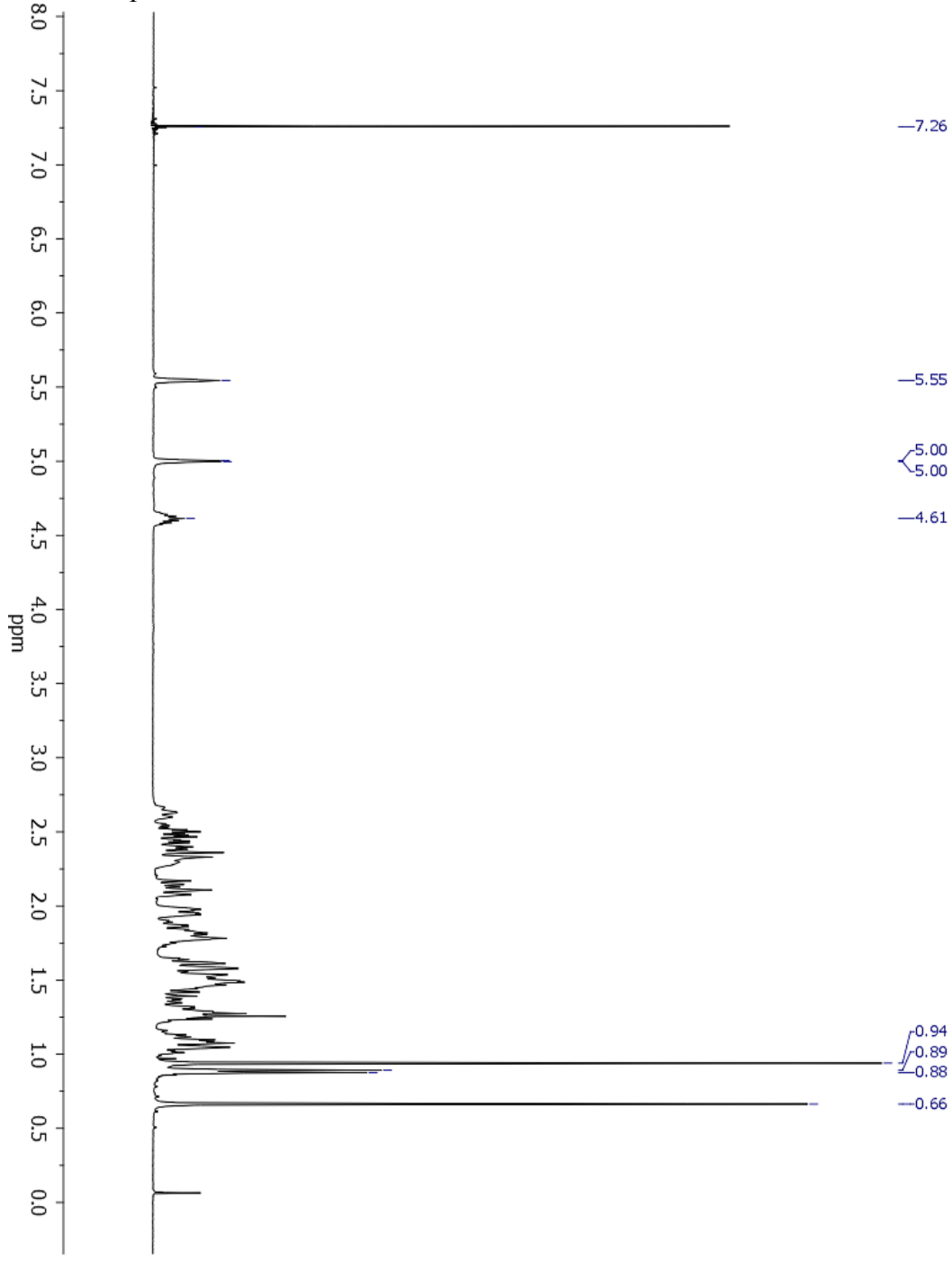

^{13}C NMR spectrum of *trans*-**N**

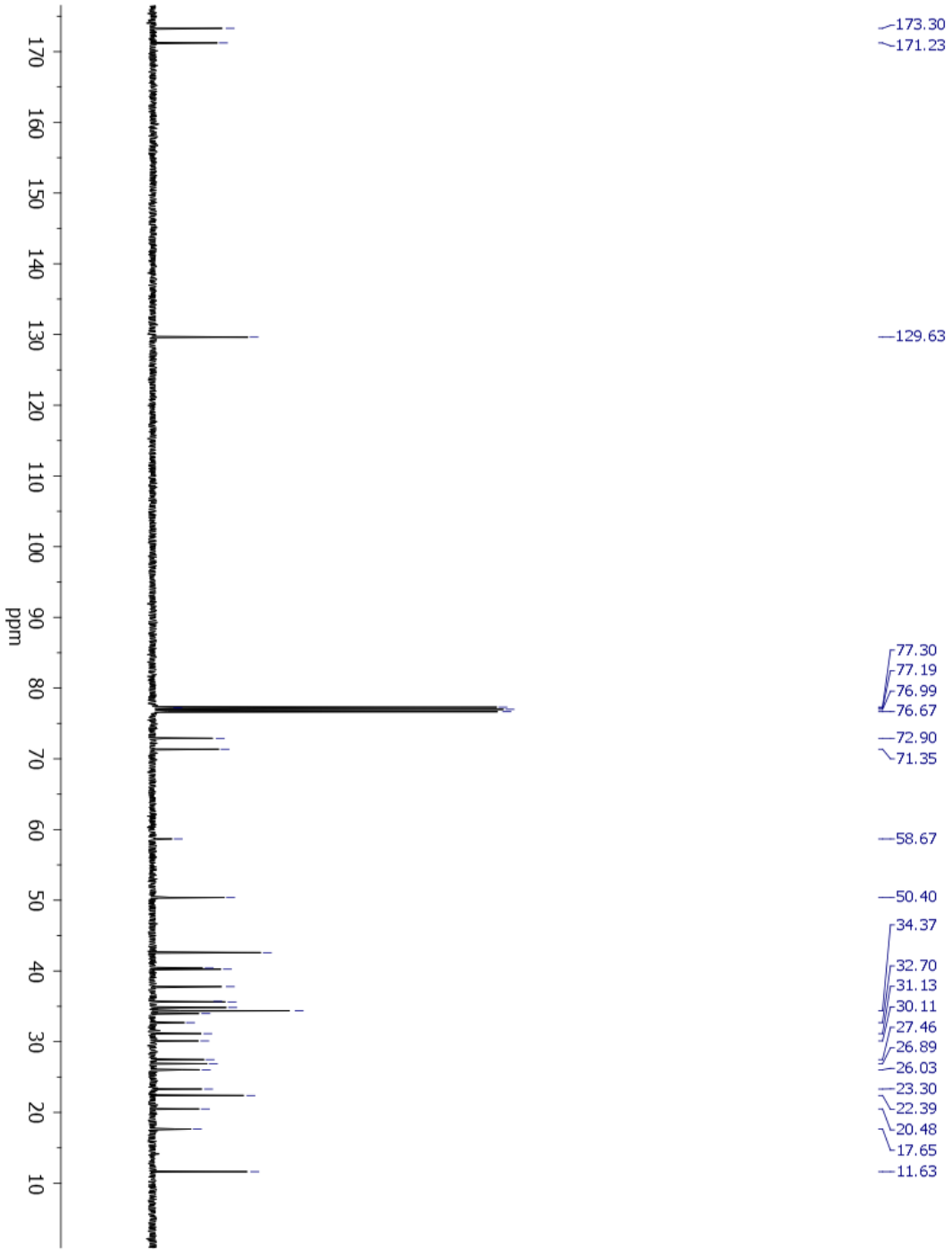

LRFAB of cyclodimer **K**

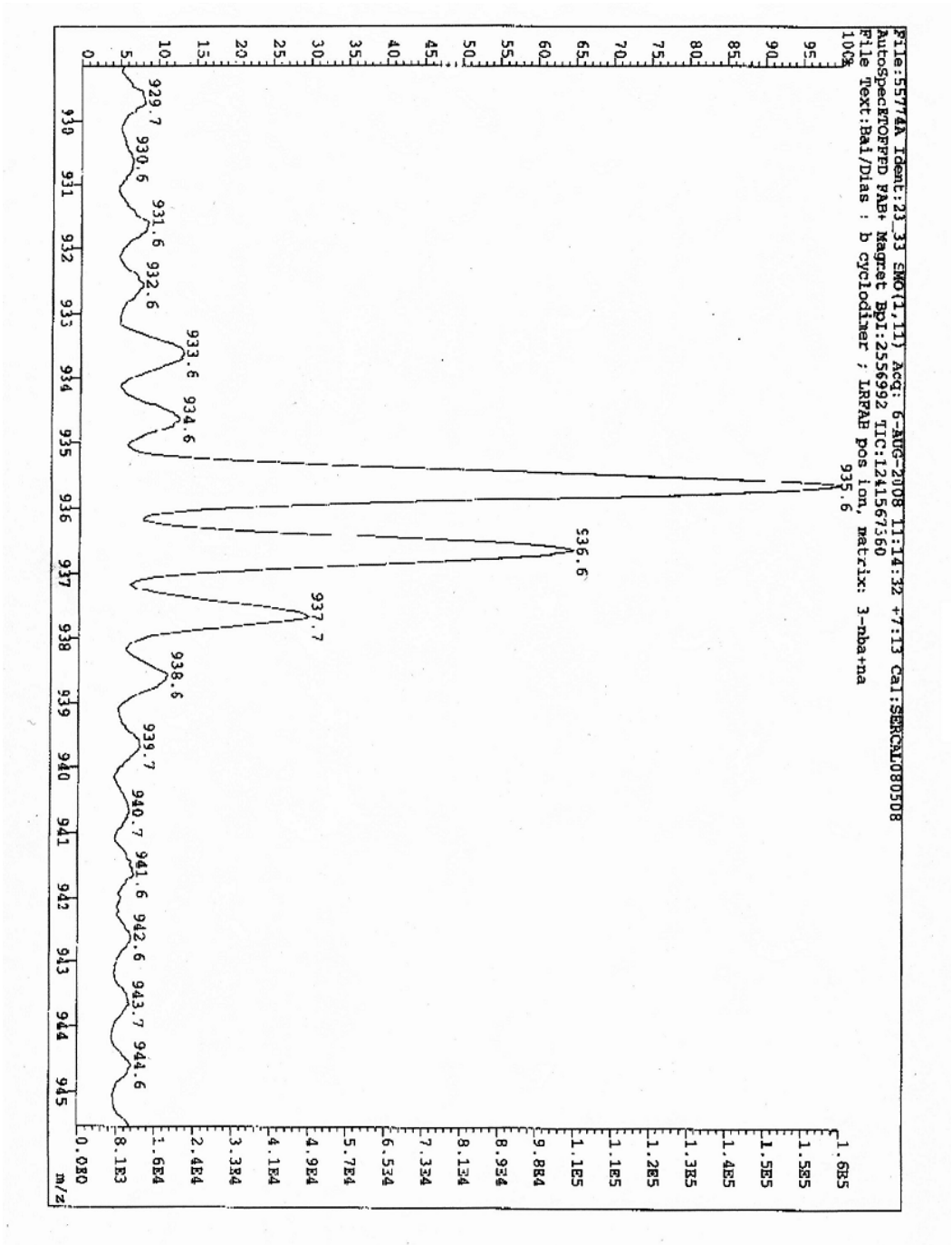

LRFAB of cyclotetramer **M**

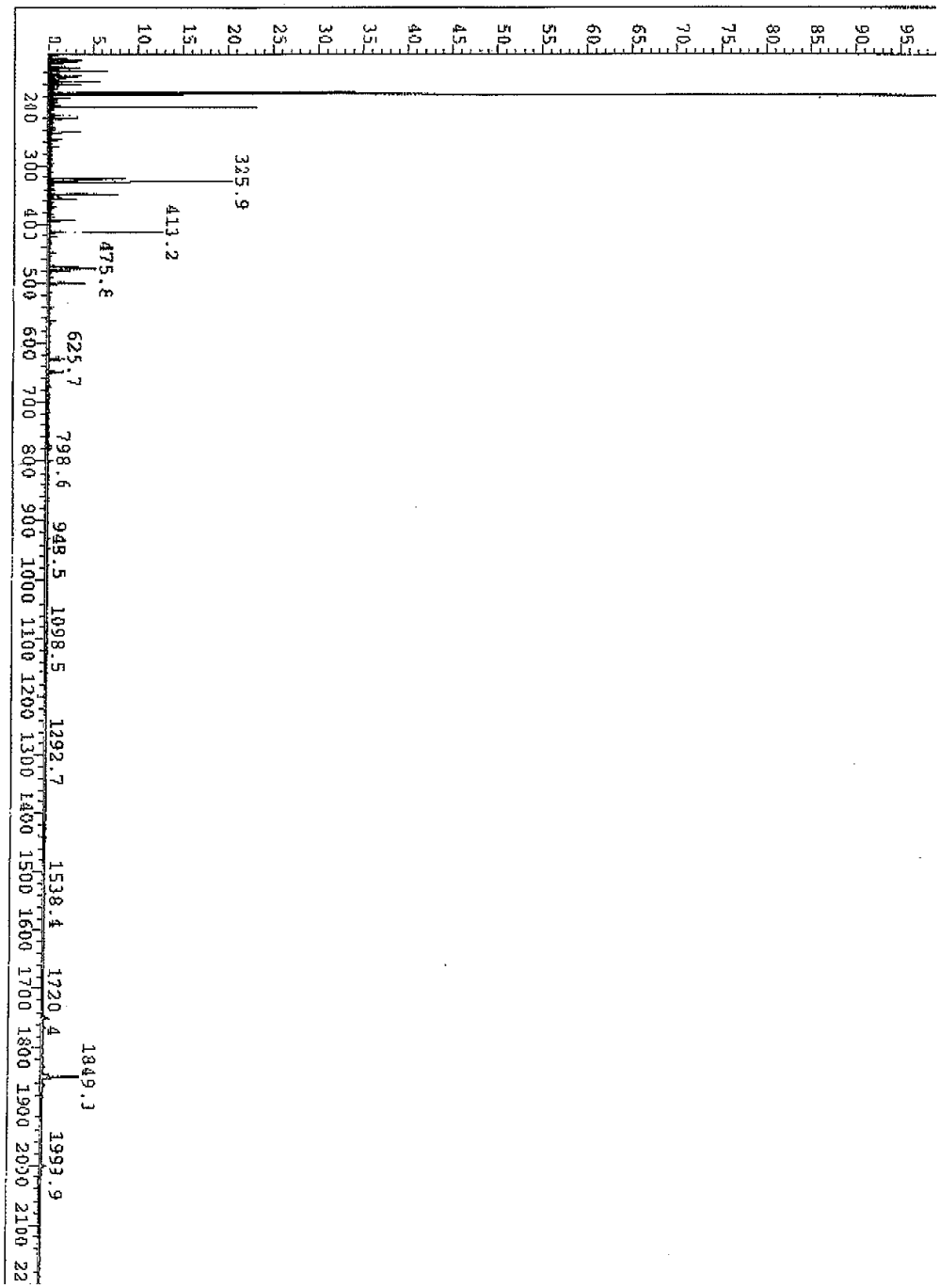

HRFAB of cyclotetramer **M**

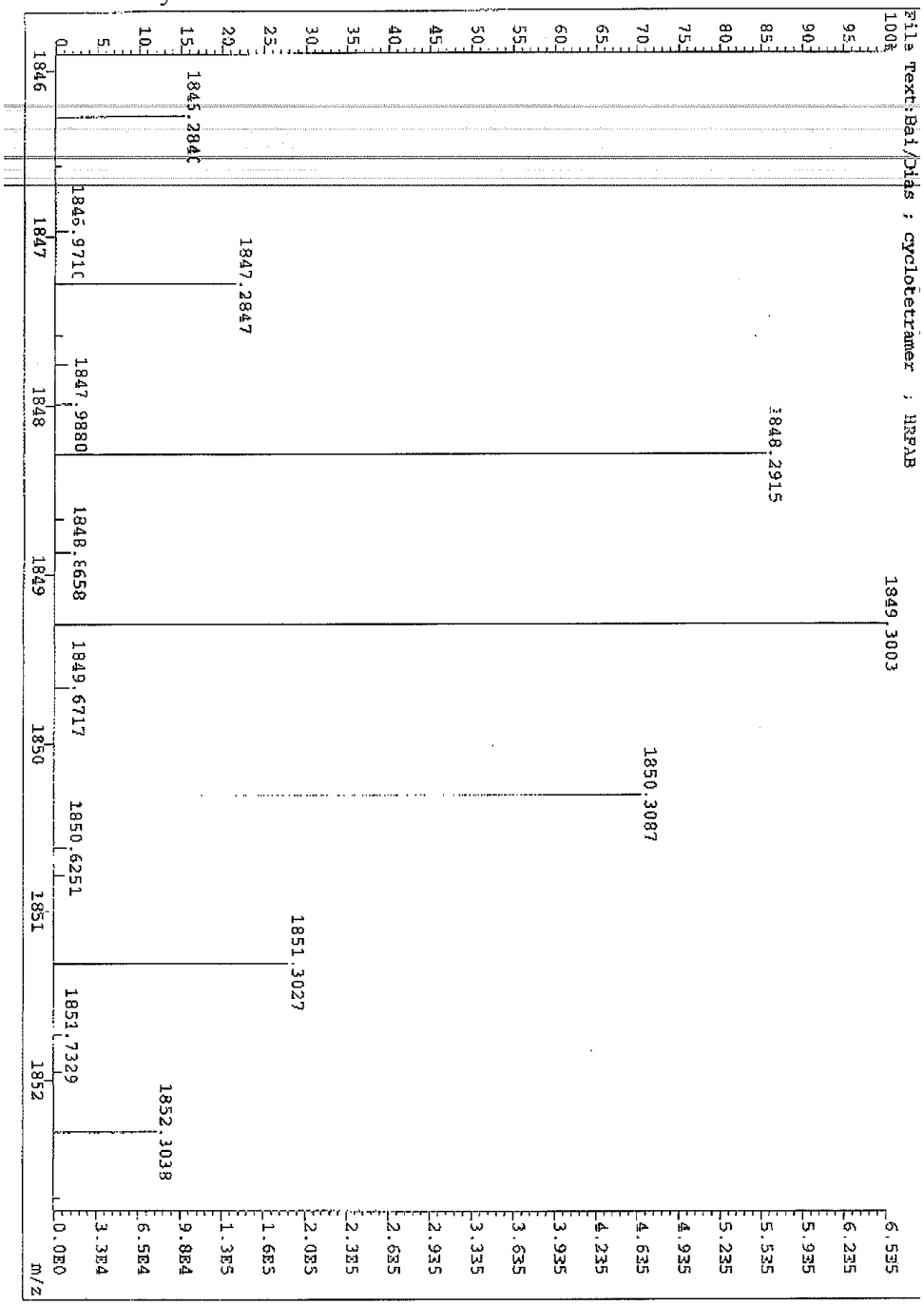

HRMS of *cis*-**5**

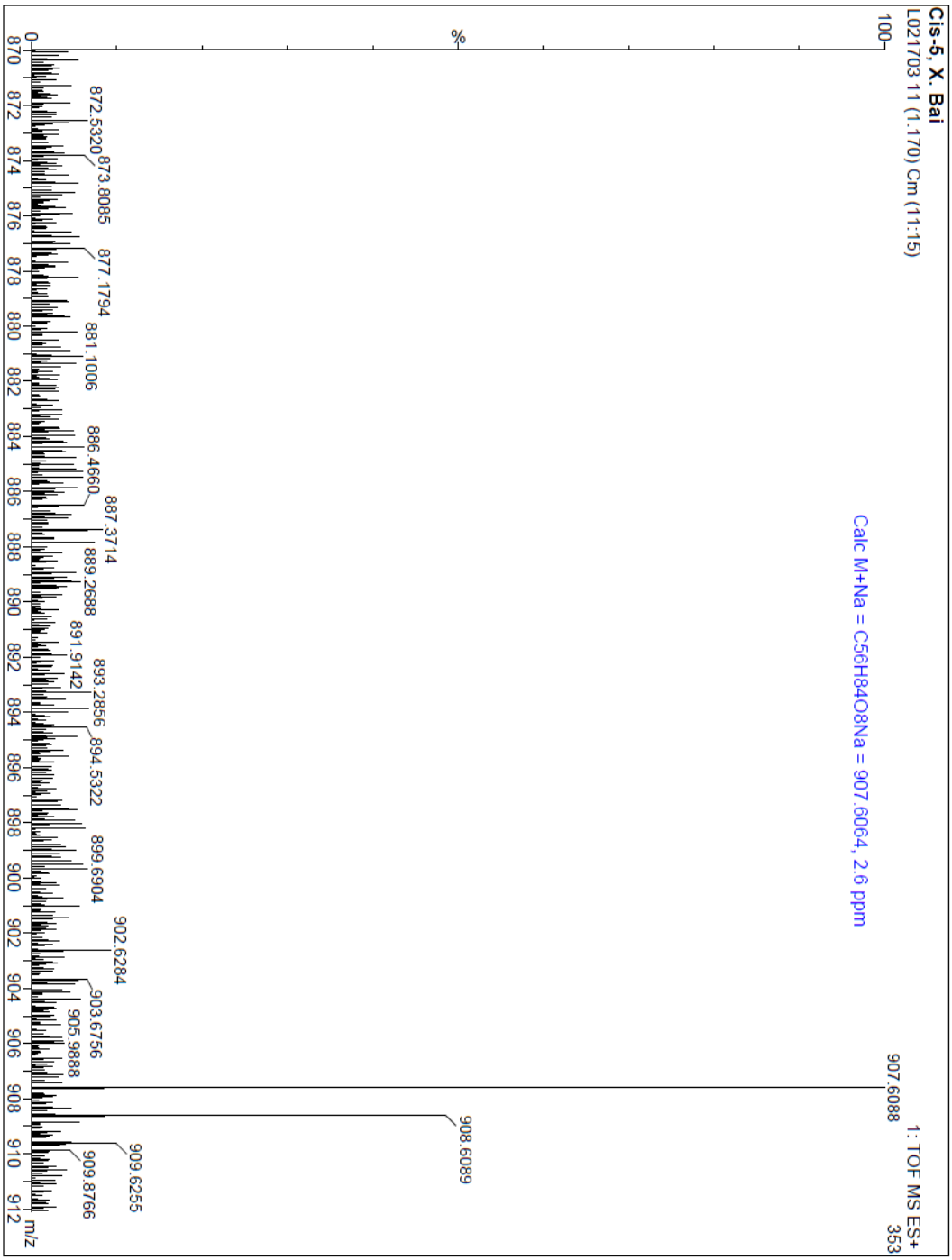
Cis-5, X. Bai
L021703 11 (1.170) Cm (11:15)
100
%
0
Calc M+Na = C56H84O8Na = 907.6064, 2.6 ppm
907.6088
908.6089
909.6255
909.8766
872.5320
873.8085
877.1794
881.1006
886.4660
887.3714
889.2688
891.9142
893.2856
894.5322
899.6904
902.6284
903.6756
905.9888
1: TOF MS ES+
353
870
872
874
876
878
880
882
884
886
888
890
892
894
896
898
900
902
904
906
908
910
912
m/z

HRMS of *trans*-**5**

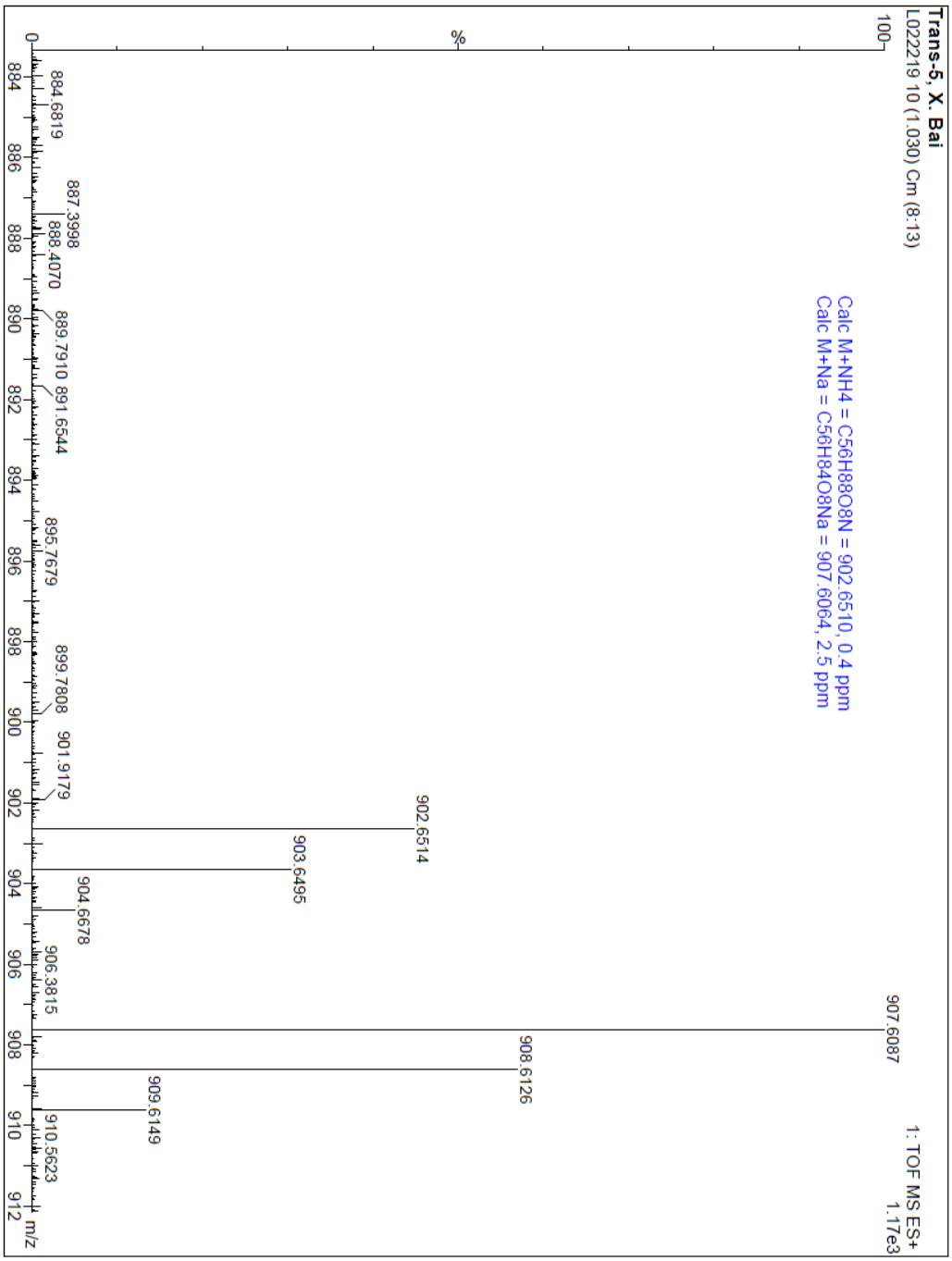

5. REFERENCES

[1] (a) Gokel,G.W.; Leevy,M.; Weber, M.E. "Crown Ethers: Sensors for Ions and Molecular Scaffolds for Materials and Biological Models," *Chem. Rev.* **2004**, *104*, 2723. (b) Izatt, E.; Bruening, R.; Krakowiak, K.; Izatt, S. "Contributions of Professor Reed M. Izatt to Molecular Recognition Technology: From Laboratory to Commercial Application," *Ind. Eng. Chem. Res.* **2000**, *39*, 3405. (c) An, H.; Bradshaw, J. S.; Izatt,R. M.; Yan, Z. "Bis- and Oligo(benzocrown ether)s," *Chem. Rev*. **1994**. *94*, 939. (d) Bradshaw. J. S.; Izatt, R. M. "Crown Ethers: The Search for Selective Ion Ligating Agents," *Acc. Chem. Res.* **1997**, *30*, 338.

[2] (a) Li,G.; Still, C.W. "An 18-Crown-6 Derivative with only One Conformation," *J. Am. Chem. Soc.* **1993**, *115***,** 3804. (b) Ji, R.; Chao, C.; Huang, Y.; Lan, Y.; Lu, C.; Luh, T. "Protonated Amino Acid-Induced One-Handed Helicity of Polynorbornene Having Monoaza-18-crown-6 Pendants," *Macromolecules* **2010**, *43*, 8813.

[3] (a) McKinlay, R.M.; Thallapally, P.K.; Atwood, J.L. "Hexameric *C*-alkylpyrogallol[4]arene Molecular Capsules Sustained by Metal-ion Coordination and Hydrogen Bonds," *Chem. Commun*. **2006**, 2956. (b) Jin, P.; Dalgarno, S. J.; Warren, J. E.; Teat, S. J.; Atwood, J. L. "Enhanced Control over Metal Composition in Mixed Ga/Zn and Ga/Cu Coordinated Pyrogallol[4]arene Nanocapsules," *Chem. Commun*. **2009**, 3348.

[4] (a) Yoon, D.; Hwang, H.; Lee, C. "Synthesis of a Strapped Calix[4]pyrrole: Structure and Anion Binding Properties," *Angew. Chem. Int. Ed*. **2002**, *41*, 1757. (b) Custelcean, R.; Delmau, L.; Moyer, B.; Sessler, J.; Cho, W.; Gross, D.; Bates, G.; Brooks, S.; Light, M.; Gale. P. "Calix[4]pyrrole: An Old yet New Ion-Pair Receptor," *Angew. Chem Int Ed*. **2005**, *44*, 2537.

[5] Sessler, J.; Kim, S.; Gross, D.; Lee, L.; Kim, J.; Lynch, V. "Crown-6-calix[4]arene-Capped Calix[4]pyrrole: An Ion-Pair Receptor for Solvent-Separated CsF Ions," *J. Am. Chem. Soc.* **2008**, *130*, 13162.

[6] Challa, R.; Ahuja, A.; Javed Ali, J.; Khar, R.K. "Cyclodextrins in Drug Delivery: An Updated Review," *AAPS Pharm. Sci. Tech.* **2005**; *6*, 43.

[7] (a) Williams, C. N. "Bile-acid metabolism and the liver," *Clinical Biochemistry* **1976**, *9*, 149. (b) Russell, D. W.; Setchell, K. D. R. "Bile Acid Biosynthesis," *Biochemistry*, **1992**, *31*, 4737.

[8] (a) Capello, A.; Moons, L. M. G.; Van de Winkel, A.; Siersema, P. D.; Dekken, Herman; Kuipers, E. J.; Kusters, J.G. "Farnesoid X Receptors and Their Role in the Etiopathogenesis of Systemic Malignancies," *American Journal of Gastroenterology* **2008**, 103, 1510. (b) Lefebvre, P.; Cariou, B.; Lien, F.; Kuipers, F.; Staels, B. "Role of Bile Acids and Bile Acid Receptors in Metabolic Regulation," *Physiol Rev*, 89, 147.

[9] (a) Alrefai, W. A.; Sarwar, Z.; Tyagi, S.; Saksena, S.; Dudeja, P. K.; Gill, R. K. "Cholesterol Modulates Human Intestinal Sodium-Dependent Bile Acid Transporter,"

Am. J. Physiol. Gastrointest. Liver Physiol. **2005**, *288*, 978. (b) Weinman, S.A.; Carruth, M. W.; Dawson. P. A. "Bile Acid Uptake via the Human Apical Sodium-Bile Acid Cotransporter Is Electrogenic," *The Journal of Biological Chemistry* **1998**, *273*, 34691.

10. Sievanen, E. "Exploitation of Bile Acid Transport Systems in Prodrug Design," *Molecules* **2007**, *12*, 1859.

[11] Swaan, P. W.; Hillgren, K. M.; Szoka, F. C., Jr.; Oie, S. "Enhanced Transepithelial Transport of Peptides by Conjugation to Cholic acid," *Bioconjugate Chem*. **1997**, *8*, 520.

[12] (a) Tolle-Sander, S.; Lentz, K. A.; Maeda, D. Y.; Coop, A.; Polli, J. E. "Increased Acyclovir Oral Bioavailability via a Bile Acid Conjugate," *Molecular Pharmaceutic*s 2004, 1, 40. (b) Balakrishnan, A.; Polli, J. E. "Apical Sodium Dependent Bile Acid Transporter (ASBT, SLC10A2): A Potential Prodrug Target," *Molecular Pharmaceutics* **2006**, *3*, 223.

[13] (a) Bonar-Law, R. P.; Davis, A. P. "Synthesis of Steroidal Cyclodimers from Cholic Acid; a Molecular Framework with Potential for Recognition and Catalysis," *Chem Commun*. **1989**, 1050. (b) Bhattarai, K. M.; Davis, A. P.; Perry, J. J.; Walter, C. J.; Menzer, S.; Williams, D. "A New Generation of "Cholaphanes": Steroid-Derived Macrocyclic Hosts with Enhanced Solubility and Controlled Flexibility," *J. Org. Chem*. **1997**, *62*, 8463.

[14] Davis, A. P.; Gilmer, J. F.; Perry, J. J. "A Steroid-Based Cryptand for Halide Anions," *Angew. Chem. Int. Ed*. **1996**, *35*, 1312.

[15] Sirikulkajorn, A.; Tuntulani, T.; Ruangpornvisuti, V.; Tomapatanaget, B.; Davis, A. P. “A Steroid-Based Receptor for Unprotected Amino Acids: the Enantioselective Recognition of l-tryptophan,” *Tetrahedron* **2010**, *66*, 7423. (b) Brotherhood, P. R.; Davis, A. P. “Steroid-Based Anion Receptors and Transporters." *Chem. Rev*. **2010**, *39*, 3633.

[16] (a) Gao, H.; Dias, J. R. “Synthesis and Characterization of Dimeric Bile Acid Ester Derivatives,” *J. Prakt. Chem*. **1997**, *339*, 187. b) Li, Y., Dias, J. R. “Dimeric and Oligiomeric Steroids,” *Chem. Rev*. **1997**, *97*, 283. (c) Gao, H.; Dias, J. R. “Synthesis of Cyclocholate Derivatives,” *Syn. Commun*. **1997**, *27*, 757. (d) Li, Y.; Dias, J. R. “Syntheses of Linear Dimeric and Cyclic Oligomeric Cholate Ester Derivatives,” *Synthesis* **1997**, 425. (e) Gao, H.; Dias, J. R. *Eur. J. Org. Chem*. “Cyclocholates with 12-Oxo and 7, 12-Oxo Groups,” **1998**, 719. (f) Gao, H.; Dias, J. R. “Synthesis of Cyclocholates and Derivatives, Part II. Selective Synthesis of Cyclocholates from Linear Dimers,” *New J. Chem.* **1998**, 579. (g) Dias, J. R.; Pascal, R. A. Jr., Morrill, J.; Holder, A. J.; Gao, H.; Barnes, C. “Remarkable Structures of Cyclotri(deoxycholate) and Cyclotetra(24-norcholate) Acetate Esters,” *J. Am. Chem. Soc*. **2002**, *124*, 4647.

[17] (a) Inanaga, J.; Hirata, K.; Saeki, H.; Katsuki, T.; Yamaguchi, M. “ a Rapid Esterification by Means of Mixed Anhydride and Its Application to Large-ring Lactonization,” *Bull. Chem. Soc. Jpn.* **1979**, *52*, 1989. (b) Storer, R. I.; Takemoto, T.; Jackson, P. S.; Brown, D. S.; Baxendale, I. R.; Ley, S. V. “Multi-Step Application of Immobilized Reagents and Scavengers: A Total Synthesis of Epothilone C,” *Chem. Eur. J.* **2004**, 10, 2529.

18. a) Jensen, L. B.; Mortensen, K.; Pavan, G. M.; Kasimova, M. R.; Jensen, D. K.; Gadzhyeva, V.; Nielsen, H. M.; Foged, C. "Molecular Characterization of the Interaction between siRNA and PAMAM G7 Dendrimers by SAXS, ITC, and Molecular Dynamics Simulations," *Biomacromolecules* **2010**, *11*, 3571. (b) Shen, Y.; Zhou, Z.; Sui, M.; Tang, J.; Xu, P.; Van Kirk, E.A.; Murdoch, W. J.; Fan, M.; Radosz, M. "Charge-Reversal Polyamidoamine Dendrimer for Cascade Nuclear Drug Delivery," *Nanomedicine* **2010**, *5*, 1205. (c) Han, L.; Huang, R.; Liu, S.; Huang, S.; Jiang, C. "Peptide-Conjugated PAMAM for Targeted Doxorubicin Delivery to Transferrin Receptor Overexpressed Tumors," *Molecular Pharmaceutics* **2010**, *7*, 2156. (d) Laza-Knoerr, A. L.; Gref, R.; Couvreur, P. "Cyclodextrins for Drug Delivery," *Journal of Drug Targeting* **2010**, *18*, 645. (e) Nagpal, K.; Singh, S. K.; Mishra, D. N. "Chitosan Nanoparticles: A Promising System in Novel Drug Delivery," *Chemical & Pharmaceutical Bulletin* **2010***, 58*, 1423.

[19] Gao, H.; Dias. J. R. "Selective Protection of the Various Hydroxyl Groups of Cholic Acid and Derivatives. A Review," *Organic Preparations and Procedures Int*. **1999**, *31*, 145.

[20] Su, C.; Williard, P. G. "Isomerization of Allyl Ethers Initiated by Lithium Diisopropylamide," *Org. Lett*. **2010**, *12*, 5378.

[21] Cyrus, K.; Wehenkel, M.; Choi, E.; Lee, H.; Swanson, H.; Kim, K. "Jostling for Position: Optimizing Linker Location in the Design of Estrogen Receptor-Targeting PROTACs," *Chem. Med. Chem.* **2010**, 5, 979.

[22] Wiles, C.; Watts, S.; Haswell, S. J.; Villar, E. P. "The Aldol Reaction of Silyl Enol Ethers within a Micro Reactor," *Lab on a Chip*. **2001**,100.

[23] (a) Saruwatari, T.; Praseuth, A. P.; Sato, M.; Torikai, K.; Noguchi, H.; Watanabe, K. "A Comprehensive Overview on Genomically Directed Assembly of Aromatic Polyketides and Macrolide Lactones Using Fungal Megasynthases," *Journal of Antibiotics* **2011**, *64*, 9. (b) Dalby, S. M.; Paterson, I. "Synthesis of Polyketide Natural Products and Analogs as Promising Anticancer Agents," *Current Opinion in Drug Discovery & Development* **2010**, *13*, 777. (c) Jarikote, D. V.; Murphy, P. V. "Metathesis and Macrocycles with Embedded Carbohydrates," *Eur. J. Org. Chem.* **2010**, 4959. (d) Hale, K. J.; Manaviazar, S. "New Approaches to the Total Synthesis of the Bryostatin Antitumor Macrolides," *Chemistry--An Asian Journal* **2010**, 5, 704. (e) Lespine, A.; Dupuy, J.; Alvinerie, M.; Comera, C.; Nagy, T.; Krajcsi, P.; Orlowski, S. "Interaction of Macrocyclic Lactones with the Multidrug Transporters: The Bases of the Pharmacokinetics of Lipid-Like Drugs," *Current Drug Metabolism* **2009**, *10*, 272.

[24] (a) Stoll, M. "Many Membered Rings and Musk Odor," *Drug & Cosmetic Industry* **1936**, *38,* 334. (b) Dhekne, V. V.; Ghatge, B. B.; Nayak, U. G.; Chakravarti, K. K.; Bhattacharyya, S. C. "Macrocyclic Musk Compounds. Part I. New Syntheses of Exaltolide, Exaltone, and Dihydrocivetone" *Journal of the Chemical Society* **1962**, 2348.

[25] (a) Livingood, C. S.; Head, E. S.; Johnson, E. A; Nilaseana, S. “Erythromycin in Local Treatment of Cutaneous Bacterial Infections,” *Journal of the American Medical Association* **1953**, *153*, 1266. (b) Guze, L. B.; Kalmanson, G. M.; “Action of Erythromycin on "Protoplasts" in Vivo,” *Science* **1964**, 146 1299.

[26] (a) Yu, X.; Guo, Z. S.; Marcu, M. G.; Neckers, L.; Nguyen, D. M.; Chen, G. A. “Modulation of p53, ErbB1, ErbB2, and Raf-1 Expression in Lung Cancer Cells by Depsipeptide FR901228,” *Journal of the National Cancer Institute* **2002**, *94*, 504. b) Zhu, W.; Otterson, G. A. “The Interaction of Histone Deacetylase Inhibitors and DNA Methyltransferase Inhibitors in the Treatment of Human Cancer Cells,” *Current medicinal chemistry* **2003**, 3, 187.

[27] (a) Parenty, A.; Moreau, X.; Campagne, J. M. “Macrocyclization by Ring-Closing Metathesis in the Total Synthesis of Natural Products: Reaction Conditions and Limitations,” *Chem. Rev*. **2006**, *106*, 911.

[28] (a) Nicolaou, K. C.; Sarabia, F.; Finlay, M. R. V.; Ninkovic, S.; King, P.N.; Vourloumis, D.; He, Y. “Total Synthesis of Oxazole- and Cyclopropane-Containing Epothilone A Analogues by the Olefin Metathesis Approach,” *Chem. Eur. J.* **1997**, *3*, 1971. (b) Seebach, D; Braendli, U; Schnurrenberger, P; Przybylski, M. “The Chemistry of 3-Hydroxy-alkanoates Poly- and Oligo-(3hydroxybutanoates (PHB, OHB),” *Helvetica Chimica Acta* **1988**, *71*, 155. (c) Jackson, R. F. W.; Sutter, M. A.; Seebach, D. “Preparation of (2*E*,4*E*,6*S*,7*S*,10*E*,12*E*,14*S*,15*S*,1′*S*)-7,15-Bis(1′-hydroxymethylethyl)-6,14-dimethyl-8,16-dioxa-2,4,10,12-cyclohexadecatetraene-1,9-dione. -A Building Block

for the Synthesis of Elaiophylin," *Liebigs Ann. Chem*. **1985**, 2313. (d) Fettes, A.; Carreira, E. M. "Leucascandrolide A: Synthesis and Related Studies," *J. Org. Chem*. **2003**, *68*, 9274.

[29] Heathcock, C. H. "Synthesis of the Macrolactone Disaccharide Subunit of Tricolorin A," *J. Org. Chem*. **1996**, *61*, 5208.

[30] Gonthier1, E.; Breinbauer, R. "Solid-Supported Reagents and Catalysts for the Preparation of Large Ring Compounds," *Molecular Diversity* **2005**, *9*, 51.

[31] Mulzer, J.; Berger, M. "Total Synthesis of the Boron-Containing Ion Carrier Antibiotic Macrodiolide Tartrolon B," *J. Org. Chem.* **2004**, *69*, 891.

PART II: Sonogashira Coupling for the Synthesis of Well-Defined π-conjugated Arylene Ethynylene Oligomers as Blue-Light-Emitting Materials

1. INTRODUCTION

1.1. The challenges for synthesis of arylene ethynylene conjugated oligomers and polymers and their applications

The fabrication of electronic and optoelectronic devices such as organic photovoltaic cells, organic field-effect transistors (OFETs) and organic light-emitting diodes (OLEDs) by using organic π-conjugated arylene ethynylene oligomers and polymers is of current interest. [1] For the past decades, great progress has been made to synthesize various rigid rod-like (poly) *p*-aryl acetylene polymers and triple-bond-containing oligomers as potential organic semiconductors; [2] however, due to the intrinsic defects of many synthetic strategies, it is impossible to make perfect highly conjugated arylene ethynylene polymers and large oligomers. Defects in the conjugated system lead to inferior electronic properties and limit their application for use in molecular electronics and photonics. [3] So far, the Sonogashira coupling reaction is the only efficient and useful method for the formation of π-conjugated triple-bond-containing systems. [4] As is known, the hetero coupling of iodo-substituted aromatic compounds with terminal alkyne is complicated by the homo coupling of the two terminal alkynes.[5] In particular, the polymerization between di-iodo-substituted aromatic compounds and dialkynes forms polymers containing a number of diyne units instead of ABAB type polymers, which breaks the conjugated system and greatly decreases their solubility, quantum yield and

purity. [6] Therefore, the synthesis of highly conjugated pure ABAB-type arylene ethynylene polymers via the Sonogashira coupling reaction is not promising. In addition, the synthesis of arylene ethynylene oligomers by Sonogashira coupling is also complicated by the presence of competing homo coupling induced by CuI and oxidizing agent. However, it is still feasible. Herein, we have conducted the systematic investigation of the unsymmetric alkynylation of electron-enriched aryl dihalides and their application to the stepwise-expansion of sp-sp^2 conjugated systems to form various pure arylene ethynylene oligomers, by using oxygen-free Sonogashira reaction conditions.

2. RESULTS AND DISCUSSION

2.1 Synthesis and characterization of mono-terminated di-*tert*-butyl-substituted oligo(phenylene ethynylene)s (OPEs).

Oxygen-free Sonogashira reaction conditions were employed for the synthesis of this series of OPEs. Un-substituted phenylene ethynylene oligomers with more than three units have very limited solubilities in most organic solvents; [7] therefore, the solubility enhancing group, *tert*-butyl, was introduced onto the conjugated system. The synthesis of oliogmers **4**, **5**, **6** and **7**, from commercially available 2, 6-di-*tert*-butylphenol is shown in Scheme 1, 2, 3 and 4. The methylation of 2, 6-di-*tert*-butylphenol was carried out using NaH and CH_3I in DMF solution to give compound **1**.[8] The subsequent iodination of compound **2** using ICl in CH_2Cl_2 formed 1, 3-di-*tert*-butyl-5-iodo-2-methoxybenzene (**2**) in high yield. The monoiodobenzene **2** was then coupled to trimethylsilylacetylene by

using oxygen-free Sonogashira coupling procedures.[6] The resulting terminal alkyne **3a** was deprotected using TBAF and THF, and was then coupled to ((4-iodophenyl)ethynyl)trimethylsilane to form oligomer **4a**. Deprotection of **4a** with TBAF provided **4b**, which was coupled with ((4-iodophenyl)ethynyl)trimethylsilane to afford trimer **5a.** Deprotection of **5a** and then coupling with ((4-iodophenyl)ethynyl)trimethylsilane produced **6a**. By repeating the deprotection and coupling steps, **6a** was converted to **7a**. Oligomers **5a-7a** have two *tert*-butyl groups on the end unit, which greatly enhances their solubilities in most organic solvents. Nevertheless, with increasing conjugation length, the solubility of the oligomers decreased.

By using a totally sealed reaction system, oxygen may be completely excluded from the reaction, according to the literature, [9] so that in principle, the homo coupling reaction induced by the co-catalyst CuI in the presence of oxygen is diminished. However, for the synthesis of this series of oligomers, we found that the homo-coupling side reaction remains non-negligible and even has the tendency to be the predominant reaction when the terminal alkynes have large bulky substitutent groups. In this study, when compound **3**, the terminal alkyne with a small substitutent group, was used for a Pd-coupling reaction, it gave the limited homo coupling side product, homo**2,** in only about 3%. With **4a**, **5a** and **6a** used as the terminal alkynes, the corresponding products homo**4**, homo**6**, and homo**8** were obtained in about 20%, 35-40%, and 60% respectively. This shows the trend that with increasing substituent group size on the terminal alkynes, the amount of

homo-coupling product is increased. This indicates that terminal alkynes with large substitute groups retard the Pd-catalyzed hetero coupling reaction and lead to more of the homo coupled product.

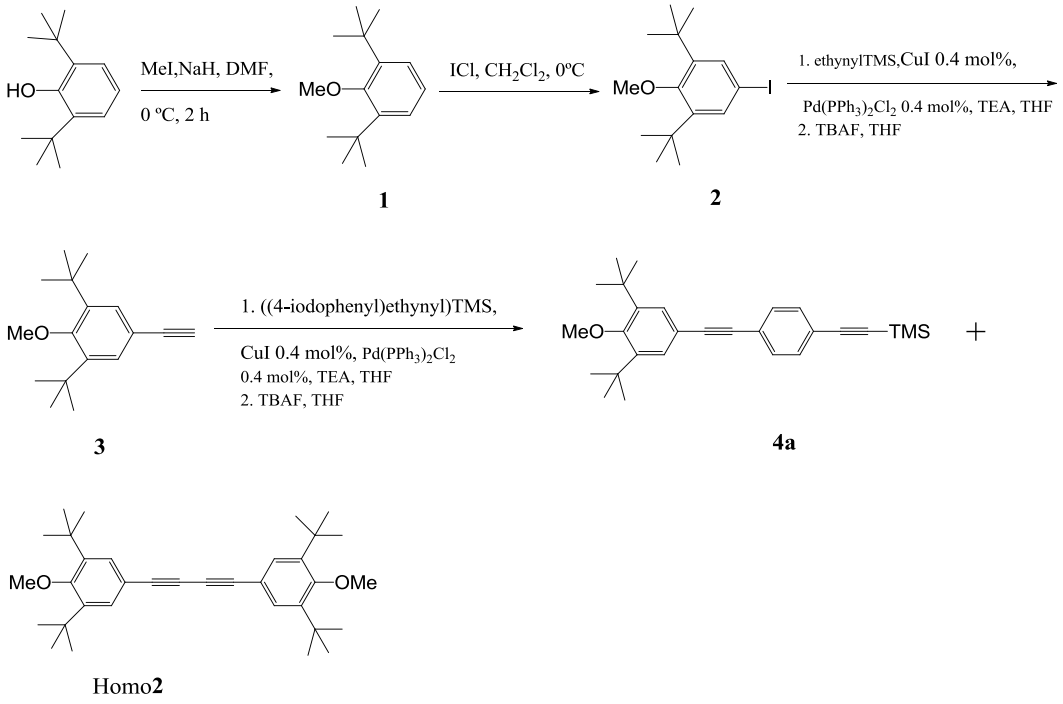

Scheme 1. The synthetic scheme for the synthesis of ((4-((3, 5-di-tert-butyl-4-methoxyphenyl) ethynyl)phenyl)ethynyl)trimethylsilane (**4a**).

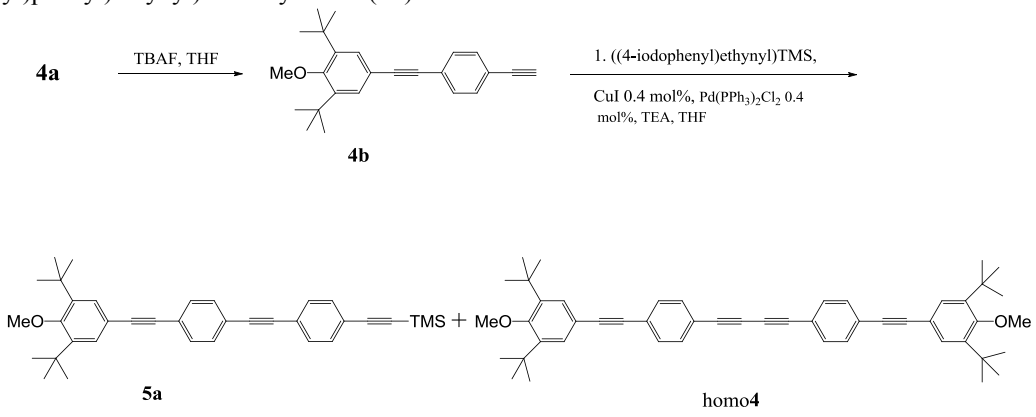

Scheme 2. The synthesis of oligomers **5a** and homo**4** by Pd-catalyzed coupling reaction.

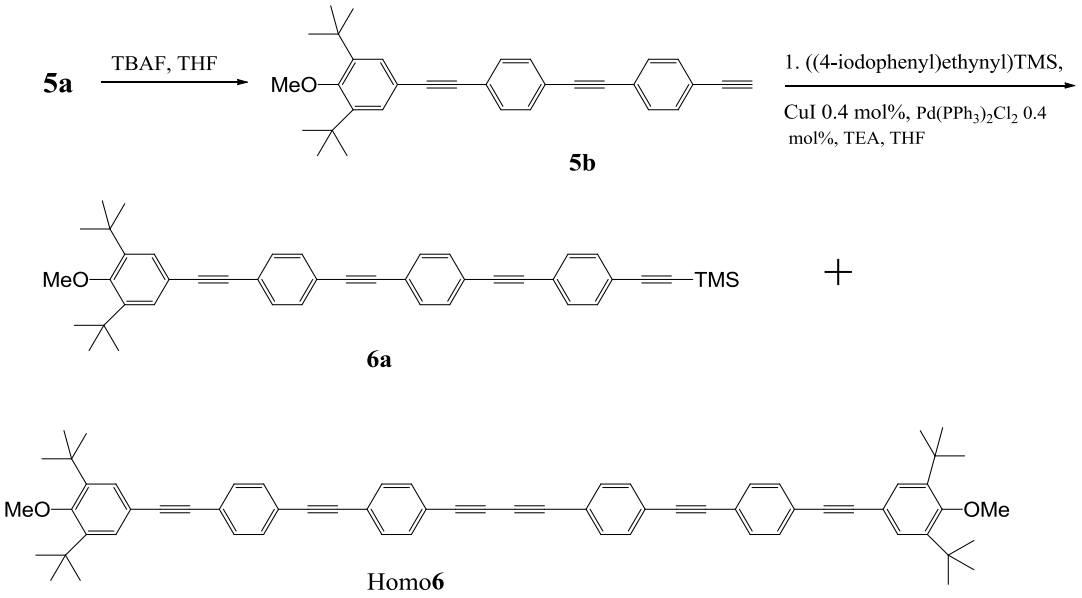

Scheme 3. The synthesis of oligomers **6a** and homo**6** by Pd-catalyzed coupling reaction.

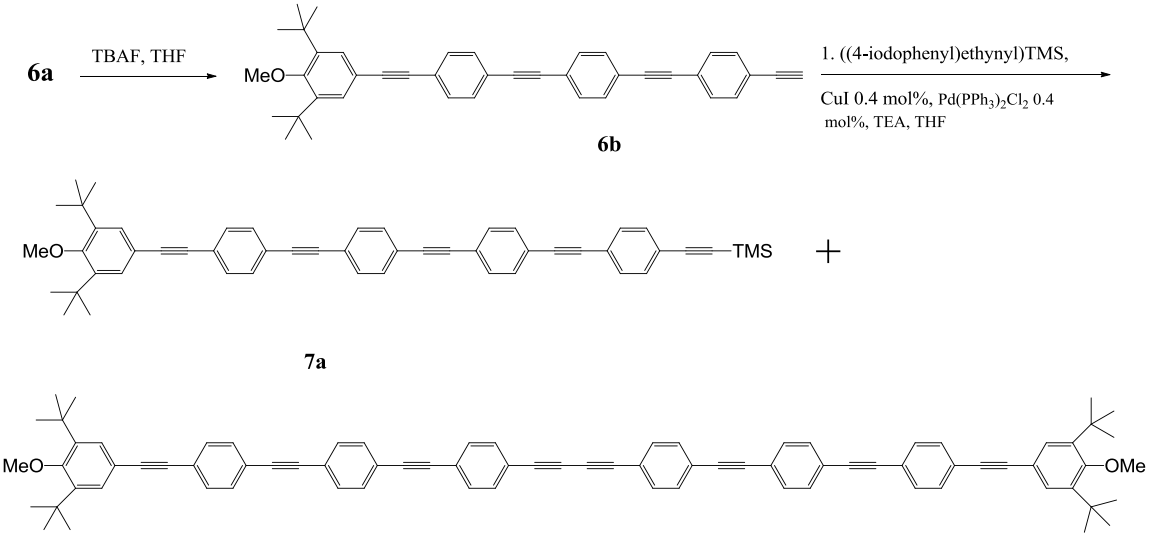

Scheme 4. The synthesis of oligomers **7a** and homo**8** by Pd-catalyzed coupling reaction.

This series of oliogmers has been fully characterized by NMR, MS (MALDI), UV and fluorescence spectroscopy. The formation of **5a**, **6a** and **7a** has been confirmed by

the integration of three signals above 7.00 ppm which represent 10, 14 and 18 protons, respectively, in Figure 1. The two protons on di-*tert*-butyl methoxyphenyl give a singlet at 7.43 ppm. The signals for four protons on the phenylethynyl trimethylsilane unit appear at 7.46 ppm and all other protons on the middle phenylene groups resonate at around 7.50 ppm.

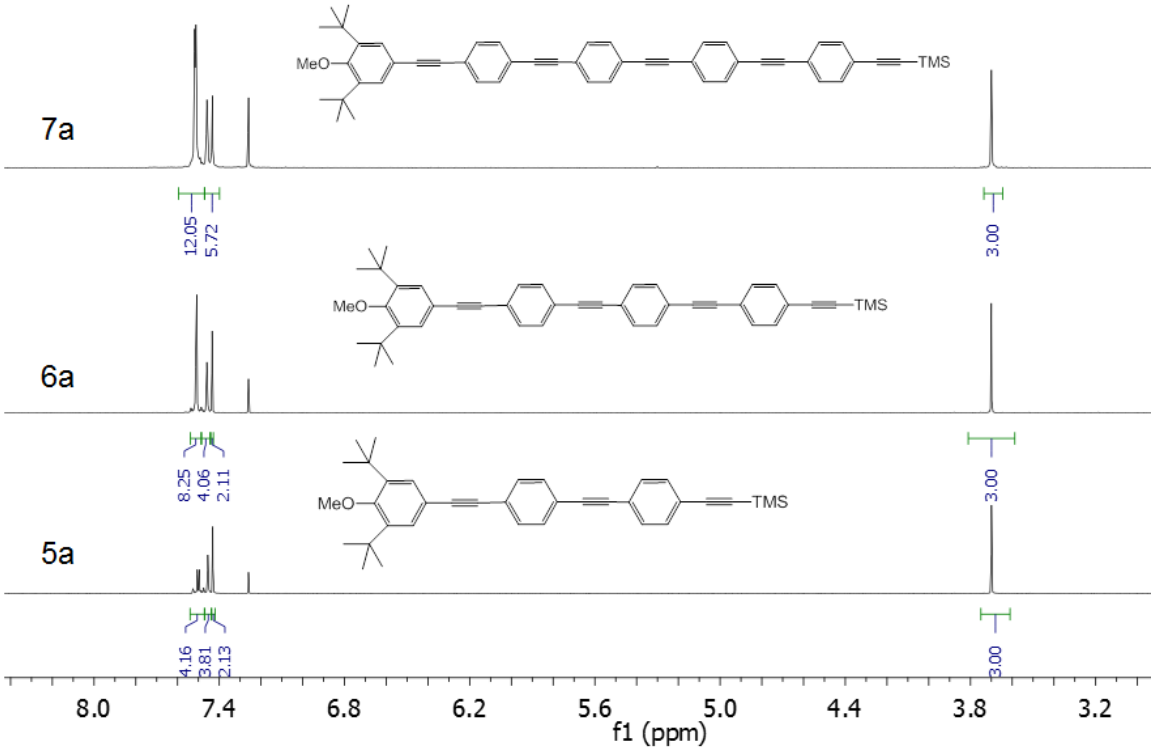

Figure 1. Partial ^{1}H NMR spectra of oligomers **5a**, **6a** and **7a** in $CDCl_3$.

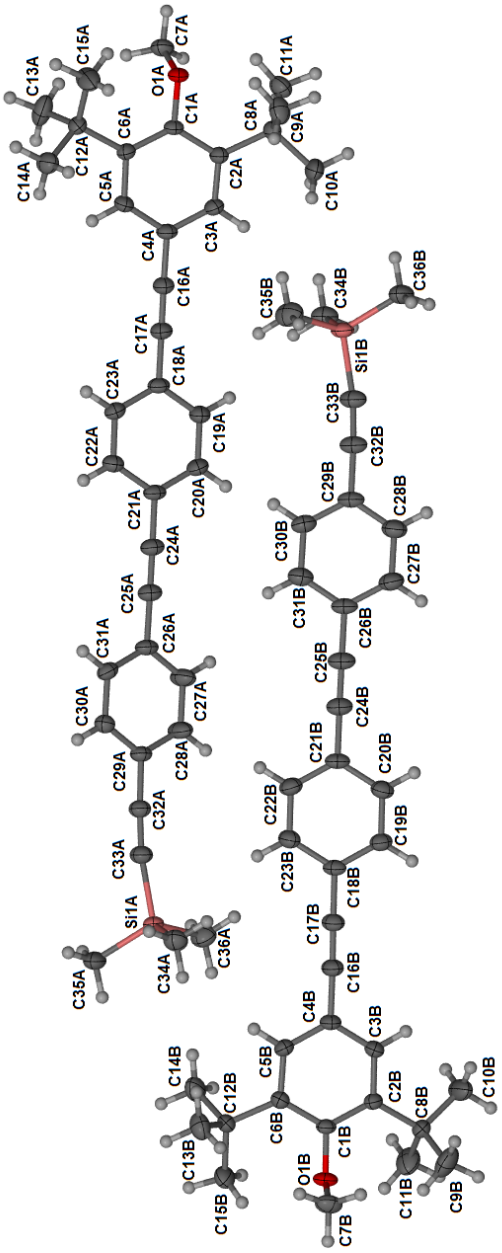

Figure 2.The crystal structure of **5a**. The displacement ellipsoids were drawn at the 50% probability level.

In addition, the structures of oligomer **5a**, **5b** and homo**4** are also confirmed by single crystal X-ray diffraction. The molecular structure of **5a** as revealed by X-ray

crystallography is shown in Figure 2. The oligomer **5a** crystallized in the triclinic space group P-1 with a basis composed of two independent molecules A & B. Molecule A and B are parallel to each other and oriented in opposite directions. Interestingly, one *tert*-butyl group on molecule B is disordered to two positions. In the drawing only the principal position is shown. Both the di-*tert*-butyl methoxyphenylene ring and the trimethylsilyl group are twisted and out of the conjugation plane. The dihedral angle between the di-*tert*-butyl methoxyphenylene ring and central ring is 160.70°. The C6-C1-C2 bond angle of **5a** is 122.4° instead of 120°, probably due to the inward squeezing of the *tert*-butyl on C(1) of **5a**, a similar phenomenon to what we found in the iodinated cyclopentadienone derivative having two *tert*-butyl groups.[10] The bond angles for C3-C4-C5, C19-C18-C23, C20-C21-C22, C27-C26-C31, and C28-C29-C30, in which the central carbons are adjacent to the triple bond, are 119°. All other bond angles on the phenylene rings are 120.5° except for the bond angles of C3-C2-C1 and C5-C6-C1 which have *tert*-butyl on C2 and C6. Their bond angles are 116.5° and 117.3° respectively.

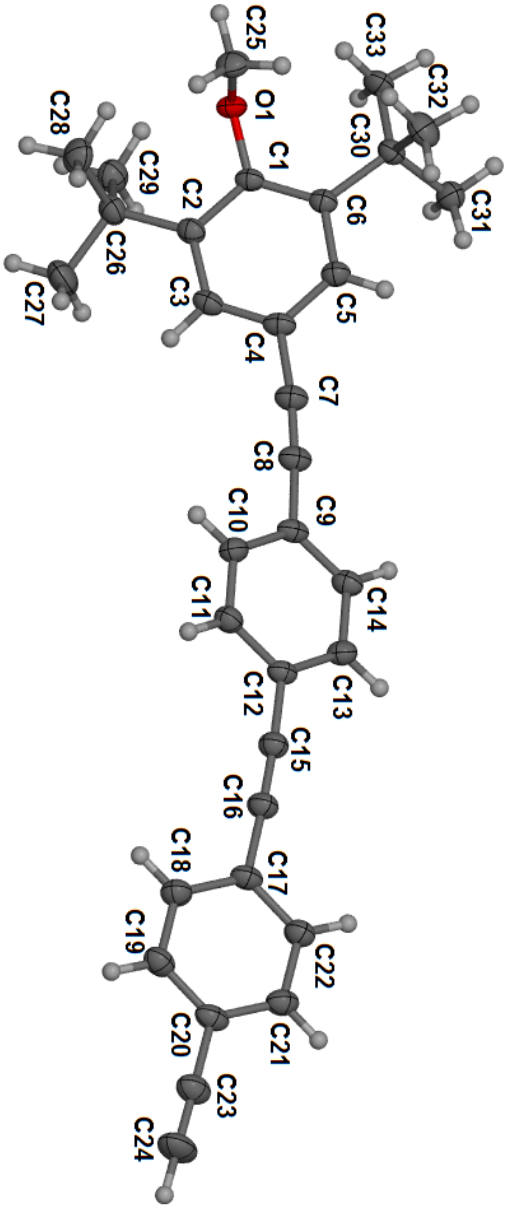

Figure 3. The crystal structure of **5b**. The displacement ellipsoids were drawn at the 50% probability level.

Compound **5b** crystalizes in the triclinic space group P-1. As shown in Figure 3, the three phenyl rings are not in the same plane, especially the di-*tert*-butyl methoxyphenyl

ring, which is significantly twisted from the conjugation plane with a torsion angle of 25.5°. Without the silyl group on the remote end of the triple bond, **5b** is more twisted and bent away from the π-π conjugation plane than the corresponding structure of **5a**.

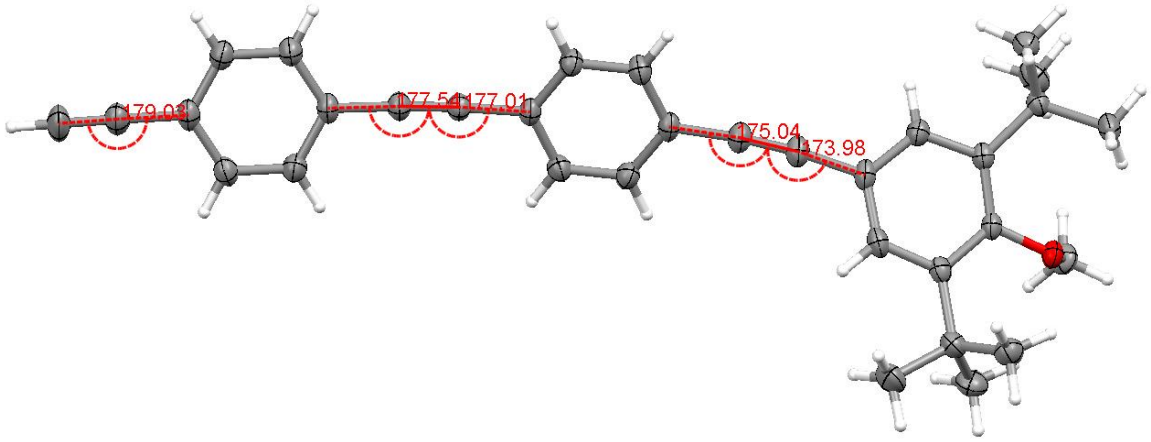

Figure 4. The crystal structure of **5b**. Bond angles between the triple bond and carbons on the phenyl ring are shown.

In addition, the bond angle between the carbons on the phenyl rings and the acetylenes, as shown in Figure 3, are 173.98, 175.04, 177.01, 177.54 and 179.03 °. It is clearly shown that the two bond angles close to the di-*tert*-butyl methoxyphenyl ring are particularly deformed and far from 180°. Probably, the two bulky *tert*-butyl groups on the phenyl ring and the unsymmetrical structure of this molecule are responsible for the bending of bond angles and the twisting of phenyl rings in the conjugation system. The twist of phenyl rings and bending both weaken the extent of sp^2-sp-sp^2-sp-sp^2 conjugation and decrease fluorescence emission. [11]

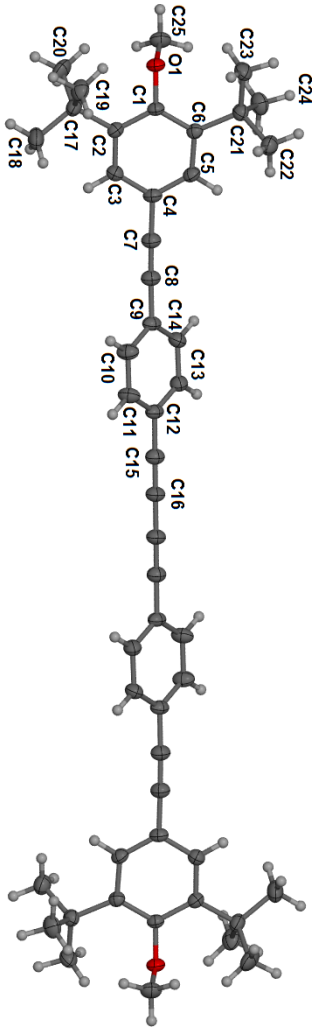

Figure 5.The crystal structure of homo **4**. The displacement ellipsoids were drawn at the 50% probabililty level.

Single crystal of homo**4** was obtained by slow evaporation of a hexanes/CH_2Cl_2 solution. The molecular structure of homo**4** is illustrated in Figure 5. It crystalized in the triclinic space group P-1.

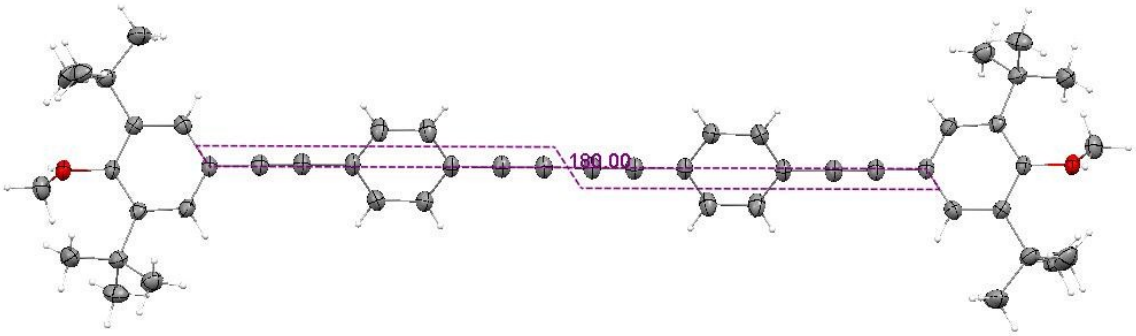

Figure 6. Torsion angle between two di-*tert*-butyl methoxy phenyl rings on homo**4**.

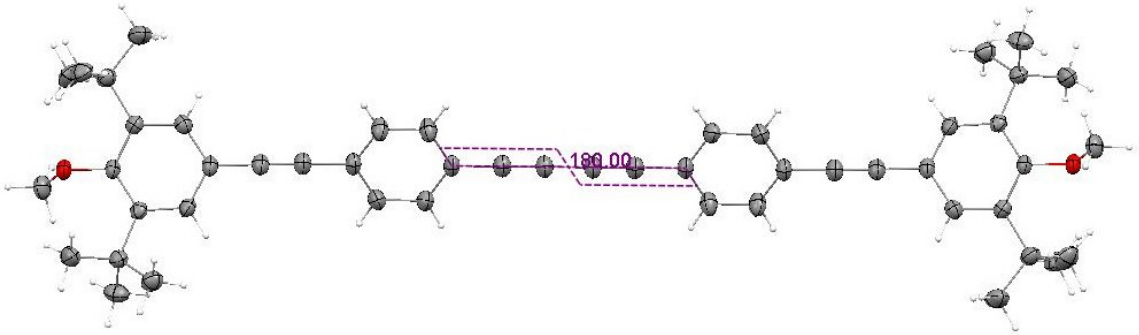

Figure 7. Torsion angle between two central phenyl rings on homo**4**.

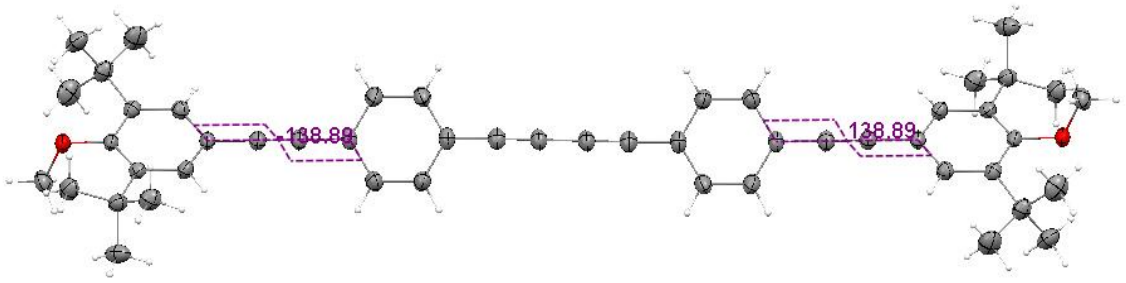

Figure 8. Torsion angle between the di-*tert*-butyl methoxy phenyl ring and its adjacent central phenyl ring on homo**4.**

From the X-ray crystal analysis, it is revealed that homo**4** is not planar, although it features a symmetrical structure. The two di-*tert*-butyl methoxyphenyl rings are in the same plane as each other, but they are twisted from the conjugated phenylene-acetylene plane. As shown in Figures 6, 7 and 8, the torsion angle between two di-*tert*-butyl methoxy phenyl rings and the torsion angle between two central phenyl rings are 180^{o}, and the torsion angle between the di-*tert*-butyl methoxyphenyl ring and the central phenyl ring is 138.89^{o}. This again indicates that the introduction of the *tert*-butyl groups for solubility enhancement is harmful to the conjugation system.

The absorption and fluorescence emission spectra for oligomers **4a**, **5a**, **6a** and **7a** in CH_2Cl_2 solution are shown in Figures 9 and 10. The spectroscopic data are summarized in Table 1. It is notable that the absorption maximum is red shifted with increasing conjugation length as repeat unit n varies from 2 to 5. There is a 38nm red shift when comparing **4a** to **5a** (n from 2 to 3), but the red shift from **6a** to **7a** is only 10 nm, which indicates that with each repeat unit increase, the red shift difference becomes smaller. The absorption spectra of the oligomers vary with the each addition of repeat unit to the conjugation system. There is almost no absorption for **4a** after 350nm, but **5a**, **6a** and

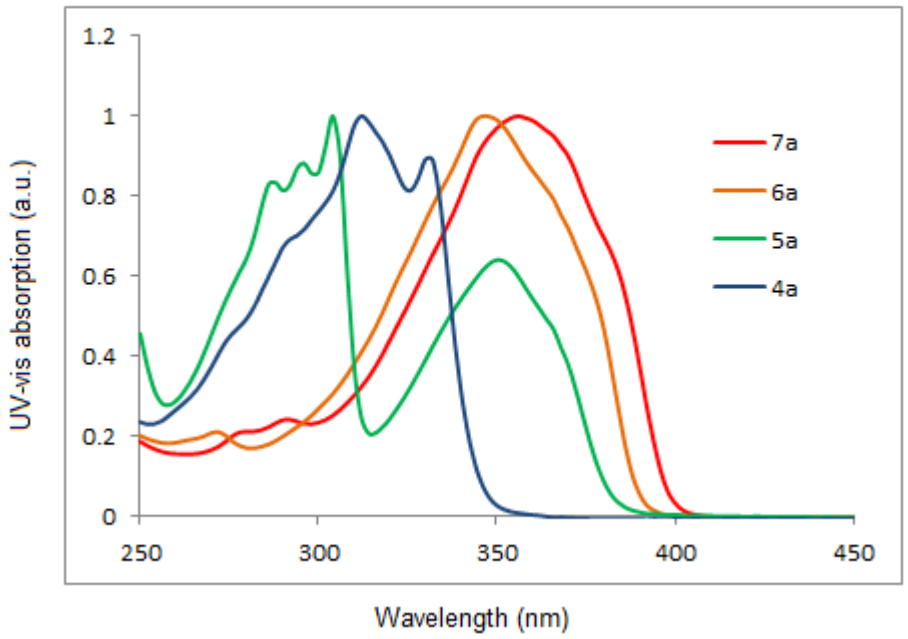

Figure 9. Normalized absorption spectra of **4a**, **5a**, **6a** and **7a** in CH_2Cl_2 solution.

7a all have the absorption maximum around 350 nm. In addition, oligomer **5a** has two distinctive peaks at 300 nm and 350 nm respectively and has the lowest absorption at 314 nm, at which **4a** has an absorption maximum instead.

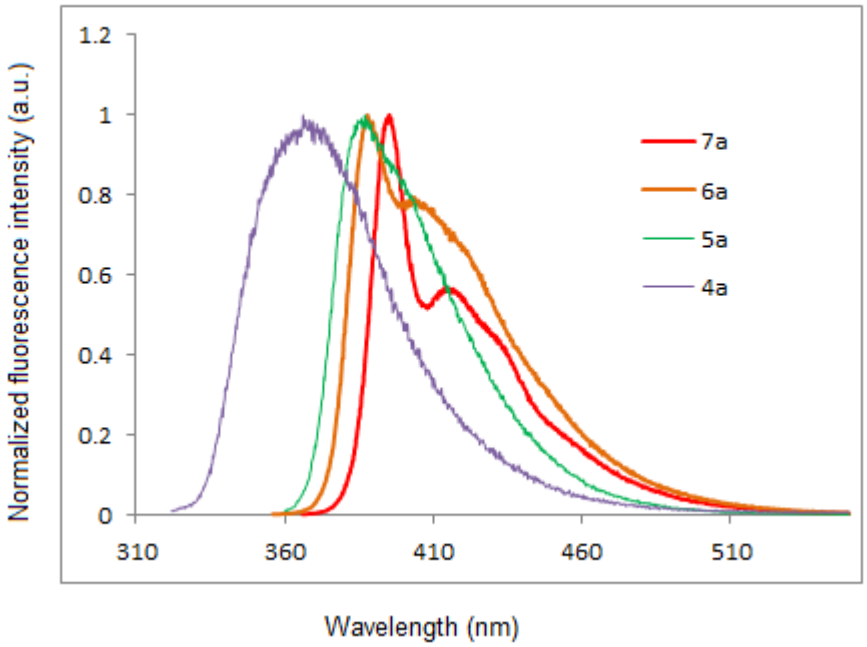

Figure 10. Fluorescence emission spectra of oligomers **4a-7a** in CH_2Cl_2 solution

Table 1. Spectroscopic Data for oligomers **4a-7a** in CH_2Cl_2 solution.

oligomer	λmax (abs) (nm)	λmax (emission) (nm)	Stokes shift (nm)	Φf
4a	312	366	54	0.343
4b	308	366	58	0.2
5a	350	387	37	0.536
5b	336	388	52	0.907
6a	346	388	42	0.986
7a	356	395	39	0.992

The photoluminescence spectra of **5a**, **5b** and **6a** with the same maximum intensity at 388 (387) nm were red-shifted by about 20 nm relative to that (366 nm) of **4a** and **4b**. In addition, the photoluminescence spectrum of **7a** has maximum emission at 395 nm and is red-shifted by 29 nm compare to that of **4a** and **4b**. The overall trend is that fluorescence maxima gradually red-shift as the number phenylene-ethylene units increases. In addition, the Stokes shift becomes smaller as the conjugation system becomes more extended. As shown in Table 1, the Stokes shift of **4a** is 54 nm, and the Stokes shift of **6a** and **7a** are 42 and 39 nm, correspondingly. As is shown in Table 1, the quantum yield is 0.34 for dimer **4a**, and 0.99 for pentamer **7a.** This shows the trend that the quantum yield of oligomers becomes higher with increasing conjugation length.

2.2 Synthesis and characterization of mono-terminated *tert*-butyl substituted mono-iodo phenylene-ethynylene oligomers.

This series of mono-iodo-substituted phenylene-ethynylene oligomers was synthesized using a sequential Sonogashira coupling/desilylation strategy (Scheme 5). The Sonogashira coupling of compound **3** with an excess of 1, 4-diiodobenzene afforded **8**. The mono-iodo oligomer **8** was coupled with ethynyltrimethysilane and was then desilylated to give **4b,** which upon further coupling with an excess of 1, 4-diiodobenzene, afforded **9**. Oligomer **10** was synthesized from **9** by repeating the reactions: coupling with the ethynyltrimethylsilane, desilylation, and reacting with an excess of 1, 4-diiodobenzene. Oligomer **11** was prepared from **10** by the same steps as for the synthesis of **10**. With increasing conjugation length of mono-iodo oligomers, solubility decreased. Due to its very limited solubility in common organic solvents, the ^{13}C NMR spectrum of oligomer **11** could not be obtained. It is difficult to synthesize and purify the mono-iodo oligomers with more than five phenyl units, especially since the iodo itself acts as a solubility decreasing group. As mentioned above, homo coupling cannot be avoided even when conducting the synthesis of mono-iodo substituted oligomers under oxygen-free conditions; the yields of mono-iodo oligomers become lower with increasing oligomer length. Meanwhile, the homo-coupling product, which is supposed to be the minor, becomes predominant with the increasing size of substituent groups on the terminal alkynes.

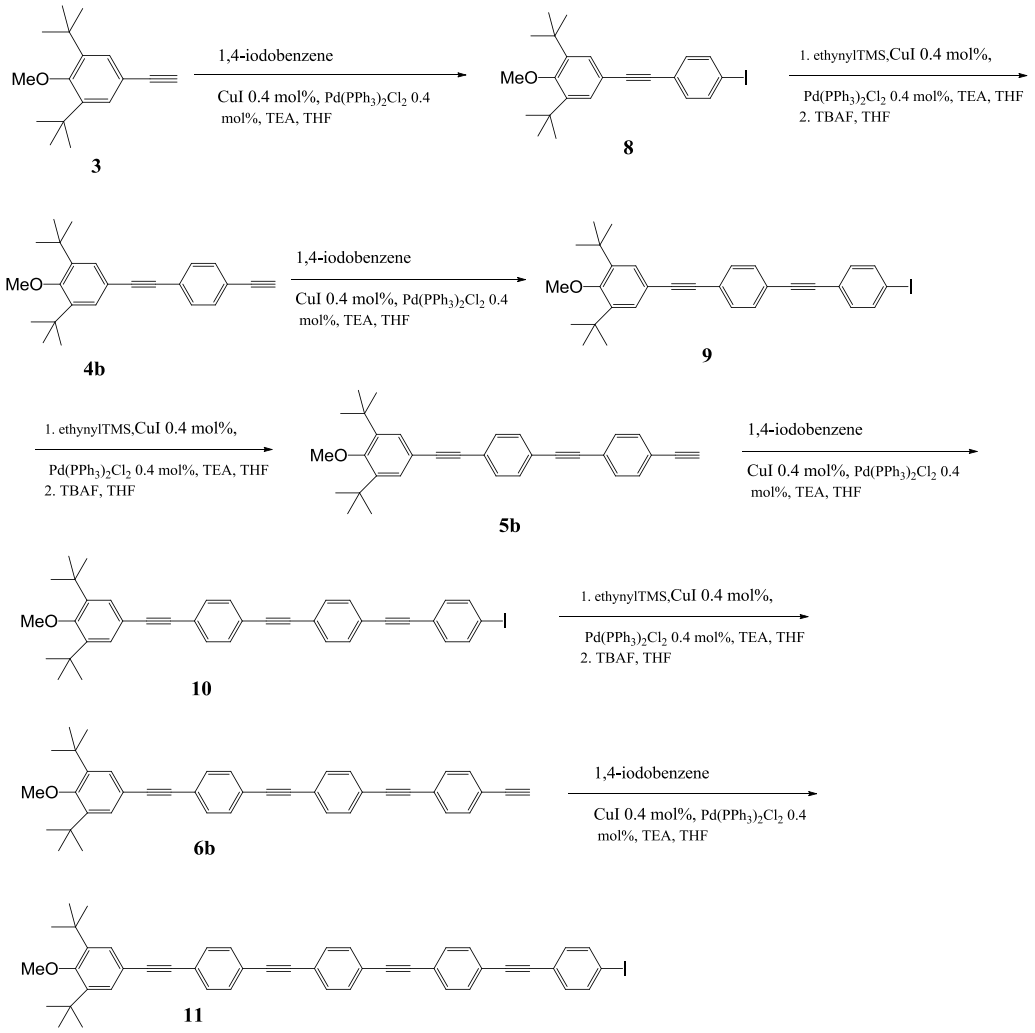

Scheme 5. The synthesis of mono-terminated *tert*-butyl-substituted mono-iodo phenylene ethynylene oligomers by Pd-coupling reaction.

2.3 Synthesis and characterization of unsymmetric phenylene-ethynylene trimers and tetramers with butoxy chains on the central units.

The synthesis of phenylene-ethynylene trimers **13a-d** is shown in Scheme 6. The ethynylbenzene was coupled with an excess of 1, 4-dibutoxy-2, 5-diiodobenzene to give the mono-iodo substituted compound **12**, followed by coupling with various terminal alkynes **a** through **d** to afford unsymmetrical trimers **13a-d**. For the synthesis of tetramers, the previously synthesized terminal alkynes, 1, 4-dibutoxy-2-ethynyl-5-(phenylethynyl) benzene, was used to couple with an excess of 1, 4-dibutoxy-2, 5-diiodobenzene, and the resulted mono-iodo oligomer **15** was then reacted with various terminal alkynes **a** through **d** to yield tetramers **16a-d**. It is observed that the yields for products **13a-d** decreases with the increasing size of the aromatic groups on the terminal alkynes despite use of the oxygen-free conditions. Again, it is confirmed that terminal alkynes with larger substituent groups contribute to higher proportions of homo coupling products. In addition, even when the *n*-butyl groups are proportionally introduced into the conjugated system with the conjugation length being grown stepwise, the resulting oligomers' solubilities still decreased with increasing conjugation length. It is noted that the solubility of tetramers with four n-butyl groups is lower than that of the corresponding trimers with two *n*-butyl groups. This means that the increase in solubility due to the butyl groups cannot offset the decrease in solubility due to the increased rigid-rod conjugation length. It is concluded that this series of phenylene-ethynylene oligomers

with butoxy chains on all central units should be completely insoluble when the conjugated system reaches to a critical length.

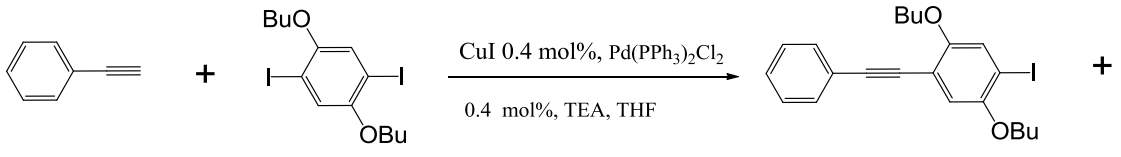

12

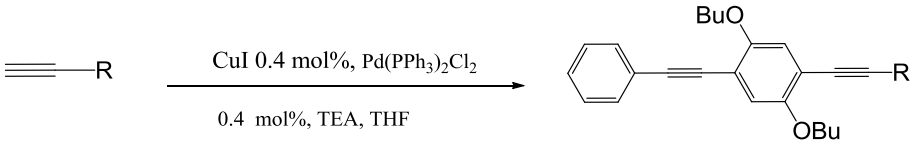

a-d

13a-d

Scheme 6. The synthesis of phenylene acetylene trimmers with various fluorescent chromophores

Entry	a-d	Product	Yield
1	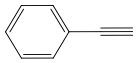	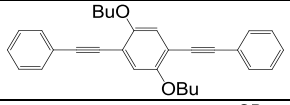	97%
2	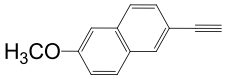	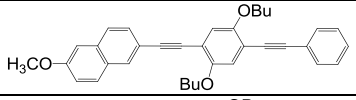	92%
3	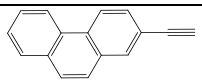	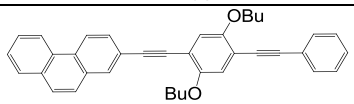	85%
4		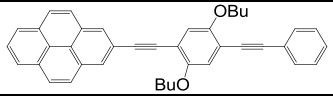	70%

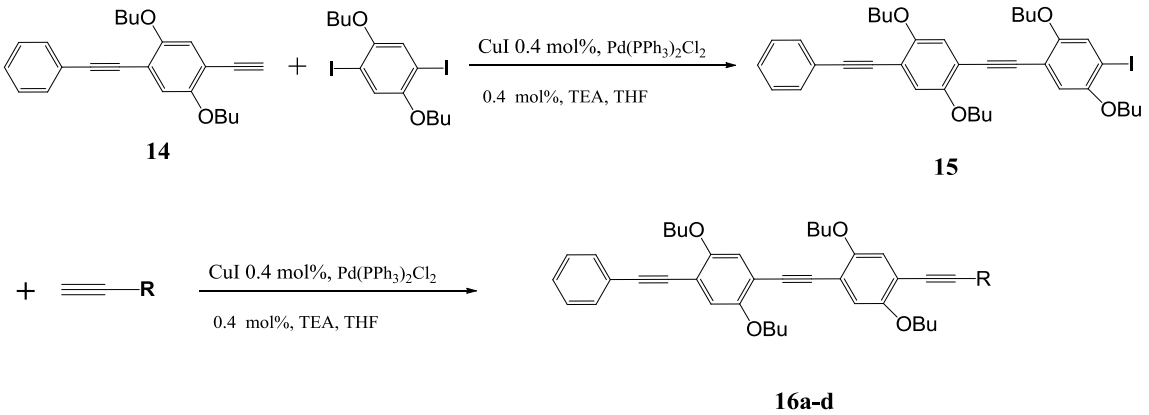

Scheme 7. The synthesis of phenylene-acetylene tetramers with various fluorescent chromophores.

Entry	13 a-d	Product	Yield
1	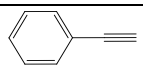	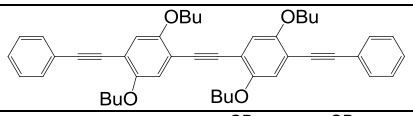	95%
2	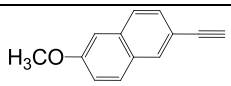	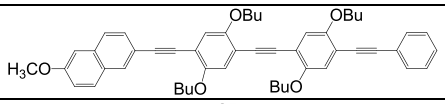	90%
3	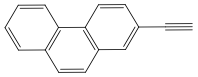	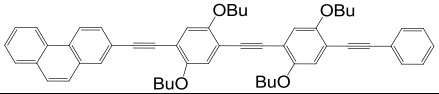	86%
4	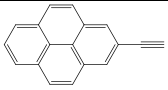	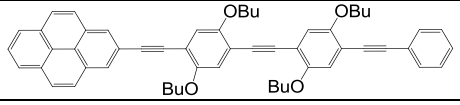	68%

The UV-vis absorption spectra for trimer **13a-d** are shown in Figure 11. The oligomers exhibit significant UV/vis bathochromic and hyperchromic shifts in their absorption spectra. Substituting the benzene ring with the more conjugated chromophores naphtalene, phenathrane, and pyrene groups, resulted in trimers **13a**, **13b**, **13c**, and **13d** having the maximum absorptions at 366, 374, 384 and 418 nm, respectively. This coincides with the fact that adding aromatic rings onto conjugated chromophores cause red shifts of these absorption bands. The emission-band trend for this series of timers is

as expected: **13a** with a benzene ending group emits at 400nm, and **13d** with a pyrene chromophore emits at 438 nm, as shown on Figure 12. The overall trend is a gradual red shift in the fluorescence maximum with additional conjugation on the chromophores. A shoulder appeared on the emission peak for all four oligomers **13a-d**.

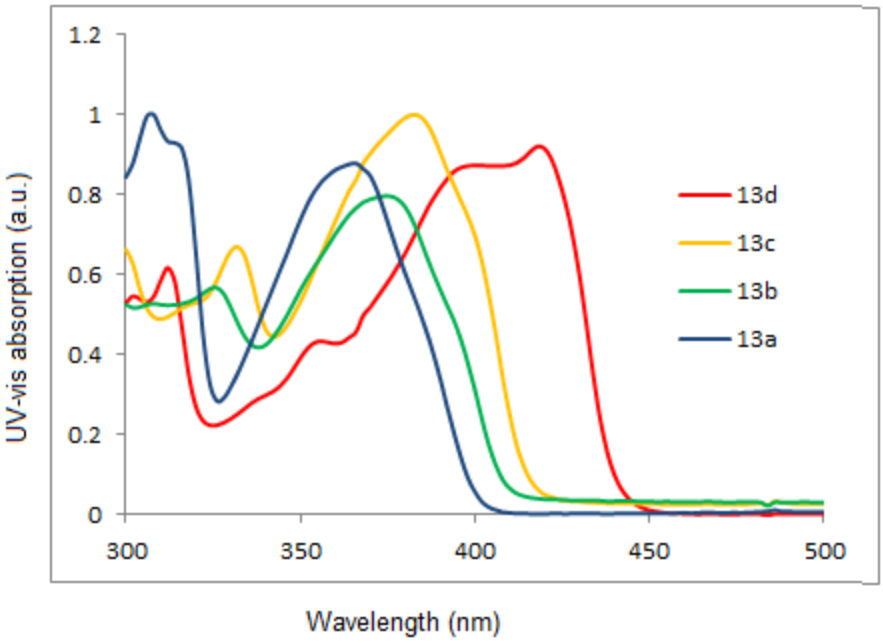

Figure 11. UV-vis absorption spectra of trimers **13a-d** in CH_2Cl_2 solution.

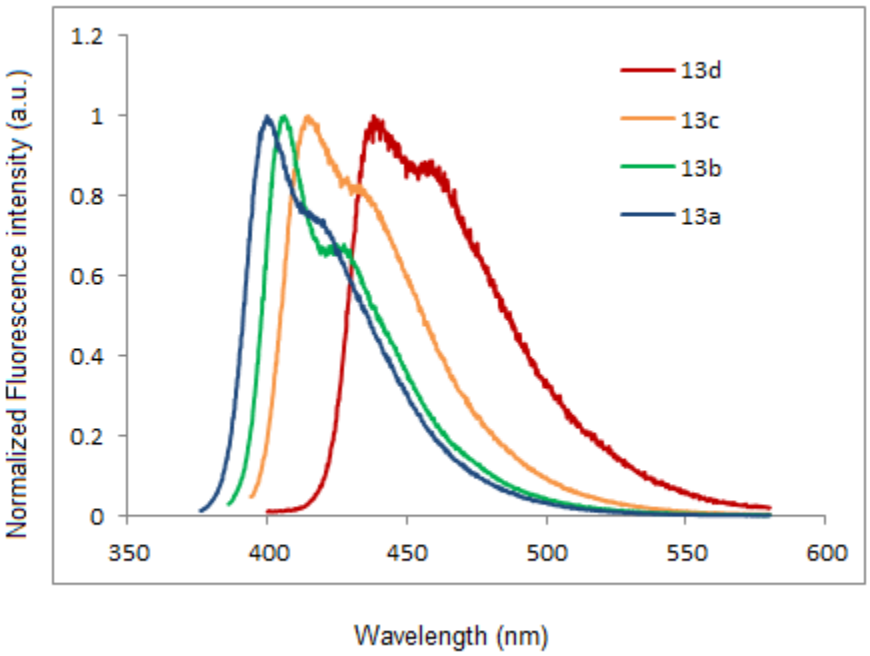

Figure 12. Fluorescence emission spectra of trimers **13a-d** in CH_2Cl_2 solution.

The absorption spectra for **16a-d** are shown in Figure 13. For tetramers **16a-d**, as chromophores varied from benzene to pyrene, the absorption peaks shift gradually from 390 nm to the longer wavelength 416 nm. In addition, all other tetramers have a red shift compared to their corresponding trimers, except for tetramer 16d. With one more phenylene-ethynylene conjugation unit than trimer **13d**, the absorption maximum of **16d** is expected to shift to a longer wavelength; however **16d** and **13d** have approximately the same absorption maxima. By further comparing the spectra of **13d** and **16d**, it is seen that the UV-*vis* absorption of **13d** ends at 450 nm, where that for **16d** has a peak shoulder around 450 nm with its asbsorption ending at 470 nm. A comparison of the absorption

maxima of tetramers with those of trimers indicates that by addition of one more repeat unit, the red shift becomes smaller for oligomers with more conjugated chromophores. As shown in Table 2, the red shift is 24 nm for **13a** to **16a**, 22 nm for **13b** to **16b**, 16 nm for **13c** to **16c** and -2 nm for **13d** to **16d**.

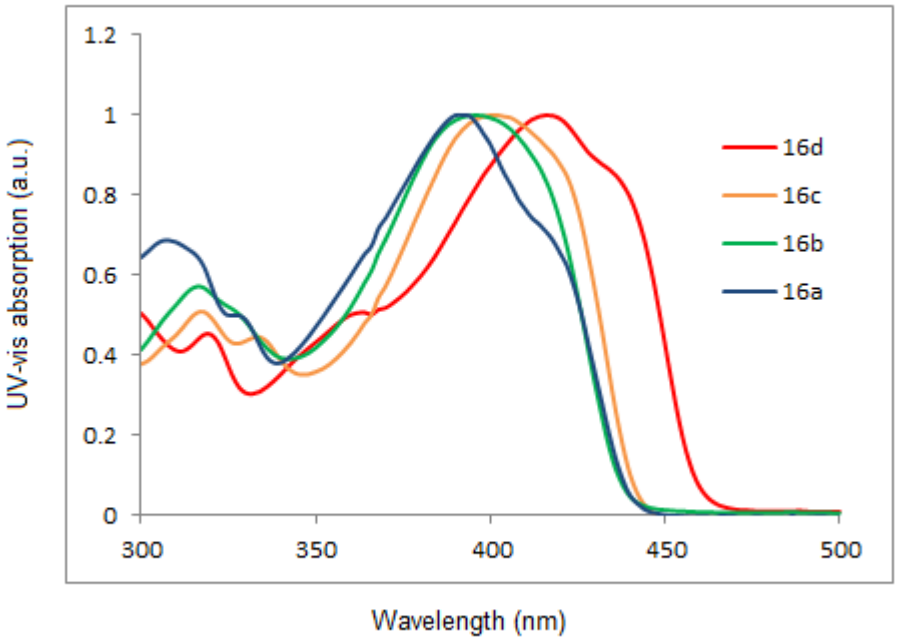

Figure 13. UV-*vis* absorption spectra of tetramers **16a-d** in CH_2Cl_2 solution.

Normalized emission spectra (Figure 14) show an expected trend with some discrepancies. Overall, the emission maxima shifted to longer wavelengths from **16a** to **16d**. The absorption peak is practically at the same position for the oligomers **16a** and **16b**, but **16b** has a much higher quantum yield than **16a**. As mentioned above, although the absorption maxima for **13d** and **16d** are the same, the emission maximum for **16d** is

higher than that of **13d** when excited by the same wavelength. The emission maximum for **16d** is 455 nm, which is red shifted about 17 nm compared with the emission maximum of **13d** (438 nm).

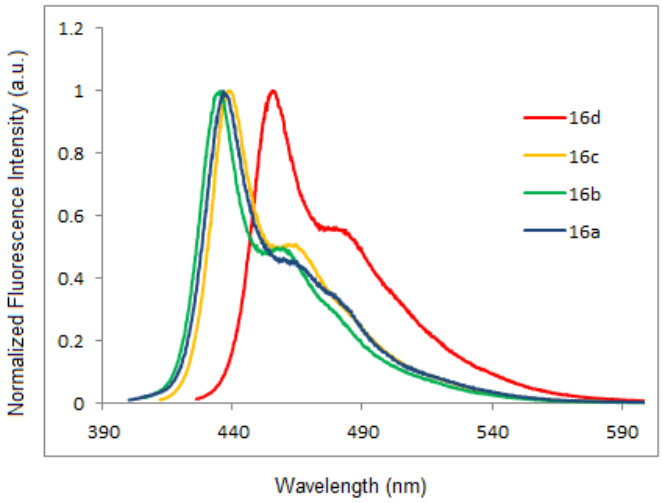

Figure 14. Fluorescence emission spectra of tetramers **16a-d** in CH_2Cl_2 solution.

Table 2. Spectroscopic Data for oligomers **13a-d** and **16a-d** in CH_2Cl_2 solution.

oligomer	λmax (nm)	λem (nm)	Stokes shift (nm)	Φf
13a	366	400	34	0.97
13b	374	406	32	0.93
13c	384	415	31	1.08
13d	418	438	20	0.63
16a	390	436	46	0.91
16b	396	435	39	1.15
16c	402	439	37	1.04
16d	416	455	39	1.00

2.4 Synthesis and characterization of unsymmetric phenylene-ethynylene compounds with allyloxy as the terminal functional group.

The phenylene-ethynylene compounds containing the allyloxy group have not previously been reported. So far there is no literature report of the Sonogashira coupling reaction taking place between terminal alkynes and aryl halides containing the allyloxy functional group. Herein, we report a new class of allyloxy-containing phenylene-ethynylene compounds. Furthermore, such phenylene-ethynylene compounds with terminal alkenes can polymerize by atom-transfer radical polymerization (ATRP) or anionic polymerization to form comb-like fluorescent polymers. The synthesis of various allyloxy-related phenylene-ethynylene compounds is shown in Schemes 7, 8 and 9. First, 4-iodophenol was used as the starting material to react with allyl bromide and sodium hydride in DMF at 0 ^{o}C to form compound **17** (1-(allyloxy)-4-iodobenzene). The allyloxy-substituted phenylene-ethynylene compounds **18a-f** were prepared by Sonogashira coupling **17** with various terminal alkynes. This series of Sonogashira coupling reactions is extremely sluggish, probably due to the existence of the terminal alkenes on the allyloxy group, which can form complexes with the Pd catalyst and which greatly decreases the Pd catalyst's reactivity. All reactions were sealed in glass flasks without oxygen or moisture for one week, with the same amount of Pd catalyst. Only the formation of **18a** gives a high yield of 90%, for other reactions, the yields are below 50%, the formation of **18b** has the lowest yield (15%).

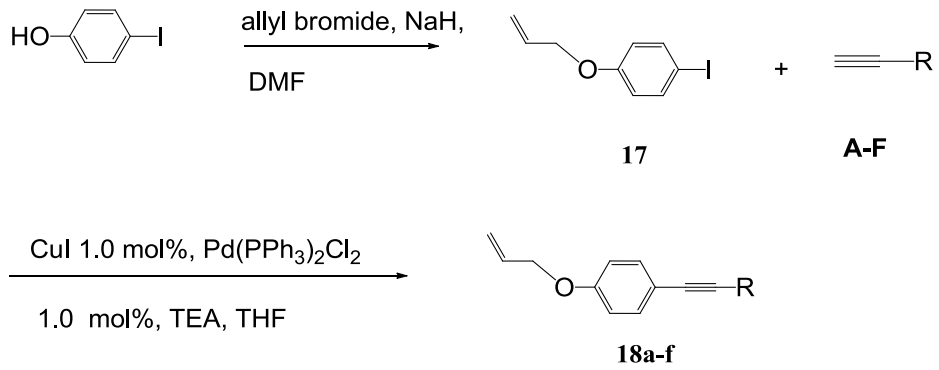

Scheme 8. The synthesis of allyloxy substituted *p*-phenylene acetylene dimers.

Entry	# A-F	Product	Yield
1	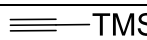	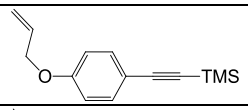	90%
2	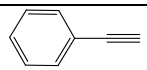	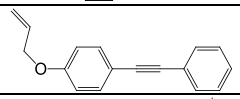	15%
3	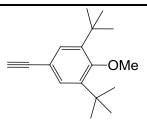	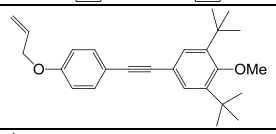	49%
4	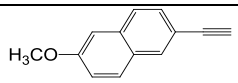	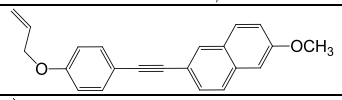	45%
5	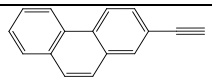	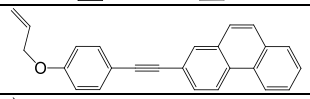	40%
6	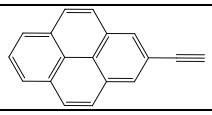	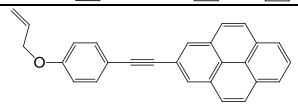	30%

The synthesis of compounds **21a-b** was conducted by using **19** desilylated from ((4-(allyloxy) phenyl) ethynyl) trimethylsilane to react with previously synthesized aryl halide compounds **12** and **20**.

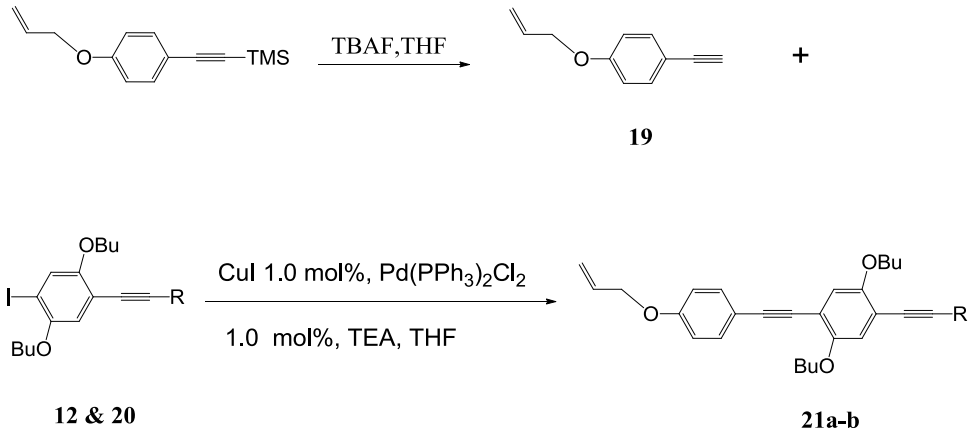

Scheme 9. The synthesis of allyloxy-substituted *p*-phenylene-acetylene trimers.

Entry	**12&20**	Product	Yield %
1	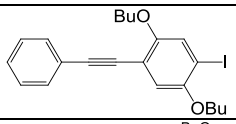	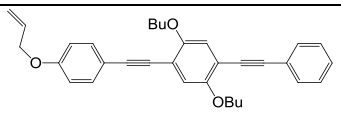	40%
2	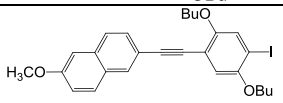	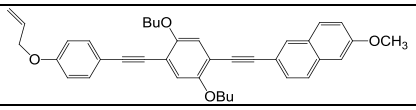	35%

The allyloxy-substituted azulene-containing π-conjugated trimer, compound **23**, was synthesized by coupling compound **19** with mono-iodo-substituted azulene derivative **21,** prepared by coupling ethynylbenzene with an excess of 1, 3-diiodo azulene.

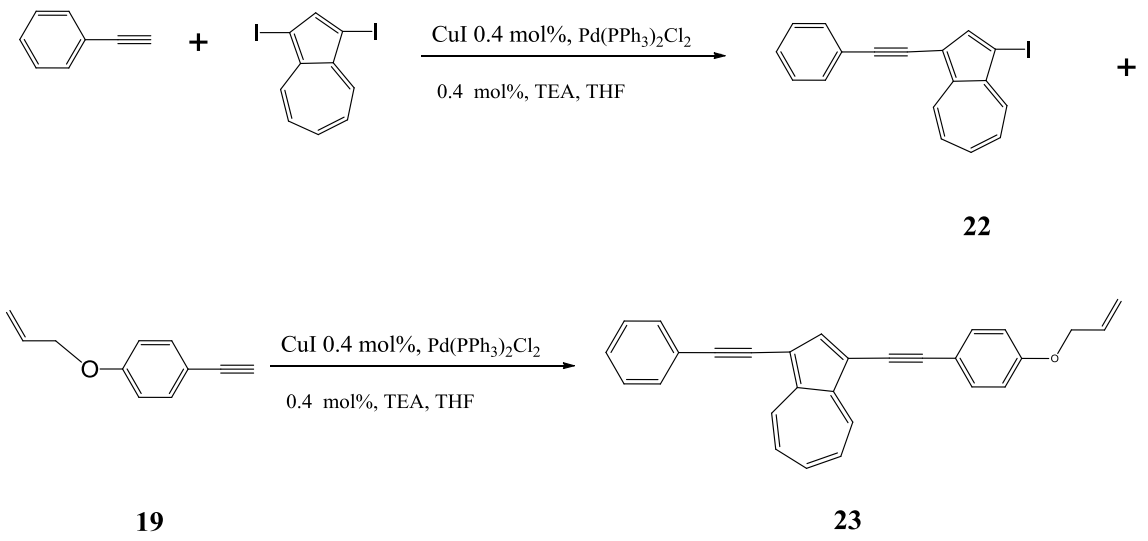

Scheme 10. The synthesis of allyloxy substituted azulene containing π-conjugated trimer.

With alkene as the end group, this type of compounds has potential as building blocks for the synthesis of fluorescent polymers with phenylene-ethylene units as side chains.

3. CONCLUSION

Four series of π-conjugated arylene ethynylene oligomers have been synthesized using Sonogashira coupling reactions. The method for the synthesis of mono-iodo substituted phenylene-ethynylene oligomers **8-11** provides a new approach for the design of pure π-conjugated oligomers with various fluorescent chormophores. Although the series of phenylene ethynylene compounds with allyl functional groups **18a-f**, **21a-b**, and **23** has been successfully synthesized, the reaction rate for the synthesis of most compounds is very slow with low yield, even with prolonged reaction periods; this type

of reaction cannot go completion. The amount of homo-coupling products is non-negligible for reactions with large or bulky substituent groups on the terminal alkynes. The structures of compound **5a**, **5b** and homo**4** have been confirmed by single crystal x-ray crystallography. The extending of π-π conjuagation and the fluorescence emission for mono-terminated di-*tert*-butyl substituted oligo (phenylene-ethynylene)s **3a-7a** were impaired due to the twisting of the di-*tert*-butyl phenylene ring and the bending of triple-bond angles. UV-vis and fluorescence studies show that there is a red shift for the series of oligomers **4a-7a**, **13a-d**, and **16a-d** either with increasing π-π conjugation of substituted chromophores or with each additional phenylene-ethylene units in the conjugated system. The quantum yields for both **13a-d** and **16a-d** are high. The synthesis of comb-like fluorescent polymers based on allyoxy substituted arylene ethynylene derivatives will be carried out in the future.

4. EXPERIMENTAL SECTION

4.1 General methods

Materials. All the chemicals and reagents were purchased from Acros Organics or Aldrich Chemical Company. THF was freshly distilled from sodium-potassium alloy unless otherwise stated. Et_3N was freshly distilled from sodium hydride.

Instrumentation. ^{1}H NMR and ^{13}C NMR spectra were recorded at 400 MHz and 100 MHz, using a Varian ANOVA NMR spectrometer. Mass spectra were obtained from University of Missouri-Kansas City, School of Biological Sciences. X-ray single crystal structural data were obtained and analyzed by Dr. Charles Barnes, department of chemistry, University of Missouri-Columbia.

4.2 Experimental procedures

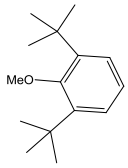

1,3-di-*tert*-butyl-2-methoxybenzene (**1**): 2,6-di-*tert*-butylphenol (10.0 g, 48 mmol), NaH(2.30 g, 58 mmol) and iodomethane (8.22g, 58 mmol) were added to DMF (50 ml) at 0 ^{o}C for 2h. The reaction mixture was poured into cold water, extracted with diethyl ether, and dried with Na_2SO_4. The crude product was purified by flash column and dried in a vacuum oven to afford **1**. ^{1}H NMR (400MHz, $CDCl_3$) δ 7.35 (d, 2H, *J* = 6.4Hz), 6.98 (m, 1H), 3.67 (s, 3H), 1.39 (s, 18H). ^{13}C NMR (100 MHz, $CDCl_3$) δ 159.65, 144.22, 126.53, 123.15, 64.40, 35.76, 31.87.

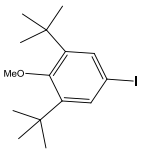

1, 3-di-*tert*-butyl-5-iodo-2-methoxybenzene (**2**): Compound **1** (5.0 g, 23 mmol): ^{1}H NMR (400MHz, $CDCl_3$) δ 7.50 (s, 2H), 3.67 (s, 3H), 1.39 (s, 18H). ^{13}C NMR (100 MHz, $CDCl_3$) δ 159.63, 146.40, 135.66, 88.11, 64.39, 35.78, 31.86.

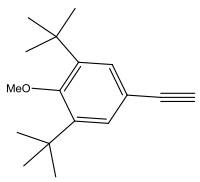

1, 3-di-*tert*-butyl-5-ethynyl-2-methoxybenzene (**3**): Compound **2** (2.0 g, 5.7 mmol), ethynyltrimethylsilane (0.67g, 6.84 mmol), Pd $(PPh_3)_2Cl_2$ (0.4 mol %), CuI (0.4 mol %), Et_3N (1.0 ml), and THF (10 ml) were placed in a specially designed long-neck round bottom flask. Gas was removed from thereaction mixture by three liquid nitrogen freeze-thaw cycles under high vacuum, and then the flask was flame-sealed. After 48h, the flask was opened and solvents were evaporated. The crude product was then purified by column chromatography and dried in the oven. The obtained product was desilylated by TBAF (1.60g, 0.005 mol) in THF; the reaction mixture was extracted with diethyl ether and dried with Na_2SO_4. The crude

product was purified by flash column and dried in a vacuum oven to afford **3.** ^{1}H NMR (400MHz, $CDCl_3$) δ 7.39 (s, 2H), 3.68 (s, 3H), 2.99 (s, 1H), 1.41 (s, 18H). ^{13}C NMR (100 MHz, $CDCl_3$) δ 160.46, 144.03, 130.59, 116.21, 84.51, 64.37, 35.72, 31.89.

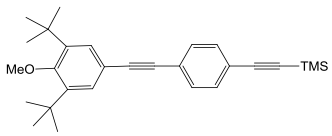

((4-((3,5-di-tert-butyl-4-methoxyphenyl)ethynyl)phenyl) ethynyl)trimethylsilane (**4a**): Compound **3** (2.0 g, 8.20 mmol), ((4-iodophenyl)ethynyl)trimethylsilane (2.9 g, 9.84 mmol), $Pd(PPh_3)_2Cl_2$ (0.4 mol%), CuI (0.4 mol %), Et_3N (0.5 ml), and THF (10 ml) were placed in a specially designed round bottom flask and reacted under our oxgen-free Sonogashra reaction conditions (similar conditions to compound **3**). The resulting products were purified by column chromatography and dried in a vacuum oven to afford **4a**. ^{1}H NMR (400MHz, $CDCl_3$) δ 7.44-7.46 (m, 4H), 7.42 (s, 2H), 3.70 (s, 3H), 1.44 (s, 18H), 0.26 (s, 9H). ^{13}C NMR (100 MHz, $CDCl_3$) δ 160.37, 144.17, 131.92, 131.36, 130.18, 123.77, 122.58, 117.22, 104.80, 96.09, 92.23, 87.64, 64.45, 35.85, 32.08, 32.01, 0.01.

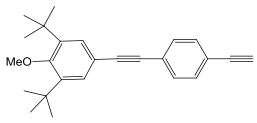

1,3-di-*tert*-butyl-5-((4-ethynylphenyl)ethynyl)-2-methoxybenzene (**4b**): Compound **4a** (2 g, 4.8 mmol) and TBAF (1.50 g, 5.76 mmol) were reacted in THF for 2h. The reaction mixture was poured into cold water, washed with diethyl ether, and dried with Na_2SO_4. The solvent was evaporated to give the crude product. Using a flash column, pure product **4b** was obtained. ^{1}H NMR (400MHz, $CDCl_3$) δ 7.43-7.48 (m, 4H), 7.42 (s, 2H), 3.69 (s, 3H), 3.17 (s, 1H), 1.41 (s, 18H). ^{13}C NMR (100 MHz, $CDCl_3$) δ 160.34, 144.11, 132.01, 131.36, 130.12, 124.12, 121.46, 117.07, 92.24, 87.37, 83.35, 78.71, 64.39, 35.78, 31.94.

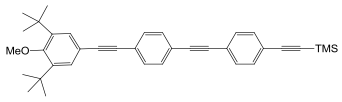

((4-((4-((3,5-di-*tert*-butyl-4-methoxyphenyl) ethynyl) phenyl) ethynyl)phenyl)ethynyl)trimethylsilane (**5a**): Compound **5a** was synthesized by the same procedure as compound **4a**. ^{1}H NMR (400MHz, $CDCl_3$) δ 7.47-7.53 (m, 4H), 7.45 (s, 4H,), 7.43 (s, 2H), 3.7 (s, 3H), 1.46 (s, 18H), 0.26 (s, 9H). ^{13}C NMR (100 MHz, $CDCl_3$) δ 160.31, 144.10, 131.48, 131.45, 131.36, 130.11, 123.69, 123.10, 123.02, 122.38, 117.13, 104.56, 96.38, 90.68, 87.59, 64.38, 35.77, 31.93, 0.10.

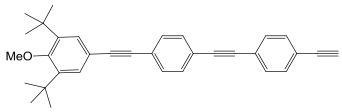

1,3-di-*tert*-butyl-5-((4-((4-ethynylphenyl)ethynyl) phenyl) ethynyl)-2-methoxybenzene (**5b**): Compound **5b** was synthesized by the same procedure as compound **4b**. ^{1}H NMR (400MHz, $CDCl_3$) δ 7.50-7.53 (m, 4H), 7.48 (s, 4H), 7.43 (s, 2H), 3.70 (s, 3H), 3.18 (s, 1H), 1.44 (s, 9H). ^{13}C NMR (100 MHz, $CDCl_3$) δ 160.32, 144.10, 132.07, 131.50, 131.45, 131.44, 130.12, 123.76, 123.54, 122.30, 121.98, 117.11, 92.30, 91.15, 90.47, 87.57, 83.22, 78.99, 64.38, 35.78, 31.93.

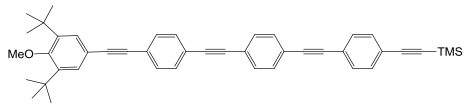

((4-((4-((4-((3,5-di-*tert*-butyl-4-methoxy phenyl) ethynyl)phenyl)ethynyl)phenyl)ethynyl) phenyl) ethynyl)trimethylsilane (**6a**): Compound **6a** was synthesized by the same procedure as compound **4a**. ^{1}H NMR (400 MHz, $CDCl_3$) δ 7.49-7.54 (m, 8H), 7.46 (s, 4H), 7.43 (s, 2H), 3.7 (s, 3H), 1.44 (s, 18H), 0.25 (s, 9H). ^{13}C NMR (100 MHz, $CDCl_3$) δ 160.30, 144.09, 131.53, 131.49, 131.45, 131.37, 130.11, 123.69, 123.08, 122.99, 122.90, 122.36, 117.10, 104.52, 96.43, 92.28, 91.19, 90.94, 90.71, 87.59, 64.38, 35.77, 31.92, 0.11.

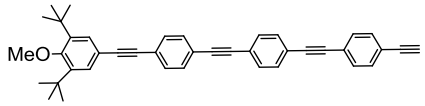

1,3-di-*tert*-butyl-5-((4-((4-((4-ethynylphenyl)ethynyl) phenyl)ethynyl)phenyl)ethynyl)-2-methoxybenzene (**6b**) Compound **6b** was synthesized by the same procedure as compound **4b**. ^{1}H NMR (400MHz, $CDCl_3$) δ 7.50-7.55 (m, 8H), 7.49 (s, 4H), 7.46 (s, 2H), 3.71 (s, 3H), 3.20 (s, 1H), 1.46 (s, 18H). ^{13}C NMR (100 MHz, $CDCl_3$) δ 160.33, 144.12, 131.57, 131.55, 131.51, 131.47, 130.13, 123.76, 123.47, 123.20, 122.87, 122.39, 122.10, 117.18, 92.36, 91.26, 90.78, 90.74, 87.64, 83.23, 79.06, 77.32, 77.01, 76.69, 64.37, 35.78, 31.95.

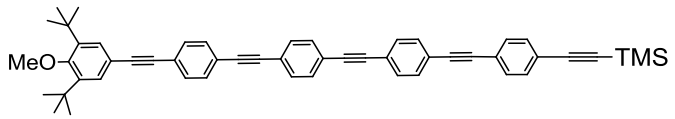

((4-((4-((4-((4-((4-((3,5-di-*tert*-butyl-4-methoxyphenyl)ethynyl)phenyl) ethynyl)phenyl)ethynyl) phenyl)ethynyl)phenyl)ethynyl)trimethylsilane (**7a**): Compound **7a** was synthesized by the same procedure as compound **4a**. ^{1}H NMR (400MHz, $CDCl_3$) δ 7.51-7.52 (m, 12H), 7.46 (s, 4H), 7.43 (s, 2H), 3.7 (s, 3H), 1.44 (s, 18H), 0.26 (s, 9H). ^{13}C NMR (100 MHz, $CDCl_3$) δ 160.34, 144.13, 131.92, 131.57, 131.51, 131.48, 131.40, 130.13, 123.77, 123.17, 123.05, 122.95, 122.41, 117.17, 104.56, 96.47, 91.24, 91.08, 91.03, 90.94, 90.74, 87.61, 64.38, 35.79, 31.95, 0.10.

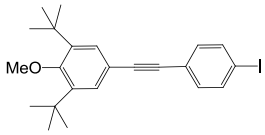

1,3-di-tert-butyl-5-((4-iodophenyl)ethynyl)-2-methoxybenzene (**8**): Compound **3** (0.5 g, 2.05 mmol), 1,4-iodobenzene (1.35 g, 4.10 mmol), $Pd(PPh_3)_2Cl_2$ (0.4 mol%), CuI (0.4 mol %), Et_3N (0.3 ml), and THF (5ml) were dissolved in THF and reacted under our previously described oxygen-free Sonogashira reaction conditions. After 3 days, the flask was opened and the solvents were evaporated,

the crude product was then purified by column chromatography and dried in an oven to afford **8**. ^{1}H NMR (400MHz, $CDCl_3$) δ 7.68 (d, 2H, *J* = 8.8Hz), 7.41 (s, 2H), 7.25 (d, 2H, *J* =8.4 Hz), 3.69 (s, 3H), 1.43 (s, 18H). ^{13}C NMR (100 MHz, $CDCl_3$) δ 160.31, 144.10, 137.42, 133.01, 130.07, 123.11, 117.03, 93.65, 91.60, 86.94, 64.37, 35.77, 31.93.

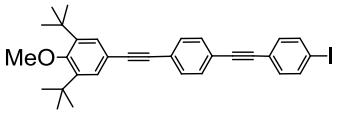

1,3-di-*tert*-butyl-5-((4-((4-iodophenyl)ethynyl)phenyl) ethynyl)-2-methoxybenzene (**9**): Compound **9** was synthesized by the same procedure as compound **8**. ^{1}H NMR (400MHz, $CDCl_3$) δ 7.67 (d, 2H, *J* =8.8 Hz), 7.48-7.53 (m, 4H), 7.43 (s, 2H), 7.25 (d, 2H, *J* = 8.4 Hz), 3.67 (s, 3H), 1.41 (s, 18H). ^{13}C NMR (100 MHz, $CDCl_3$) δ 160.54, 144.33, 137.76, 133.27, 131.68, 130.34, 123.96, 122.79, 122.50, 117.32, 94.54, 92.51, 90.79, 90.31, 87.79, 64.61, 36.00, 32.16.

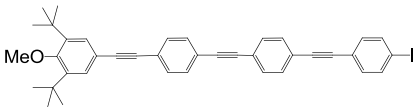

1,3-di-*tert*-butyl-5-((4-((4-((4-iodophenyl)ethynyl)phenyl) ethynyl)phenyl)ethynyl)-2-methoxybenzene (**10**): Compound **10** was synthesized by the same procedure as compound **8**. ^{1}H NMR (400MHz, $CDCl_3$) δ 7.70 (d, 2H, *J* =8.8 Hz), 7.51 (m, 8H), 7.43 (s, 2H), 7.25 (d, 2H, *J* =8.4 Hz), 3.70 (s, 3H), 1.44 (s, 18H). ^{13}C NMR (100 MHz, $CDCl_3$) δ 160.31, 144.10, 137.55, 131.54, 131.49, 130.11, 123.71, 122.80, 122.48, 122.34, 117.09, 94.41, 91.21, 90.36, 87.58, 64.38, 35.78, 31.93.

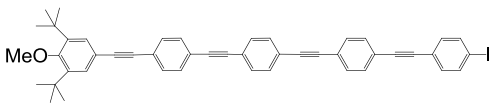

1,3-di-*tert*-butyl-5-((4-((4-((4-((4-iodophenyl)

ethynyl)phenyl)ethynyl)phenyl)ethynyl)pheny l)ethynyl)-2-methoxybenzene (**11**): Compound **11** was synthesized by the same procedure as compound **8**. ^{1}H NMR (400MHz, $CDCl_3$) δ 7.70 (d, 2H, *J* =8.8 Hz), 7.51(m, 12H), 7.41 (s, 2H), 7.25 (d, 2H, *J* = 8.4 Hz), 3.70 (s, 3H), 1.44 (s, 18H).

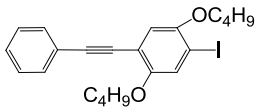

1,4-dibutoxy-2-iodo-5-(phenylethynyl)benzene (**12**): Compound **12** was synthesized by the same procedure as compound **8**. ^{1}H NMR (400 MHz, $CDCl_3$) δ ^{13}C NMR (100 MHz, $CDCl_3$) δ 154.35, 151.85, 131.51, 128.31, 128.24, 123.92, 123.41, 115.97, 113.69, 91.17, 87.46, 85.55, 69.80, 69.62, 31.33, 31.27, 19.33, 19.21, 13.86, 13.84.

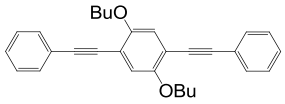

((2,5-dibutoxy-1,4-phenylene)bis(ethyne-2,1-diyl))dibenzene (**13a**): Compound 12 (0.1g, 0.22 mmol), ethynylbenzene (0.027 g, 0.26 mmol), $Pd(PPh_3)_2Cl_2$ (0.4 mol%), CuI (0.4 mol %), Et_3N (0.3 ml), and THF (3ml) were added to a round bottom flask and reacted under our previously described oxgen-free Sonogashira reaction conditions for 3 days. The resulting products were purified by column chromatography and dried in a vacuum oven to afford **13a**. ^{1}H NMR (400MHz, $CDCl_3$) δ 7.50-7.53 (m, 4H), 7.30-7.35 (m, 6H), 7.00 (s, 2H), 4.02 (t, 4H, *J* = 6.4 Hz), 1.78-1.84 (m, 4H), 1.52-1.57 (m, 4H), 0.98 (t, 6H, *J* = 7.2Hz). ^{13}C NMR (100 MHz, $CDCl_3$) δ 153.64, 131.55, 128.31, 128.23, 123.47, 116.99, 113.99, 94.80, 85.95, 69.35, 31.37, 19.26, 13.89.

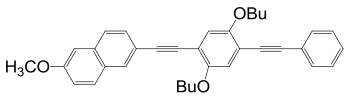

2-((2,5-dibutoxy-4-(phenylethynyl)phenyl)ethynyl)-6-

methoxy naphthalene (**13b**): Compound **13b** was synthesized by the same procedure as compound **13a**. ^{1}H NMR (400MHz, $CDCl_3$) δ 7.99 (s, 1H), 7.70-7.74 (m, 2H), 7.55-7.57 (m, 3H), 7.35-7.39 (m, 3H), 7.17 (d, 1H, *J* = 12 Hz), 7.12 (s, 1H), 7.06 (d, 2H, *J* = 7.2 Hz), 4.08 (t, 2H, *J* = 6.4 Hz), 4.07 (t, 2H, *J* = 6.4 Hz), 1.84-1.90 (m, 4H), 1.57-1.66 (m, 4H), 1.01-1.06 (m, 6H). ^{13}C NMR (100 MHz, $CDCl_3$) δ 158.35, 153.71, 153.67, 134.14, 131.54, 131.22, 129.35, 128.98, 128.52, 128.30, 128.19, 126.78, 123.53, 119.36, 118.41, 117.07, 117.00, 114.29, 113.87, 105.87, 95.50, 94.78, 86.05, 85.72, 69.41, 69.38, 55.32, 31.42, 31.38, 19.30, 19.26, 13.92, 13.88.

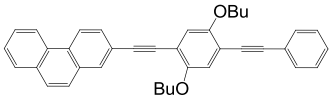

2-((2,5-dibutoxy-4-(phenylethynyl)phenyl)ethynyl) phenanthrene (**13c**): Compound **13c** was synthesized by the same procedure as compound **13a**. ^{1}H NMR (400MHz, $CDCl_3$) δ 8.67-8.78 (m, 3H), 8.11 (s, 1H), 7.89 (d, 1H, *J* = 8.0 Hz), 7.58-7.75 (m, 6H), 7.36-7.41 (m, 3H), 7.17 (s, 1H), 7.10 (s, 1H), 4.13 (t, 2H, *J* = 6.4 Hz), 4.11 (t, 2H, *J* = 6.4Hz), 1.97-2.02 (m, 2H), 1.85-1.90 (m, 2H), 1.58-1.68 (m, 4H), 1.07 (t, 6H, *J* = 7.2 Hz). ^{13}C NMR (100 MHz, $CDCl_3$) δ 153.96, 153.64, 131.57, 131.48, 131.32, 131.21, 130.32, 130.09, 128.56, 128.33, 128.25, 127.39, 127.05, 126.92, 123.52, 122.66, 122.62, 120.01, 117.01, 116.29, 114.20, 113.81, 94.96, 93.39, 90.79, 86.11, 69.47, 69.09, 31.60, 31.42, 19.33, 19.28, 13.95, 13.90.

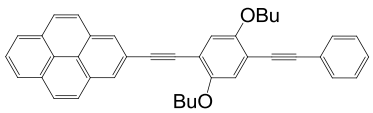

2-((2,5-dibutoxy-4-(phenylethynyl)phenyl)ethynyl)pyrene (**13d**): Compound **13d** was synthesized by the same procedure as compound **13a**. ^{1}H NMR (400MHz, $CDCl_3$) δ ^{1}H NMR (400MHz, $CDCl_3$) δ 8.86 (d, 1H, *J* = 9.2 Hz), 8.02-8.25 (m, 8H), 7.57-7.59 (m, 2H), 7.34-7.41 (m, 3H), 7.20

(s, 1H), 7.11 (s, 1H), 7.16 (t, 2H, *J* = 6.4 Hz), 4.12 (t, 2H, *J* = 6.4 Hz), 2.01-2.08 (m, 2H), 1.86-1.93 (m, 2H), 1.57-1.72 (m, 4H), 1.04-1.09 (m, 6H). ^{13}C NMR (100 MHz, $CDCl_3$) δ 153.83, 153.62, 132.02, 131.57, 131.25, 131.23, 131.12, 129.29, 128.33, 128.26, 128.14, 127.26, 126.20, 125.97, 125.57, 124.53, 124.48, 124.30, 123.47, 118.07, 116.78, 116.20, 114.00, 113.91, 94.97, 94.40, 91.93, 86.10, 69.41, 69.05, 31.62, 31.41, 19.38, 19.29, 14.01, 13.93.

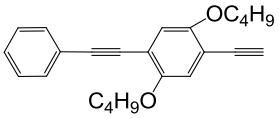

1,4-dibutoxy-2-ethynyl-5-(phenylethynyl)benzene (**14**): ^{1}H NMR (400MHz, $CDCl_3$) δ ^{1}H NMR (400MHz, $CDCl_3$) δ 7.52-7.54 (m, 2H), 7.34-7.36 (m, 3H), 6.90 (d, 2H, *J* = 7.2 Hz), 4.02 (t, 2H, *J* = 6.4 Hz), 4.00 (t, 2H, *J* = 6.4 Hz), 3.34 (s, 1H), 1.79-1.84 (m, 4H), 1.49-1.59 (m, 4H), 0.99 (t, 3H, *J* = 7.6 Hz), 1.00 (t, 3H, *J* = 7.6 Hz).

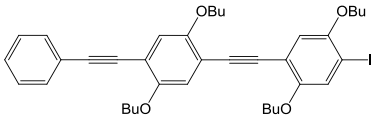

1,4-dibutoxy-2-((2,5-dibutoxy-4-(phenylethynyl) phenyl) ethynyl)-5-iodobenzene (**15**): Compound **14** (2g, 5.8 mmol), 1,4-dibutoxy-2,5-diiodobenzene (5.47 g, 11.6 mmol), $Pd(PPh_3)_2Cl_2$ (0.4 mol%), CuI (0.4 mol %), Et_3N (4 ml), and THF (15 ml) were added to a round bottom flask and reacted under our oxygen-free Sonogashira reaction conditions for 6 days. The resulting products were purified by column chromatography and dried in a vacuum oven to afford **15.** ^{1}H NMR (400MHz, $CDCl_3$) δ ^{1}H NMR (400MHz, $CDCl_3$) δ7.52-7.55 (2H), 7.31-7.36 (m, 3H), 7.01 (d, 2H, *J* = 7.2 Hz), 6.92 (d, 2H, *J* = 7.2 Hz), 3.95-4.06 (m, 8H), 1.79-1.86 (m,8H), 1.53-1.60 (m, 8H), 0.97-1.02 (m, 12H). ^{13}C NMR (100 MHz, $CDCl_3$) δ 154.24, 153.67, 153.52, 151.90, 131.56, 128.32, 128.24, 124.15, 123.51, 117.22, 117.18, 116.19,

114.25, 114.13, 114.04, 94.87, 91.00, 90.79, 87.54, 86.00, 69.78, 69.76, 69.45, 69.36, 31.39, 31.38, 31.29, 19.34, 19.26, 19.23, 13.93, 13.90, 13.86, 13.82.

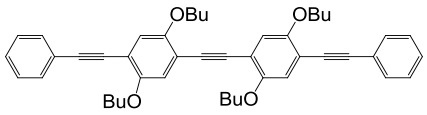

1,2-bis(2,5-dibutoxy-4-(phenylethynyl)phenyl)ethyne (**16a**): Compound 15 (0.1 g, 0.14 mmol), ethynyl benzene (0.017 g, 0.17 mmol), $Pd(PPh_3)_2Cl_2$ (0.4 mol%), CuI (0.4 mol %), Et_3N (0.3 ml), and THF (3ml) were added to a round bottom flask and reacted under our previously described oxygen-free Sonogashira reaction procedures. The resulting products were purified by column chromatography and dried in a vacuum oven to afford **16a.** ^{1}H NMR (400MHz, $CDCl_3$) δ 7.51-7.55 (m, 4H), 7.30-7.36 (m, 6H), 6.99 (s, 4H), 4.01 (t, 4H, *J* = 6.4 Hz), 3.99 (t, 4H, *J* =6.4 Hz), 1.80-1.87 (m, 8H), 1.46-1.57 (m, 8H), 1.25-1.37 (m, 72H), 0.85-0.89 (m, 12H). ^{13}C NMR (100 MHz, $CDCl_3$) δ 154.98, 153.46, 131.61, 128.31, 123.34, 117.67, 116.90, 115.11, 112.50, 95.49, 85.82, 79.51, 79.25, 69.77, 69.59, 31.92, 29.71, 29.69, 29.66, 29.63, 29.44, 29.37, 29.31, 29.14, 26.08, 25.93, 22.69, 14.12.

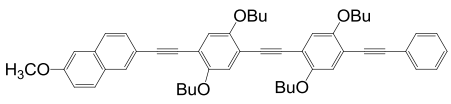

2-((2,5-dibutoxy-4-((2,5-dibutoxy-4-(phenylethynyl) phenyl)ethynyl)phenyl)ethynyl)-6-methoxy naphtha lene (**16b**): Compound **16b** was synthesized by the same procedure as compound **16a**. ^{1}H NMR (400MHz, $CDCl_3$) δ 7.98 (s, 1H), 7.70-7.73 (m, 2H), 7.54-7.57 (m, 3H), 7.34-7.36 (m, 3H), 7.13-7.18 (m, 2H), 7.03-7.06 (m, 4H), 4.03-4.09 (m, 8H), 3.94 (m, 3H), 1.84-1.90 (m, 4H), 1.56-1.65 (m, 4H), 1.05-1.30 (m, 8H), 0.99-1.06 (m, 12H). ^{13}C NMR (100 MHz, $CDCl_3$) δ 158.31, 153.59, 153.57, 153.49, 153.45, 131.54, 131.23, 129.37, 128.98, 128.49, 128.31, 128.22, 126.78, 123.46, 119.38, 118.36, 117.08, 117.01, 116.94,

114.25, 114.19, 114.03, 113.92, 105.80, 95.57, 94.86, 91.52, 91.43, 85.99, 85.72, 69.37, 69.27, 69.24, 55.34, 31.91, 31.38, 31.35, 30.15, 29.69, 29.36, 22.69, 19.30, 19.26, 14.18, 14.12, 13.96, 13.94.

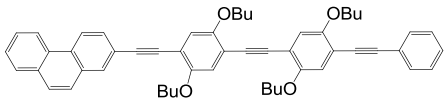

2-((2,5-dibutoxy-4-((2,5-dibutoxy-4-(phenylethynyl) phenyl) ethynyl) phenyl)ethynyl)phenanthrene (**16c**): Compound **16c** was synthesized by the same procedure as compound **16a**. ^{1}H NMR (400MHz, $CDCl_3$) δ 8.60-8.68 (m, 3H), 8.02(s, 1H), 7.81 (d, 1H, *J* = 8.0 Hz), 7.46-7.61 (m, 6H), 7.27-7.28 (m, 2H), 7.18 (s, 1H), 7.08(s, 1H), 6.97-7.01 (m, 3H), 3.96-4.06 (m, 8H), 1.90-1.94 (m, 2H), 1.76-1.83 (m, 6H), 1.51-1.60 (m, 8H), 0.90-0.99 (m, 12H). ^{13}C NMR (100 MHz, $CDCl_3$) δ 153.89, 153.60, 153.48, 153.43, 131.55, 131.48, 131.30, 131.18, 130.31, 130.06, 128.58, 128.32, 128.24, 127.42, 127.34, 127.06, 126.93, 123.46, 122.66, 122.64, 119.97, 117.08, 117.01, 116.97, 116.34, 114.37, 114.20, 113.99, 113.72, 94.89, 93.44, 91.62, 90.81, 85.99, 69.48, 69.38, 69.25, 68.98, 31.58, 31.41, 31.39, 31.36, 19.33, 19.28, 19.26, 13.98, 13.89.

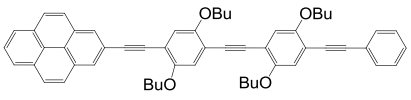

2-((2,5-dibutoxy-4-((2,5-dibutoxy-4-(phenylethynyl) phenyl)ethynyl)phenyl)ethynyl)pyrene(**16d**): Compound **16d** was synthesized by the same procedure as compound **16a**. 1H NMR (400MHz, CDCl3) δ 8.86 (d, 1H, *J* =9.2 Hz), 8.04-8.25 (m, 8H), 7.54-8.02 (m, 2H), 7.34-7.38 (m, 3H), 7.19 (s, 1H), 7.11 (s, 1H), 7.05 (d, 2H, *J* = 4.8 Hz), 4.04-4.17 (m, 8H), 2.02-2.06 (m, 2H), 1.82-1.92 (m, 6H), 1.56-1.72 (m, 8H), 1.00-1.09 (m, 12H).). ^{13}C NMR (100 MHz, $CDCl_3$) δ 153.89, 153.70, 153.57, 132.07, 131.57, 131.31, 131.28, 131.17, 129.33,

128.33, 128.23, 128.15, 127.28, 126.22, 126.00, 125.58, 125.52, 124.55, 124.36, 123.54, 118.17, 117.26, 117.21, 117.09, 116.54, 114.45, 114.38, 114.12, 114.07, 94.91, 94.47, 92.04, 91.67, 91.65, 86.06, 69.60, 69.50, 69.37, 69.12, 31.65, 31.48, 31.45, 31.41, 19.39, 19.31, 19.27, 13.97, 13.88.

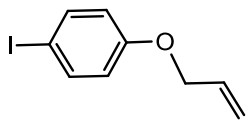

1-(allyloxy)-4-iodobenzene (**17**): 4-iodophenol (5 g, 22.7 mmol), allyl bromide (3.27 g, 27.0 mmol), and NaH (0.82g, 34.1 mmol) were added to DMF (30 ml) and reacted for 2 h at 0 ºC. The reaction mixture was poured into the cold ice, extracted with di-ethyl ether, and dried using Na_2SO_4. The crude product was purified using a flash column and dried in a vacuum oven to afford compound **17**. ^{1}H NMR (400MHz, $CDCl_3$) δ 7.55 (d, 2H, *J* = 8.8 Hz), 6.69 (d, 2H, *J* = 8.8 Hz), 5.98-6.07 (m, 1H), 5.27-5.42(m, 2H), 4.50(d, 2H, *J* = 7.2 Hz). ^{13}C NMR (100 MHz, $CDCl_3$) δ 158.5, 138.2, 132.8, 117.89, 117.17, 82.87, 68.85.

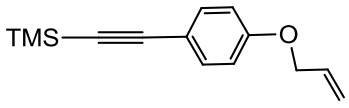

((4-(allyloxy)phenyl)ethynyl)trimethylsilane(**18a**):Compound **17** (0.5 g, 1.92 mmol), ethynyltrimethylsilane (0.23 g, 2.31 mmol), $Pd(PPh_3)_2Cl_2$ (0.8 mol%), CuI (0.8 mol %), Et_3N (1 ml), and THF (5 ml) were added to a round bottom flask and reacted under our oxygen-free Sonogashira reaction conditions for 7 days. The resulting product was purified by column chromatography and dried in an oven to afford compound **18a**. ^{1}H NMR (400MHz, $CDCl_3$) δ 7.39(d, 2H, *J* = 8.8 Hz), 6.83(d, 2H, *J* = 8.8 Hz), 6.00-6.07(m, 1H), 5.28-5.42

(m, 2H), 4.53 (d, 2H, J = 7.2 Hz), 0.24(s, 9H). ^{13}C NMR (100 MHz, $CDCl_3$) δ 158.68, 133.42, 132.80, 117.91, 115.35, 114.52, 105.11, 92.47, 68.72, 0.05.

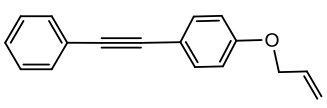

1-(allyloxy)-4-(phenylethynyl) benzene (**18b**): Compound **18b** was synthesized by the same procedure as compound **18a.** ^{1}H NMR (400MHz, $CDCl_3$) δ 7.53 (d, 2H, J = 8.8 Hz), 7.48(d, 2H, J =8.8Hz), 7.37-7.32(m, 3H), 6.90 (d, 2H, J =8.8 Hz), 6.02-6.11 (m, 1H), 5.30-5.46(m, 2H), 4.56 (d, 2H, J =7.2Hz). ^{13}C NMR (100 MHz, $CDCl_3$) δ 158.54, 138.13, 132.98, 132.82, 131.39, 128.26, 127.89, 123.50, 117.89, 117.08, 115.44, 114.69, 89.29, 88.06, 68.73.

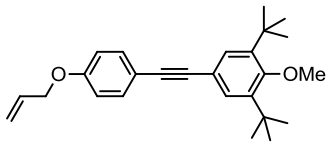

5-((4-(allyloxy) phenyl)ethynyl)-1,3-di-tert-butyl-2-methoxy benzene (**18c**): Compound **18c** was synthesized by the same procedure as compound **18a.** ^{1}H NMR (400MHz, $CDCl_3$) d 7.46 (d, 2H, J =8.8Hz), 7.41(s, 2H), 6.88 (d, 2H, J =8.8Hz), 6.01-6.08 (m, 1H), 5.28-5.44 (m, 2H), 4.54 (d, 2H, J =7.2Hz), 3.69(s, 3H), 1.42(s, 18H). ^{13}C NMR (100 MHz, $CDCl_3$) d 159.82, 158.34, 143.88, 132.88, 129.91, 117.85, 117.66, 115.79, 114.65, 88.73, 87.69, 68.73, 64.32, 35.72, 31.94, 29.67.

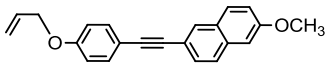

2-((4-(allyloxy) phenyl)ethynyl)-6-methoxynaphthalene (**18d**): Compound **18d** was synthesized by the same procedure as compound **18a.** ^{1}H NMR (400MHz, $CDCl_3$) δ 7.97 (s, 1H), 7.71 (t, 2H, J = 8.4 Hz), 7.50-7.56(m, 3H,), 7.17(d, 1H, J = 7.6 Hz), 7.12(s, 1H), 6.91(d, 2H, J =8.8 Hz), 6.04-6.10 (m, 1H), 5.31-5.46 (m, 2H), 4.56 (d, 2H, J =7.2 Hz), 3.92 (s, 3H). ^{13}C NMR (100 MHz, $CDCl_3$) δ 158.46, 158.12,

133.88, 132.94, 132.84, 130.89, 128.96, 128.47, 126.73, 119.29, 118.41, 117.85, 115.64, 114.71, 105.72, 88.97, 88.63, 68.72, 55.27.

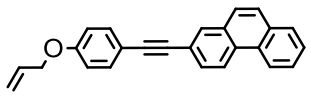

2-((4-(allyloxy)phenyl)enthynyl)phenanthrene (**18e**): Compound **18e** was synthesized by the same procedure as compound **18a.** ^{1}H NMR (400MHz, $CDCl_3$) δ 8.58-8.72 (m, 3H), 8.08(s, 1H), 7.08 (d, 1H, *J* = 8.8Hz), 7.63-7.73 (m, 7H), 6.97 (d, 2H, *J* = 8.8 Hz), 6.05-6.13 (m, 1H), 5.33-5.48 (m, 2H), 4.58(d, 2H, *J* =7.2Hz). ^{13}C NMR (100 MHz, $CDCl_3$) δ 158.70, 133.11, 132.80, 131.35, 131.27, 131.11, 130.07, 130.04, 128.44, 127.23, 126.97, 126.95, 126.87, 122.72, 122.55, 119.88, 117.91, 115.53, 114.80, 93.96, 86.42, 68.75.

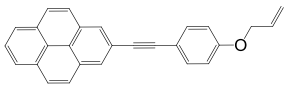

2-((4-(allyloxy) phenyl)enthynyl)pyrene (**18f**): Compound **18f** was synthesized by the same procedure as compound **18a.** ^{1}H NMR (400MHz, $CDCl_3$) δ 8.66 (d, 1H, *J* =12Hz), 8.0-8.22 (m, 8H), 7.67 (d, 2H, *J* = 6.8Hz), 6.98 (d, 2H, *J* = 8.8Hz), 6.06-6.13(m, 1H), 5.33-5.49 (m, 2H), 4.59 (d, 2H, *J* = 7.2 Hz). ^{13}C NMR (100 MHz, $CDCl_3$) d 158.73, 133.14, 132.86, 131.69, 131.25, 131.08, 130.97, 129.43, 128.16, 127.94 , 127.24, 126.17, 125.60, 125.49, 125.45, 124.52, 124.48, 124.33, 118.18, 117.99, 115.78, 114.88, 95.18, 87.41, 68.82.

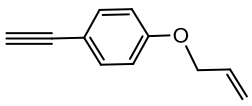

1-(allyloxy)-4-ethynylbenzene (**19**): Compound **19** was synthesized by the same procedure as compound **4b.** ^{1}H NMR (400MHz, $CDCl_3$) d 7.42 (d, 2H, *J* = 8.8 Hz), 6.86 (d, 2H, *J* = 8.8 Hz), 5.99-6.08 (m 1H), 5.29-5.44 (m, 2H), 4.54 (d, 2H, *J*=7.2 Hz), 3.00 (s, 1H). ^{13}C NMR (100 MHz, $CDCl_3$) δ 158.88, 133.54, 132.77, 117.95, 114.65, 114.25, 83.60, 75.80, 68.74.

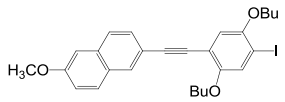

2-((2,5-dibutoxy-4-iodophenyl)ethynyl)-6-methoxynaphthalene (**20**): Compound **20** was synthesized by the same procedure as compound **8**. ^{1}H NMR (400MHz, $CDCl_3$) δ 7.98 (s, 1H), 7.69-7.72 (m, 2H), 7.55 (d, 2H, *J* =8.4 Hz), 7.33 (s, 1H), 7.17 (d, 1H, *J* = 8.8 Hz), 7.11 (s, 1H), 6.96 (s, 1H), 4.02 (t, 2H, *J* = 6.4Hz), 3.99 (t, 2H, *J* = 6.4 Hz), 3.92 (s, 3H), 1.80-1.87 (m, 4H), 154-1.60 (m, 4H), 0.99-1.05 (m, 6H). ^{13}C NMR (100 MHz, $CDCl_3$) δ 158.27, 154.27, 151.77, 134.07, 131.16, 129.30, 128.88, 128.42, 126.76, 123.77, 119.37, 118.24, 115.81, 113.80, 105.74, 94.80, 87.20, 85.23, 69.68, 69.55, 55.29, 31.32, 31.23, 19.31, 19.24, 13.90, 13.84.

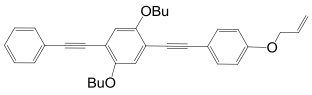

1-((4-(allyloxy)phenyl)ethynyl)-2,5-dibutoxy-4-(phenyl ethynyl) benzene (**21a**): Compound **12** (0.5 g, 1.11 mmol), Compound **19** (0.21 g, 1.34 mmol), $Pd(PPh_3)_2Cl_2$ (0.8 mol%), CuI (0.8 mol %), Et_3N (1ml), and THF (4 ml) were added to a round bottom flask and reacted under our oxygen-free Sonogashira reaction conditions for 7 days. The resulting product was purified by column chromatography and dried in an oven to afford compound **21a**. ^{1}H NMR (400MHz, $CDCl_3$) δ 7.46-7.55 (m, 4H), 7.32-7.36 (m, 3H,), 7.01 (d, 2H, *J* = 4.0 Hz), 6.99(d, 2H, *J* =8.8Hz), 6.01-6.08 (m, 1H), 5.29-5.44 (m, 2H), 4.54 (d, 2H, *J* =7.2 Hz), 4.03 (t, 4H, *J* =6.4 Hz), 1.80-1.85 (m, 4H), 1.55-1.62 (m, 4H), 1.00 (t, 6H, *J* =7.2 Hz). ^{13}C NMR (100 MHz, $CDCl_3$) δ 158.56, 153.57, 153.36, 132.93, 132.80, 131.46, 128.25, 128.14, 123.43, 117.84, 116.86, 116.70, 115.65, 114.67, 114.29, 113.43, 94.85, 94.61, 85.98, 84.65, 69.23, 68.70, 31.31, 19.20, 13.86.

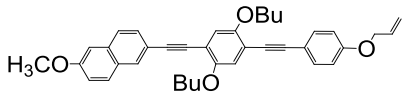

2-((4-((4-(allyloxy)phenyl)ethynyl)-2,5-dibutoxy phenyl)ethynyl)-6-methoxynaphthalene(**21b**): Compound **20** (0.5 g, 0.95 mmol), Compound **19** (0.18 g, 1.14 mmol), $Pd(PPh_3)_2Cl_2$ (0.8 mol%), CuI (0.8 mol %), Et_3N (1ml), and THF (4 ml) were added to a round bottom flask and reacted under our oxygen-free Sonogashira reaction conditions for 7 days. The resulting product was purified by column chromatography and dried in an oven to afford compound **21b**. ^{1}H NMR (400MHz, $CDCl_3$) δ 7.97 (s, 1H), 7.69-7.71 (m, 2H), 7.54 (d,1H, *J* = 8.4 Hz), 7.47 (d, 2H, *J* = 8.8Hz), 7.12-7.17 (m, 2H), 7.05 (s, 1H), 7.02 (s, 1H), 6.90 (d, 2H, *J* = 8.8Hz), 6.05-6.12 (m, 1H), 5.32-5.47 (m, 2H), 4.59 (d, 2H, *J* = 7.2 Hz), 4.06 (t, 2H, *J* = 6.4 Hz), 4.05 (s , 2H, *J* = 6.4 Hz), 3.69 (s, 3H), 1.85-1.91 (m, 4H), 1.58-1.67 (m, 4H), 1.03(t, 3H, *J* = 7.6 Hz), 1.01 (t, 3H, *J* =7.6 Hz). ^{13}C NMR (100 MHz, $CDCl_3$) δ 158.59,158.27, 153.60, 153.44, 134.07, 132.98, 132.85, 131.18, 129.35, 128.98, 128.47 , 126.75, 119.36, 117.93, 116.78, 115.74, 114.71, 114.15, 113.72, 105.78, 95.32, 94.84, 85.72, 84.72, 69.31, 69.30, 55.34, 31.40, 31.36, 19.30, 19.26, 13.95, 13.91.

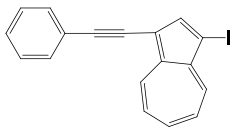

1-iodo-3-(phenylethynyl)azulene(**22**): Compound **22** was synthesized by the same procedure as compound **8**. ^{1}H NMR (400MHz, $CDCl_3$) δ 8.57 (d, 1H, *J* = 8.8 Hz), 8.23(d, 1H, *J* = 9.6 Hz), 8.10 (s, 1H), 7.61(t, *J* = 4Hz), 7.59-7.61 (m, 2H), 7.29-7.39 9m, 5H). ^{13}C NMR (100 MHz, $CDCl_3$) δ 145.62, 141.66, 140.59, 139.67, 139.62, 136.12, 131.31, 128.38, 127.91, 125.42, 125.03, 123.74, 112.31, 94.72, 84.41, 77.33, 77.01, 76.69, 74.58.

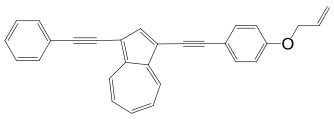

1-((4-(allyloxy) phenyl)ethynyl)-3-(phenylethynyl)azulene (**23**): Compound 22 (0.5 g, 1.41 mmol), Compoudn **19** (0.27 g, 1.69 mmol) $Pd(PPh_3)_2Cl_2$ (0.8 mol%), CuI (0.8 mol %), Et_3N (1ml), and THF (4 ml) were added in a round bottom flask and reacted under our oxygen-free Sonogashira reaction conditions for 7 d. The resulted product was purified by column chromatography and dried in the oven to afford compound **23.** ^{1}H NMR (400MHz, $CDCl_3$) δ 8.57-8.60 (q, 2H, J=4Hz), 8.12 (s, 1H), 7.26-7.70 (m, 10H), 6.93 (d, 2H, *J* =8.8 Hz), 6.03-6.13 (m, 1H), 5.31-5.47 (m, 2H), 4.58 (d, 2H, *J* =7.2Hz).). ^{13}C NMR (100 MHz, $CDCl_3$) δ 158.35, 141.73, 141.65, 141.21, 139.92, 137.06, 136.97, 133.97, 132.87, 132.80, 131.35, 128.35, 127.83, 125.42, 123.83, 118.02, 117.91, 116.07, 114.81, 114.77, 110.91, 110.40, 94.01, 93.90, 84.91, 83.40, 68.78.

Homo**4**: ^{1}H NMR (400MHz, $CDCl_3$) δ 7.50 (s, 8H), 7.43 (s, 4H), 3.70 (s, 6H), 1.44 (s, 36H). ^{13}C NMR (100 MHz, $CDCl_3$) δ 160.63, 144.36, 132.59, 131.69, 130.37, 124.81, 121.20, 117.20, 109.98, 93.26, 87.68, 82.35, 77.22, 76.90, 75.67, 64.62, 36.00, 32.15.

Homo**6:** ^{1}H NMR (400MHz, $CDCl_3$) δ, 7.33 (s, 16H), 7.09 (s, 4H), 3.53 (s, 6H), 1.27 (s, 36H).

Homo**8**: ^{1}H NMR (400MHz, $CDCl_3$) δ 7.52 (s) 7.44 (s, 4H), 3.68 (s, 6H), 1.44 (s, 36H).

5. SUPPORTING SPECTRA

^{1}H NMR spectrum of 1, 3-di-tert-butyl-5-iodo-2-methoxybenzene (**2**)

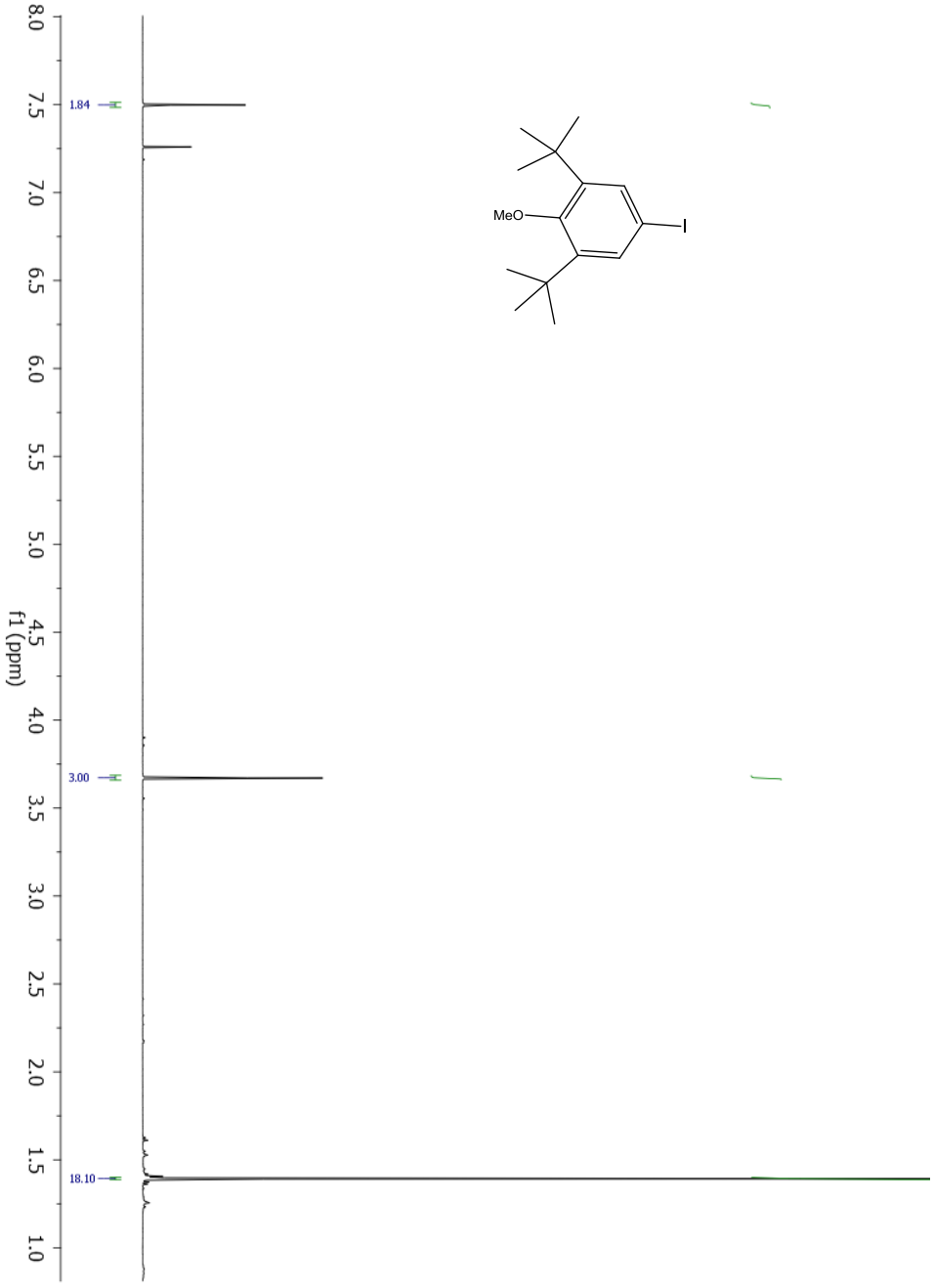

^{13}C NMR spectrum of 1, 3-di-tert-butyl-5-iodo-2-methoxybenzene (**2**)

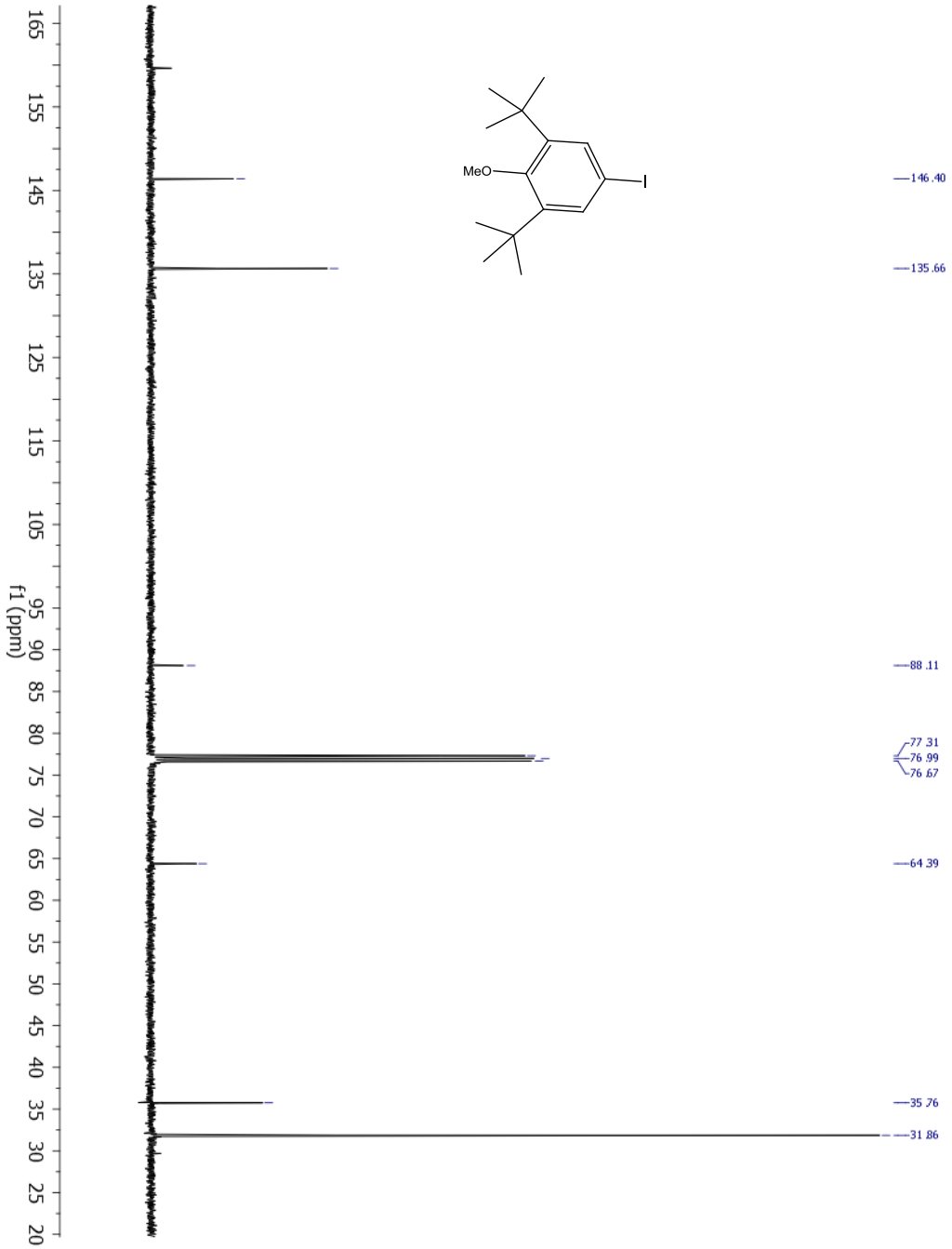

^{1}H NMR spectrum of 1, 3-di-tert-butyl-5-iodo-2-methoxybenzene (**3**)

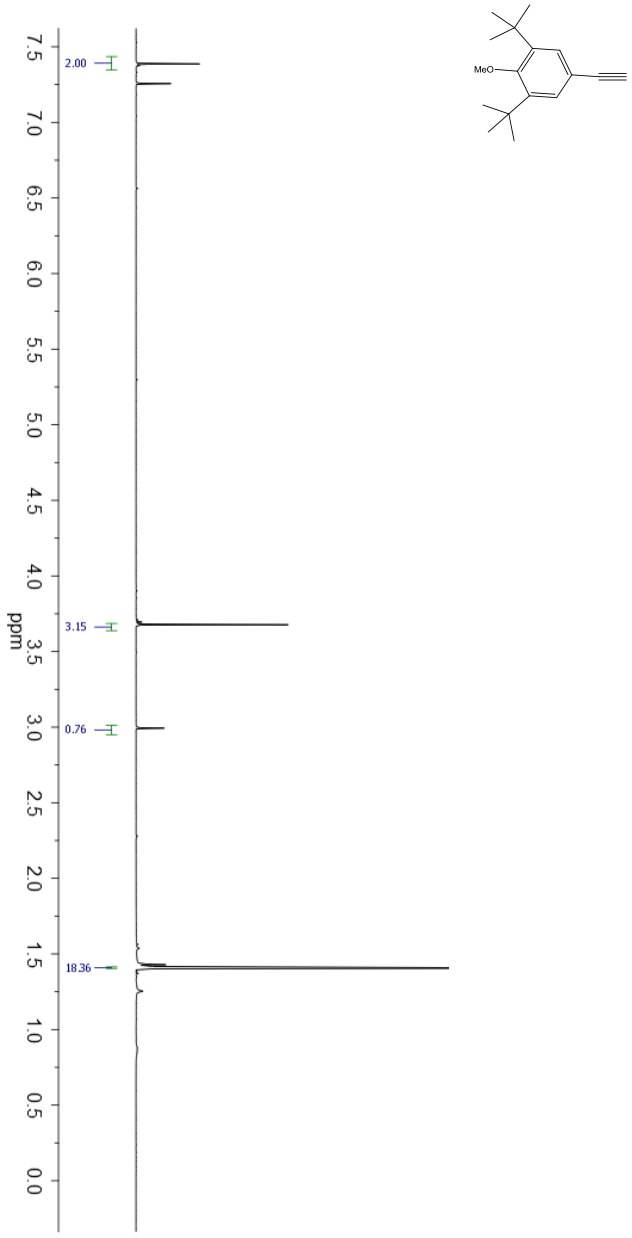

^{13}C NMR spectrum of 1, 3-di-tert-butyl-5-iodo-2-methoxybenzene (**3**)

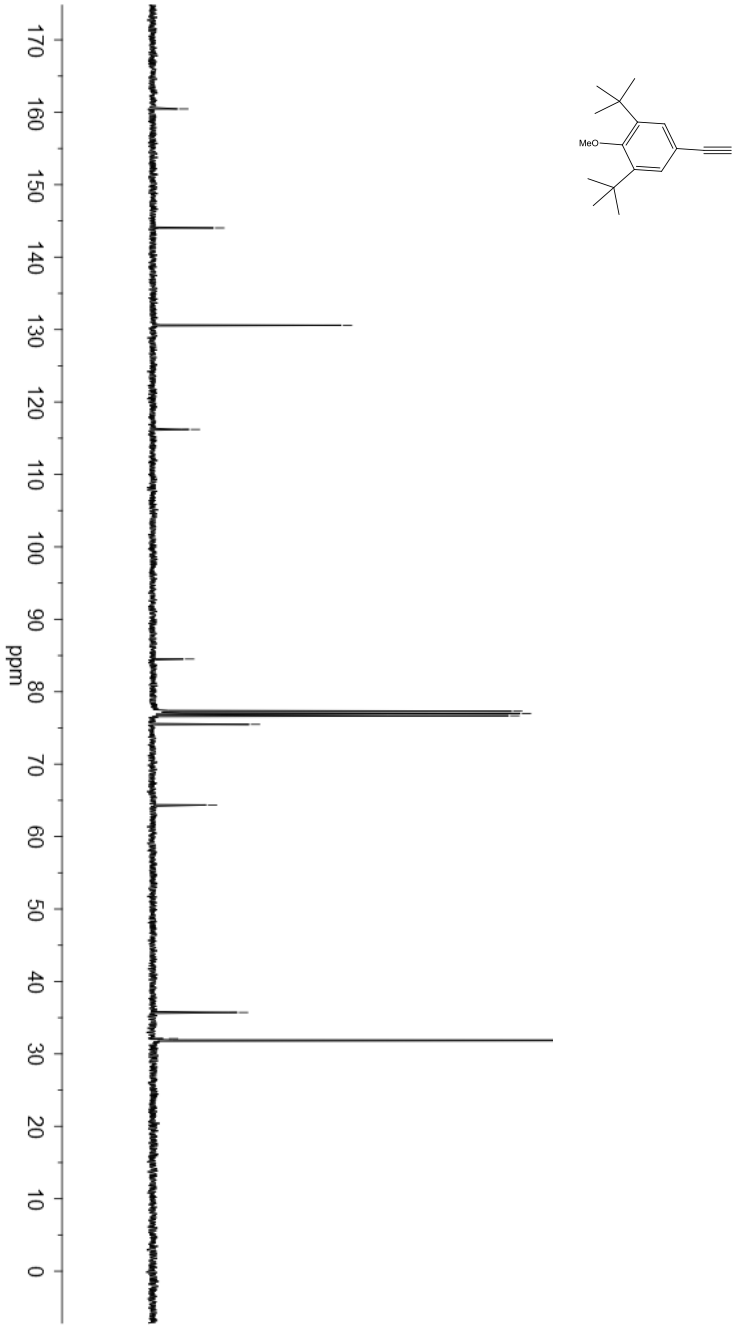

^{1}H NMR spectrum of compound (**4a**)

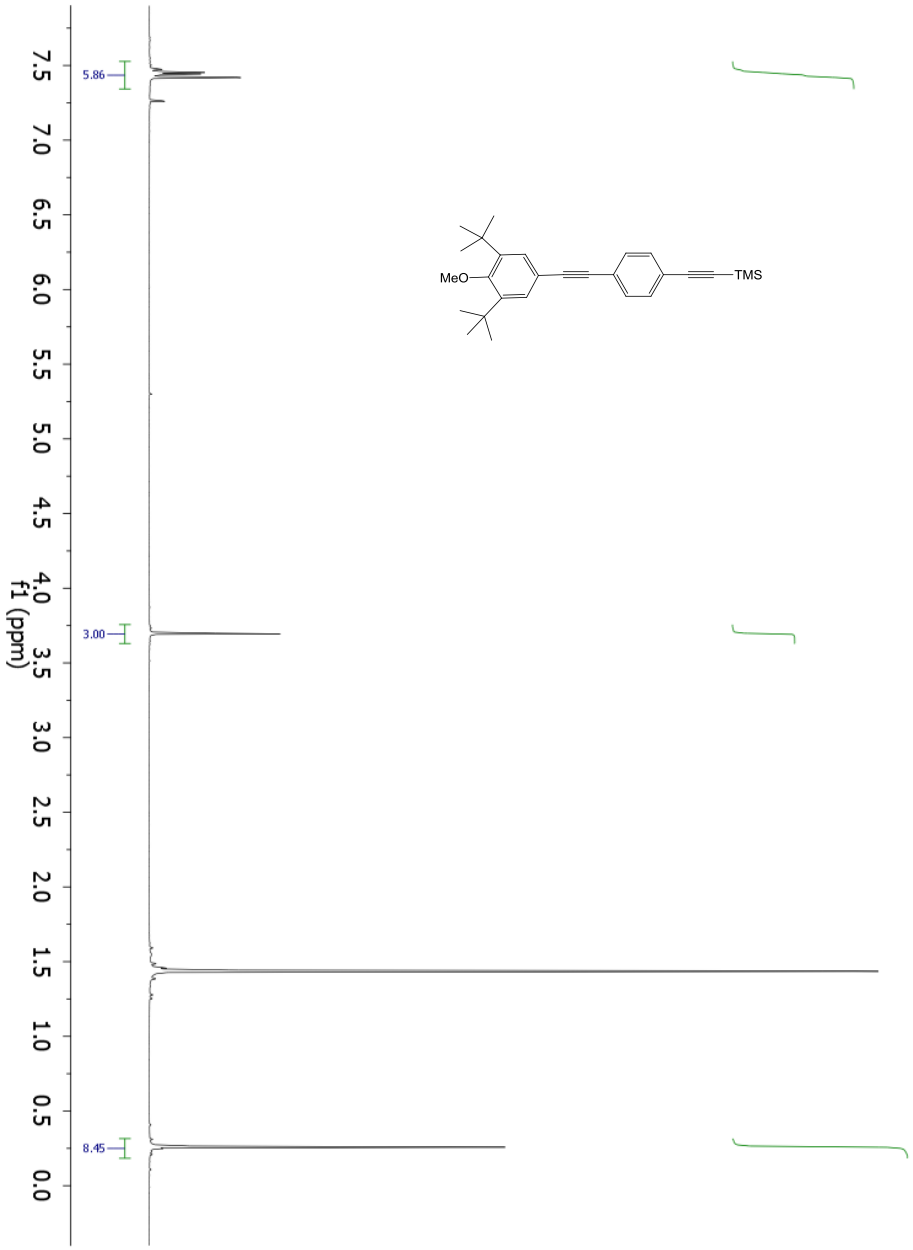

^{13}C NMR spectrum of compound (**4a**)

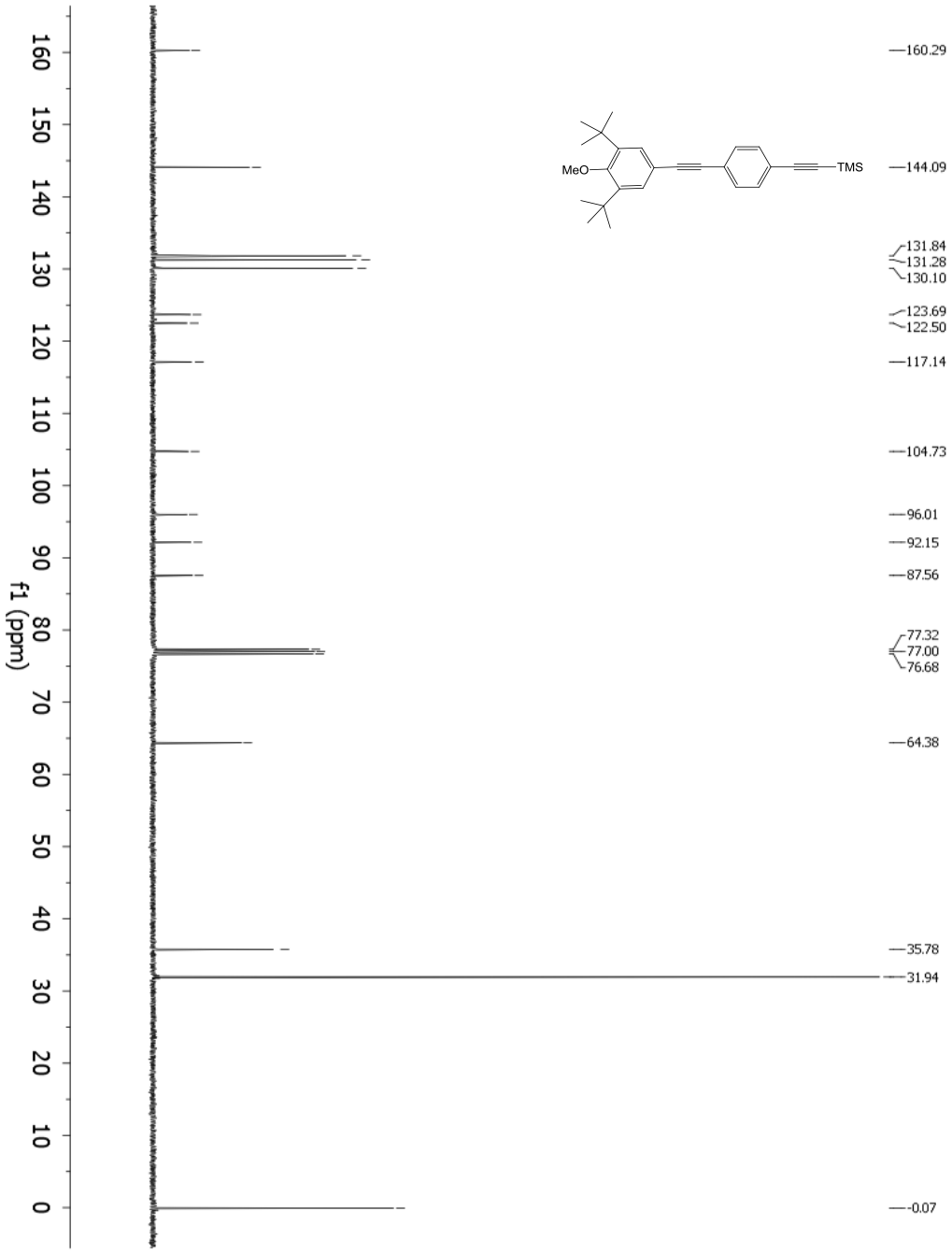

^{1}H NMR spectrum of compound (**4b**)

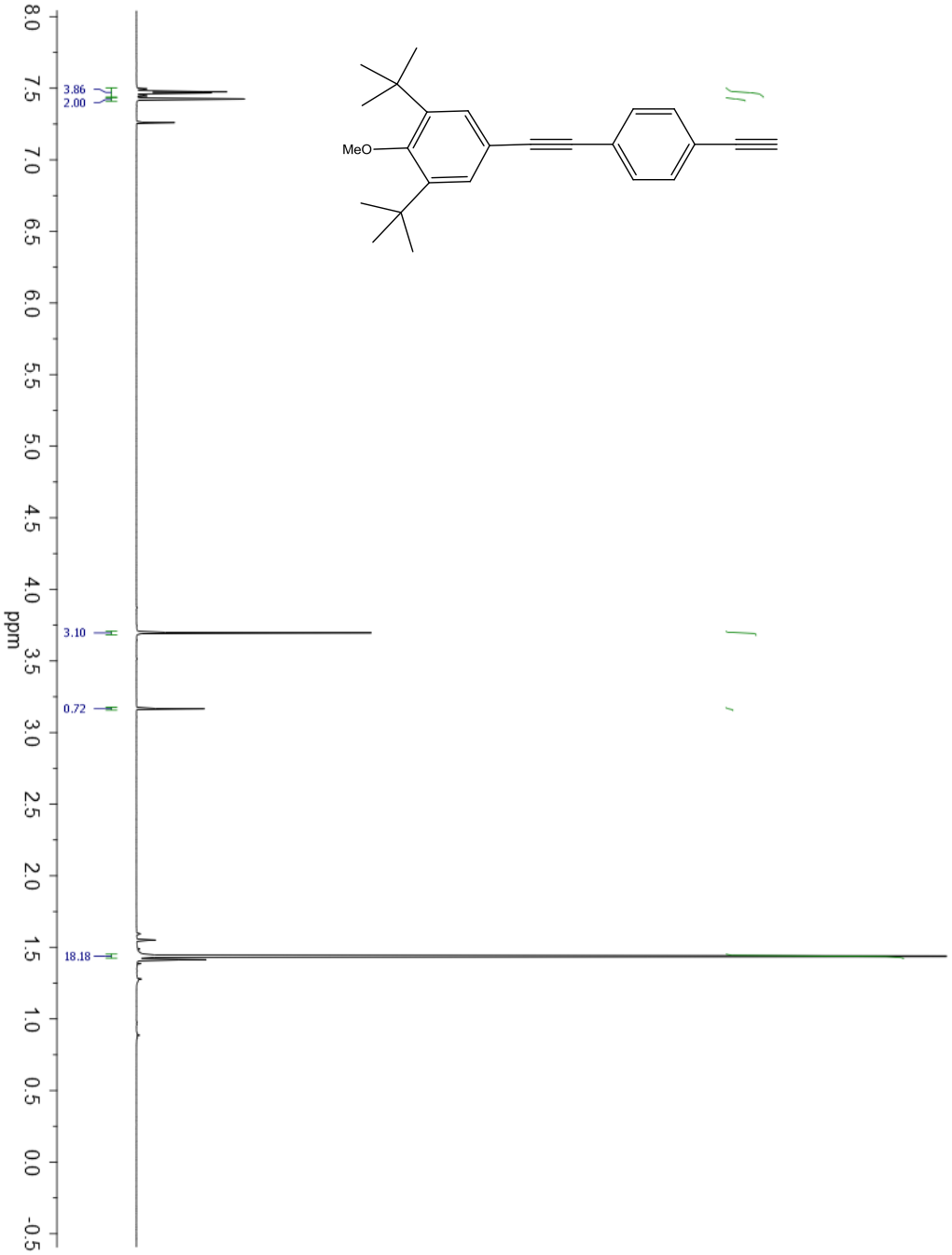

^{13}C NMR spectrum of compound (**4b**)

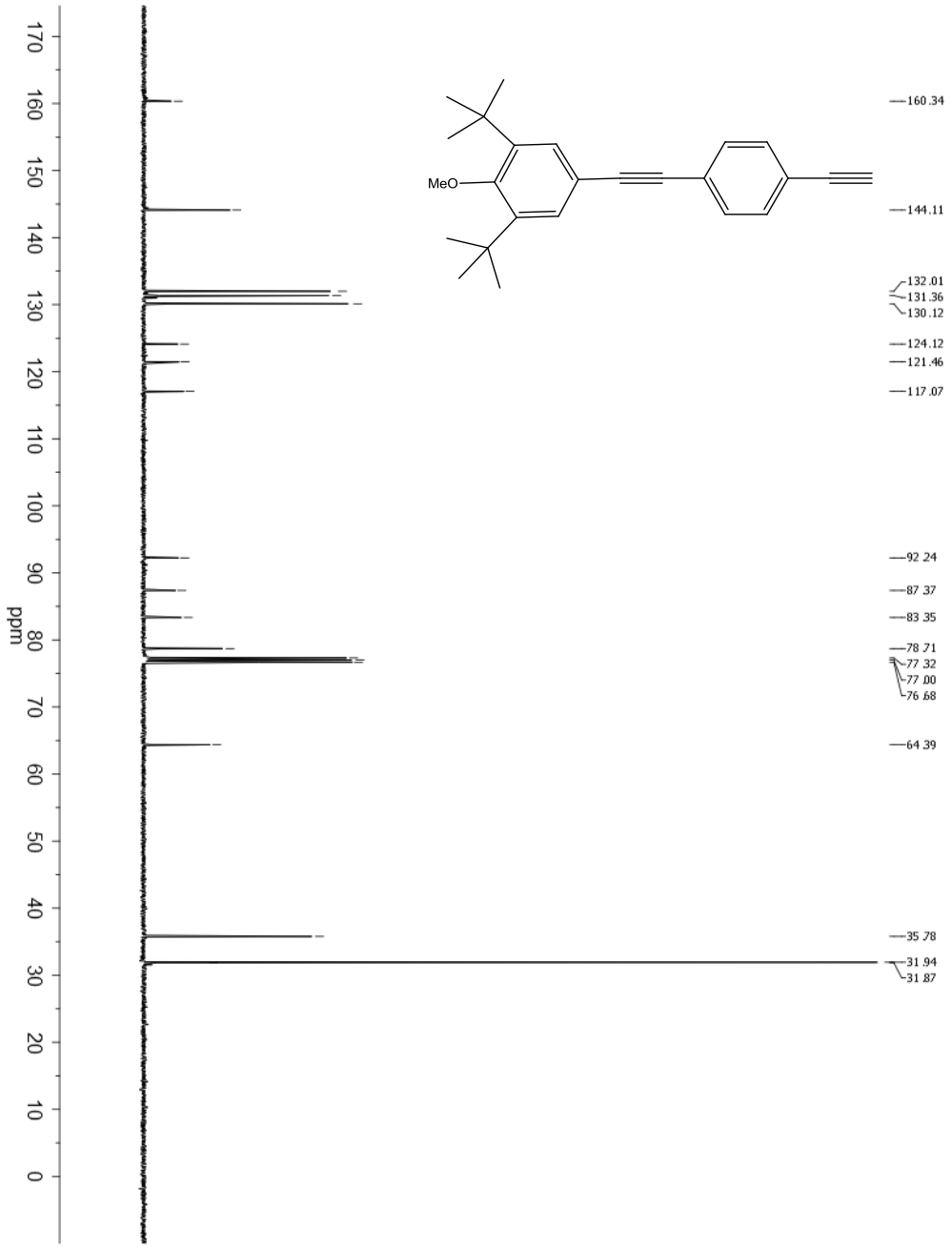

^{1}H NMR spectrum of compound (**5a**)

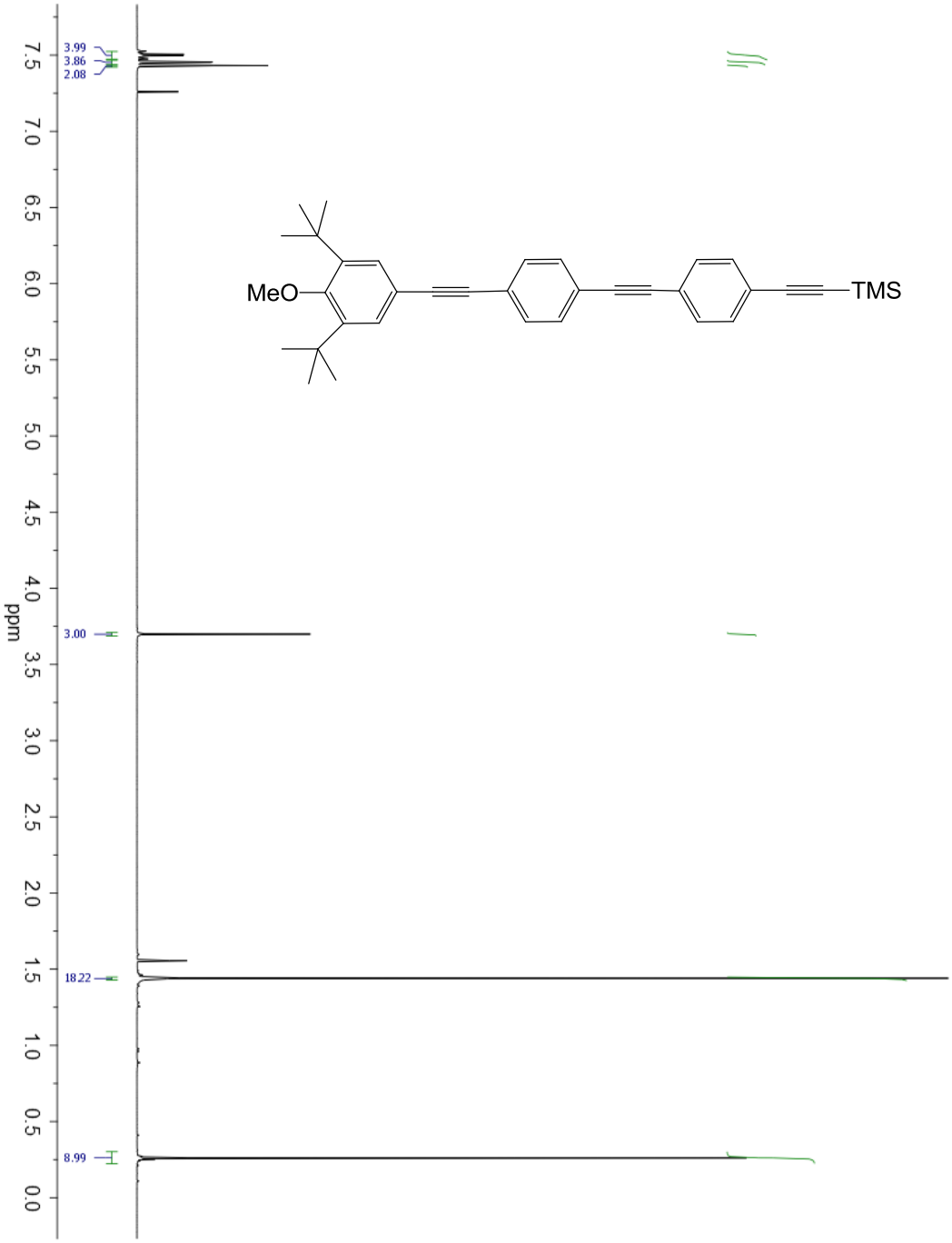

^{13}C NMR spectrum of compound (**5a**)

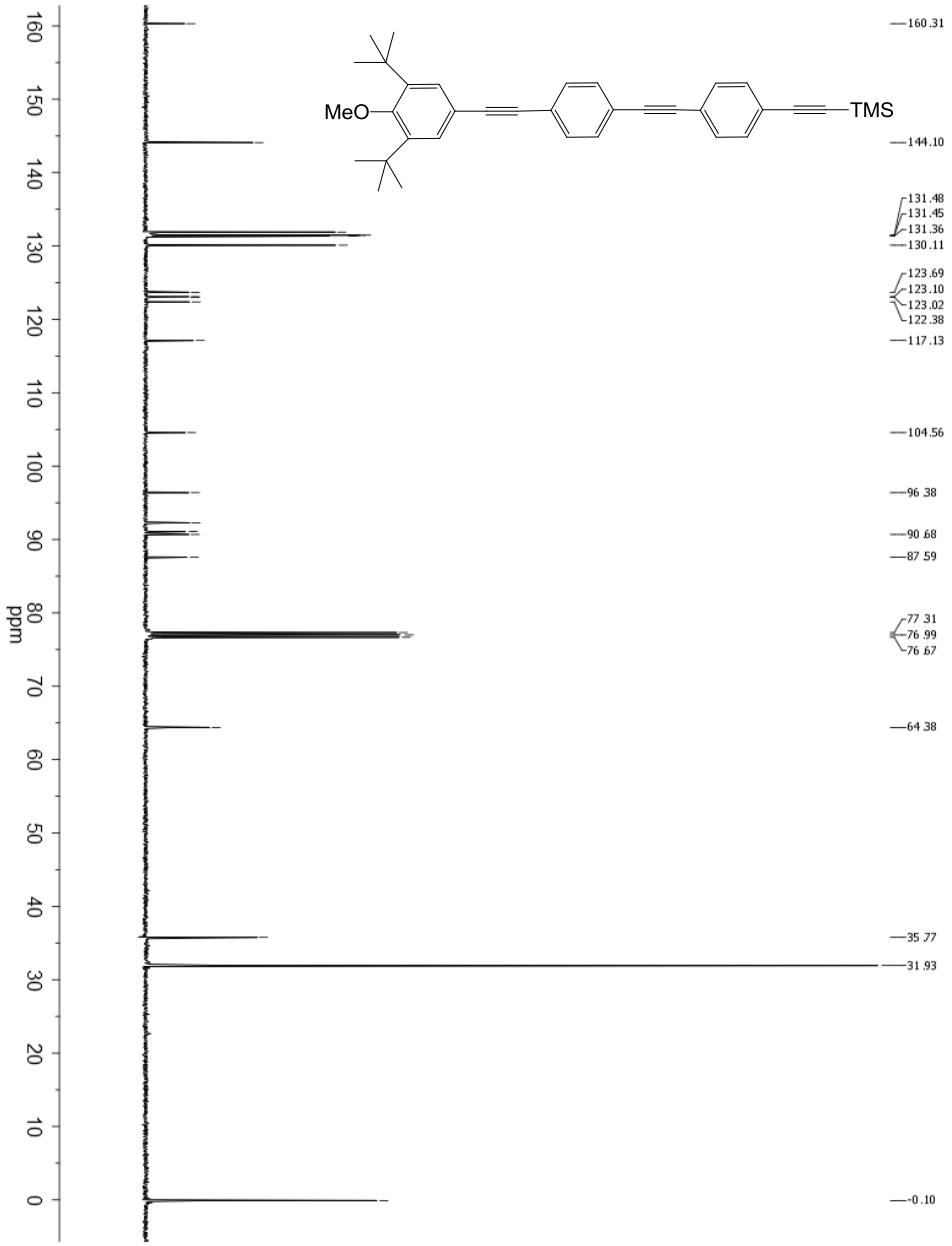

^{1}H NMR spectrum of compound (**5b**)

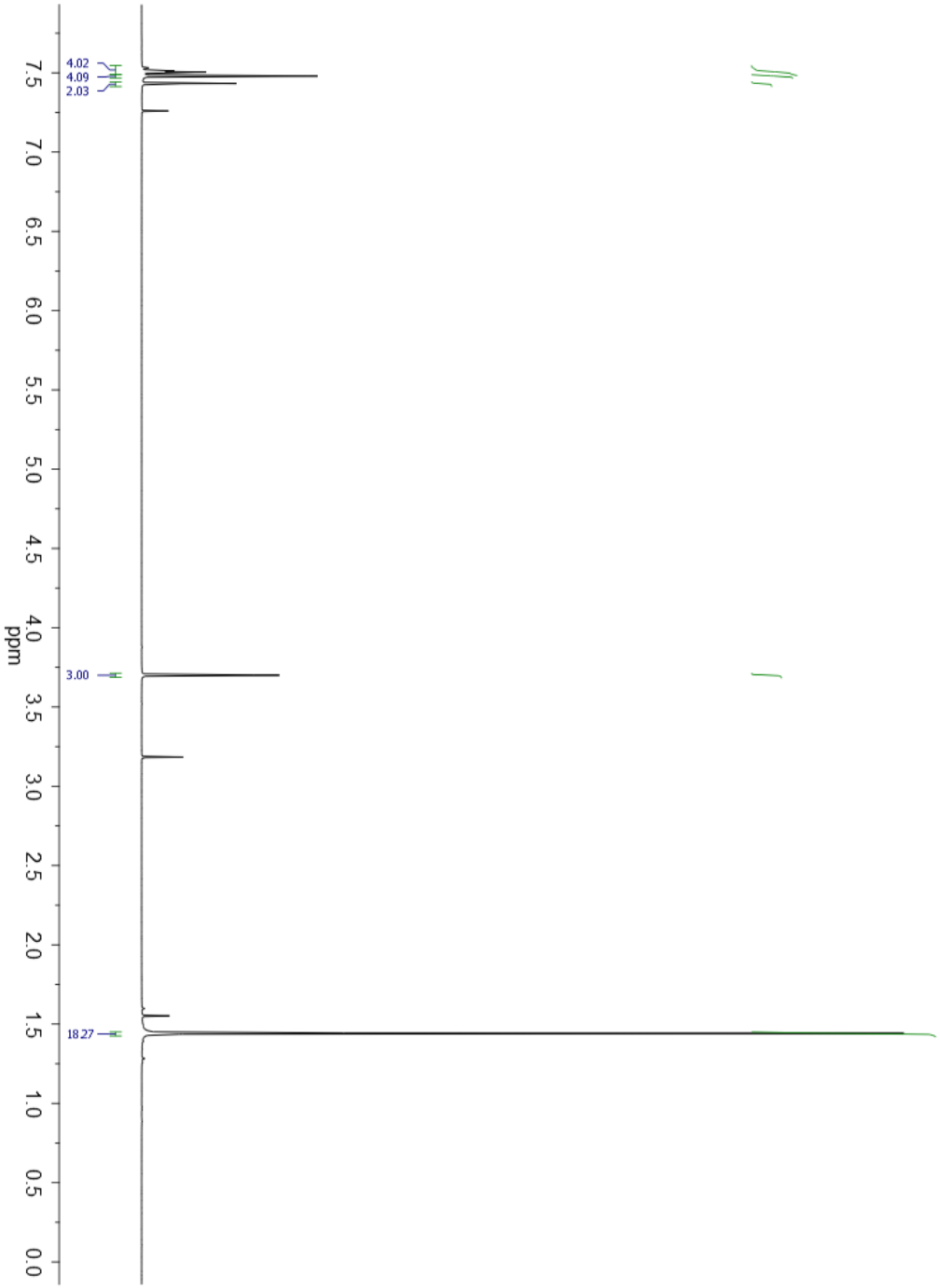

^{13}C NMR spectrum of compound (**5b**)

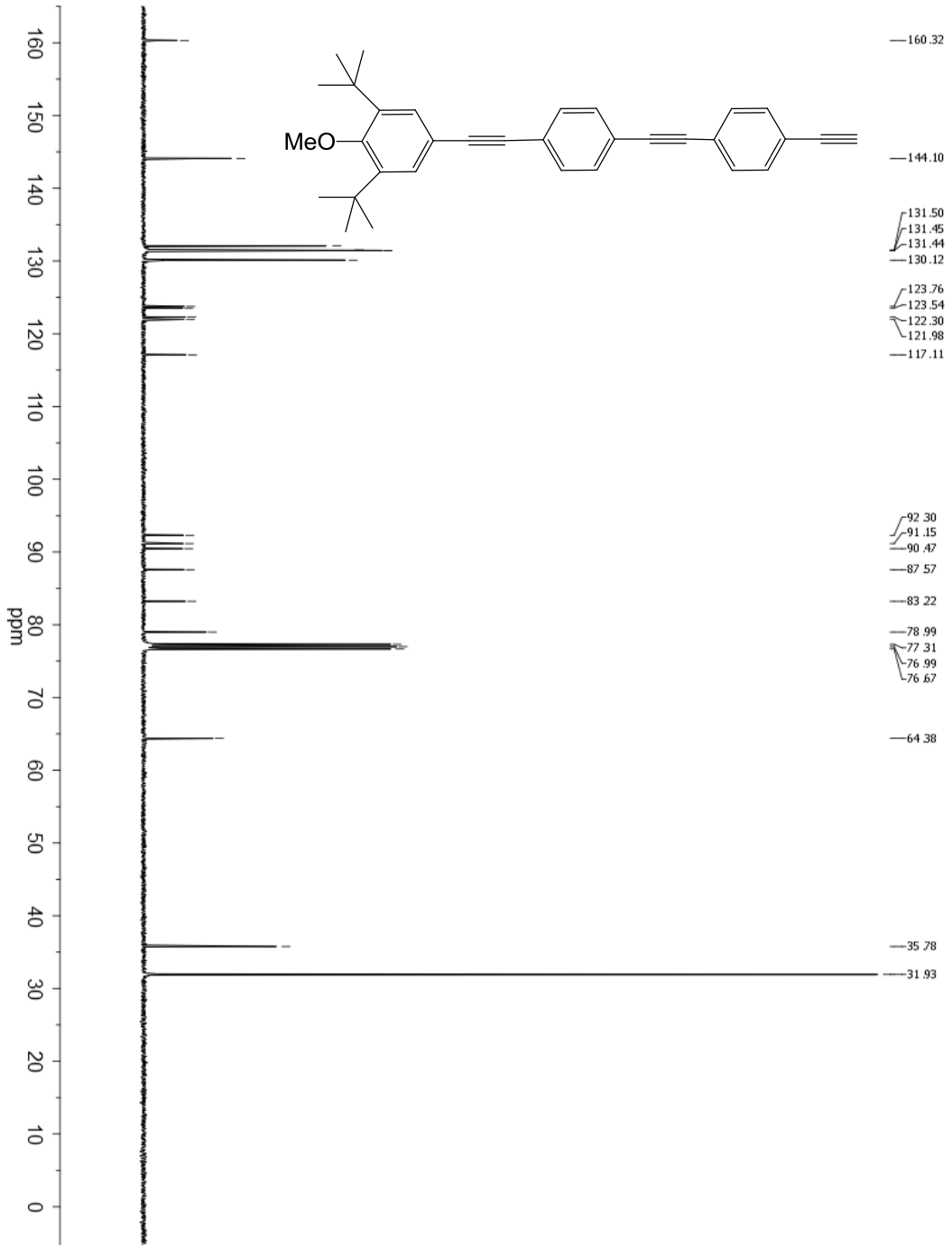

^{1}H NMR spectrum of compound (**6a**)

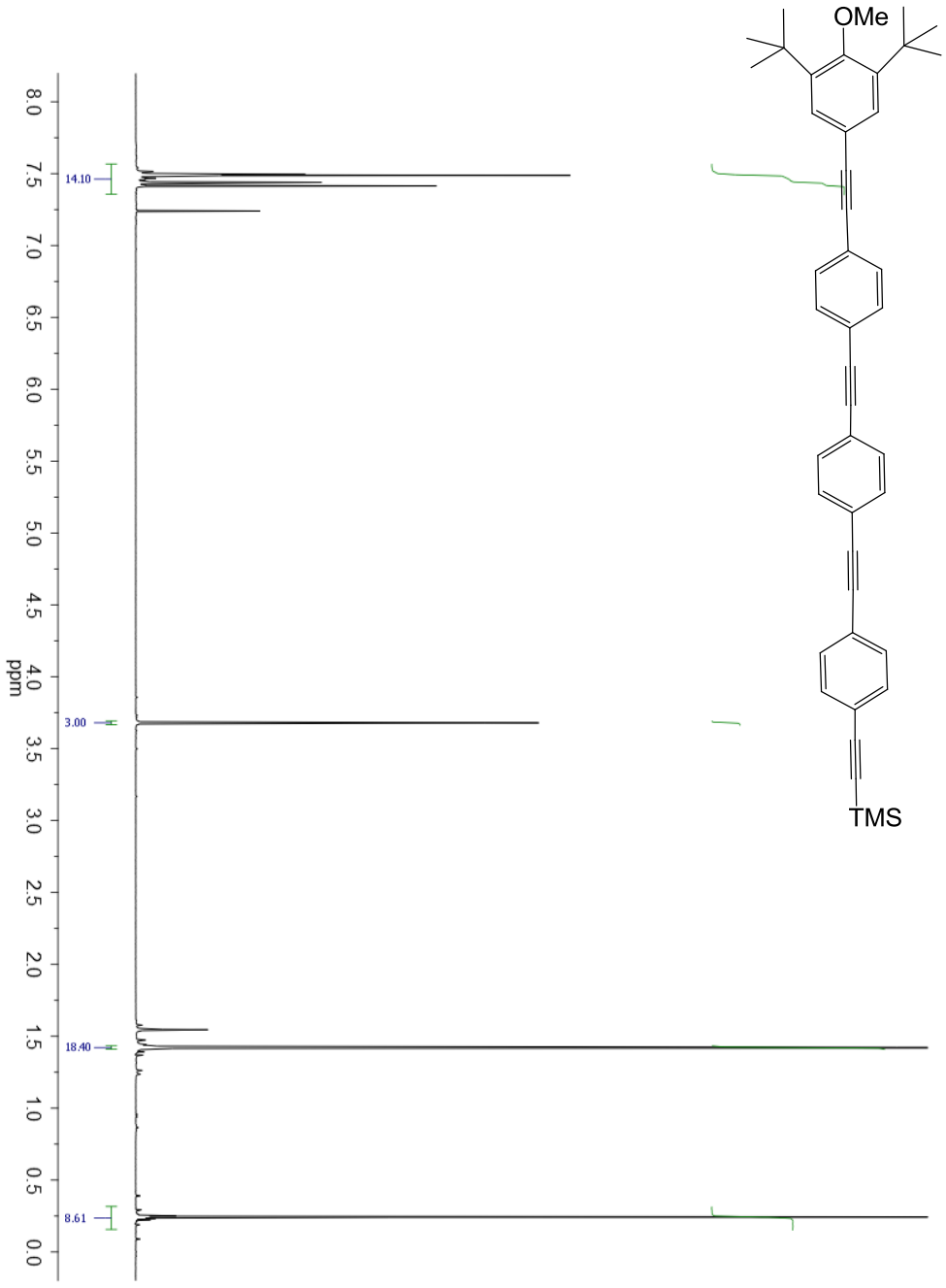

^{13}C NMR spectrum of compound (**6a**)

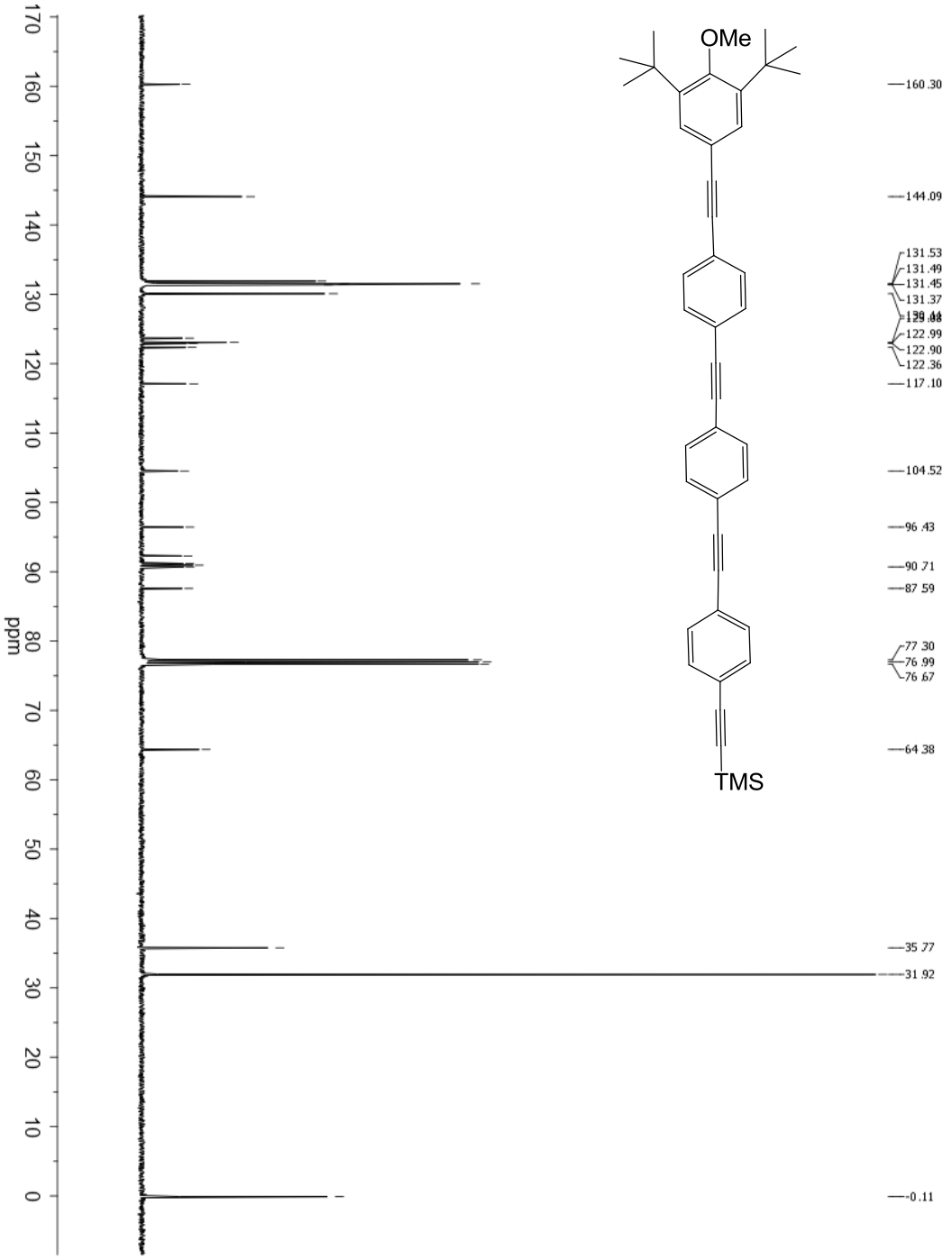

^{1}H NMR spectrum of compound (**6b**)

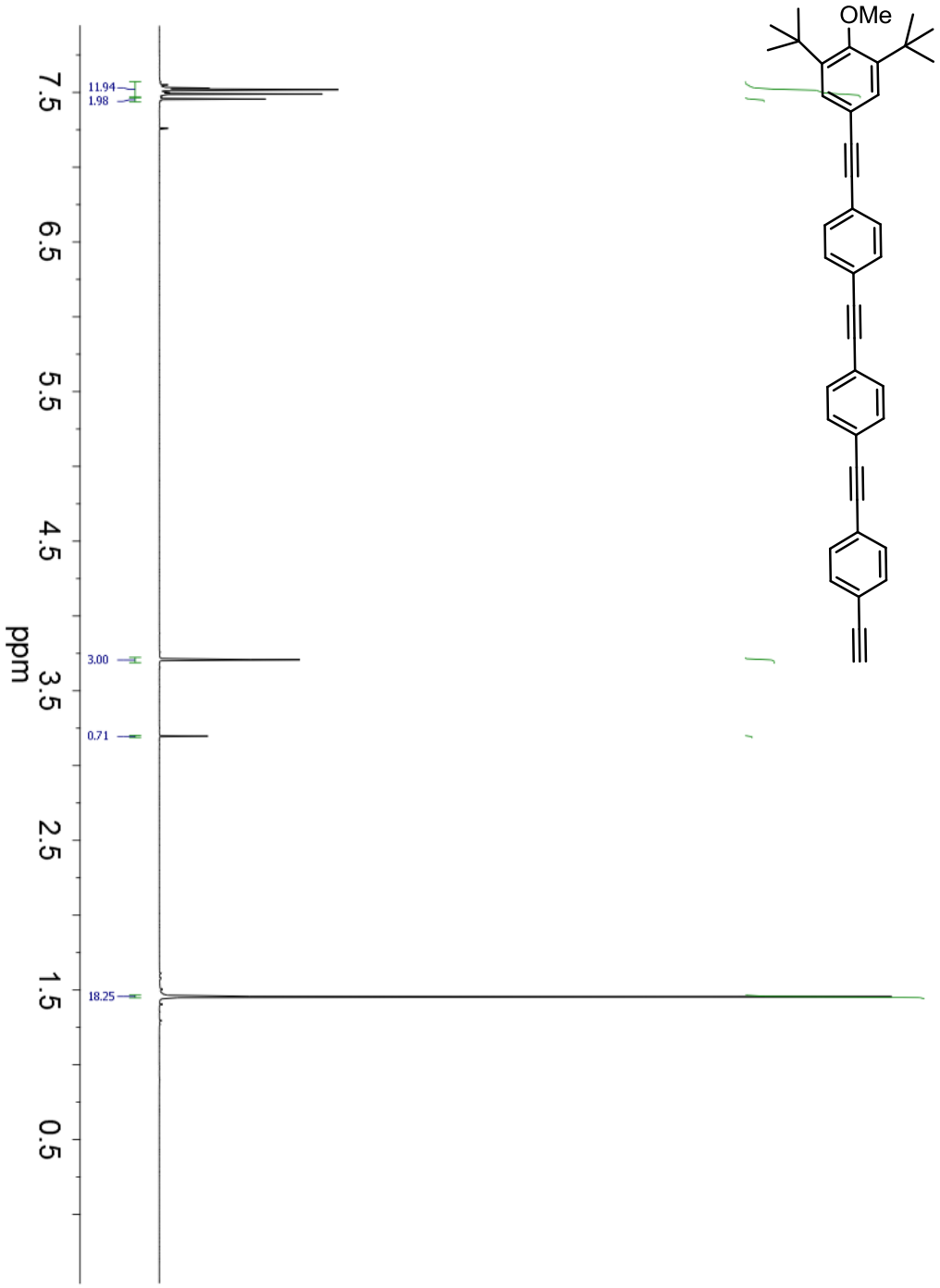

^{13}C NMR spectrum of compound (**6b**)

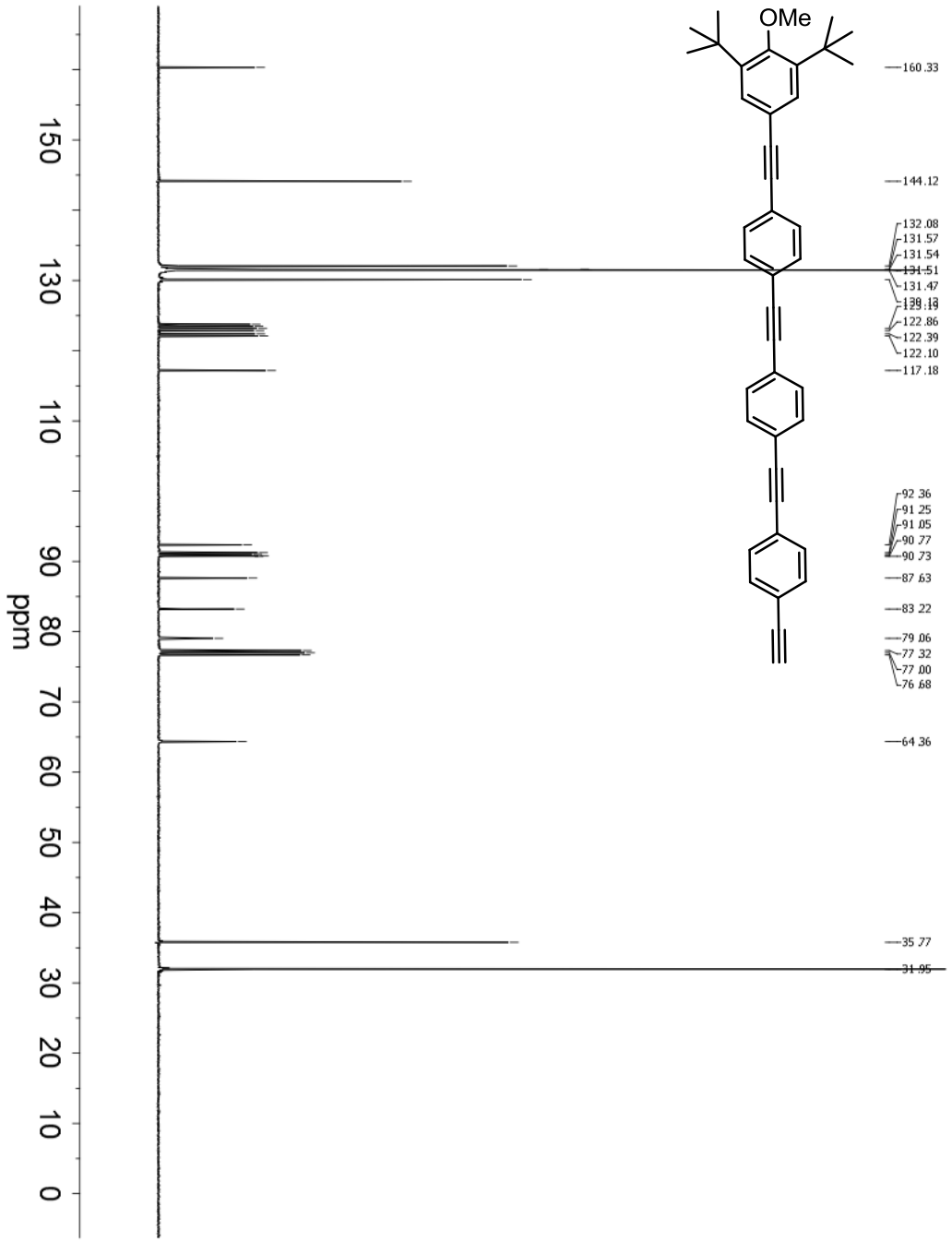

^{1}H NMR spectrum of compound (**7a**)

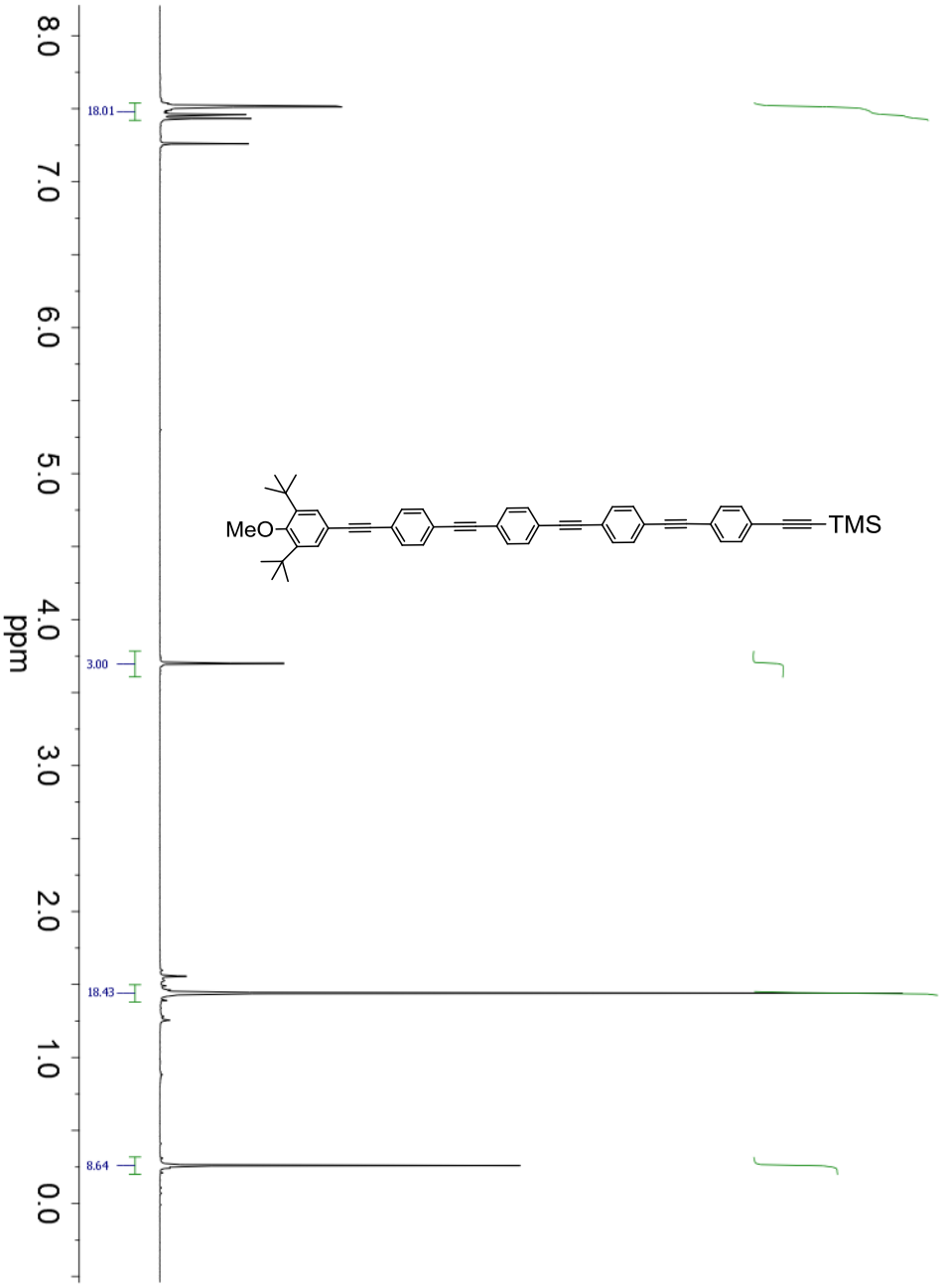

^{13}C NMR spectrum of compound (**7a**)

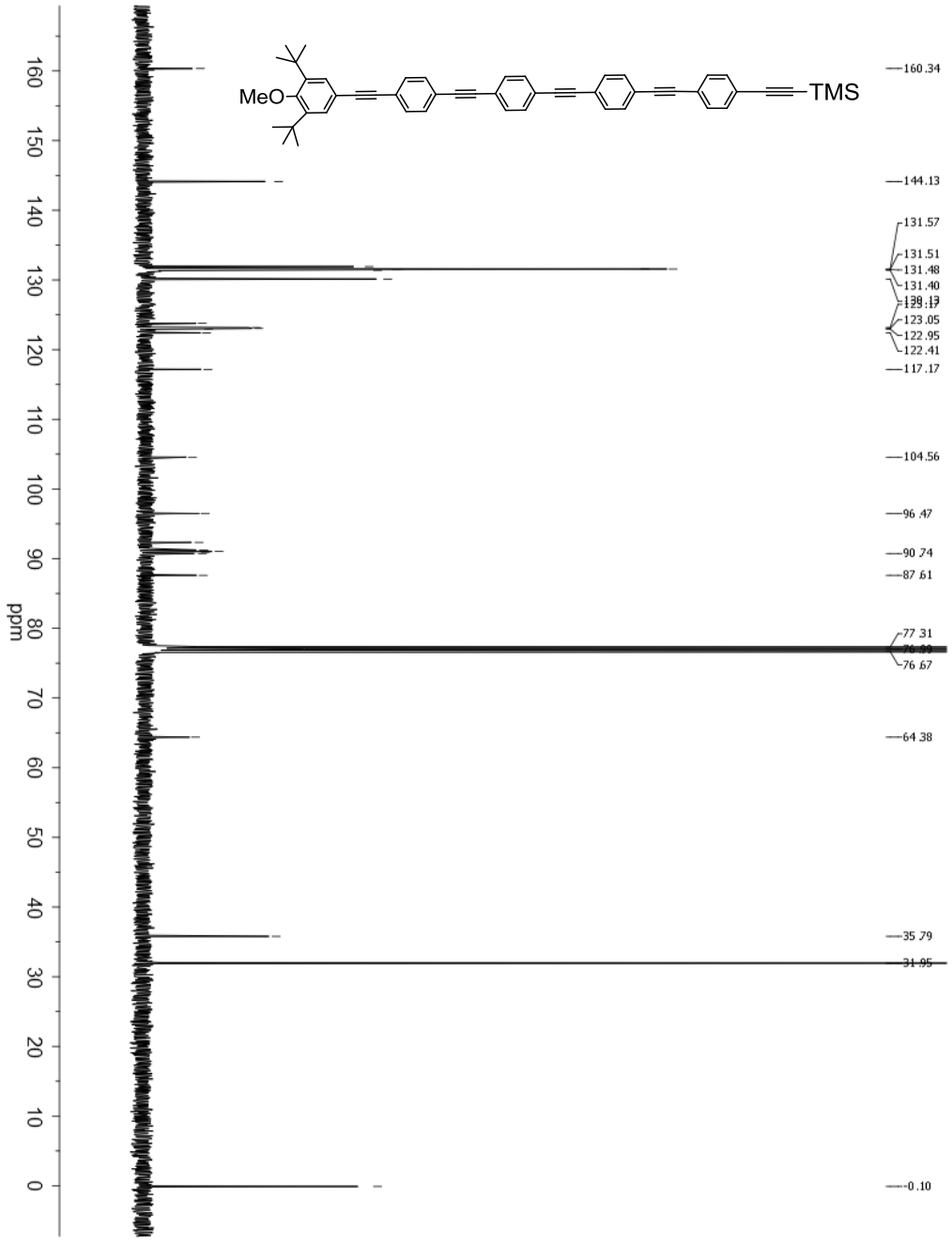

^{1}H NMR spectrum of compound (**8**)

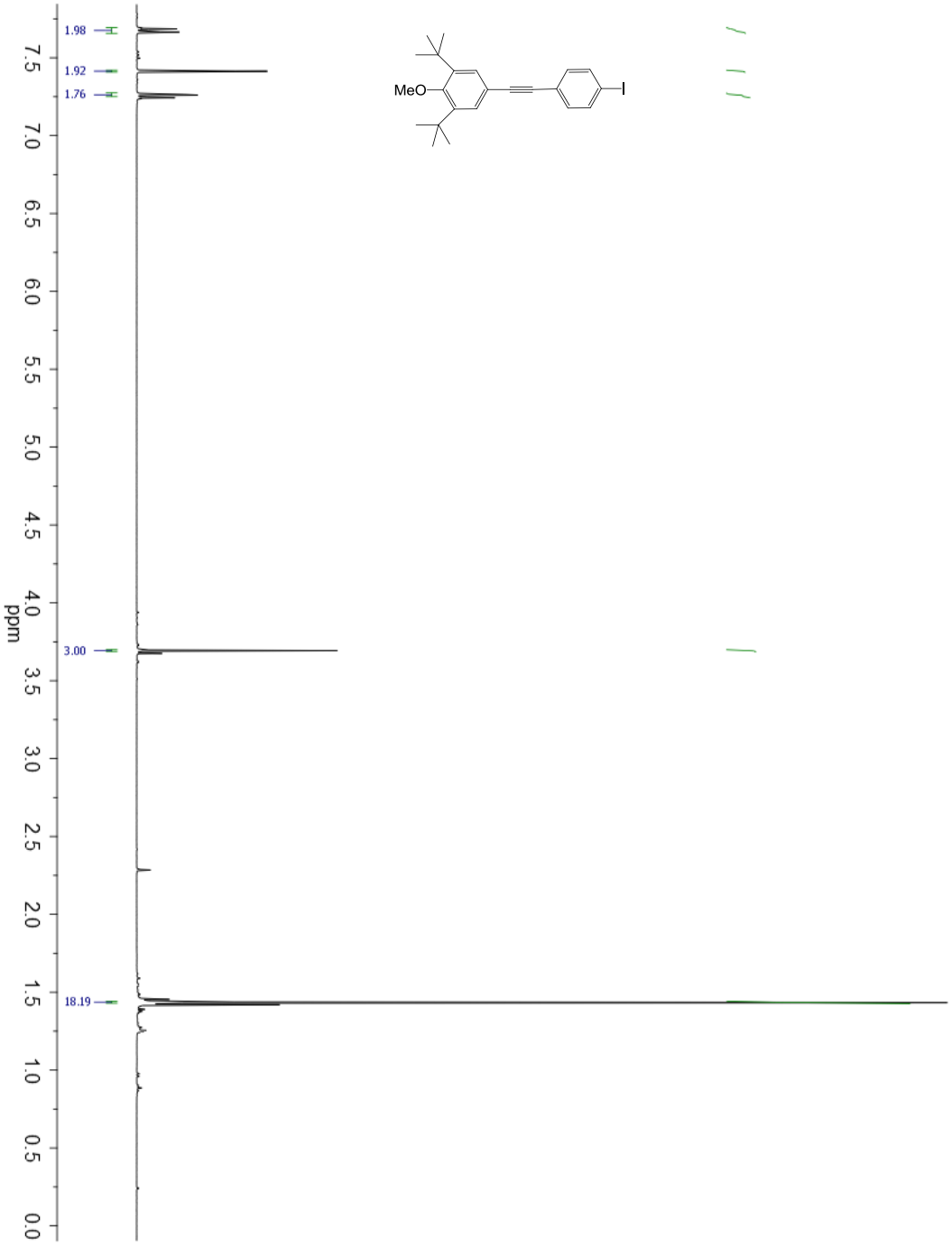

^{13}C NMR spectrum of compound (**8**)

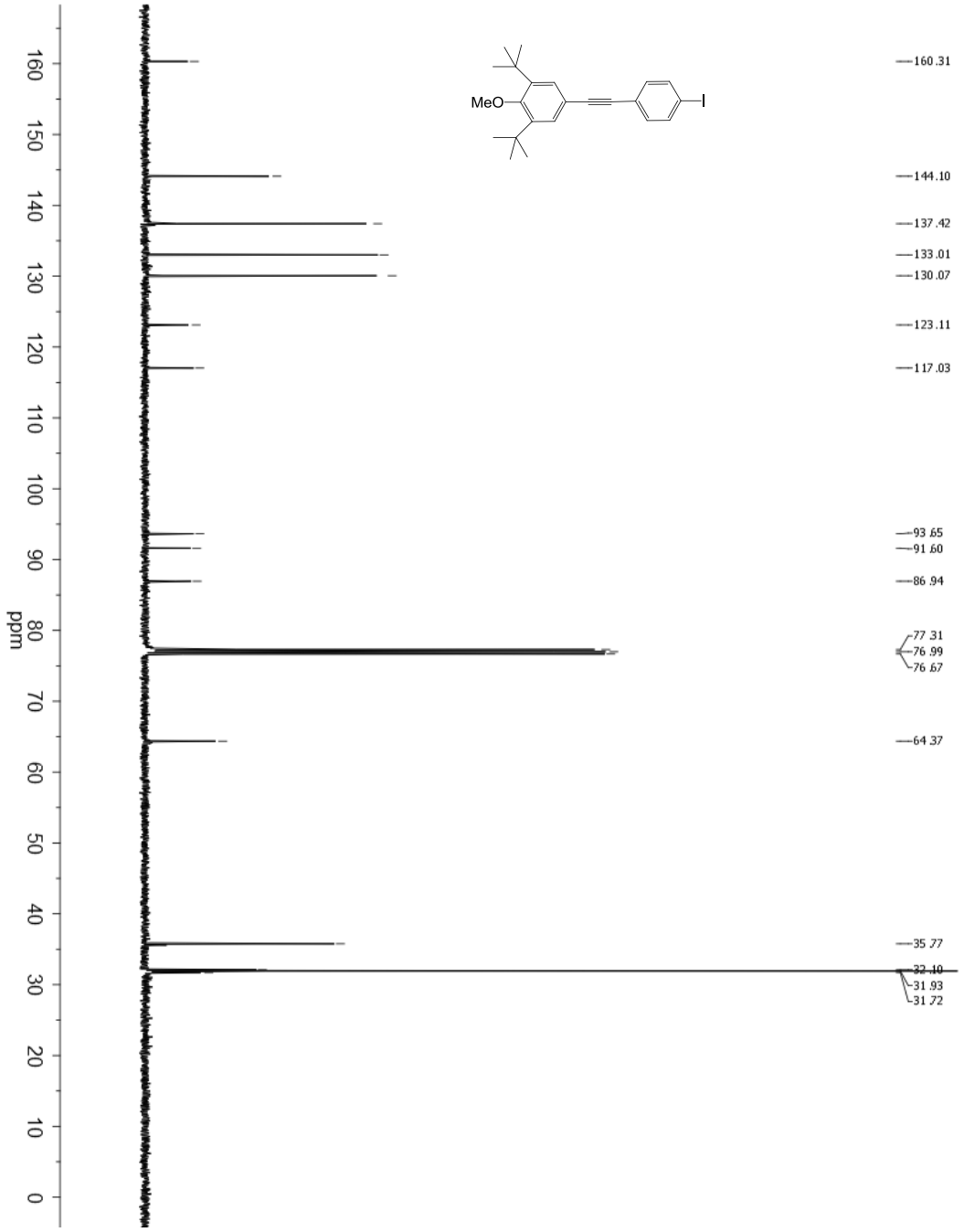

^{1}H NMR spectrum of compound (**9**)

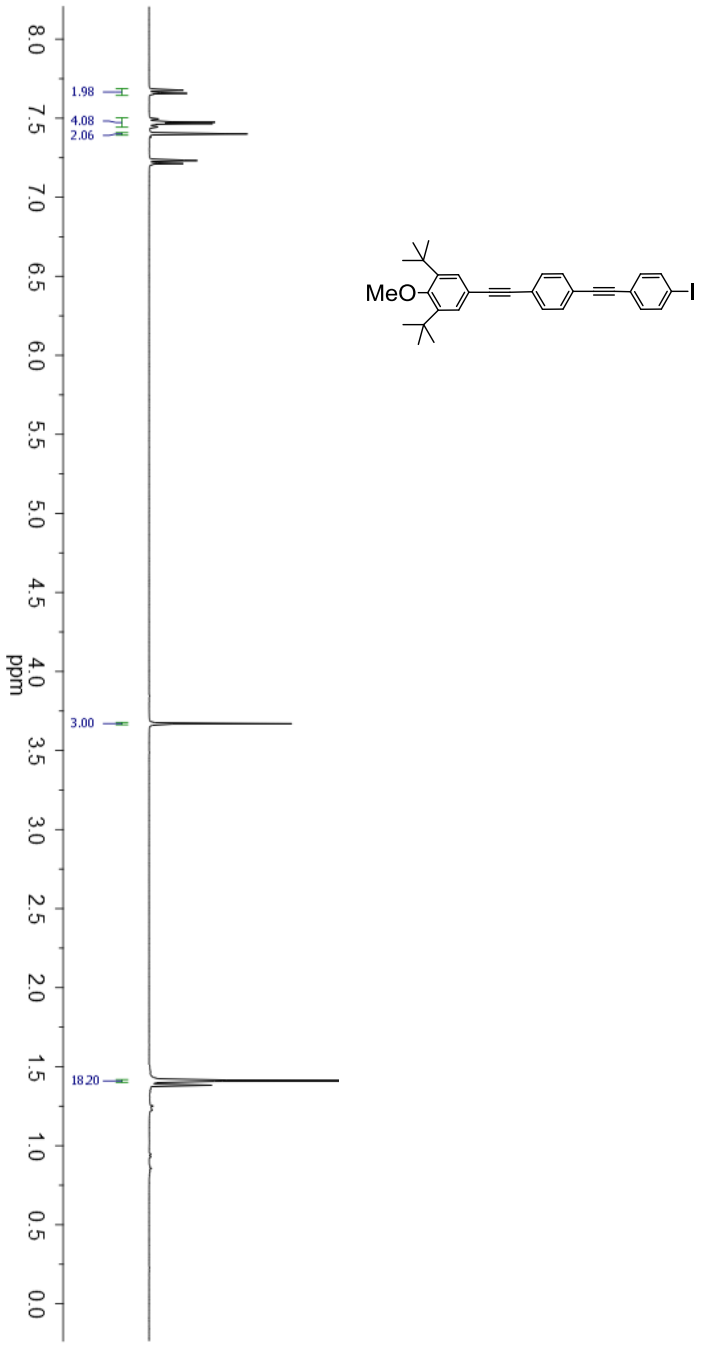

^{13}C NMR spectrum of compound (**9**)

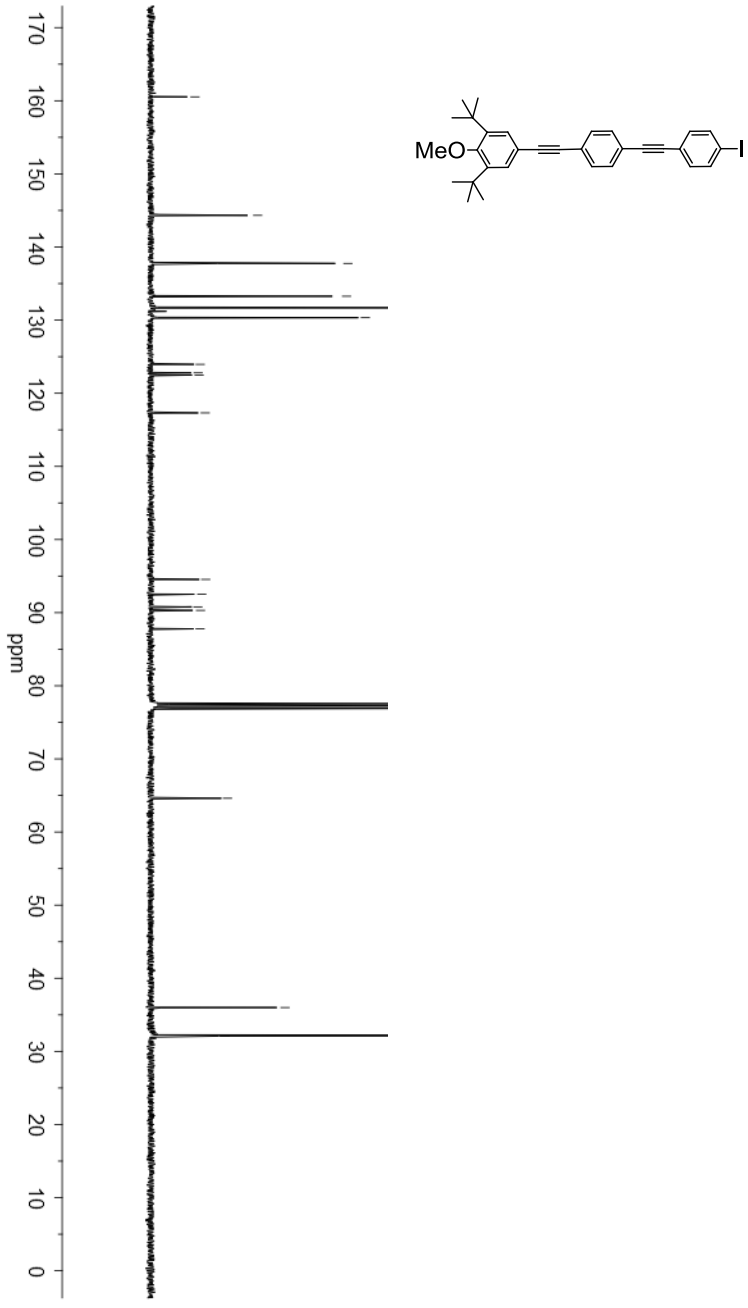

^{1}H NMR spectrum of compound (**10**)

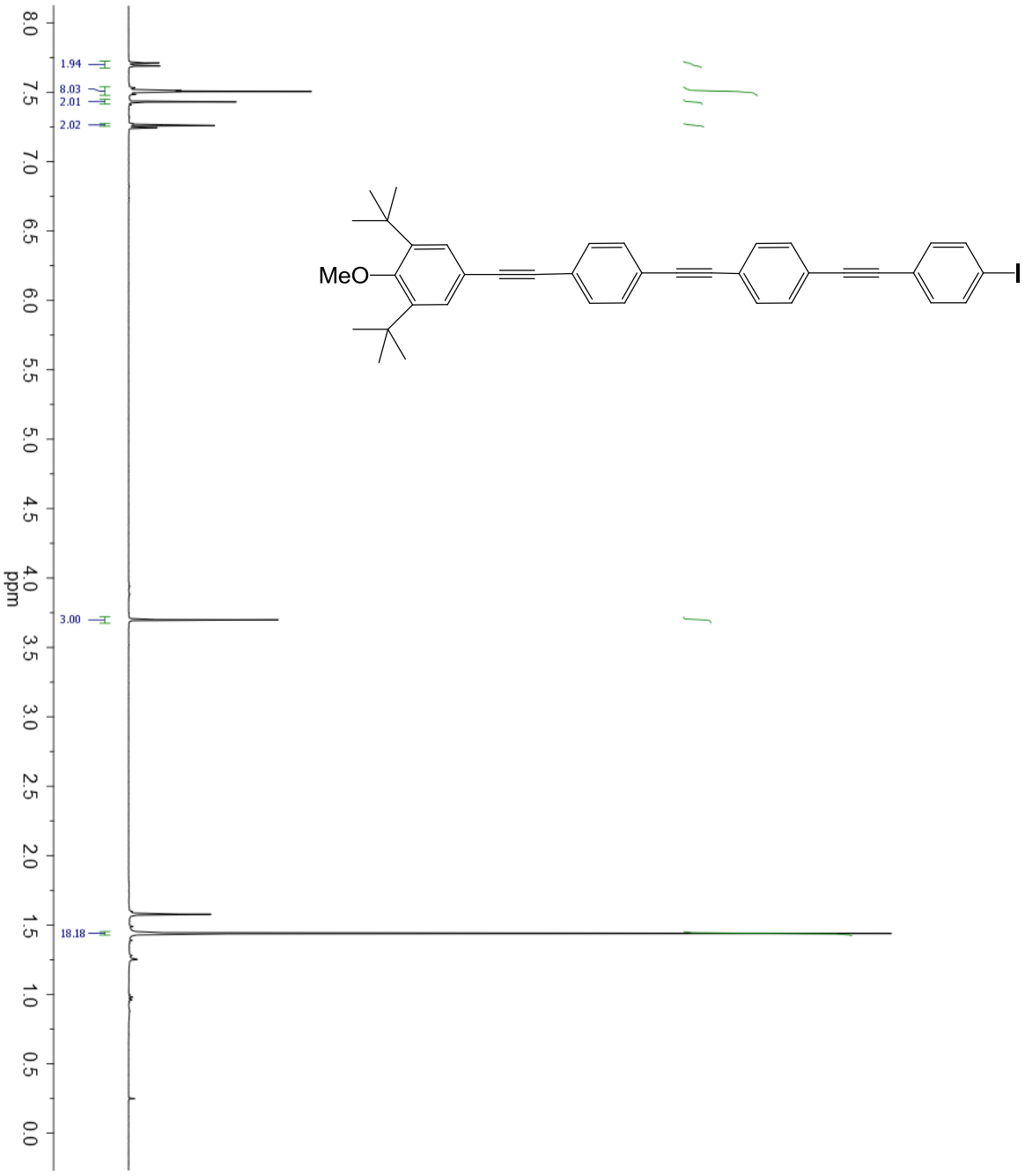

^{13}C NMR spectrum of compound (**10**)

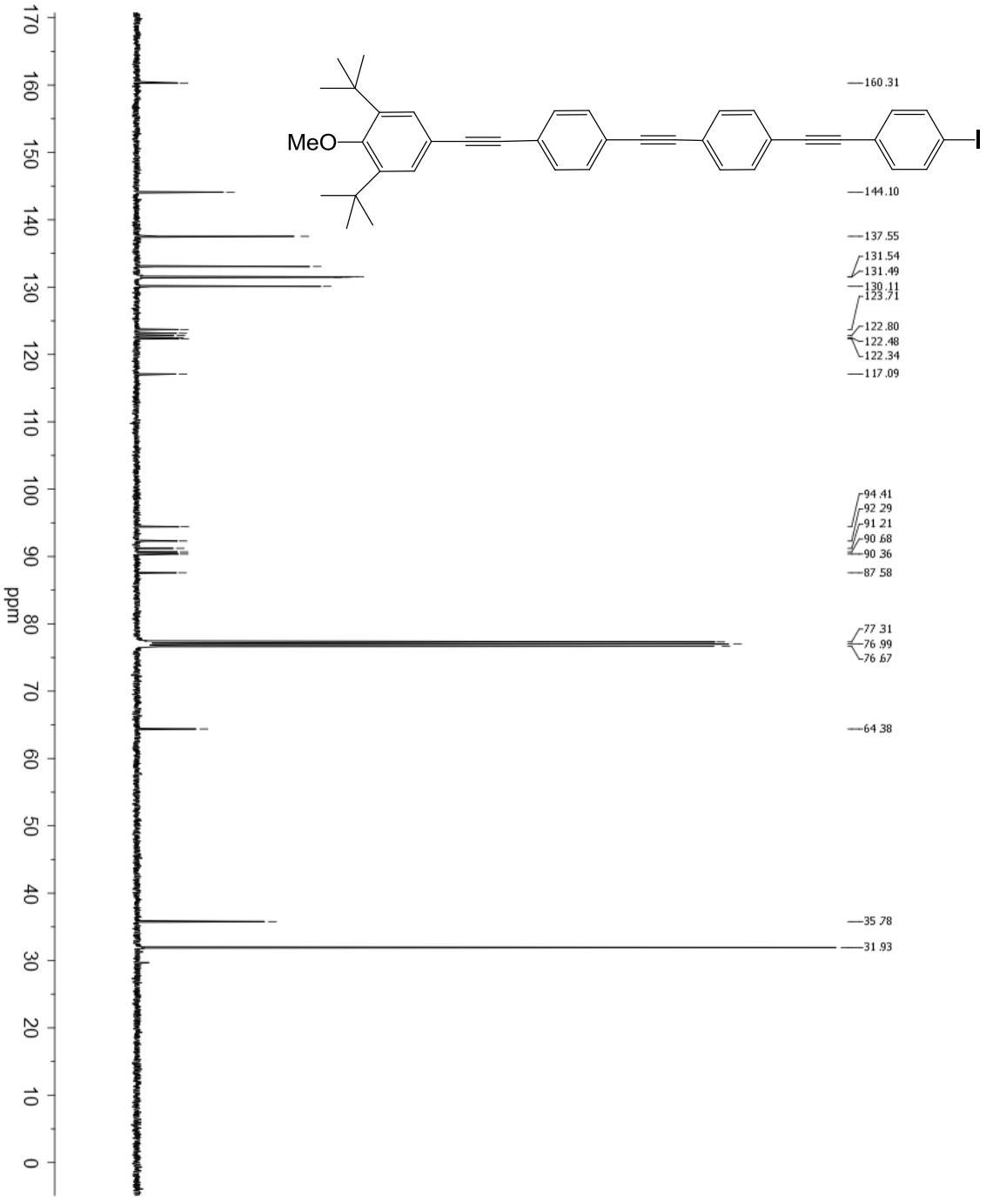

^{1}H NMR spectrum of compound (**11**)

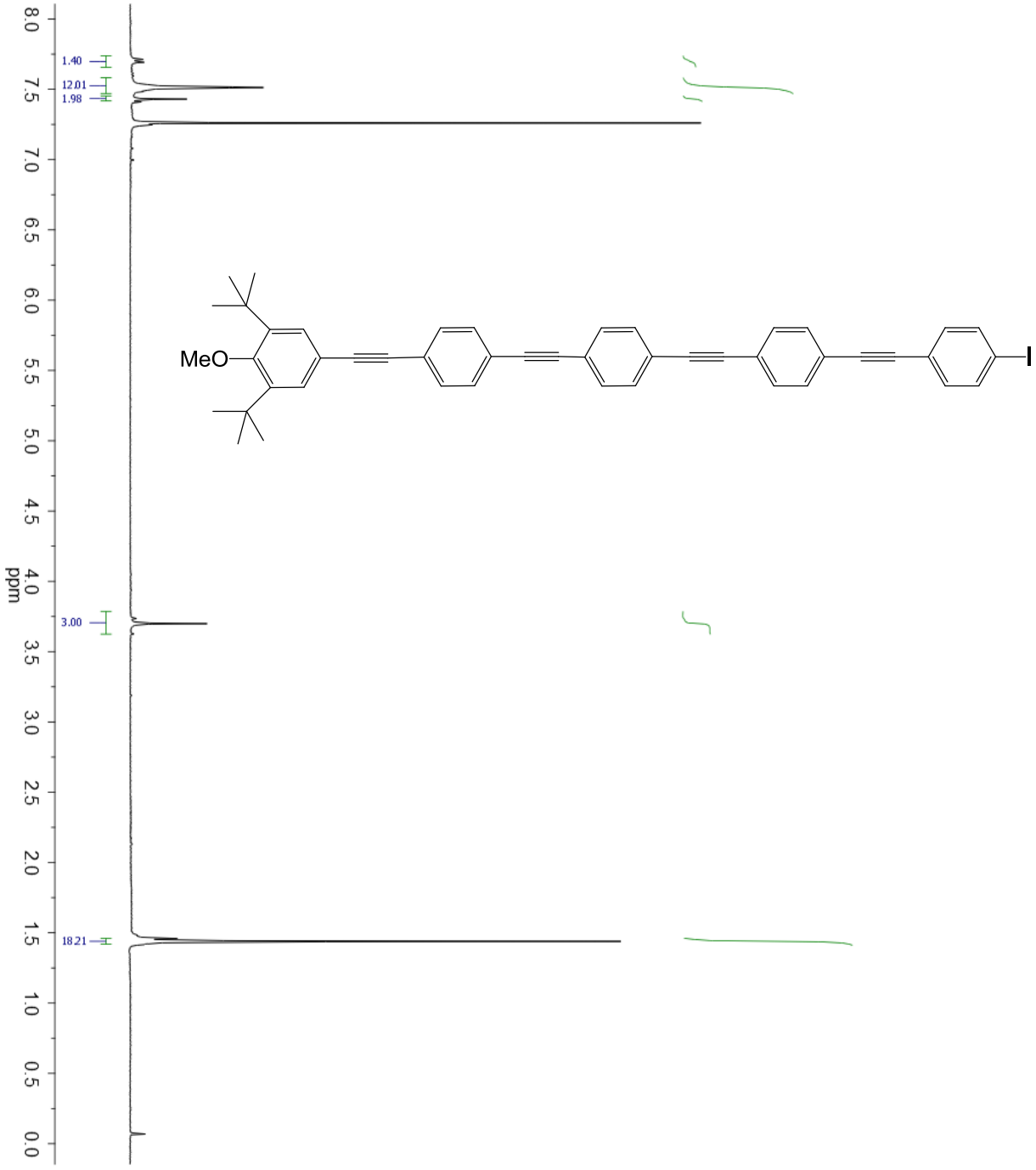

^{1}H NMR spectrum of compound (**12**)

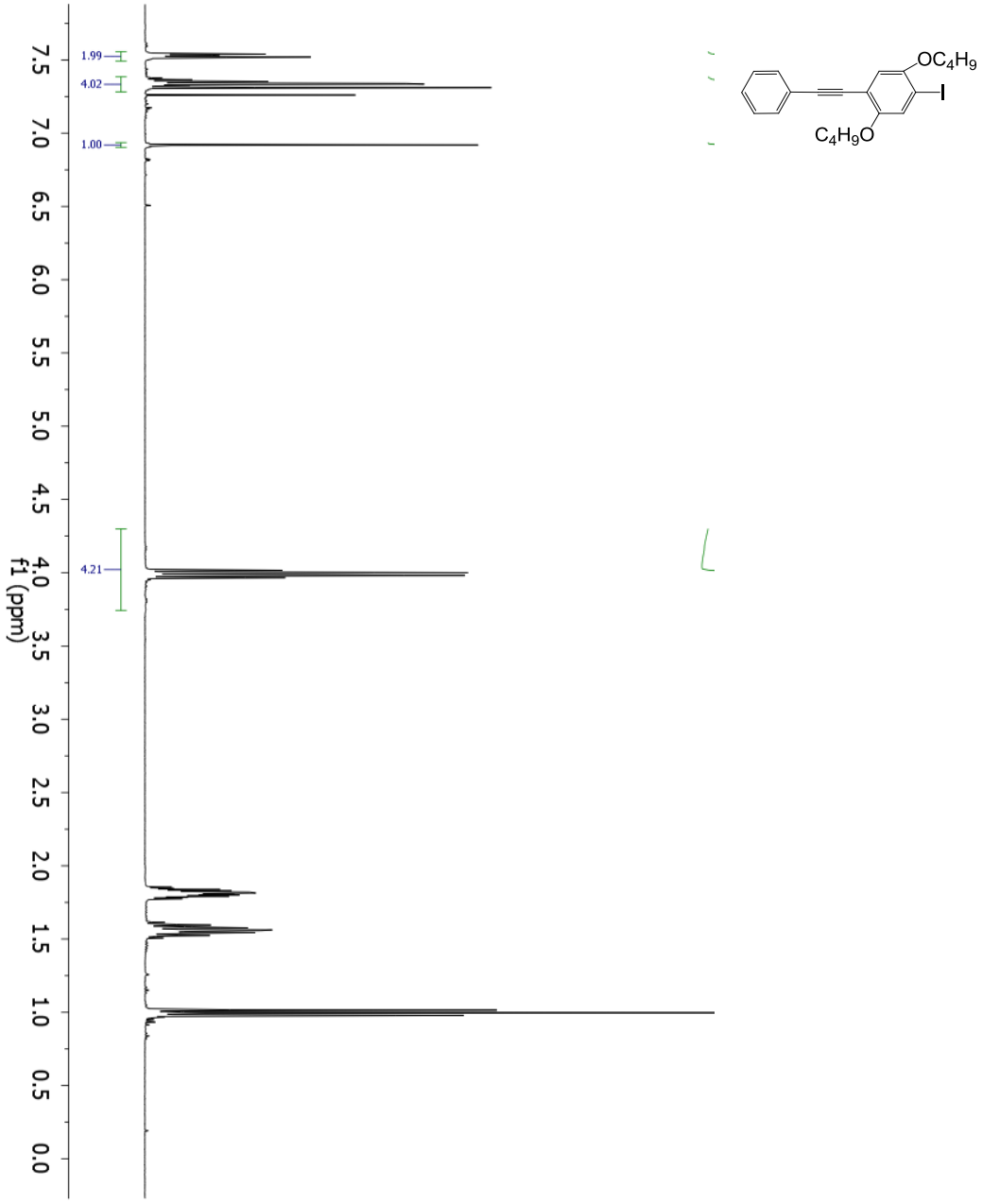

^{13}C NMR spectrum of compound (**12**)

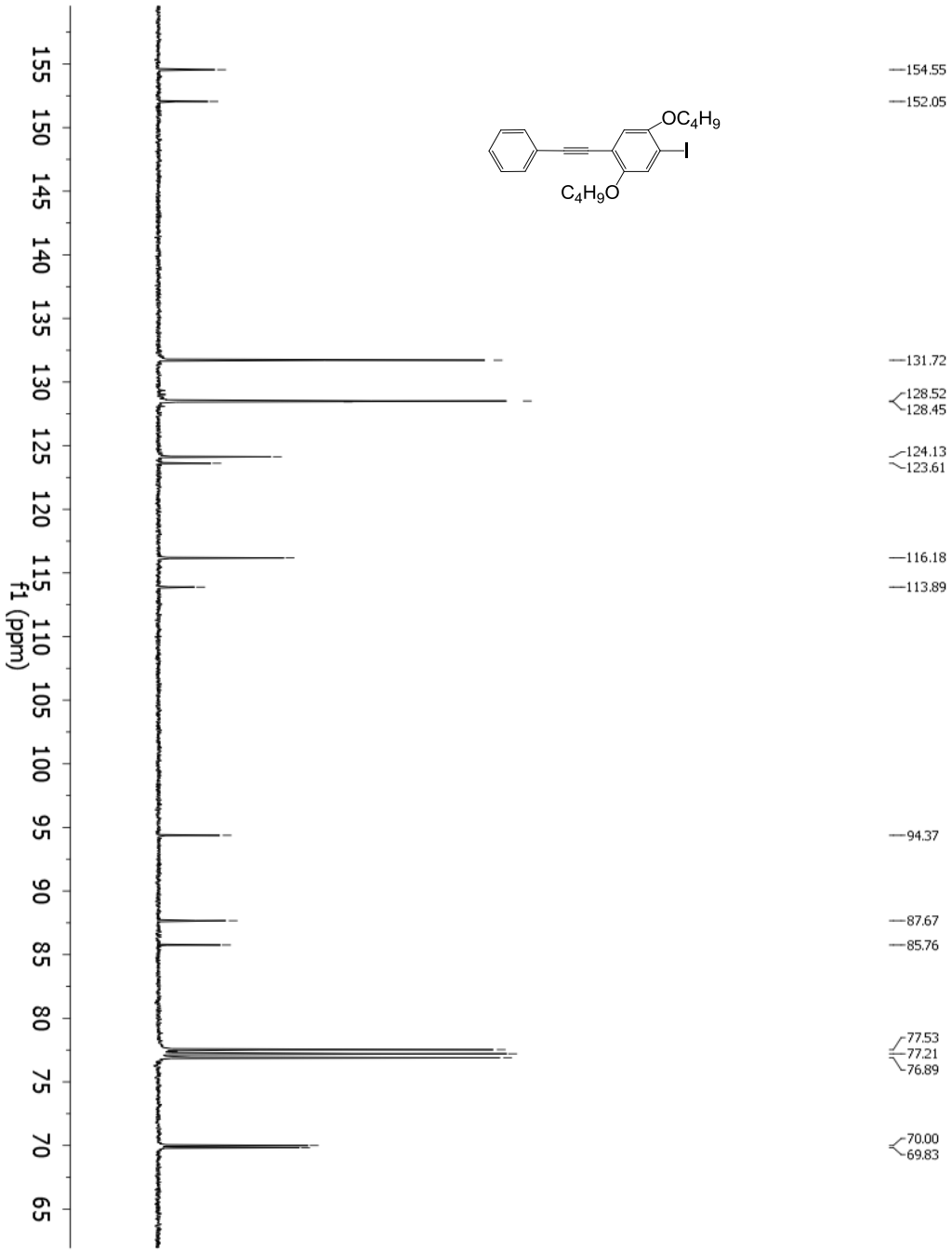

^{1}H NMR spectrum of compound (**13a**)

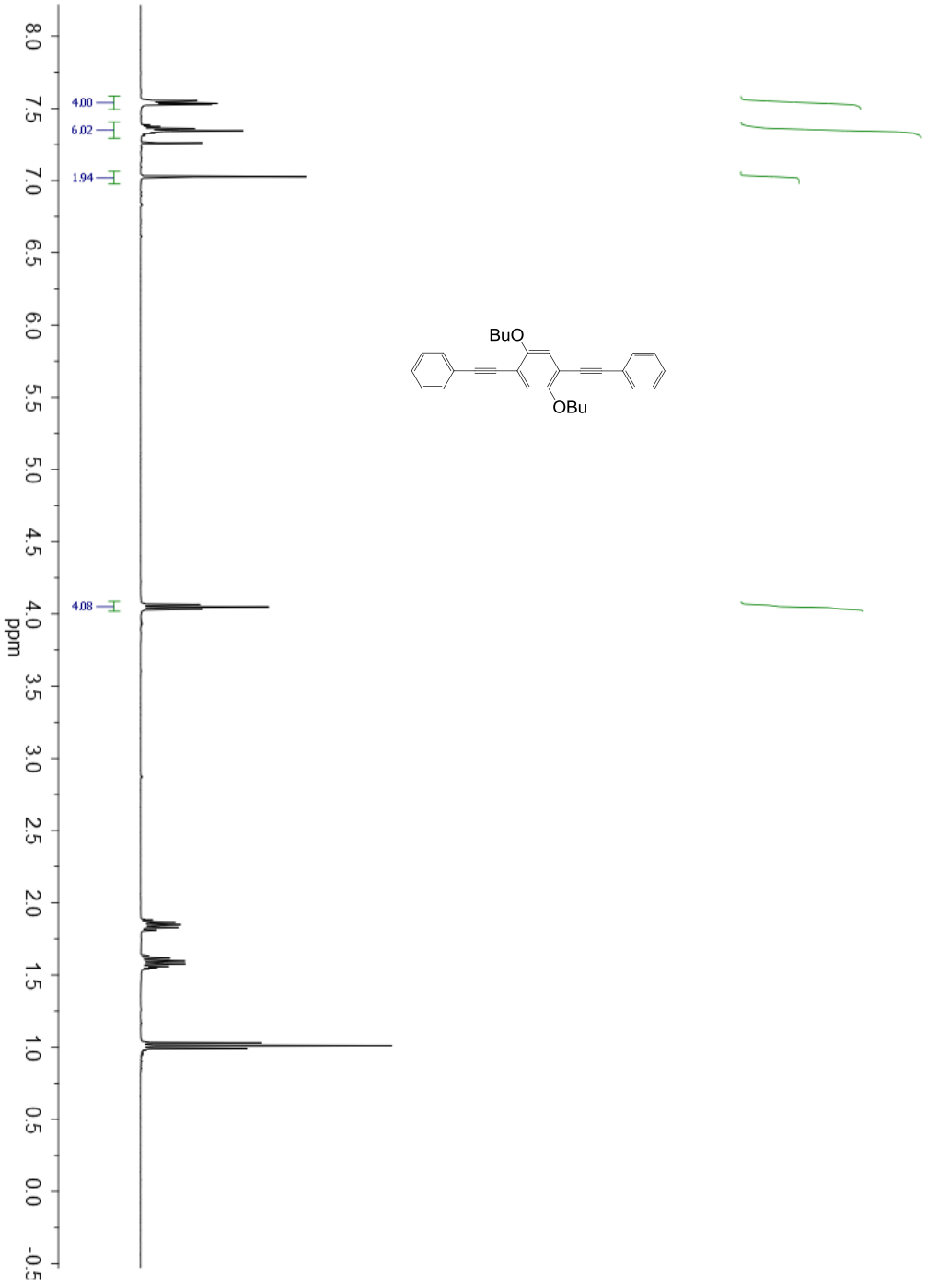

^{13}C NMR spectrum of compound (1**3a**)

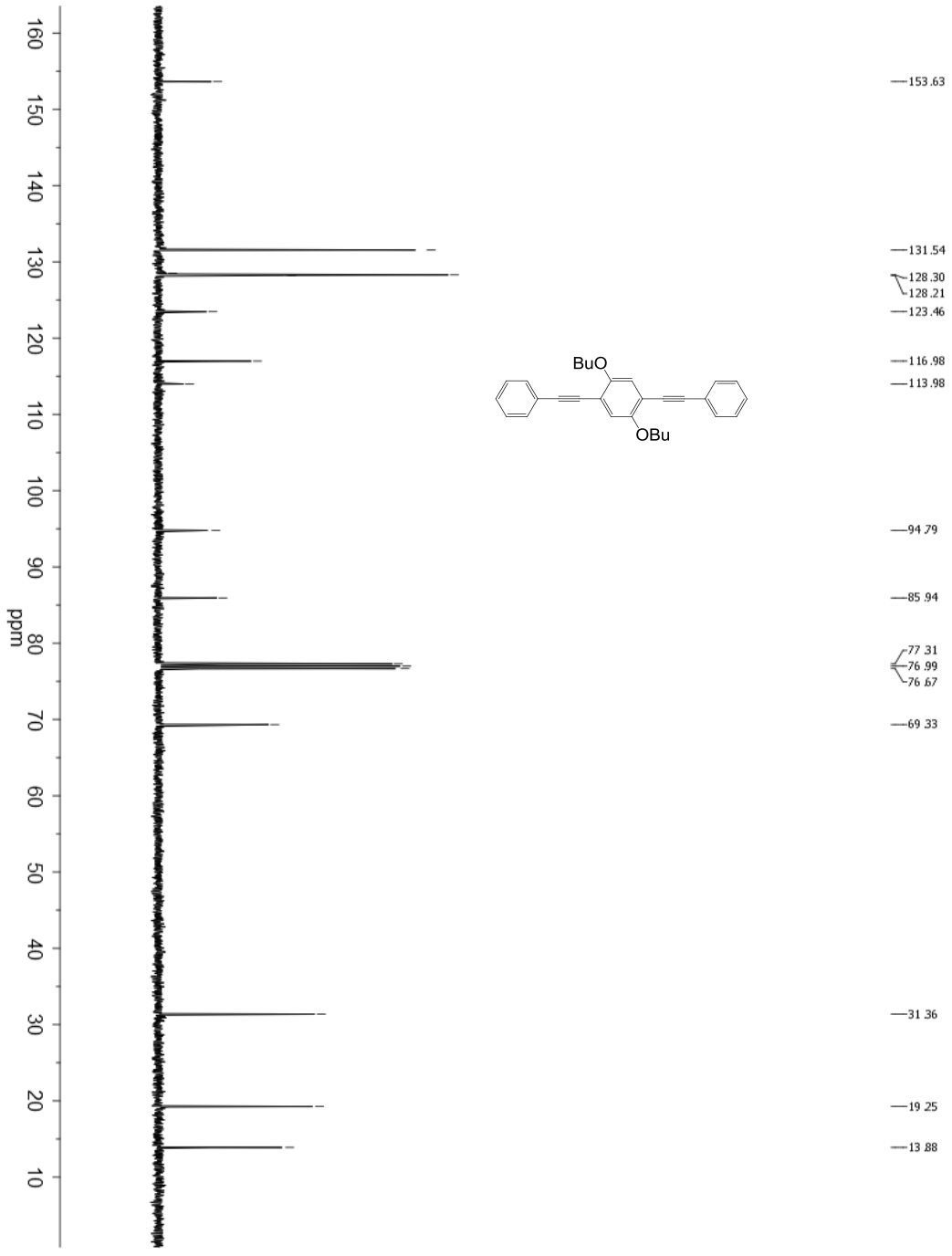

^{1}H NMR spectrum of compound (**13b**)

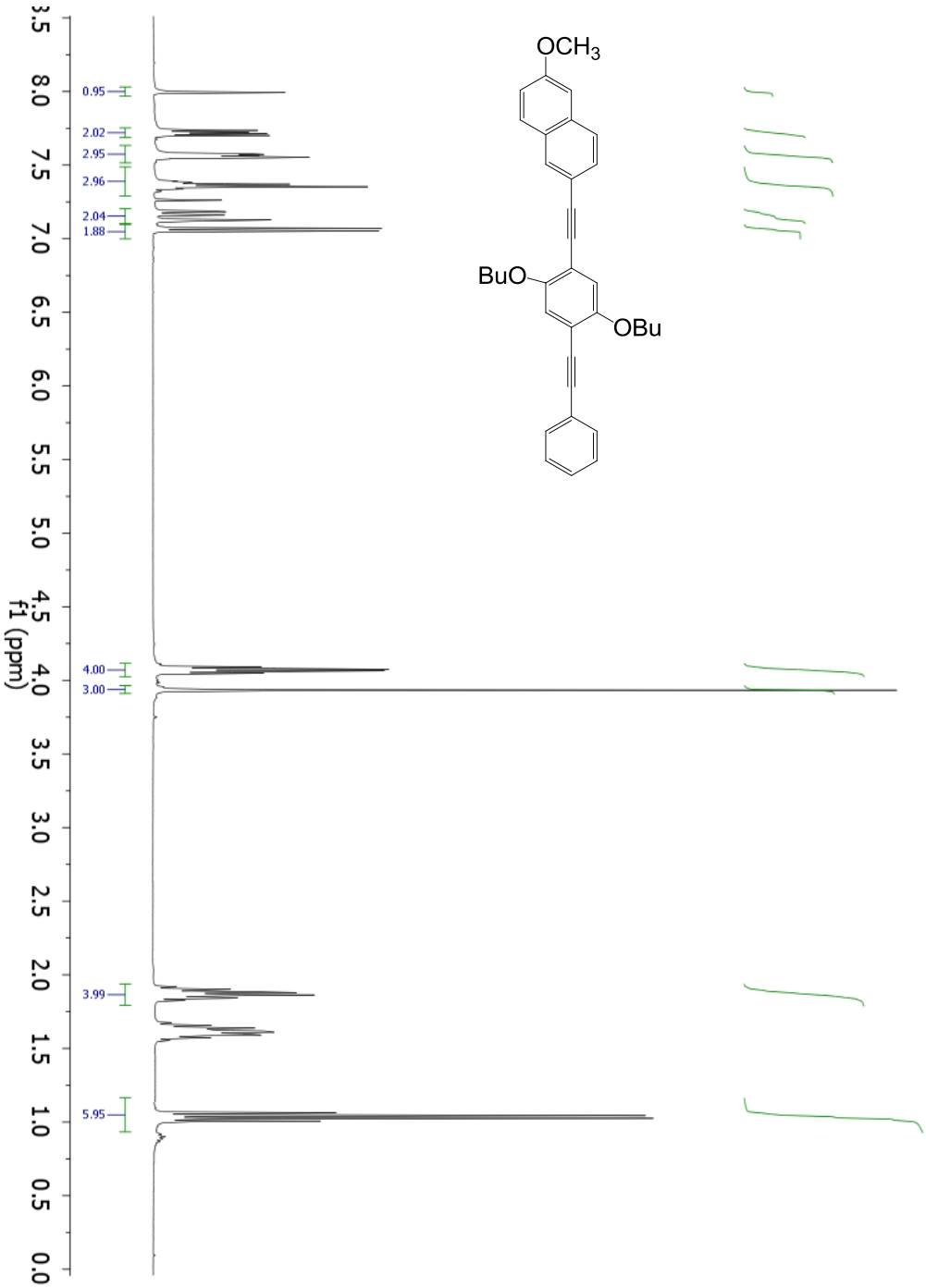

^{13}C NMR spectrum of compound (1**3b**)

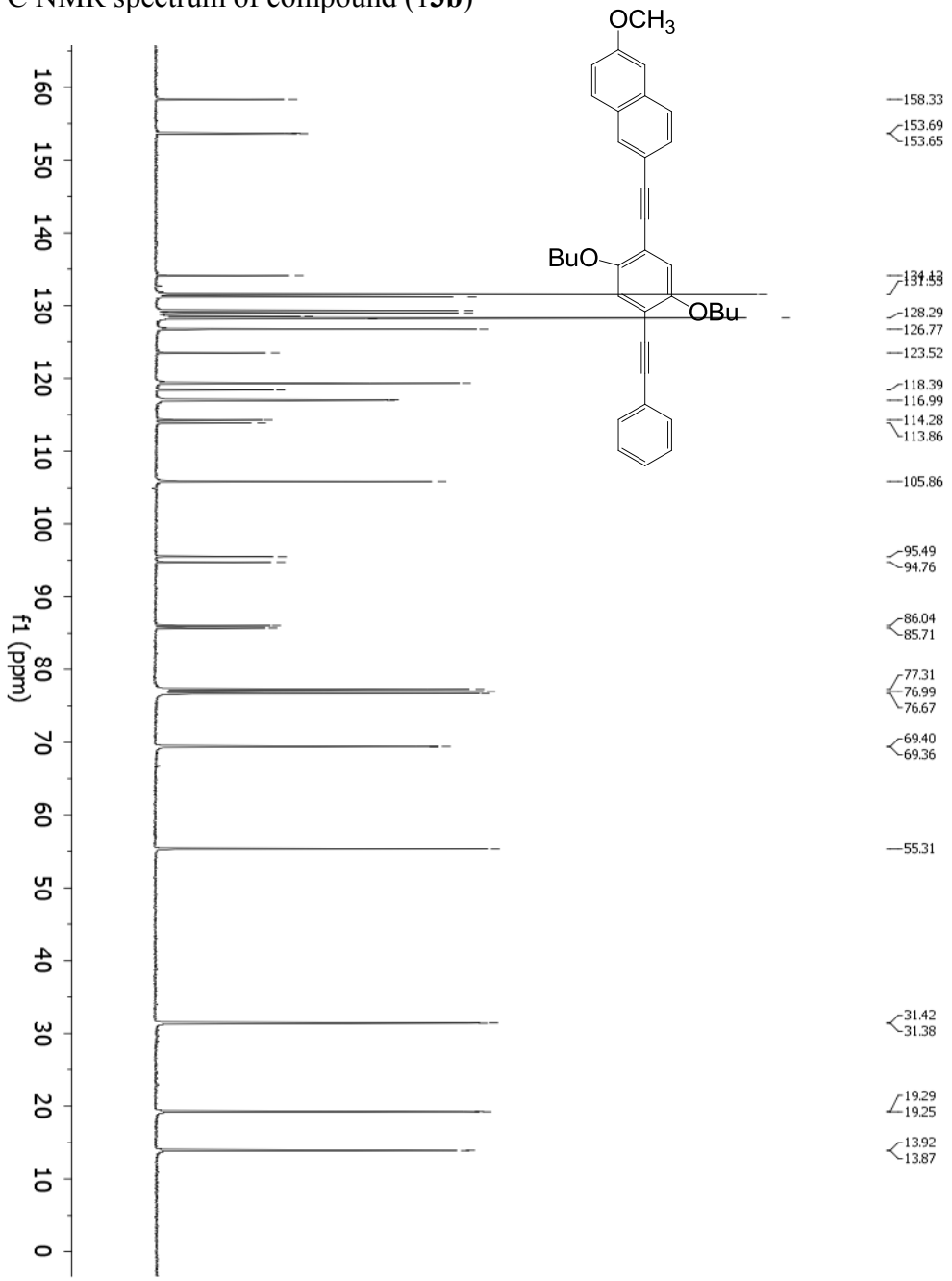

^{1}H NMR spectrum of compound (**13c**)

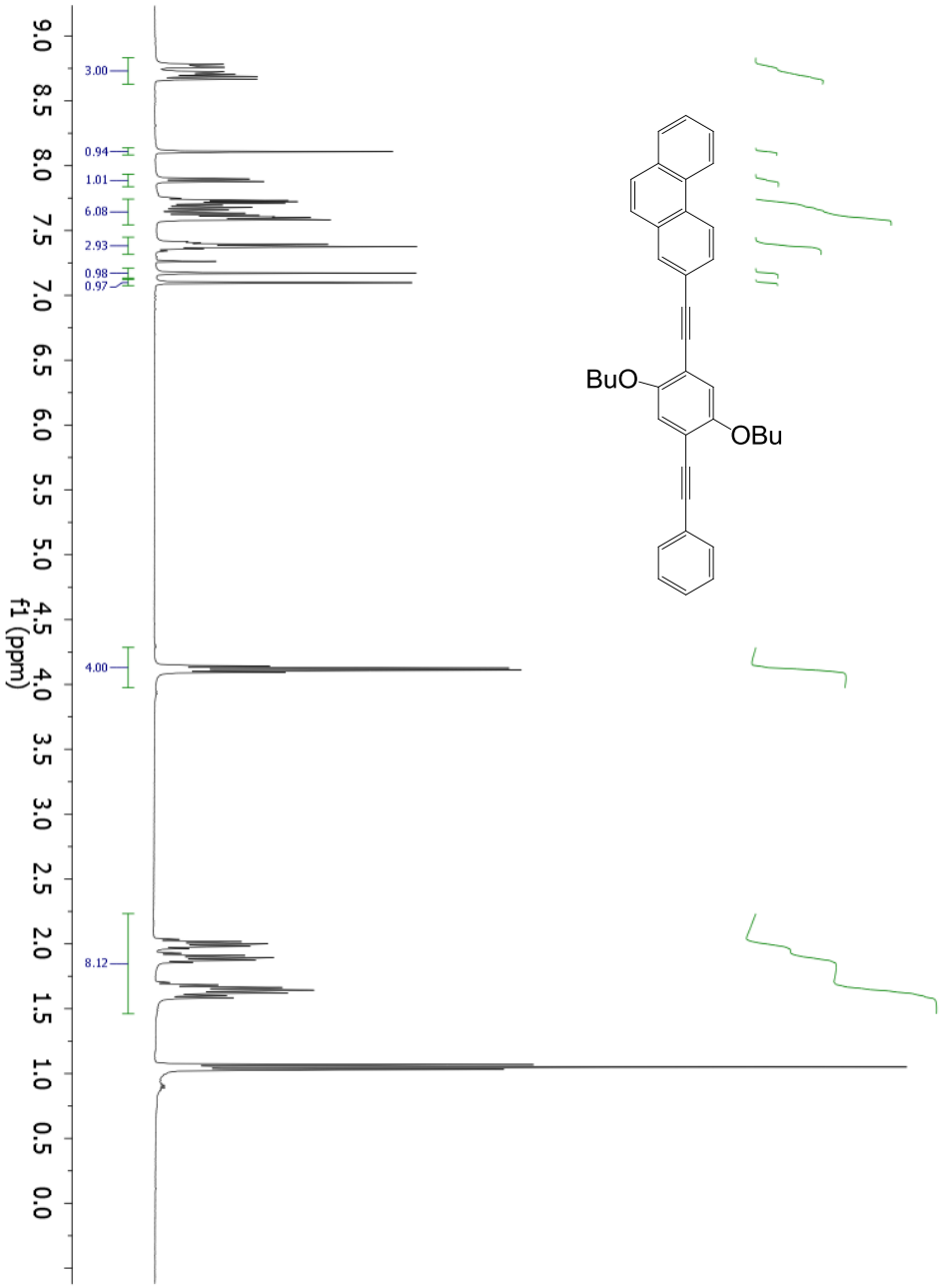

^{13}C NMR spectrum of compound (1**3c**)

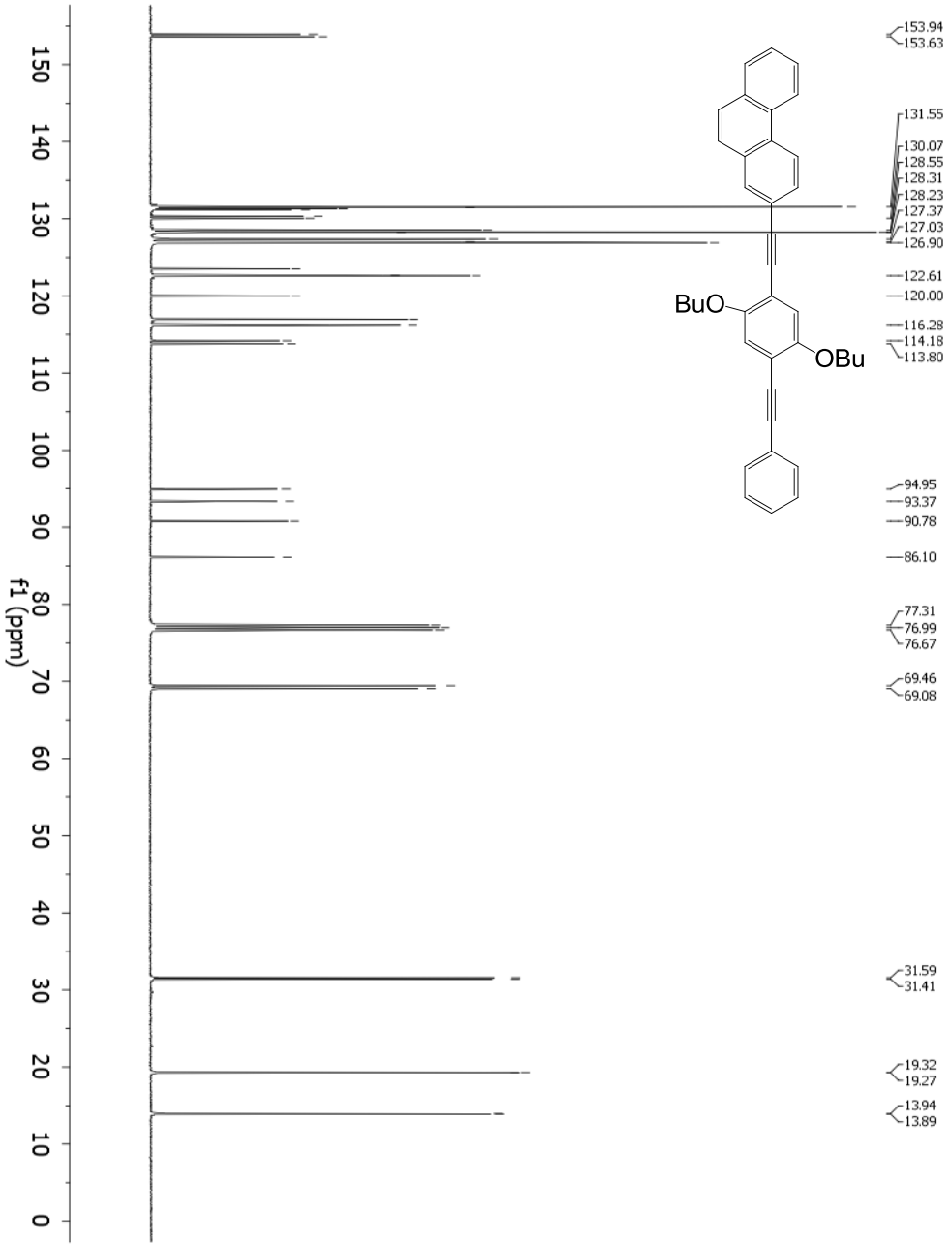

^{1}H NMR spectrum of compound (**13d**)

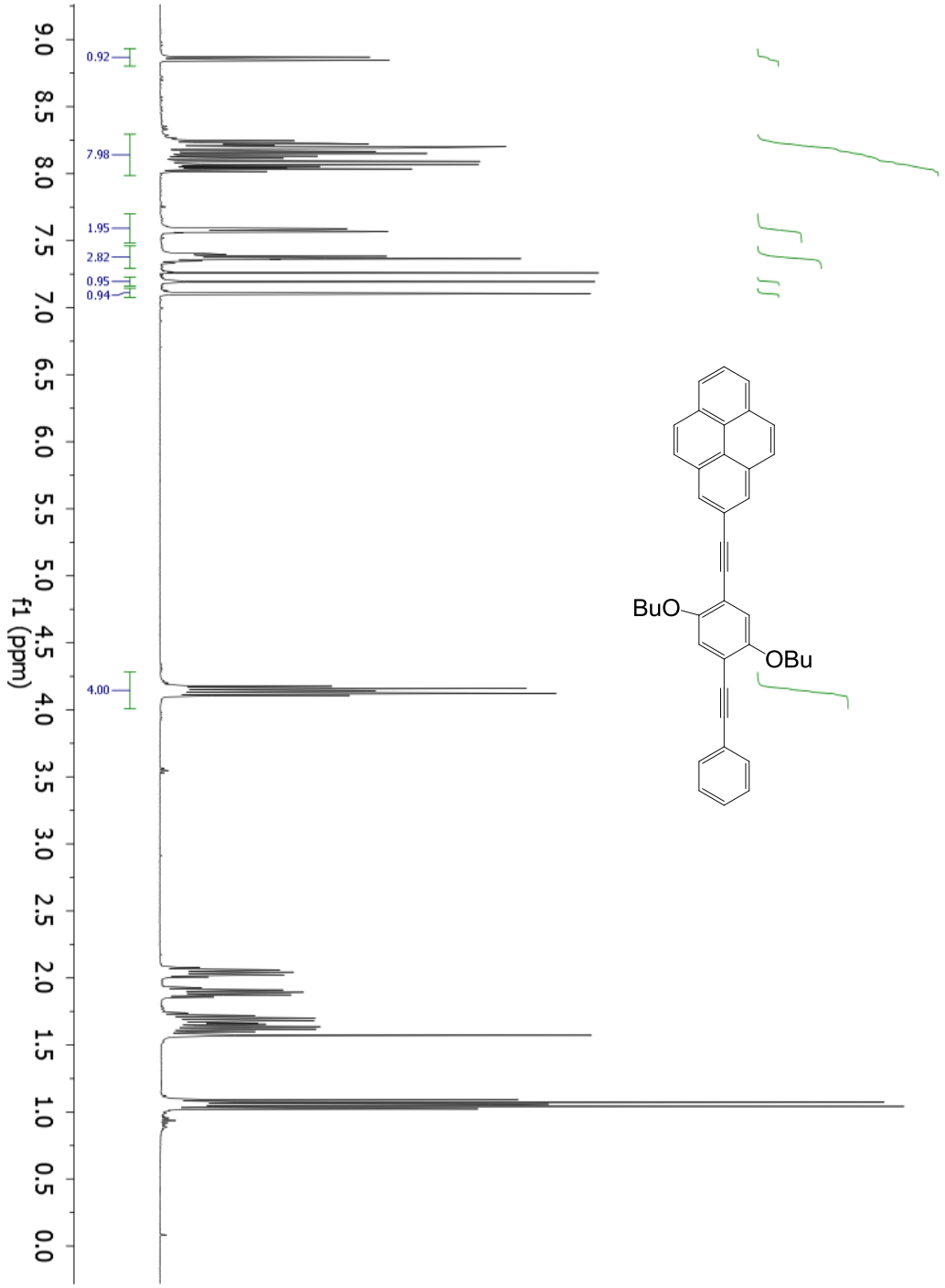

^{13}C NMR spectrum of compound (1**3d**)

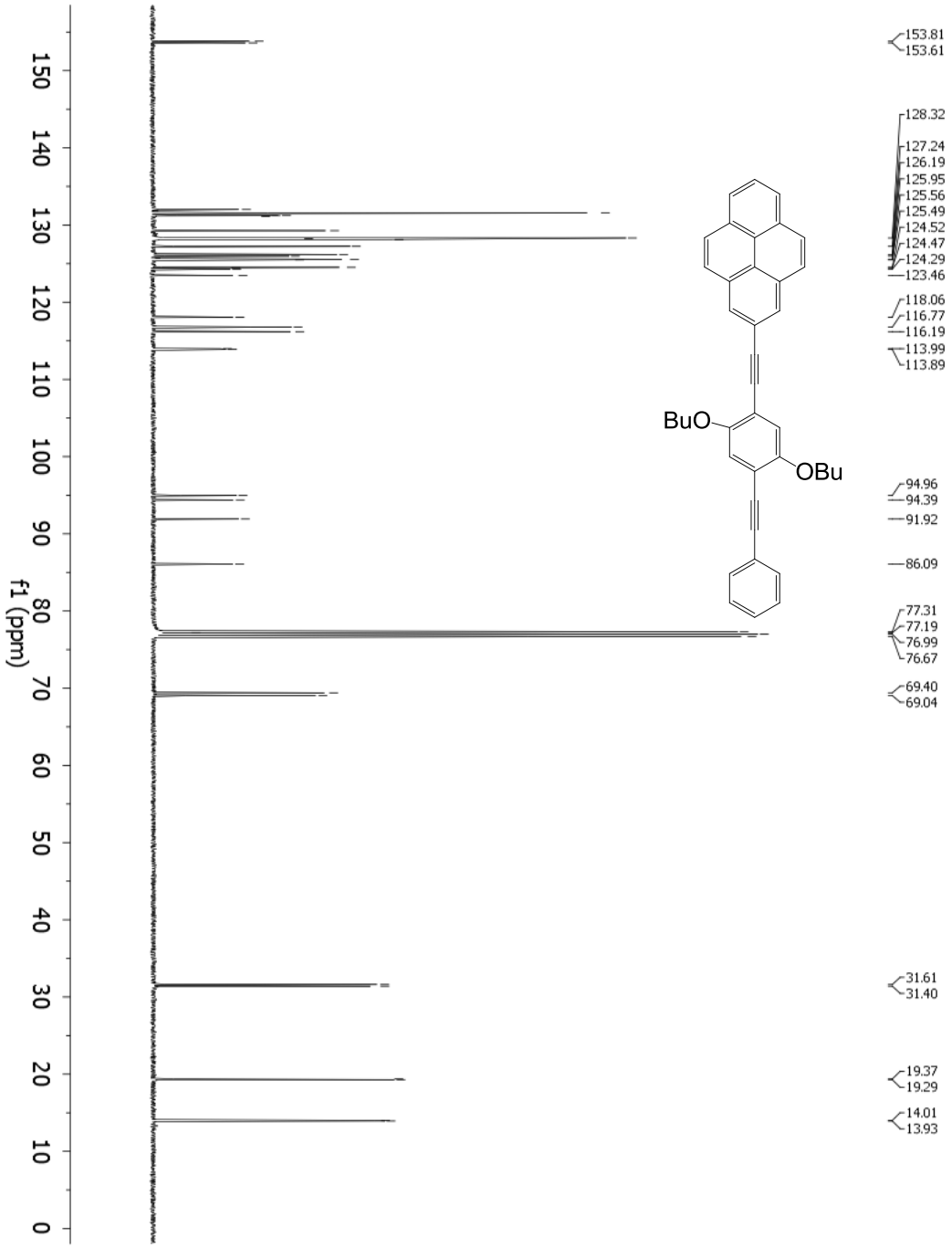

^{1}H NMR spectrum of compound (**14**)

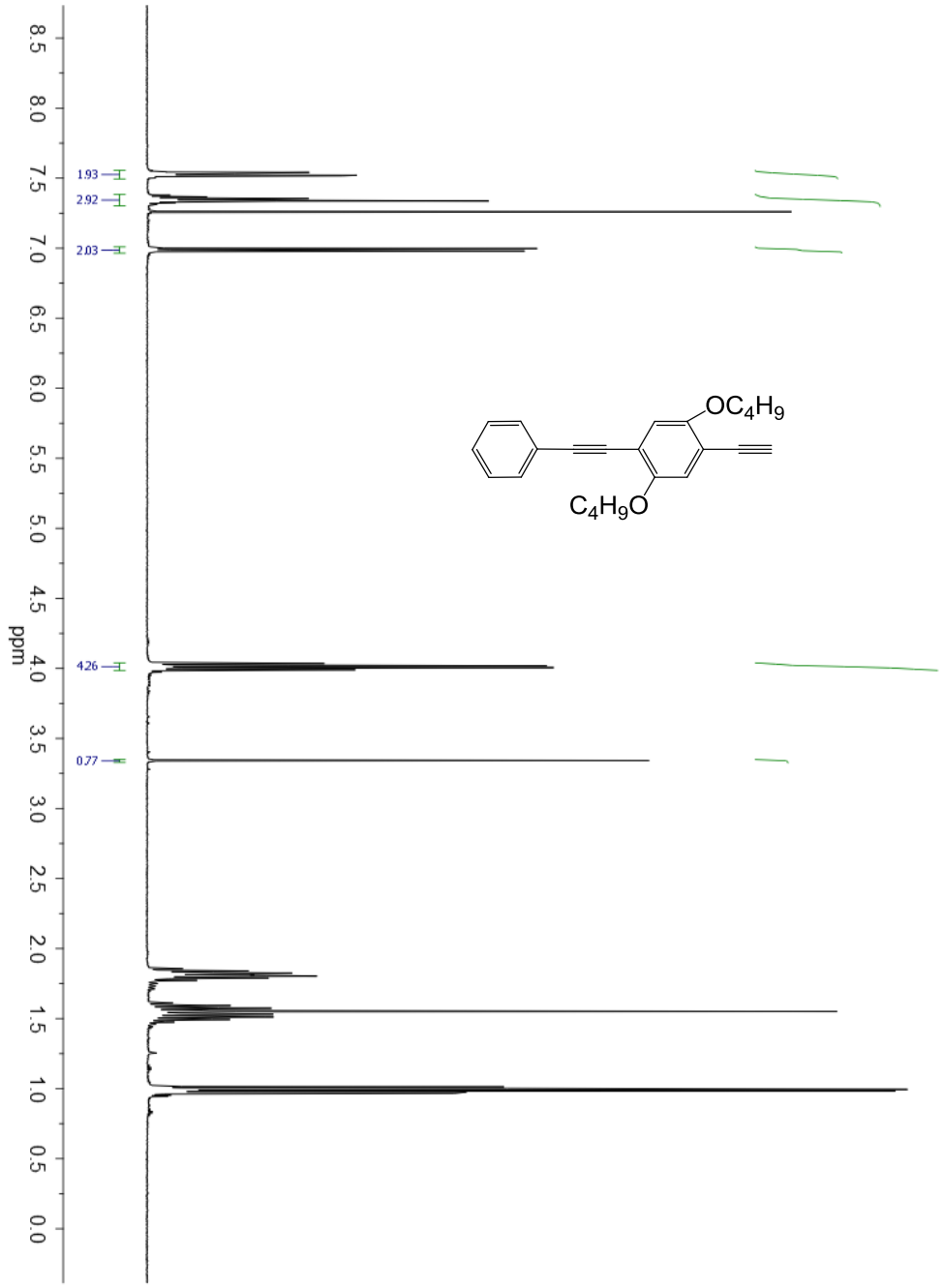

^{1}H NMR spectrum of compound (**15**)

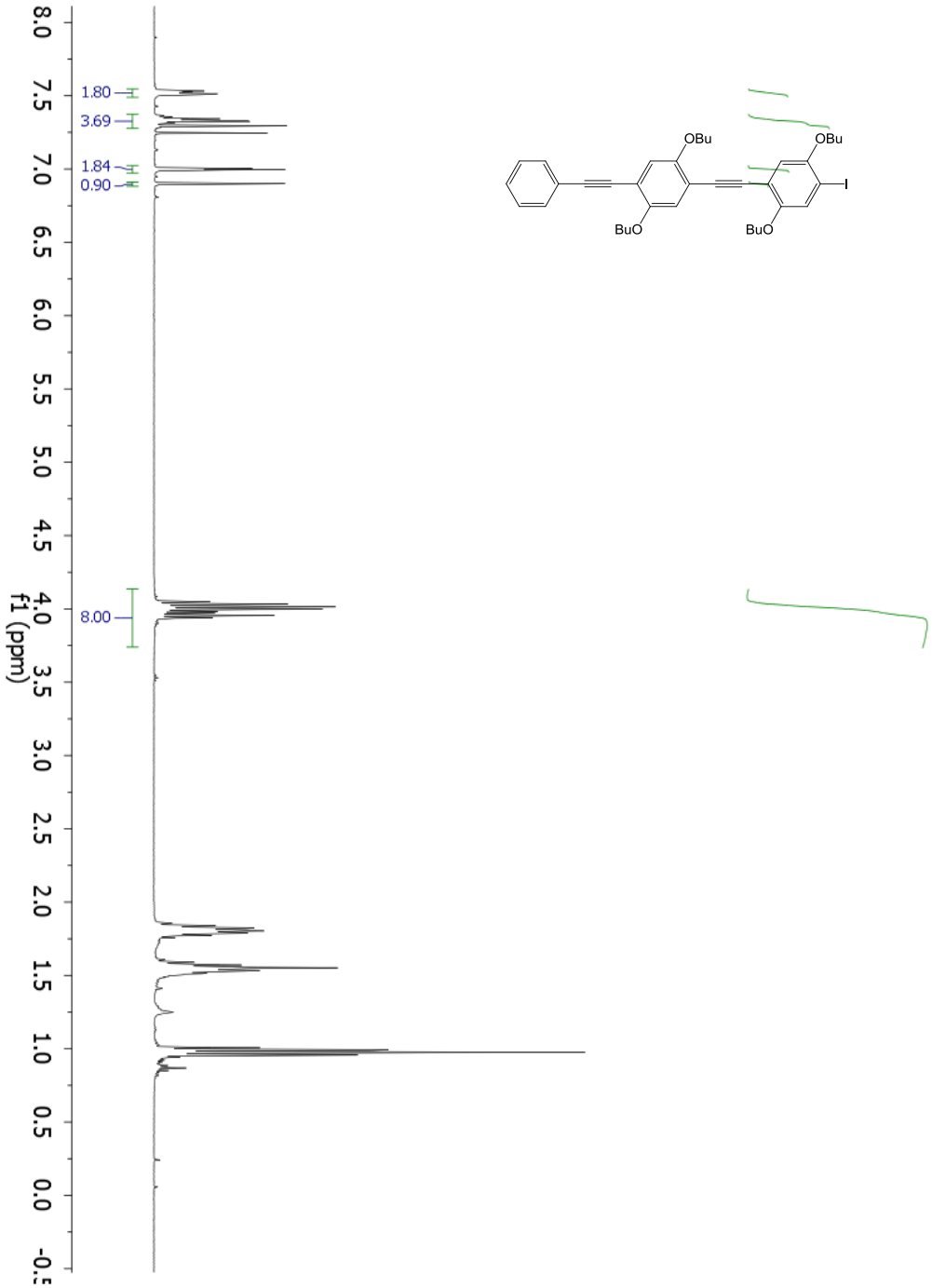

^{13}C NMR spectrum of compound (1**5**)

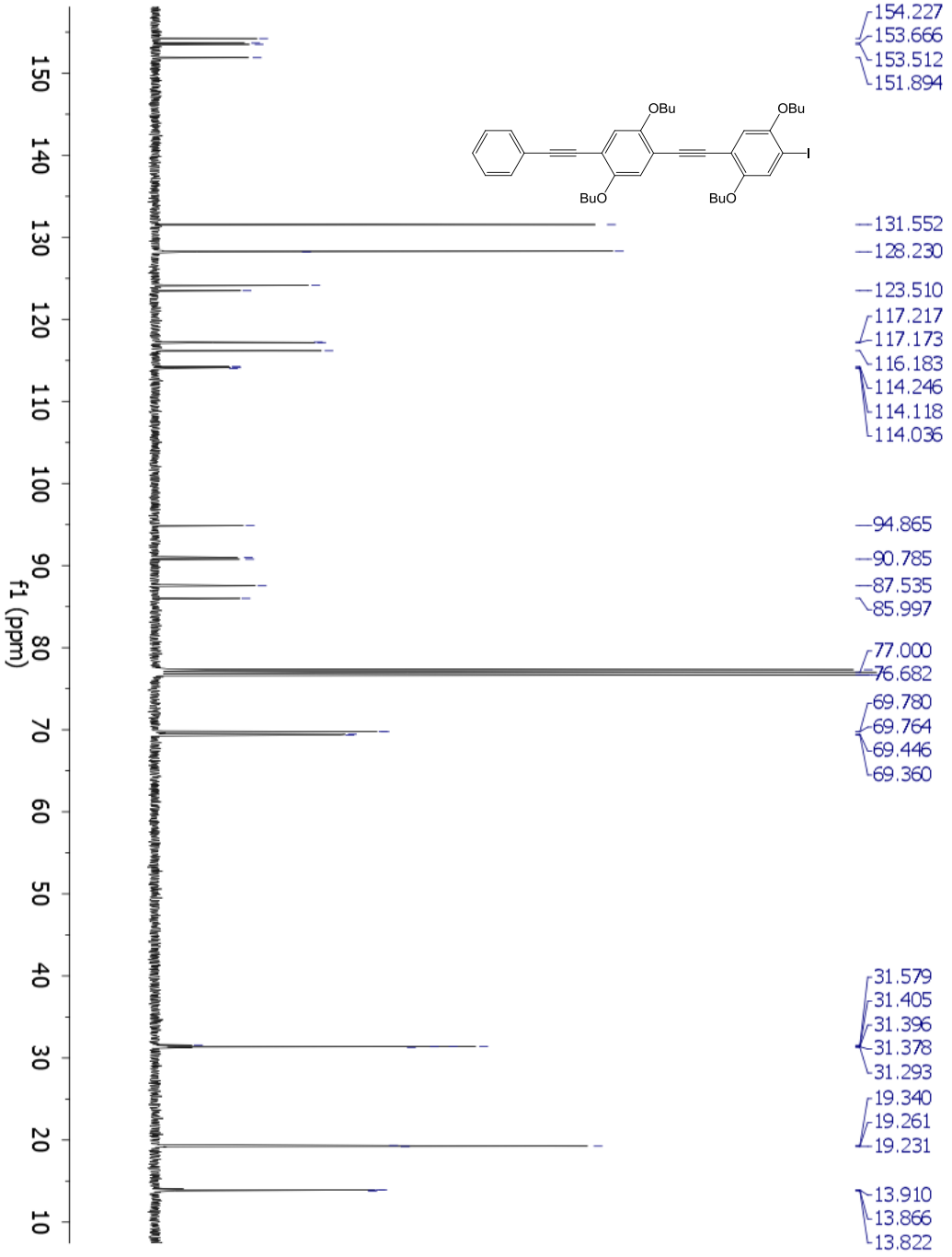

^{1}H NMR spectrum of compound (**16a**)

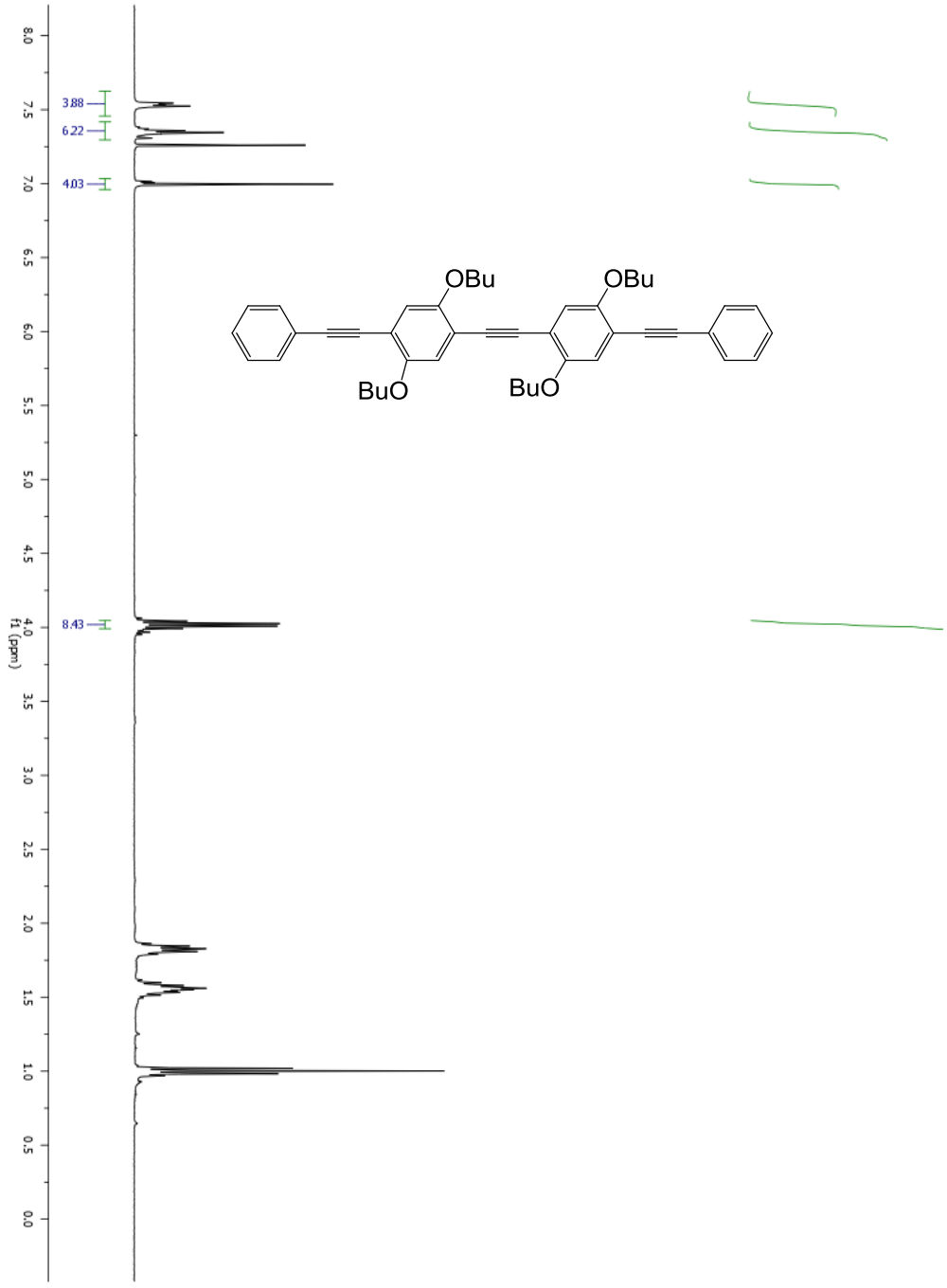

^{13}C NMR spectrum of compound (**16a**)

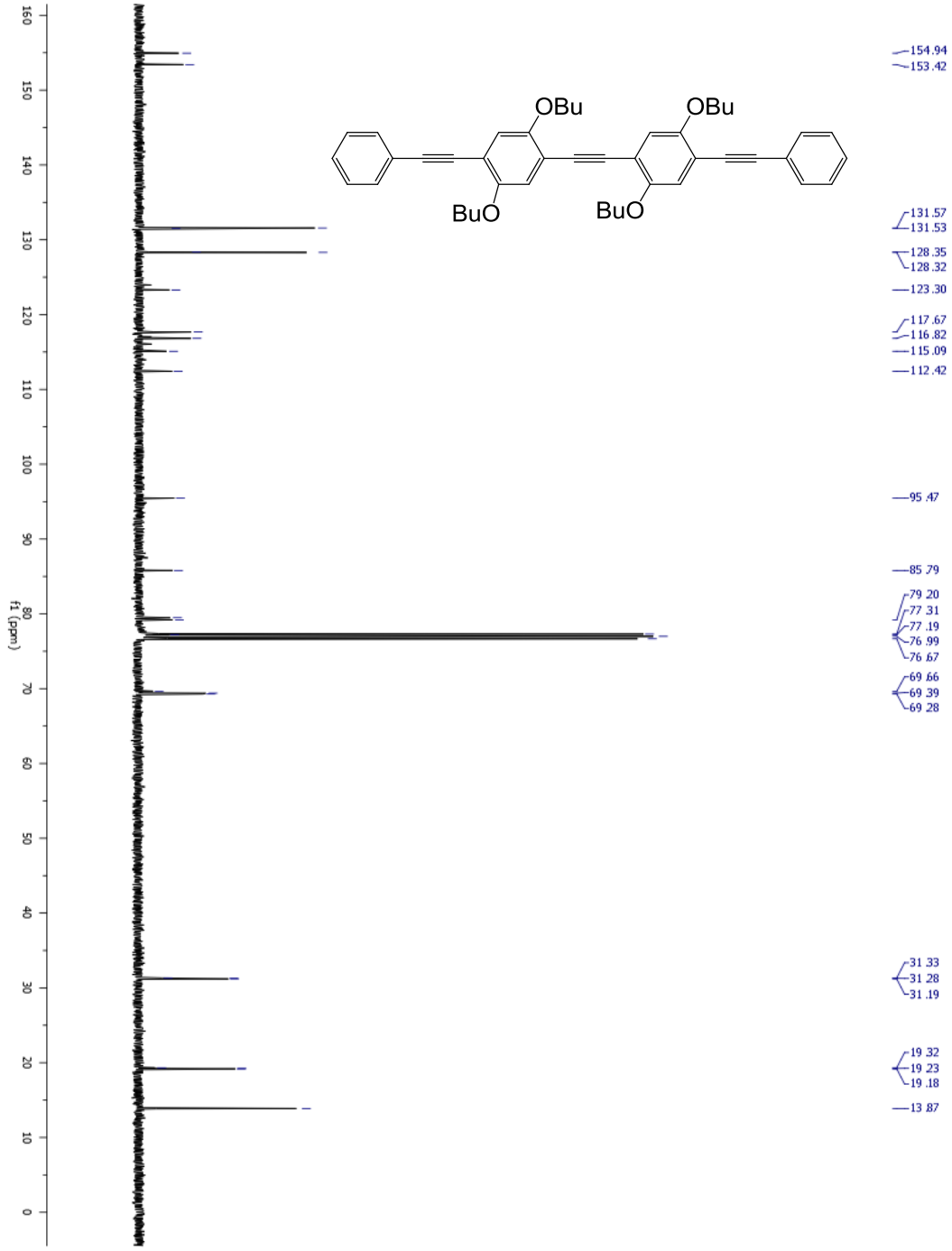

^{1}H NMR spectrum of compound (**16b**)

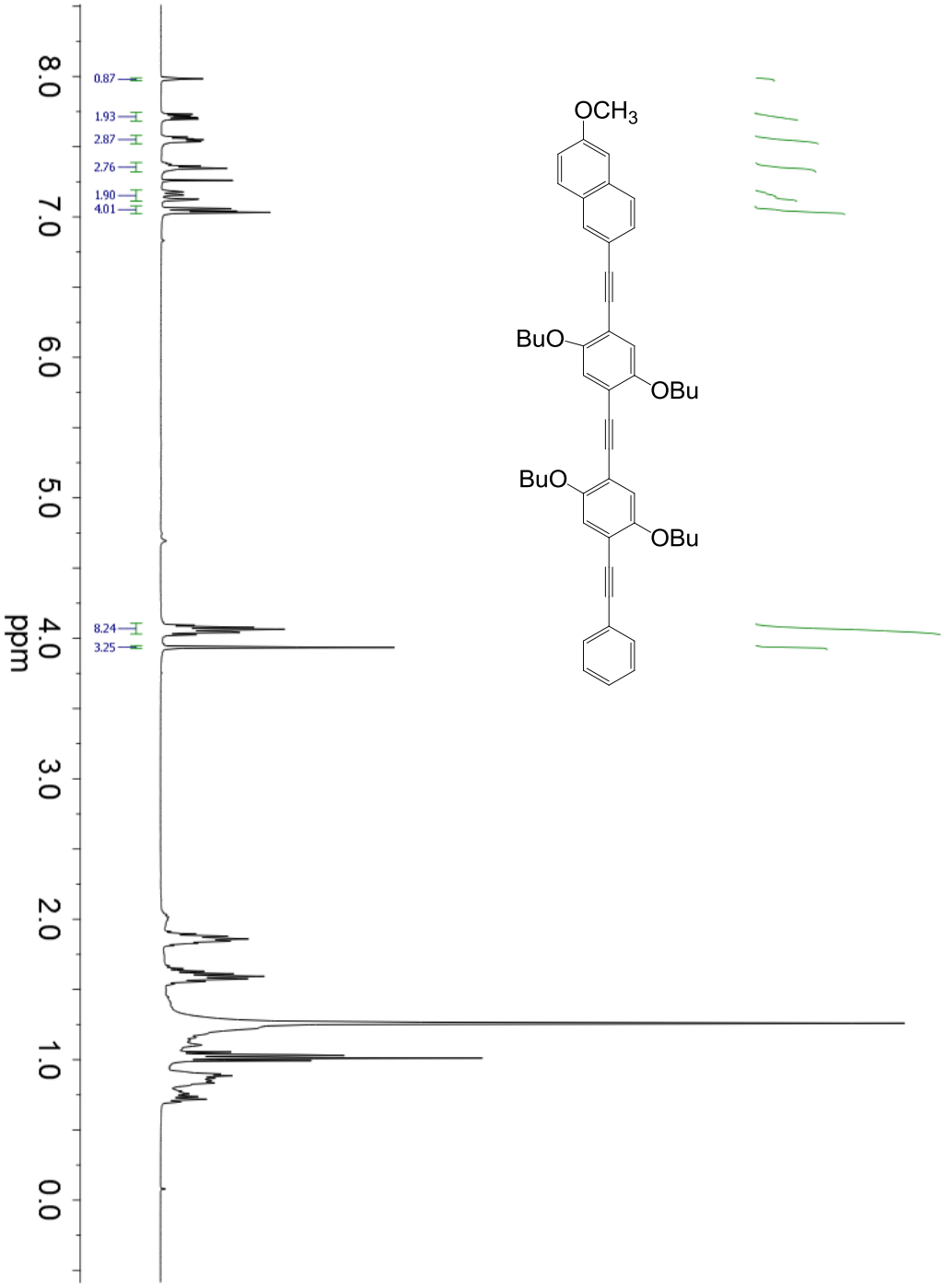

^{13}C NMR spectrum of compound (**16b**)

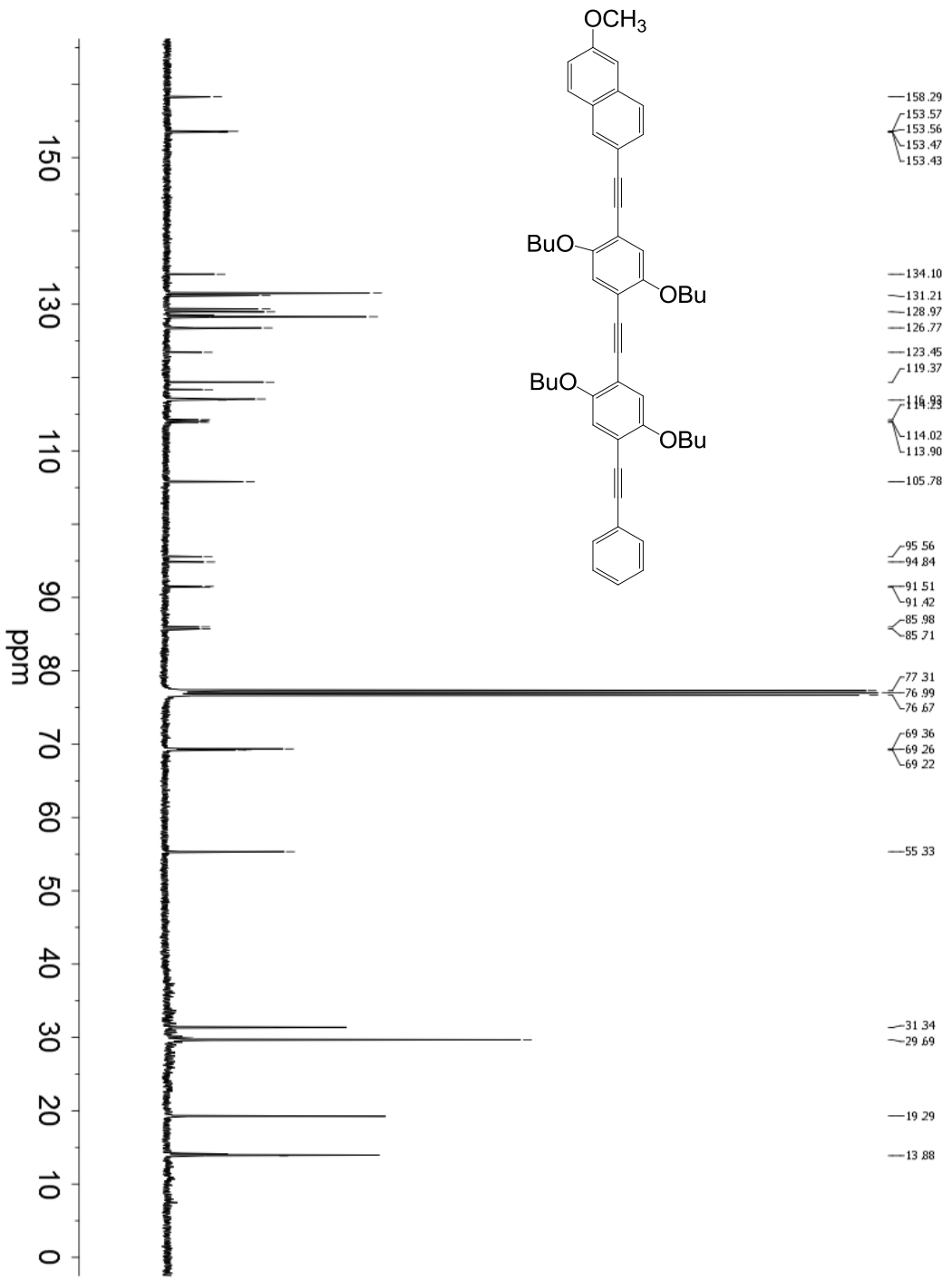

^{1}H NMR spectrum of compound (**16c**)

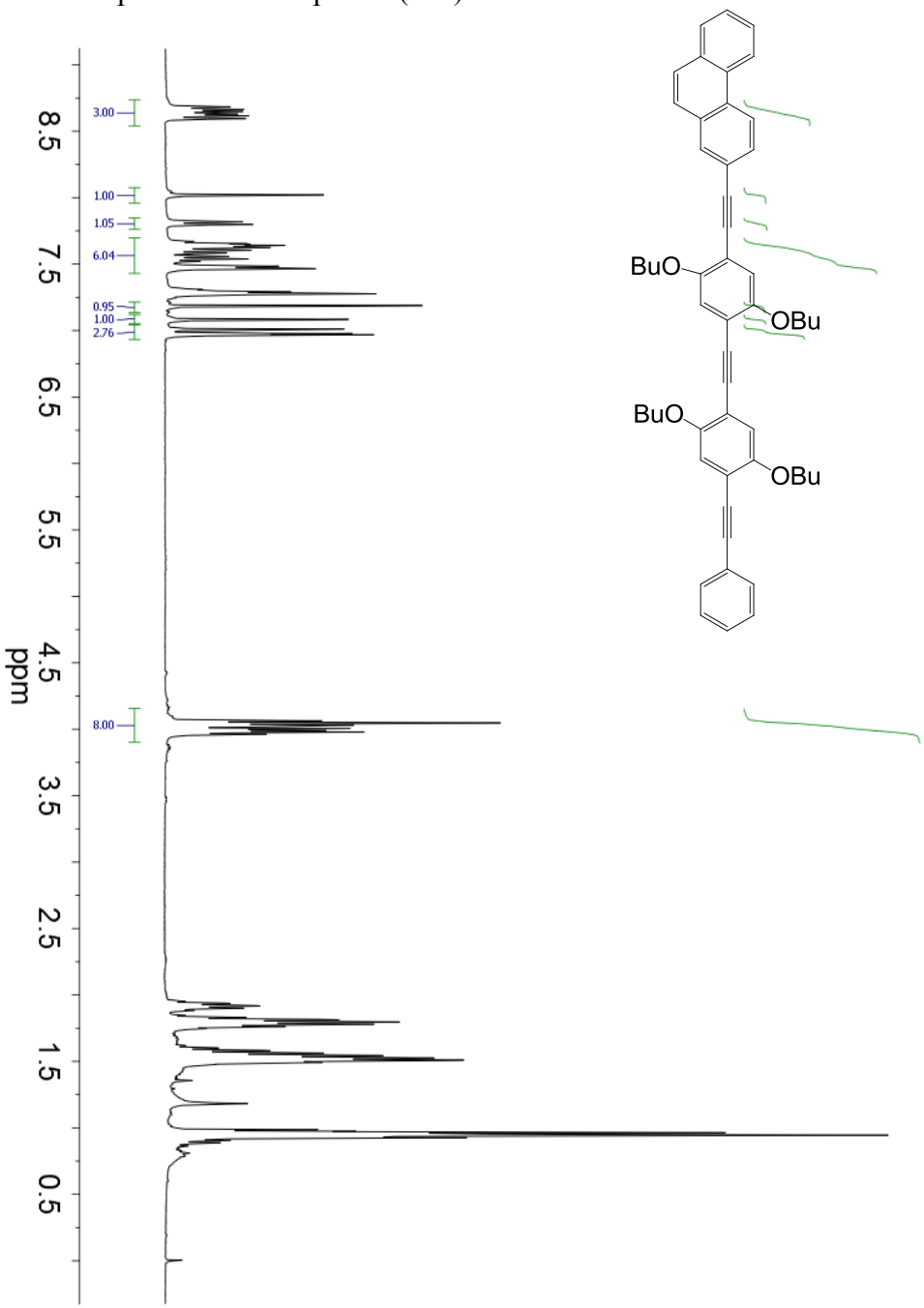

^{13}C NMR spectrum of compound (**16c**)

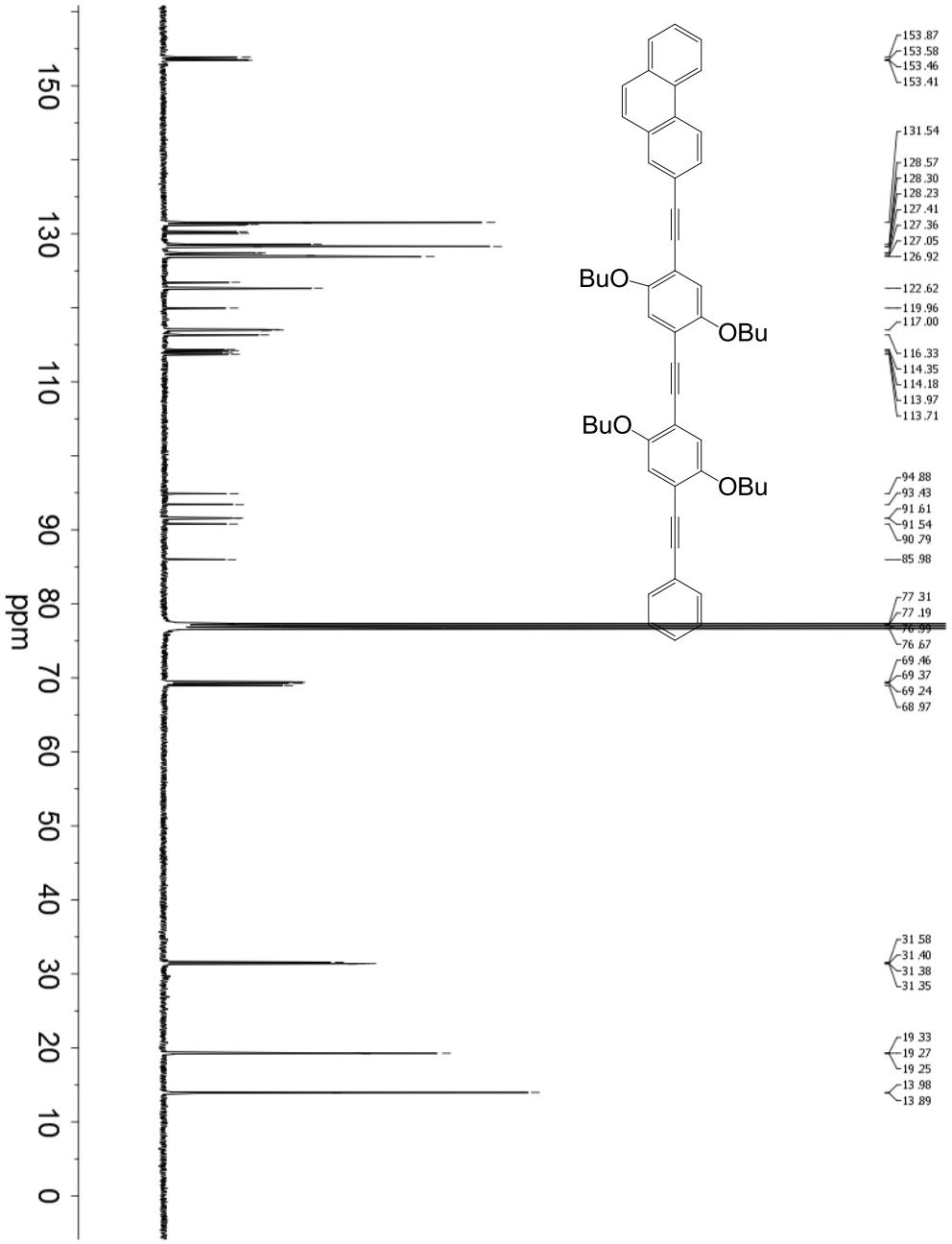

^{1}H NMR spectrum of compound (**16d)**

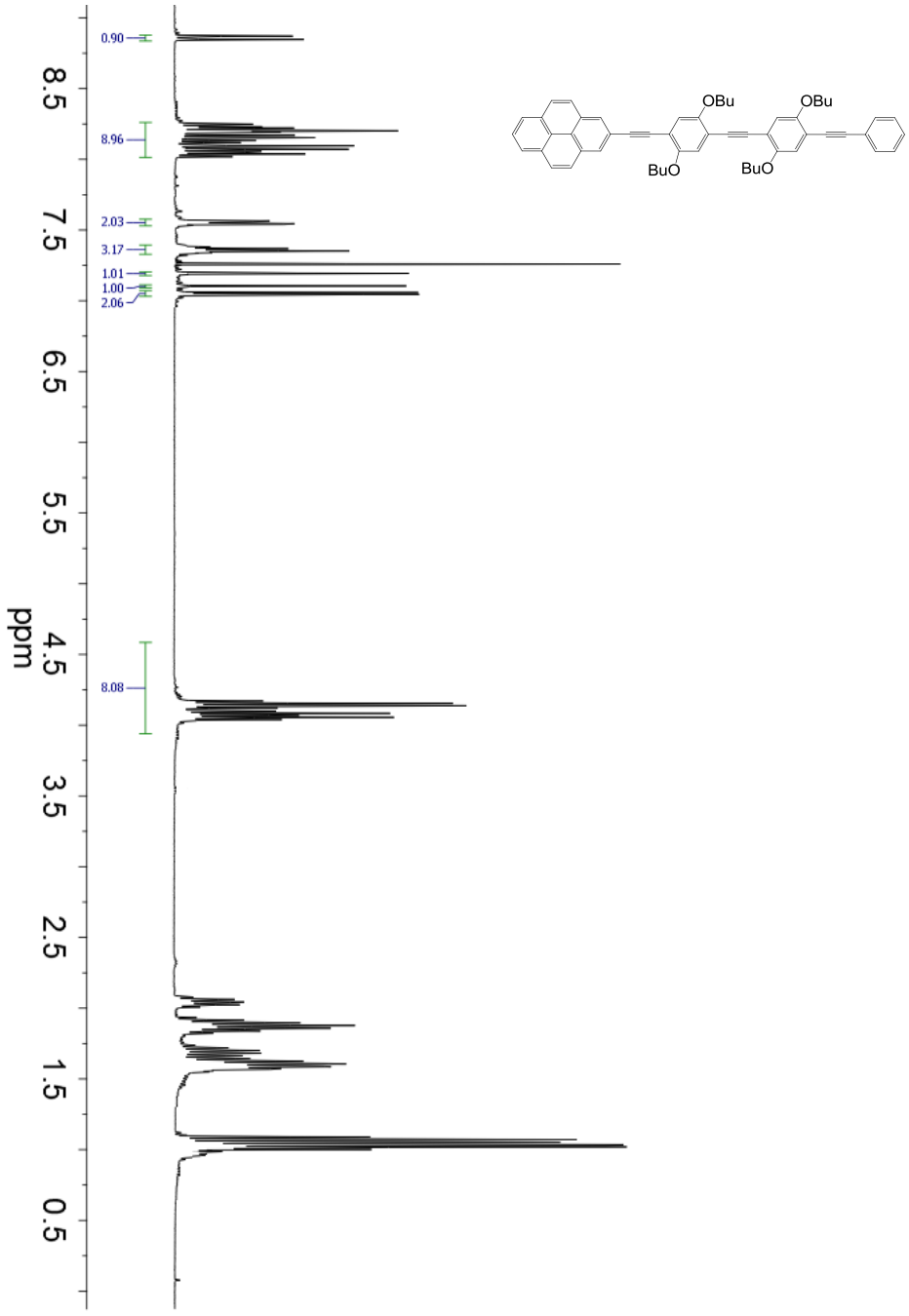

^{13}C NMR spectrum of compound (**16d)**

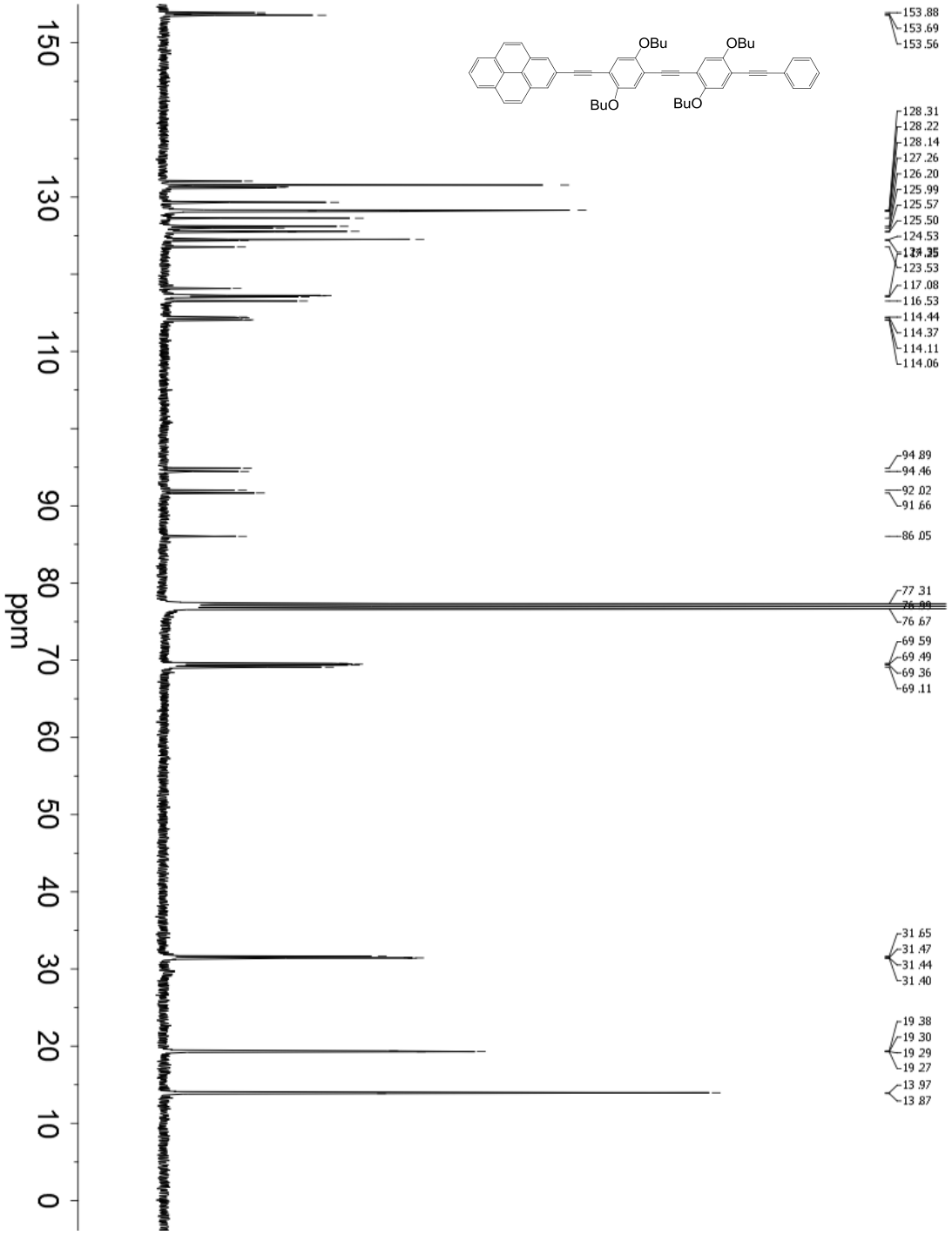

^{1}H NMR spectrum of compound (**17)**

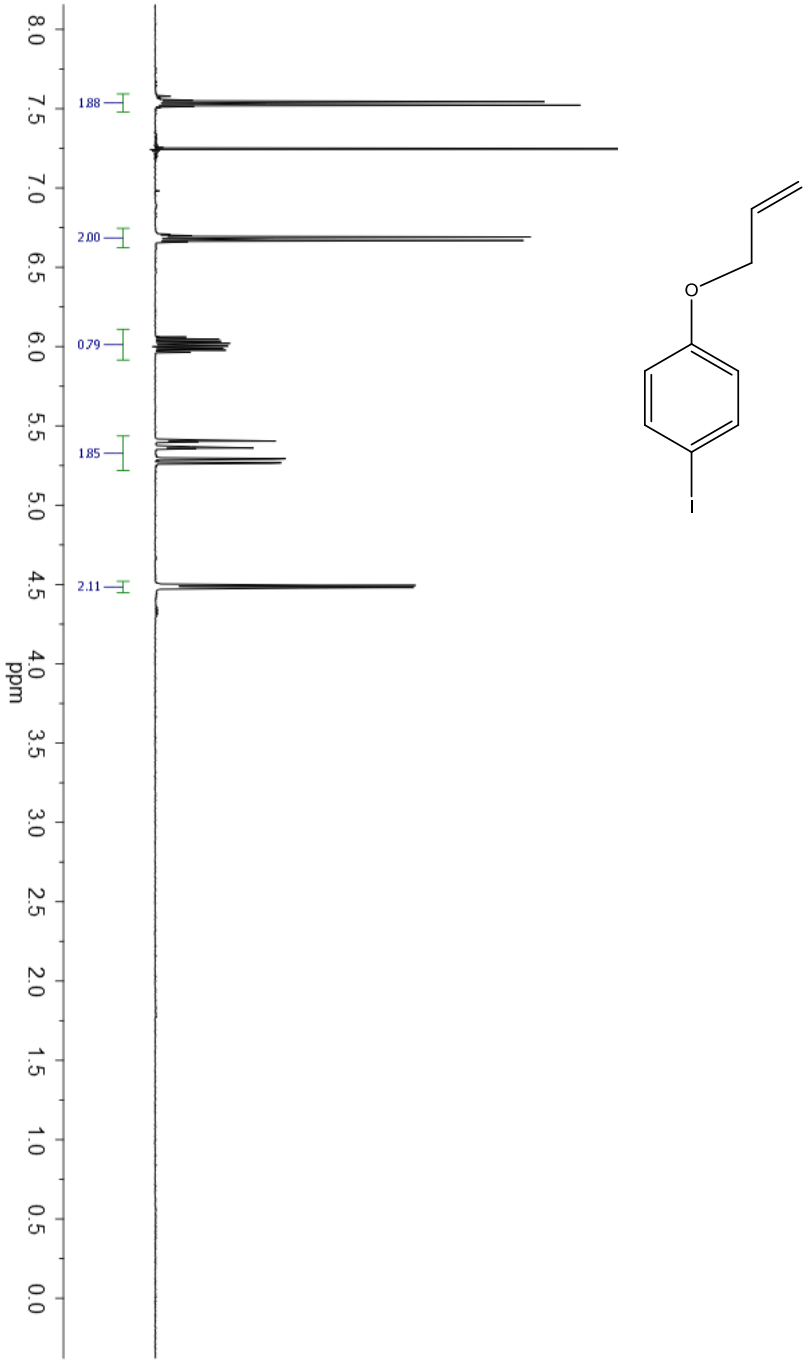

^{13}C NMR spectrum of compound (**17)**

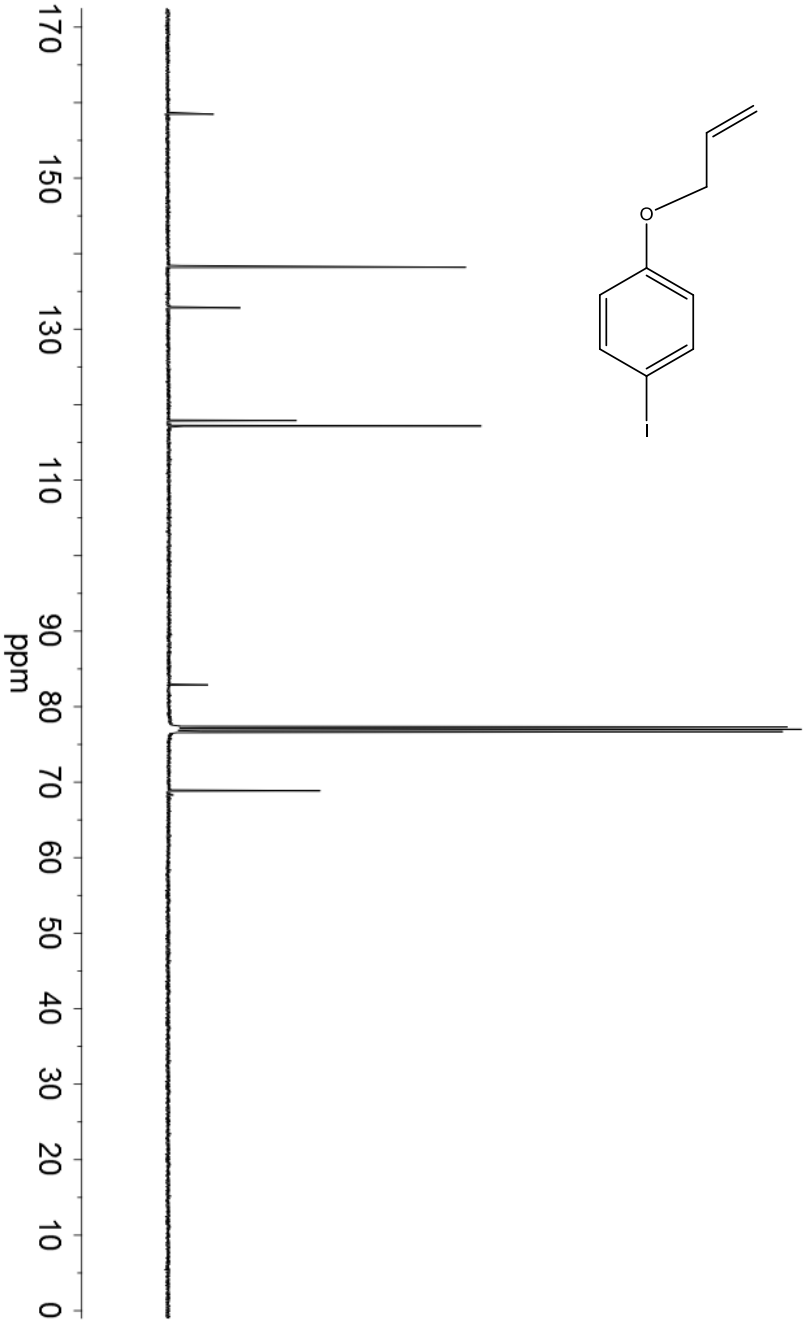

^{1}H NMR spectrum of compound (**18a)**

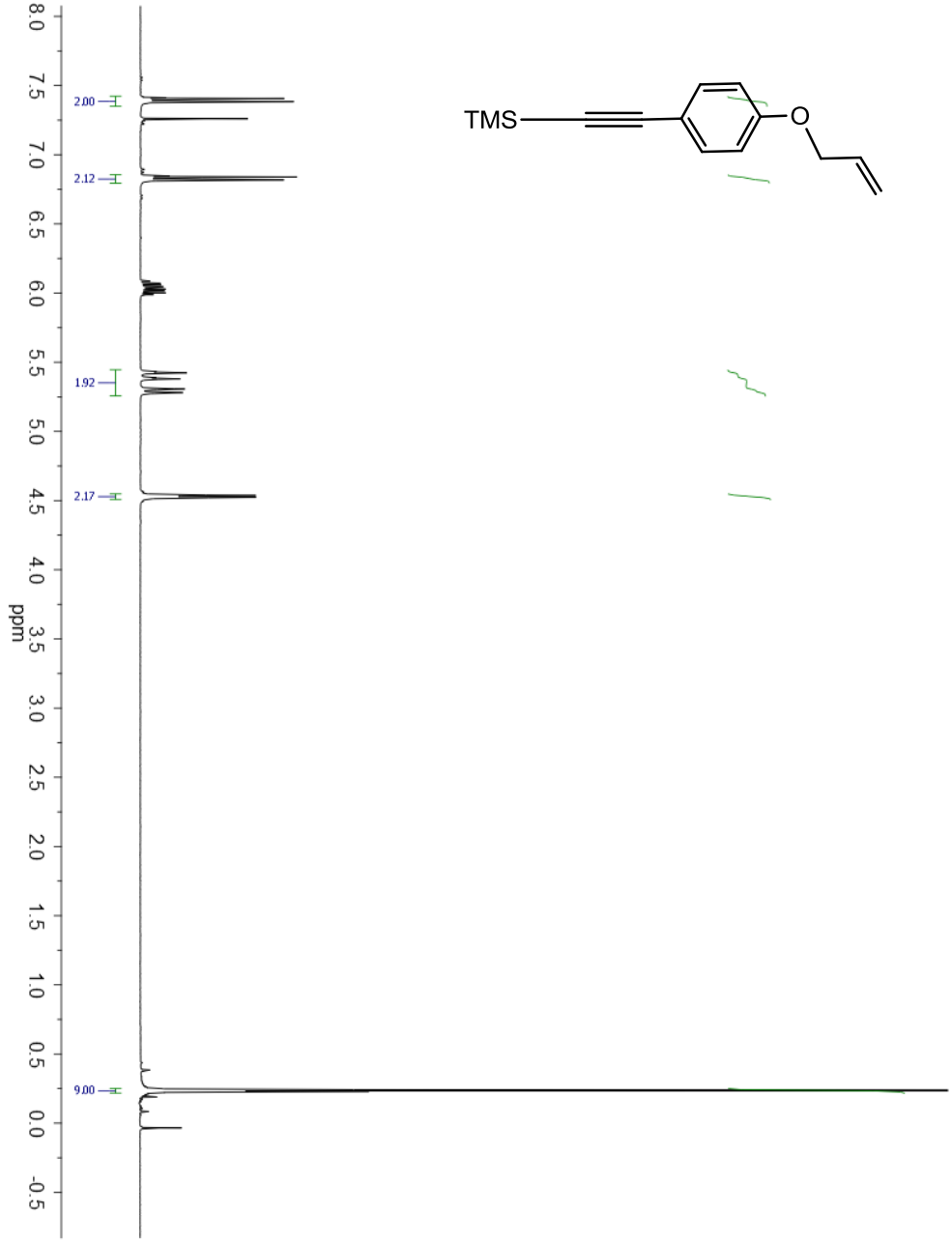

^{13}C NMR spectrum of compound (**18a)**

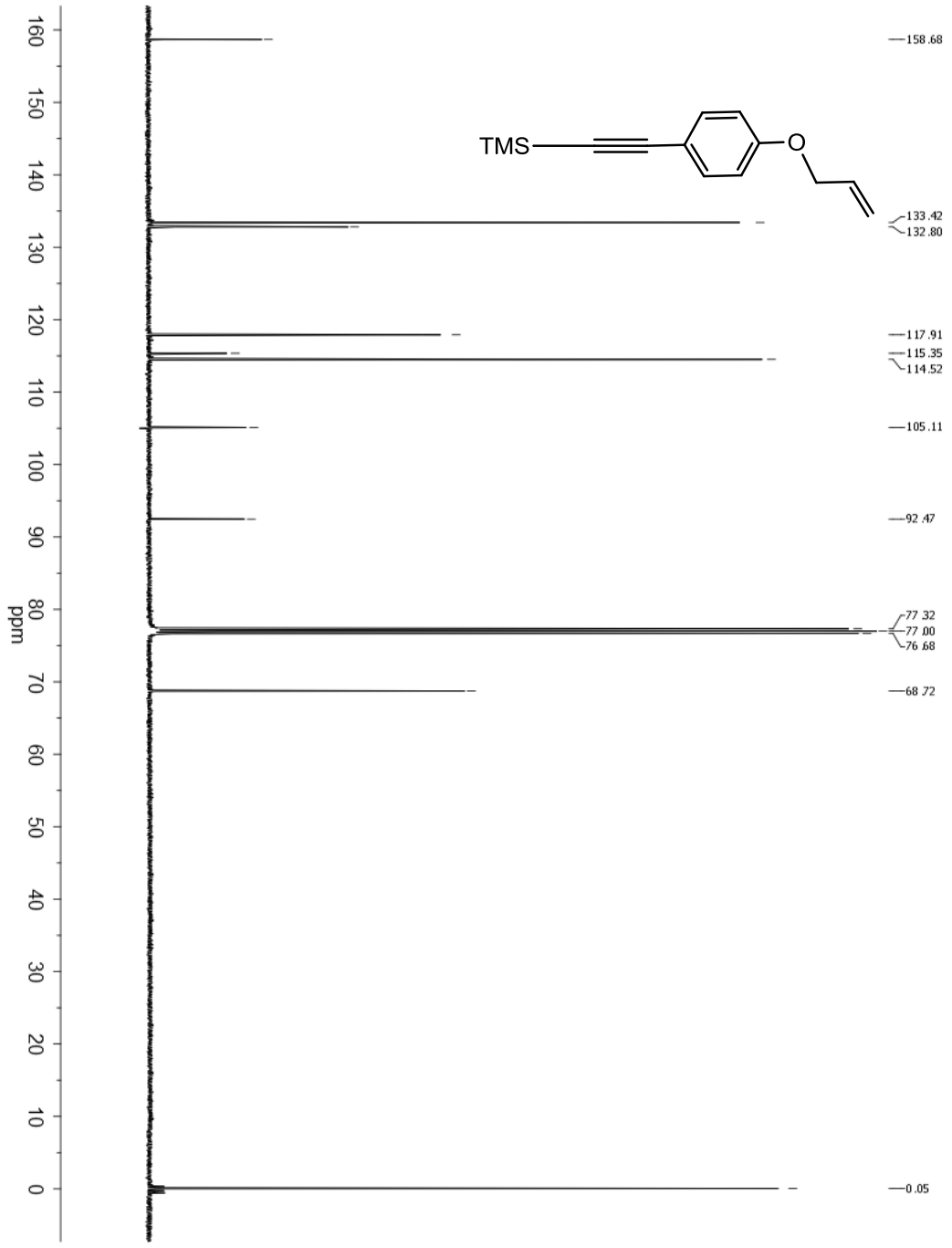

^{1}H NMR spectrum of compound (**18b)**

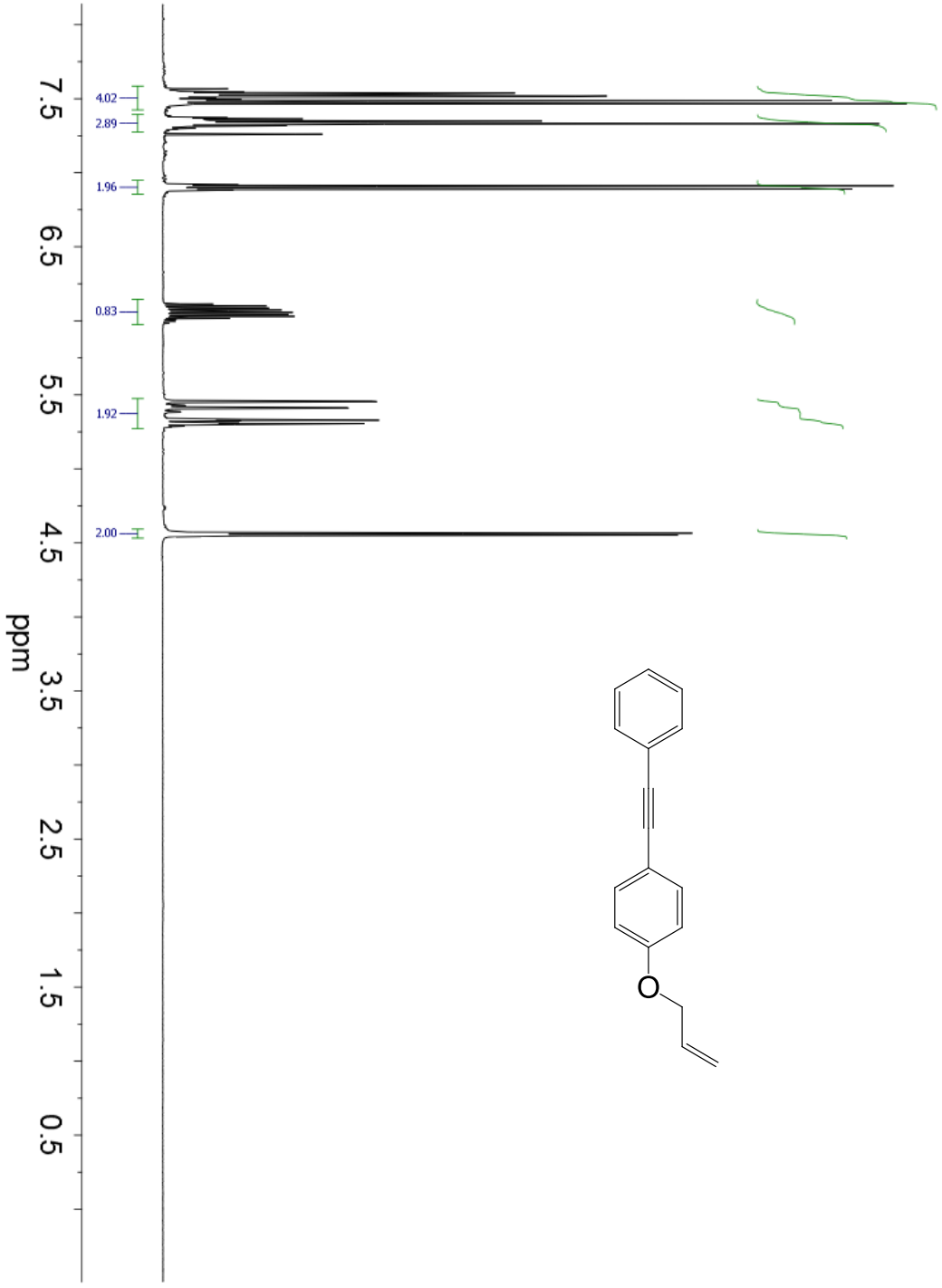

^{13}C NMR spectrum of compound (**18b)**

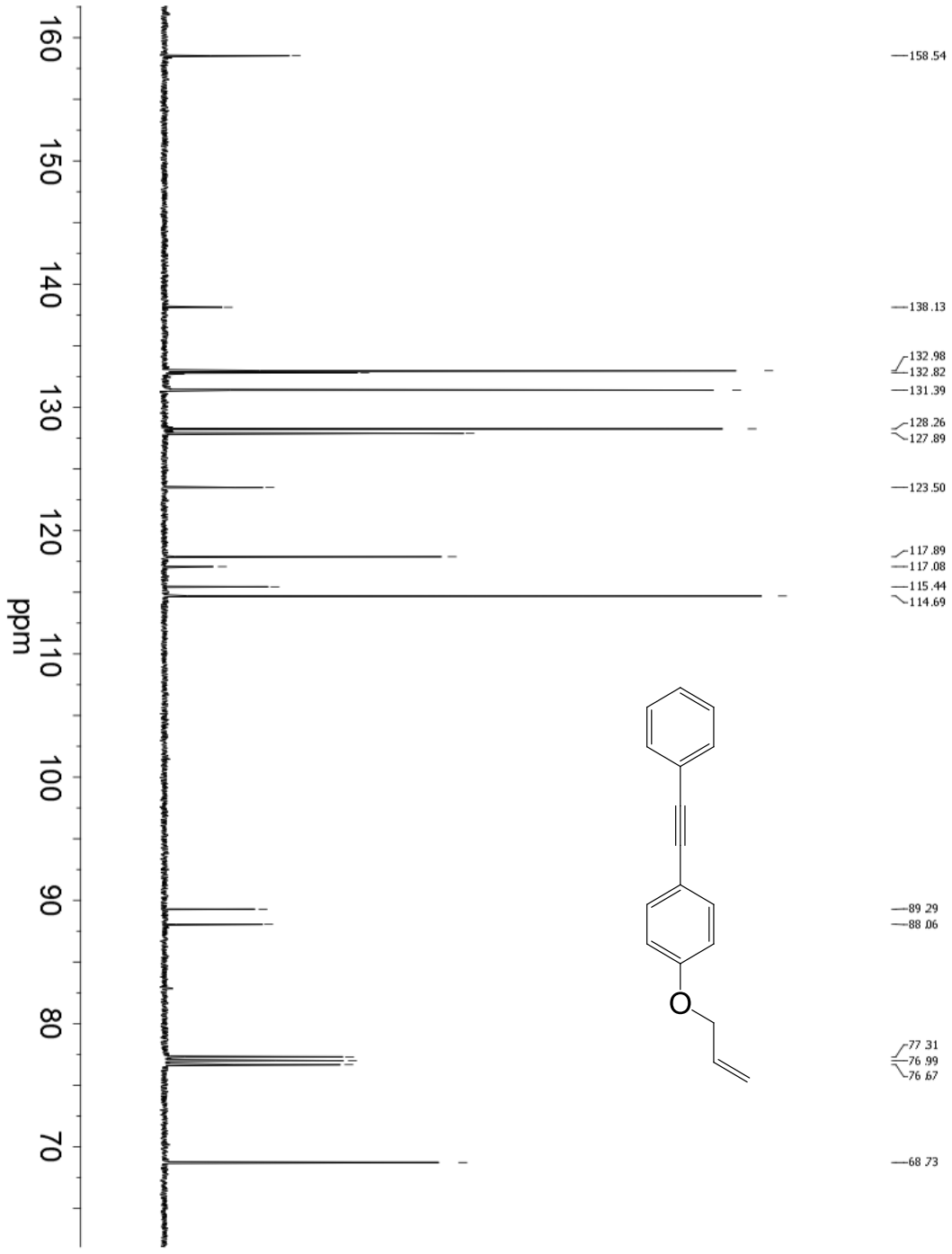

^{1}H NMR spectrum of compound (**18c**)

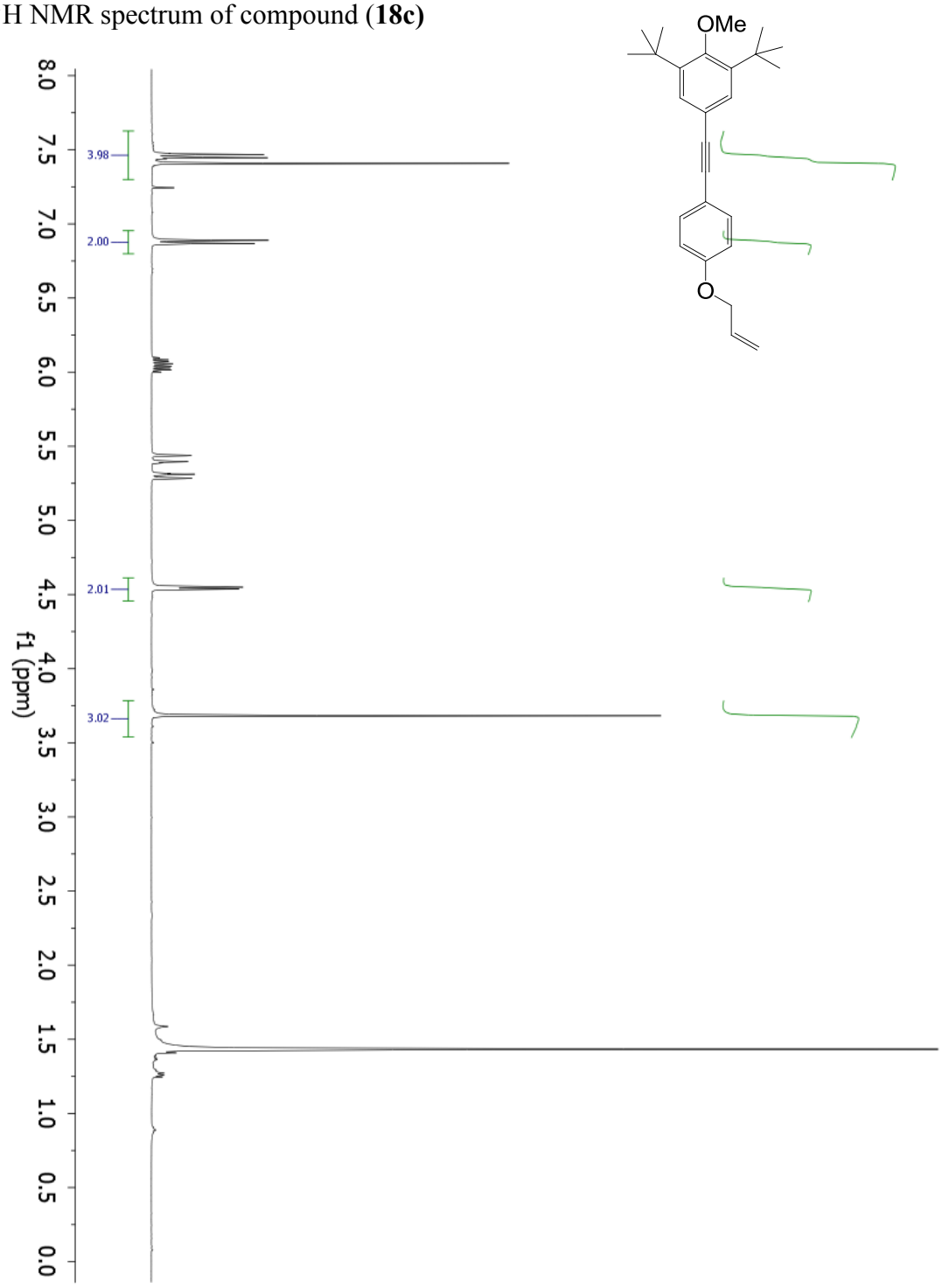

^{13}C NMR spectrum of compound (**18c)**

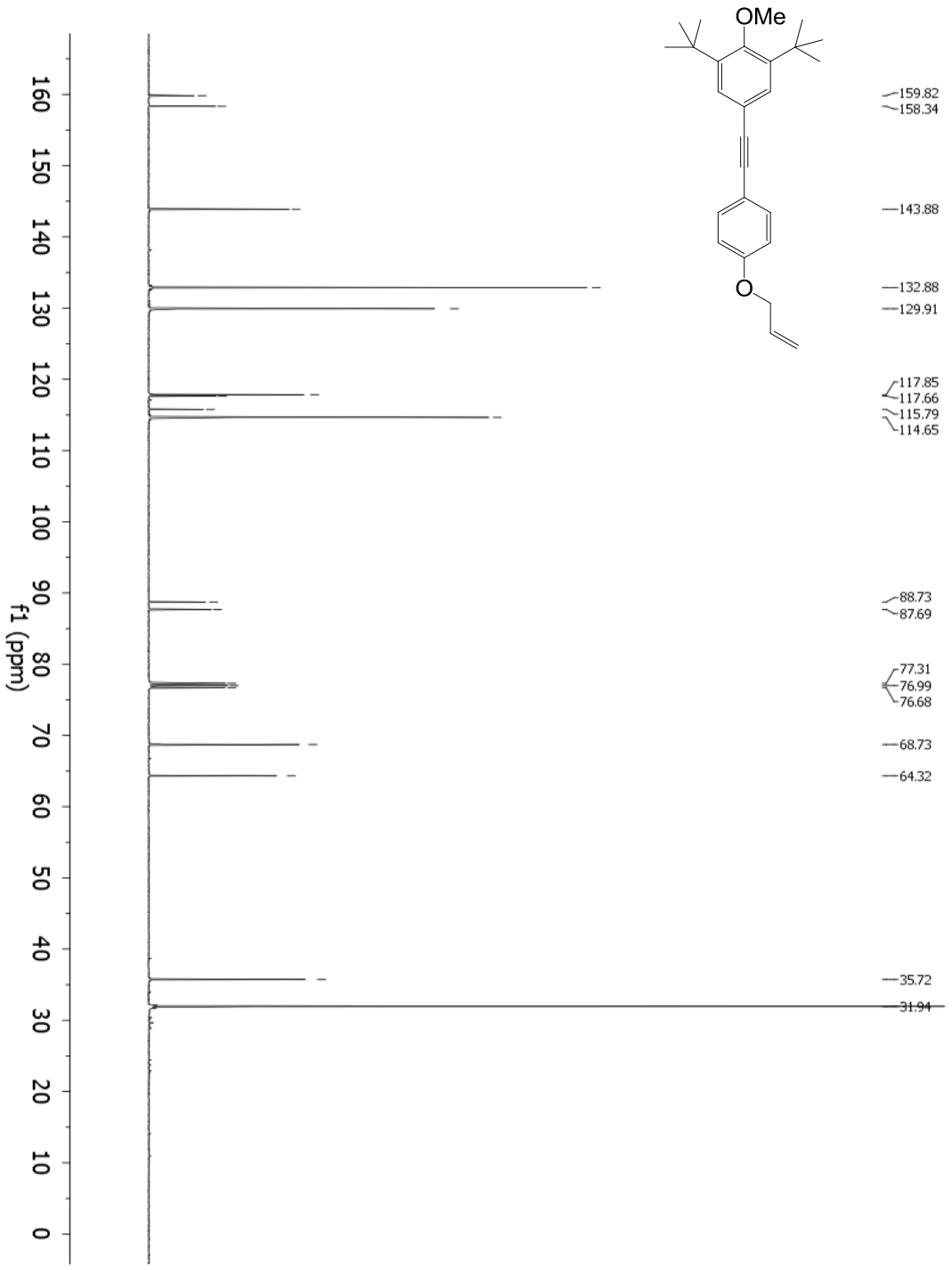

^{1}H NMR spectrum of compound (**18d)**

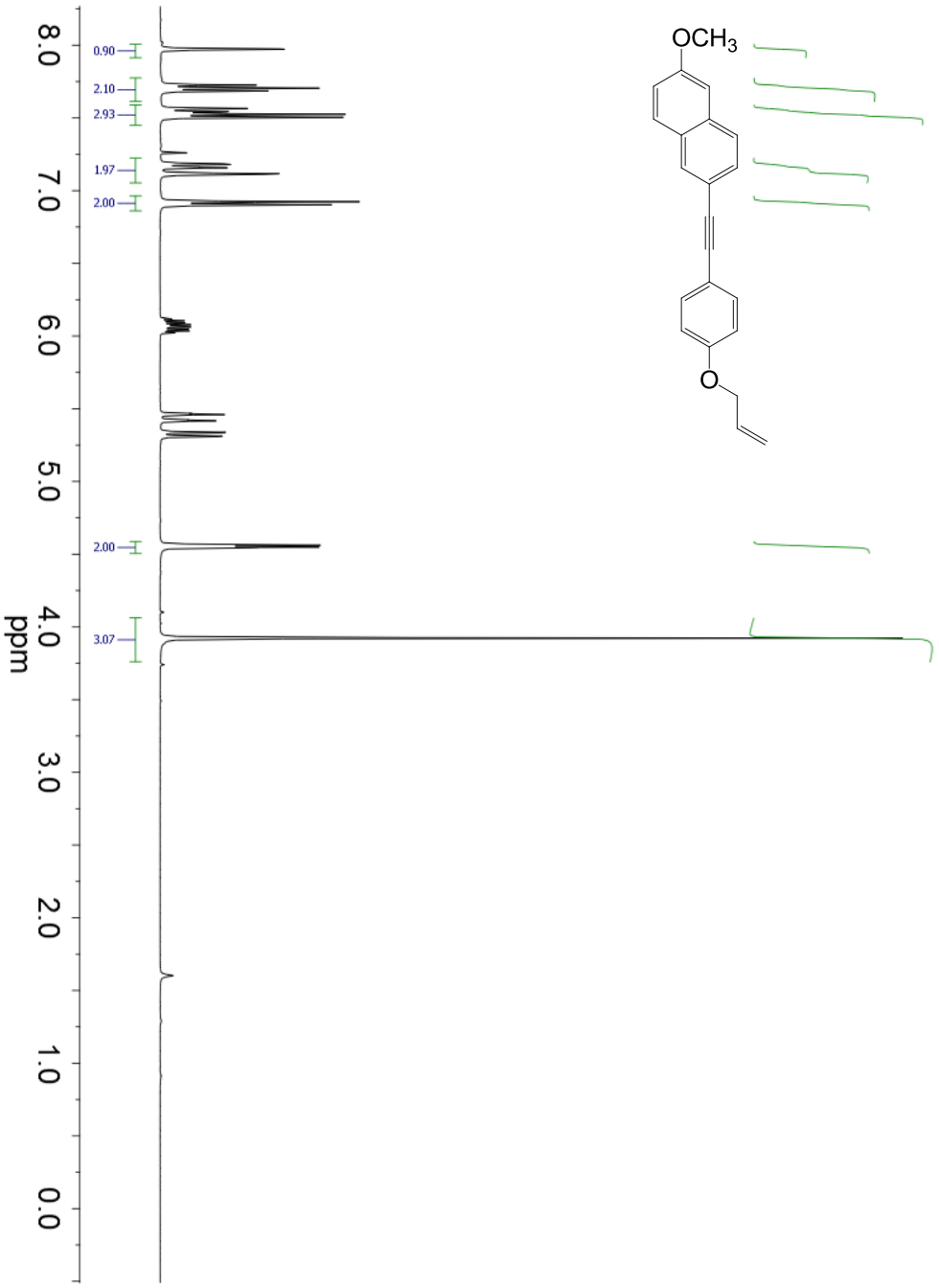

^{13}C NMR spectrum of compound (**18d)**

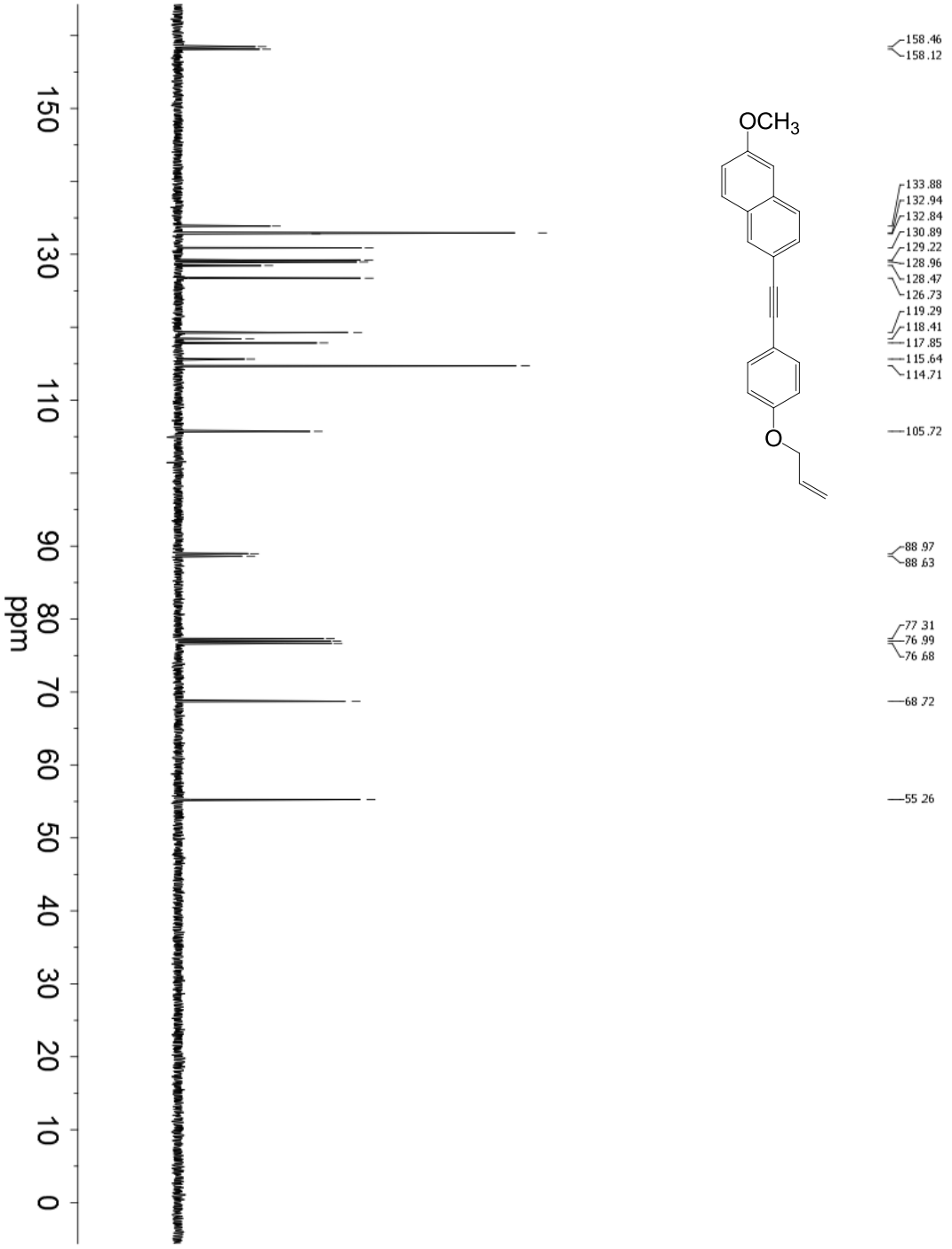

^{1}H NMR spectrum of compound (**18e)**

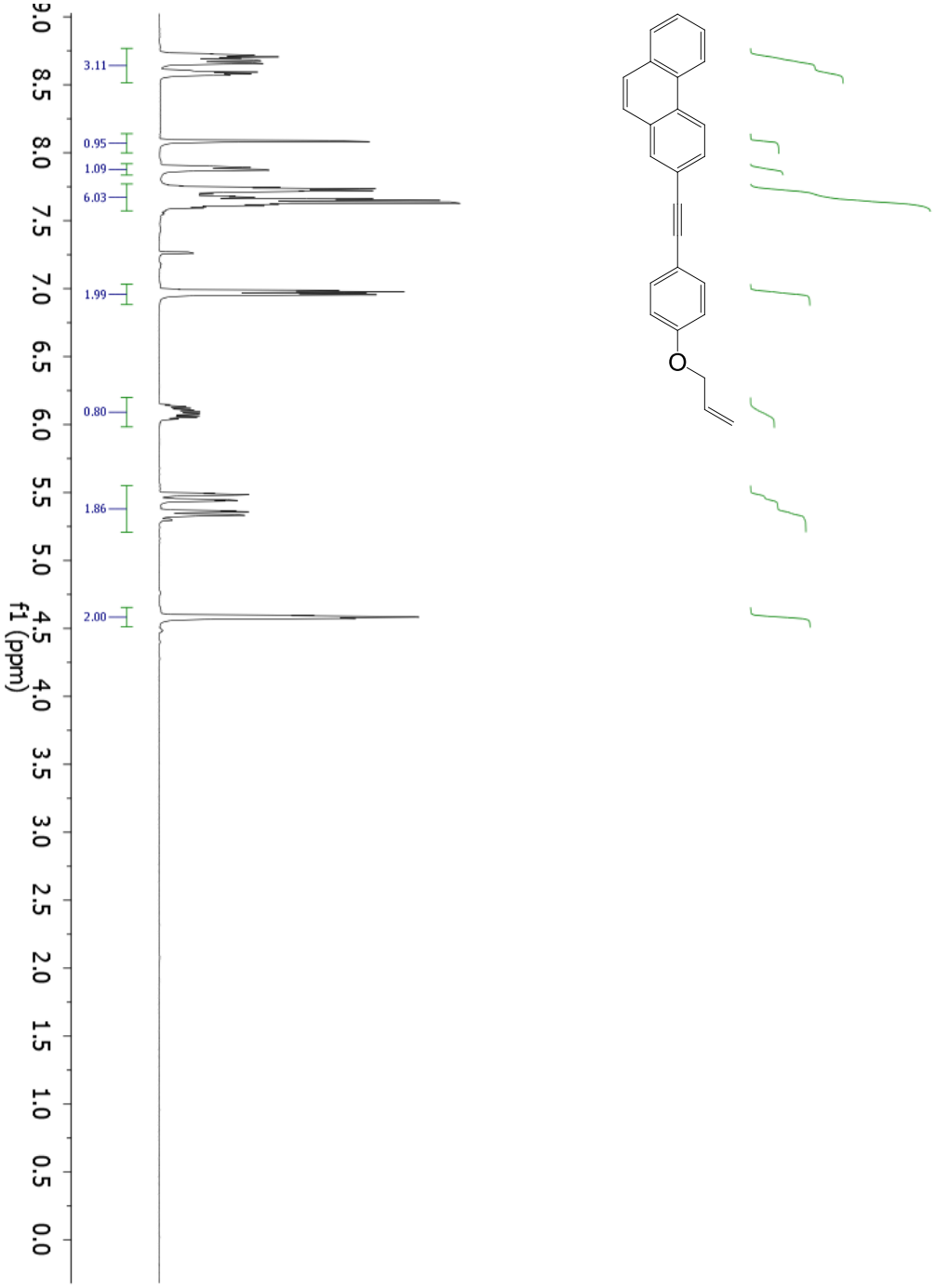

^{13}C NMR spectrum of compound (**18e)**

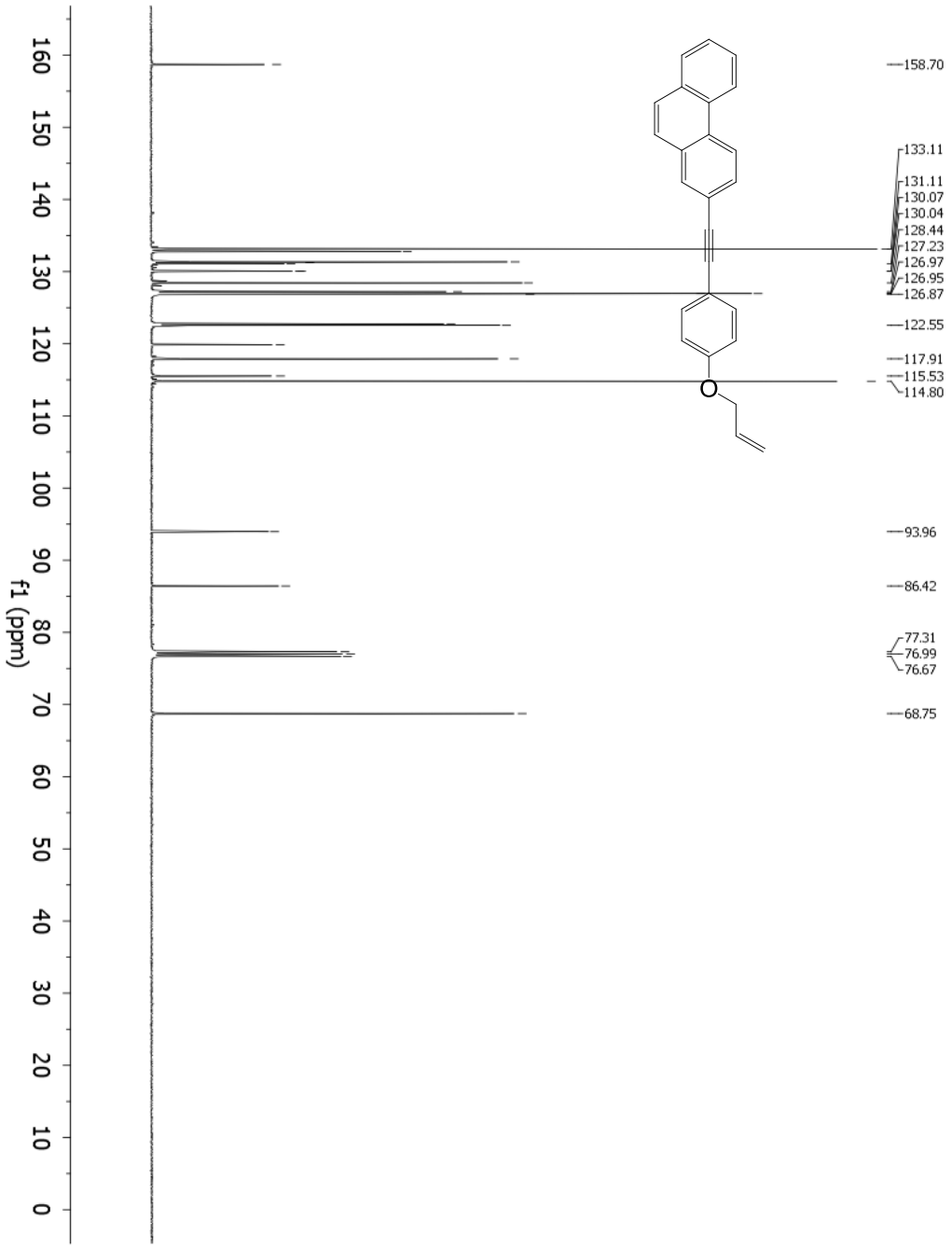

^{1}H NMR spectrum of compound (**18f)**

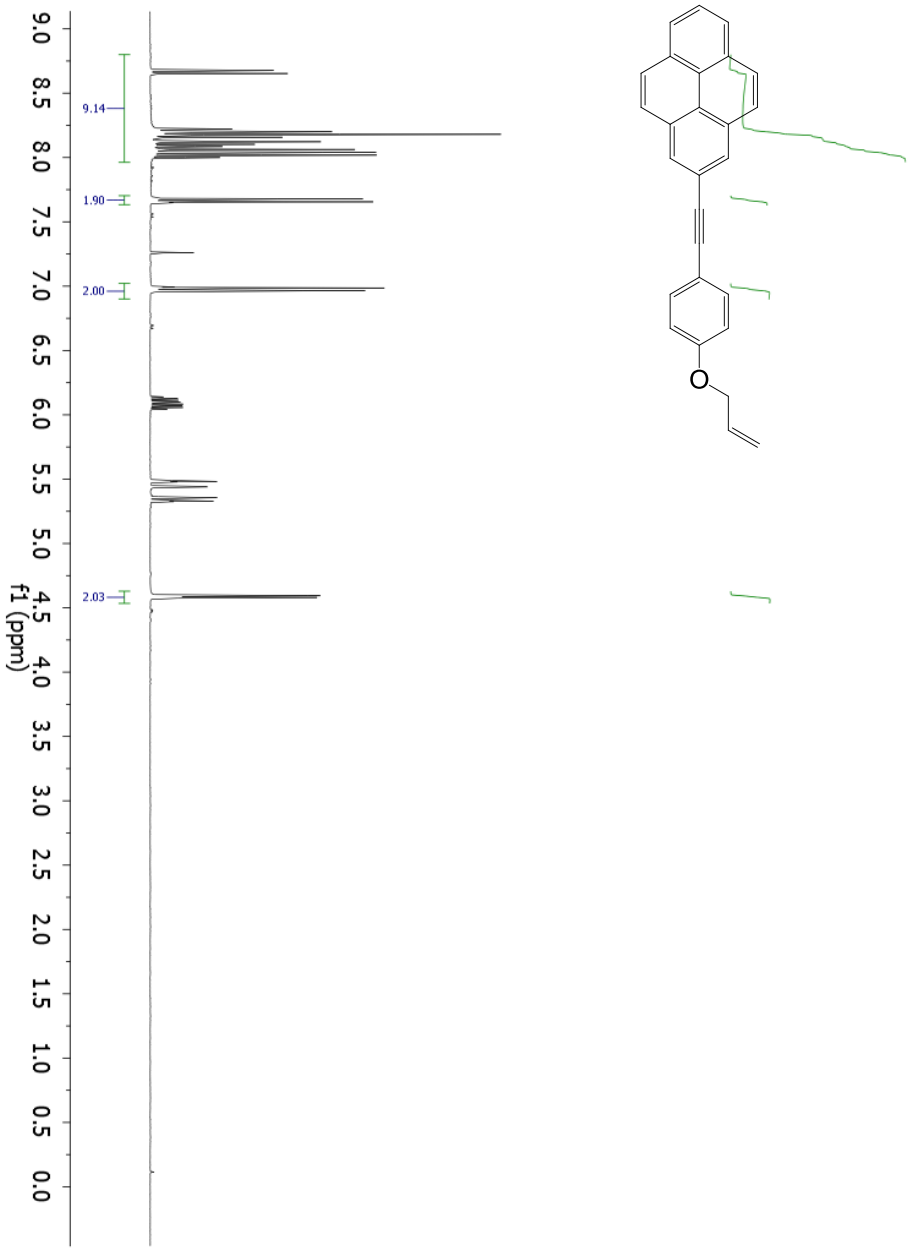

^{13}C NMR spectrum of compound (**18f)**

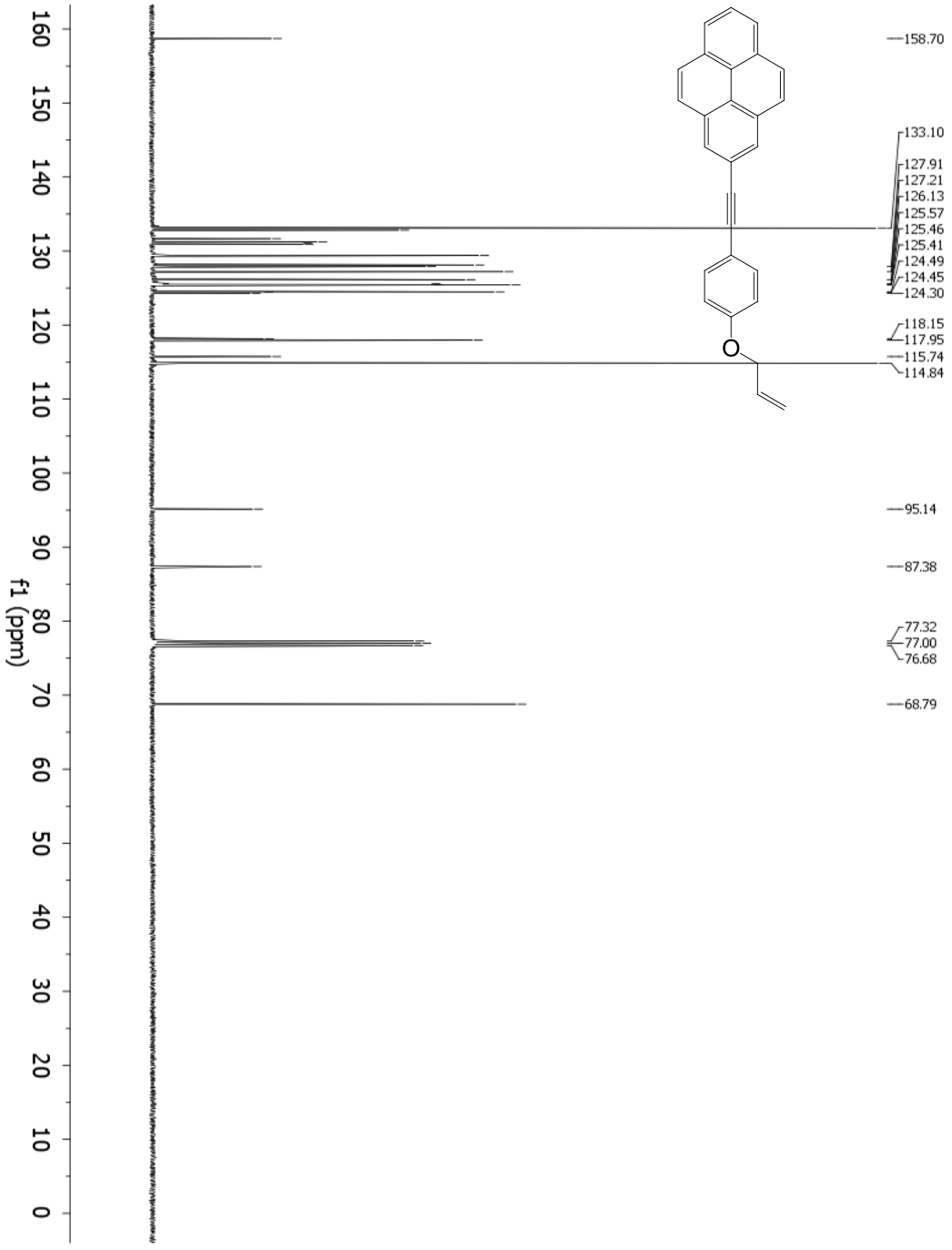

^{1}H NMR spectrum of compound (**19)**

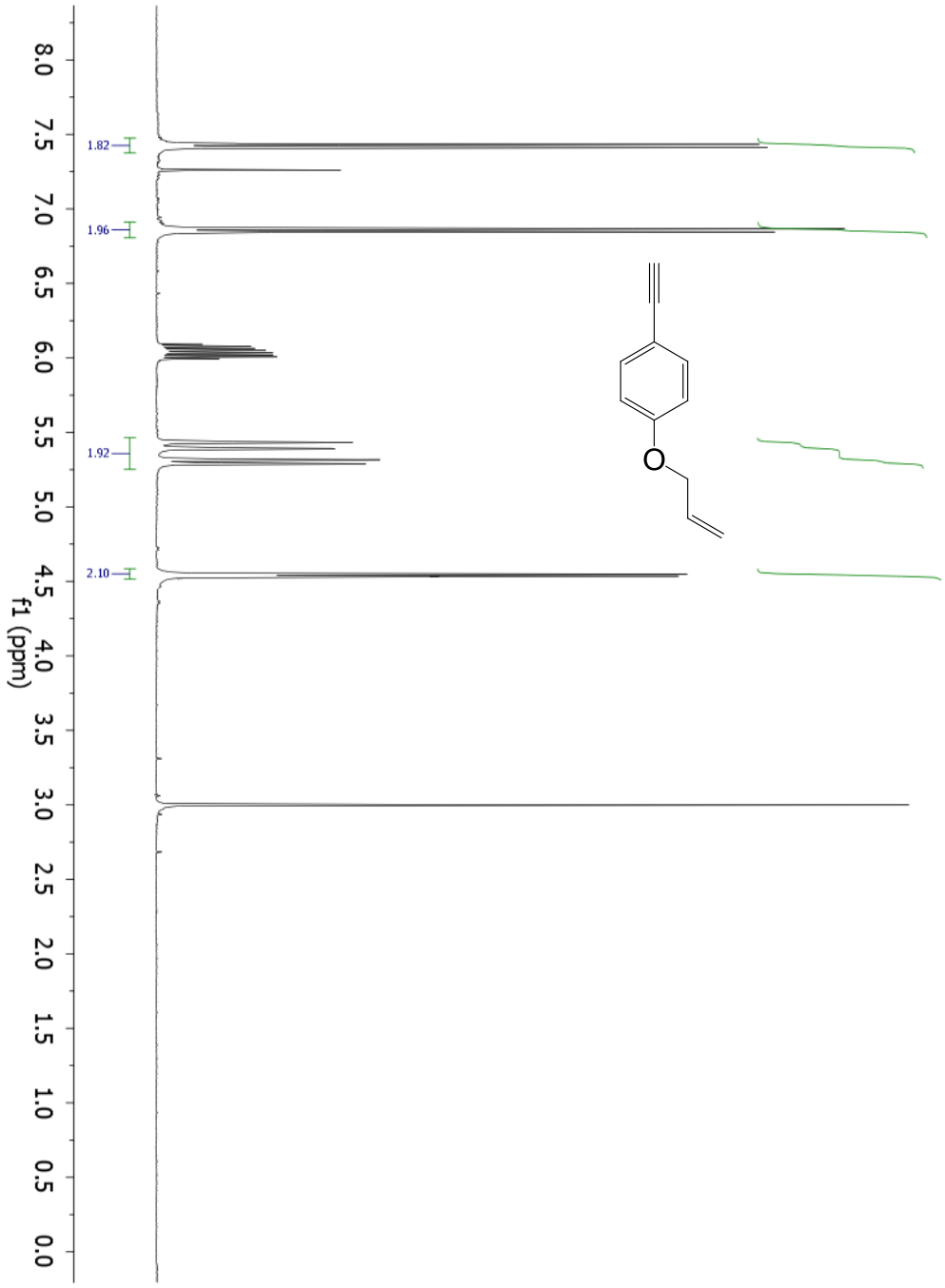

^{13}C NMR spectrum of compound (**19)**

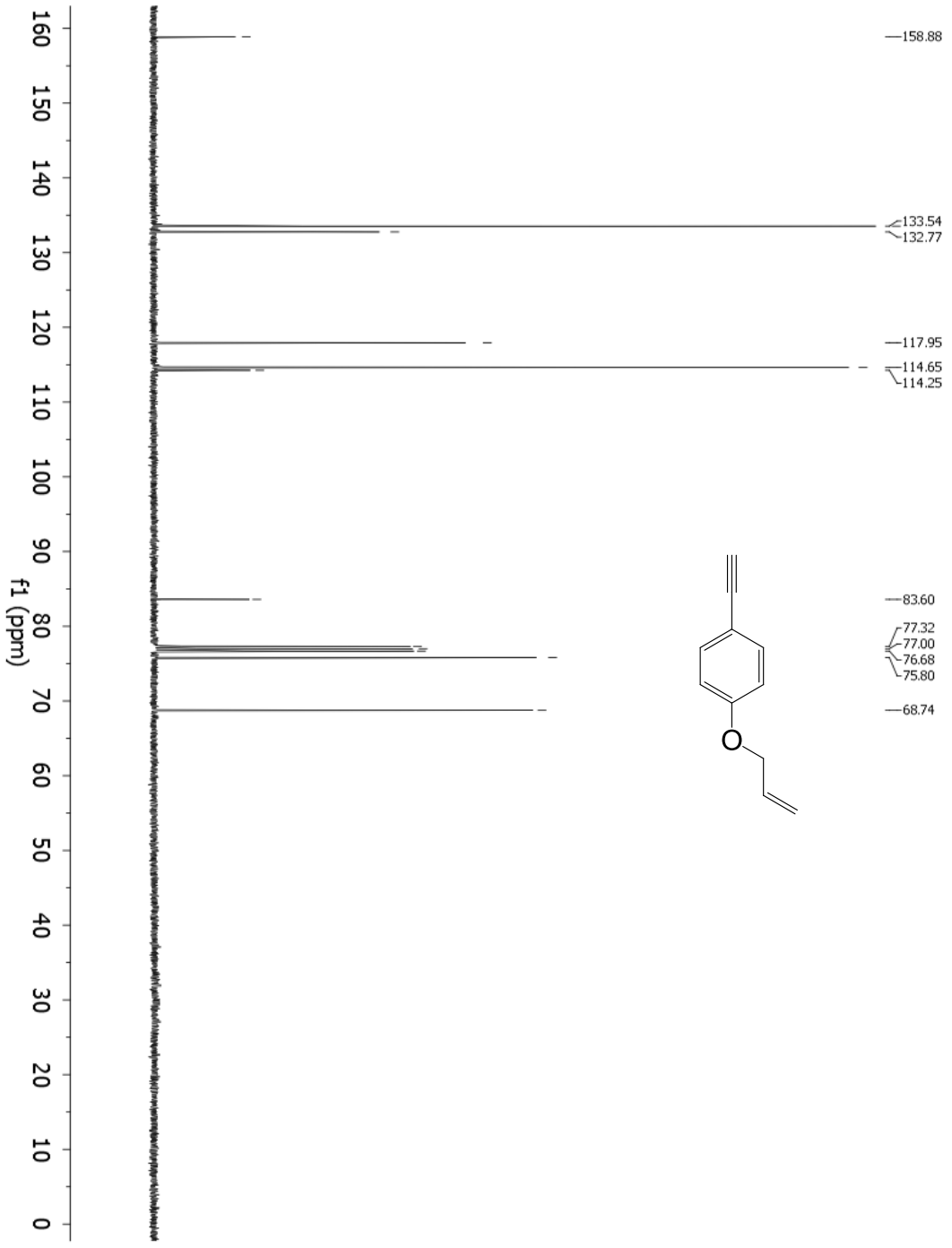

^{1}H NMR spectrum of compound (**20**)

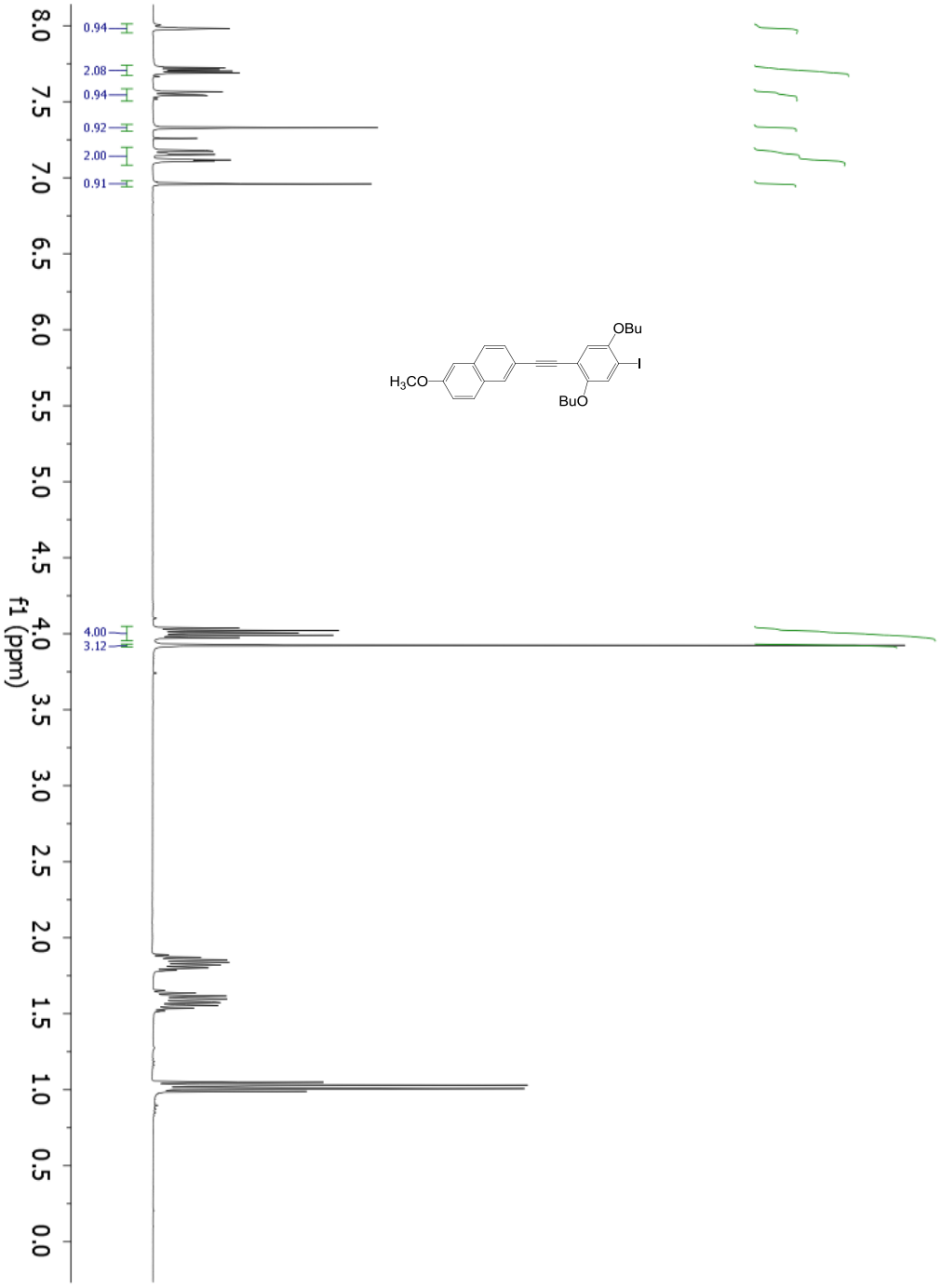

^{13}C NMR spectrum of compound (**20)**

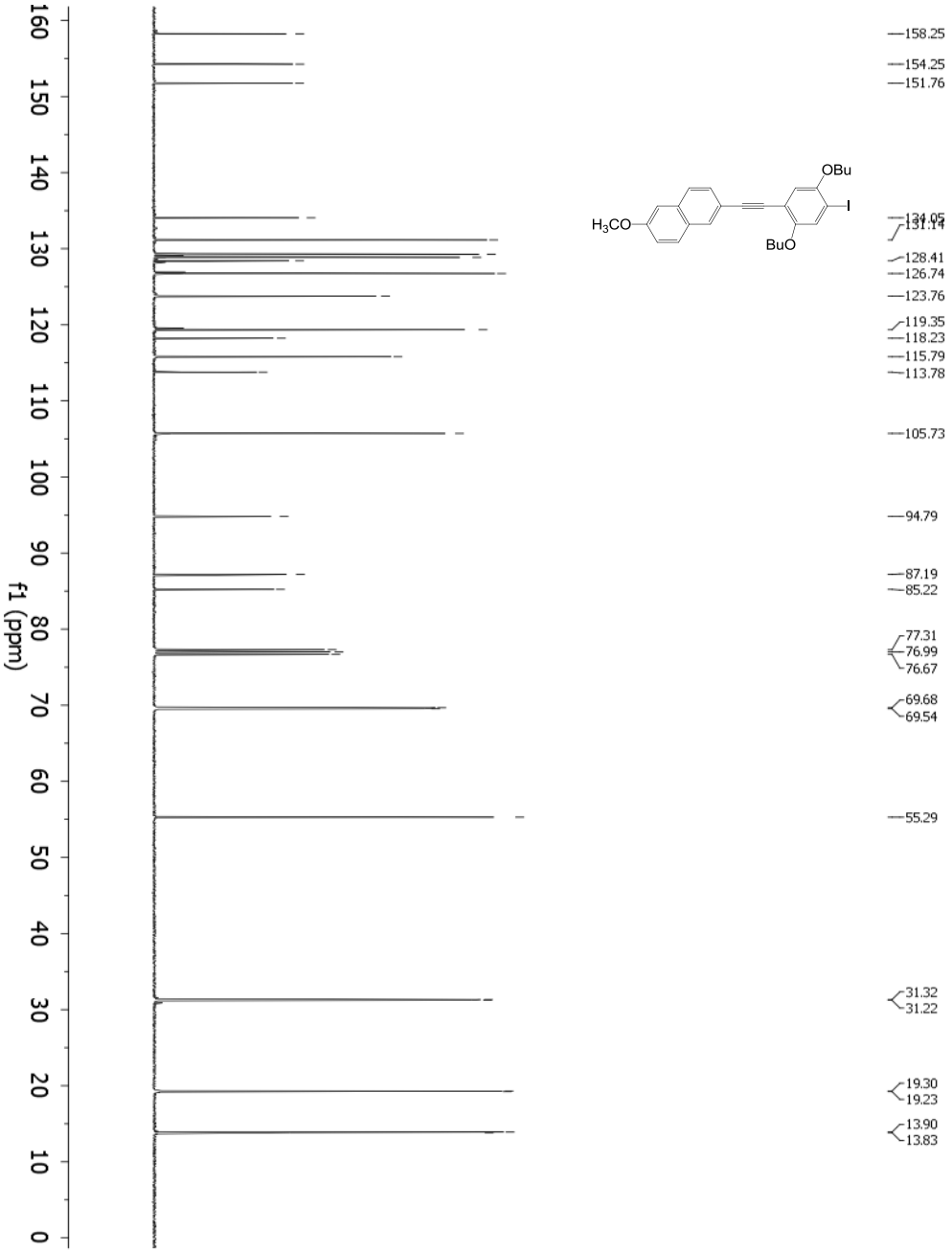

^{1}H NMR spectrum of compound (**21a)**

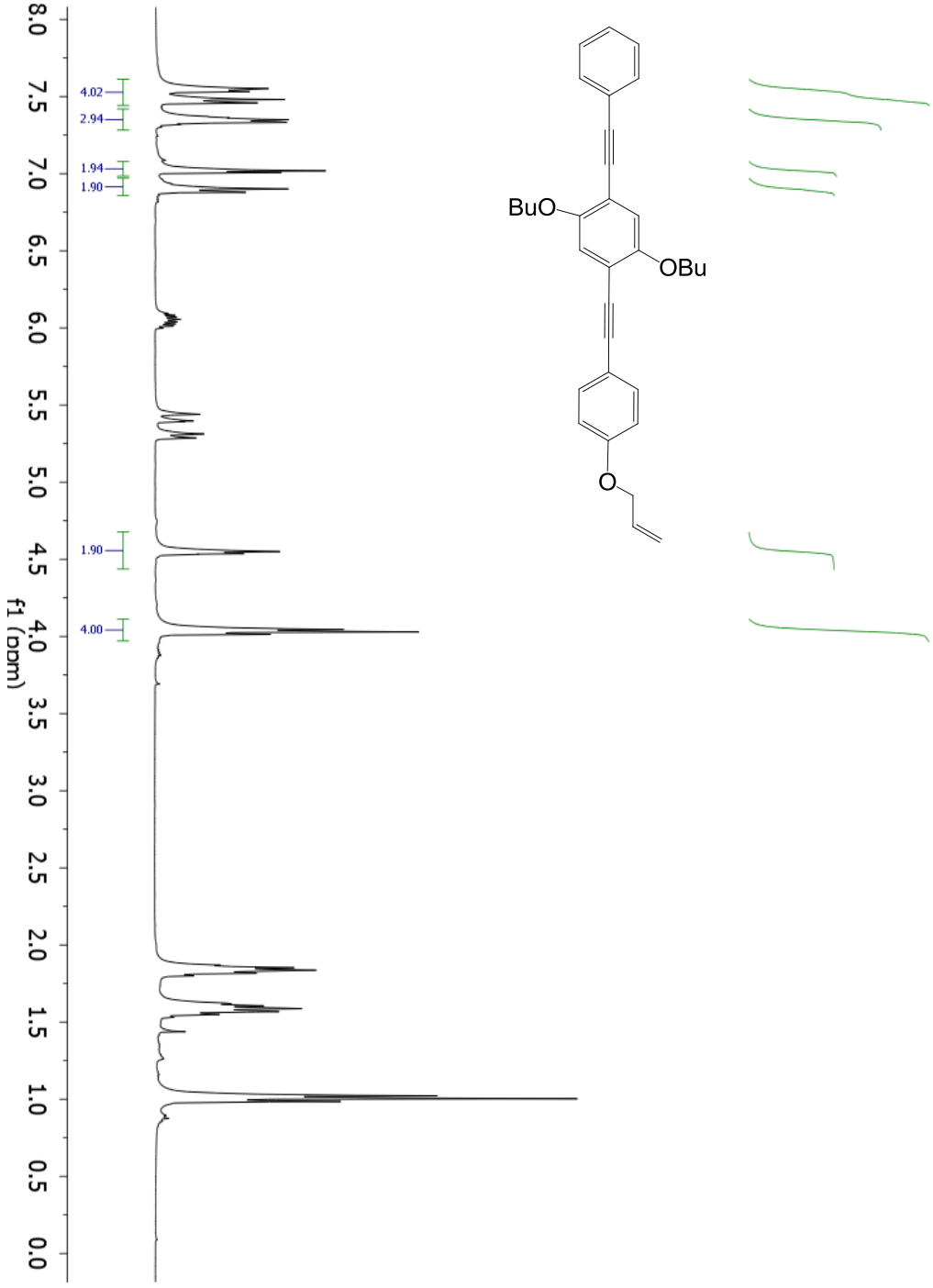

^{13}C NMR spectrum of compound (**21a)**

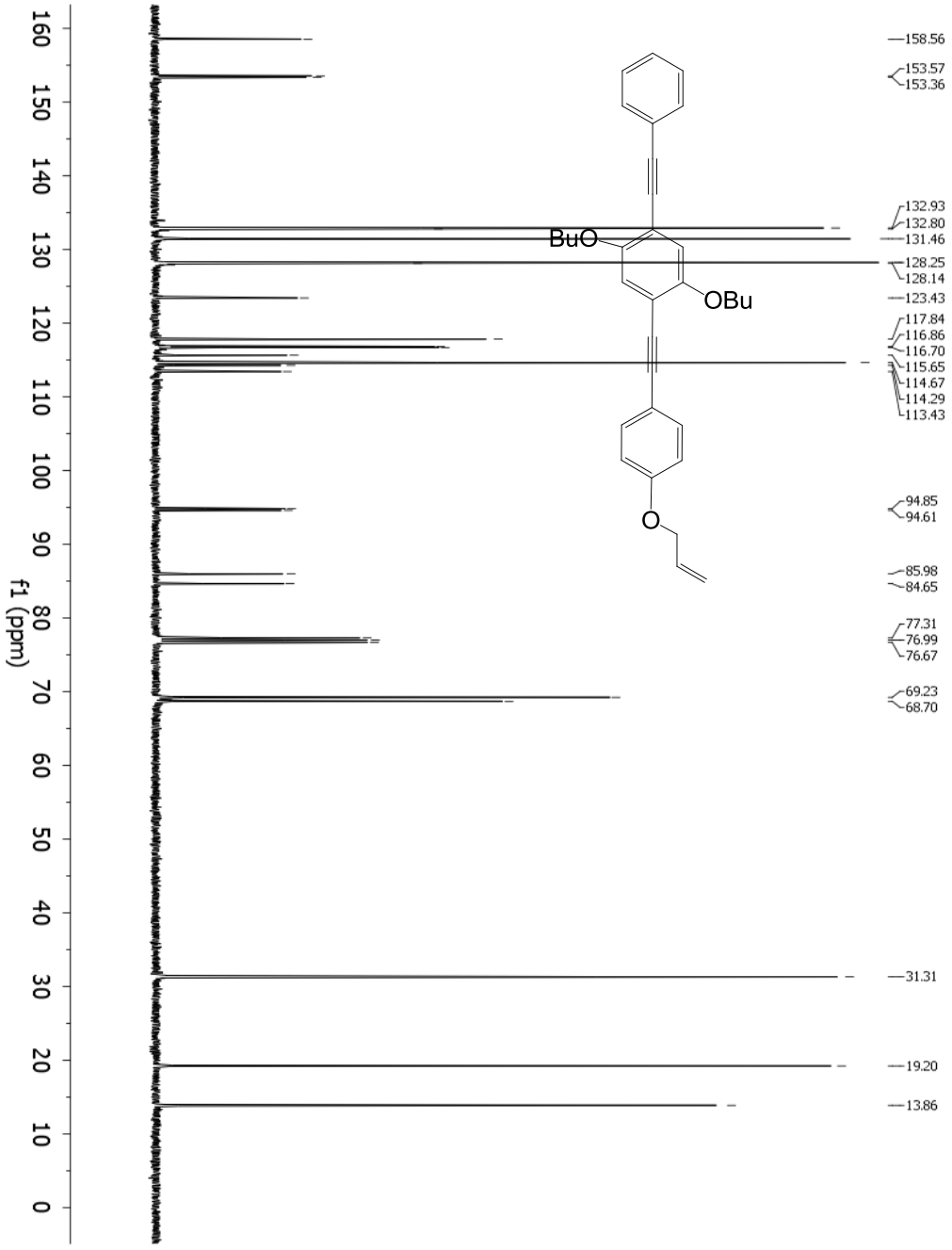

^{1}H NMR spectrum of compound (**21b)**

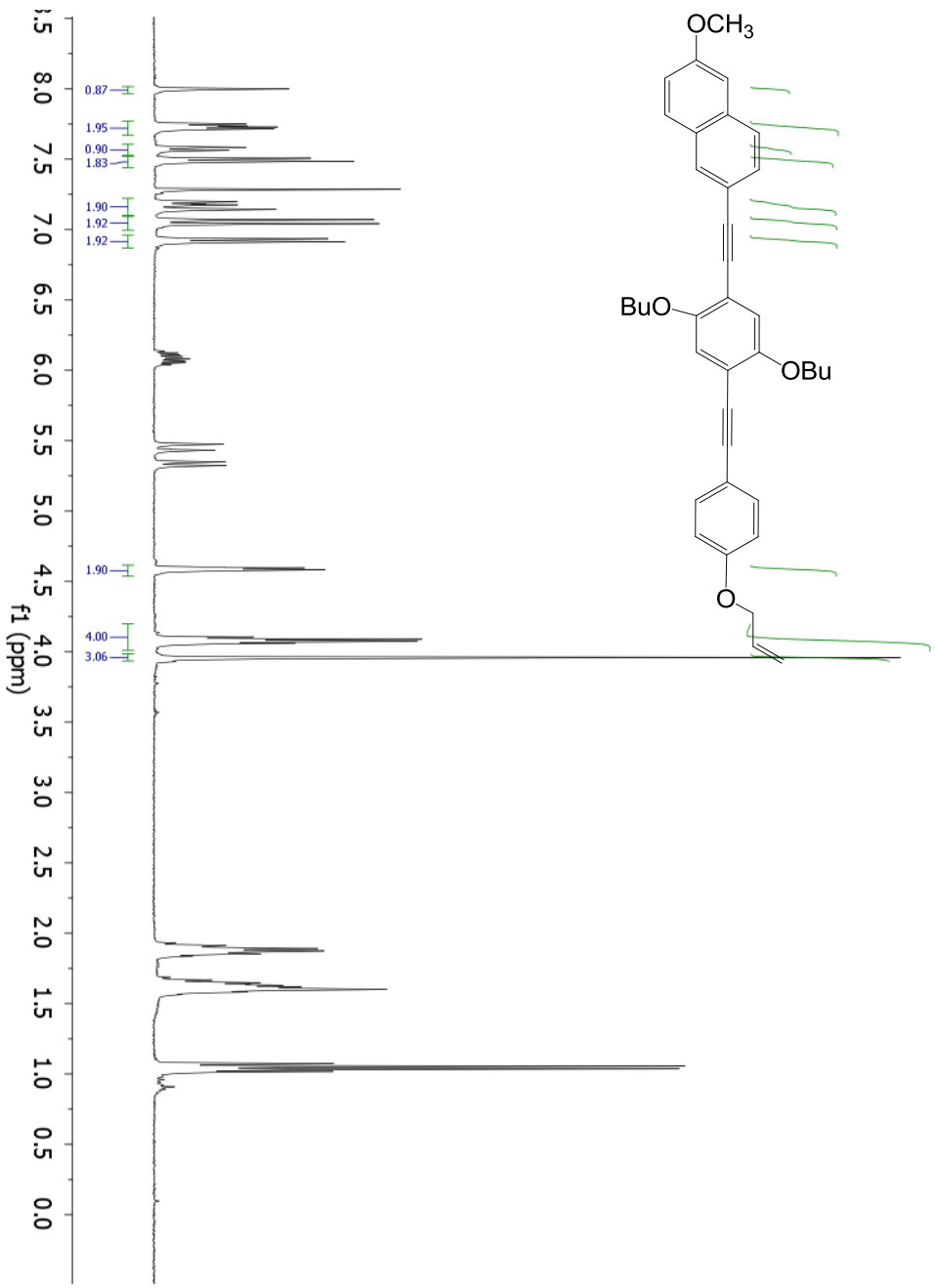

^{13}C NMR spectrum of compound (**21b)**

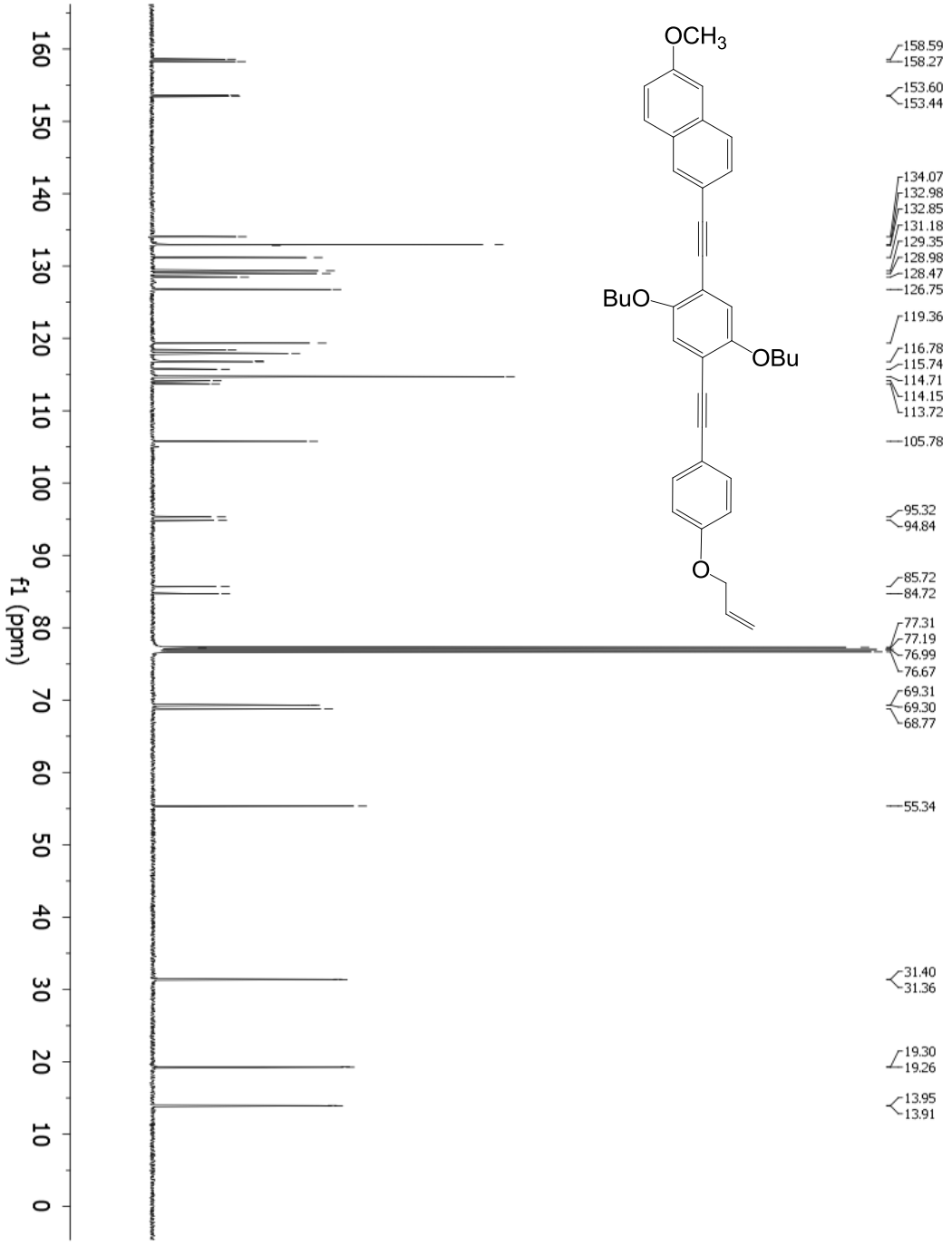

^{1}H NMR spectrum of compound (**22**)

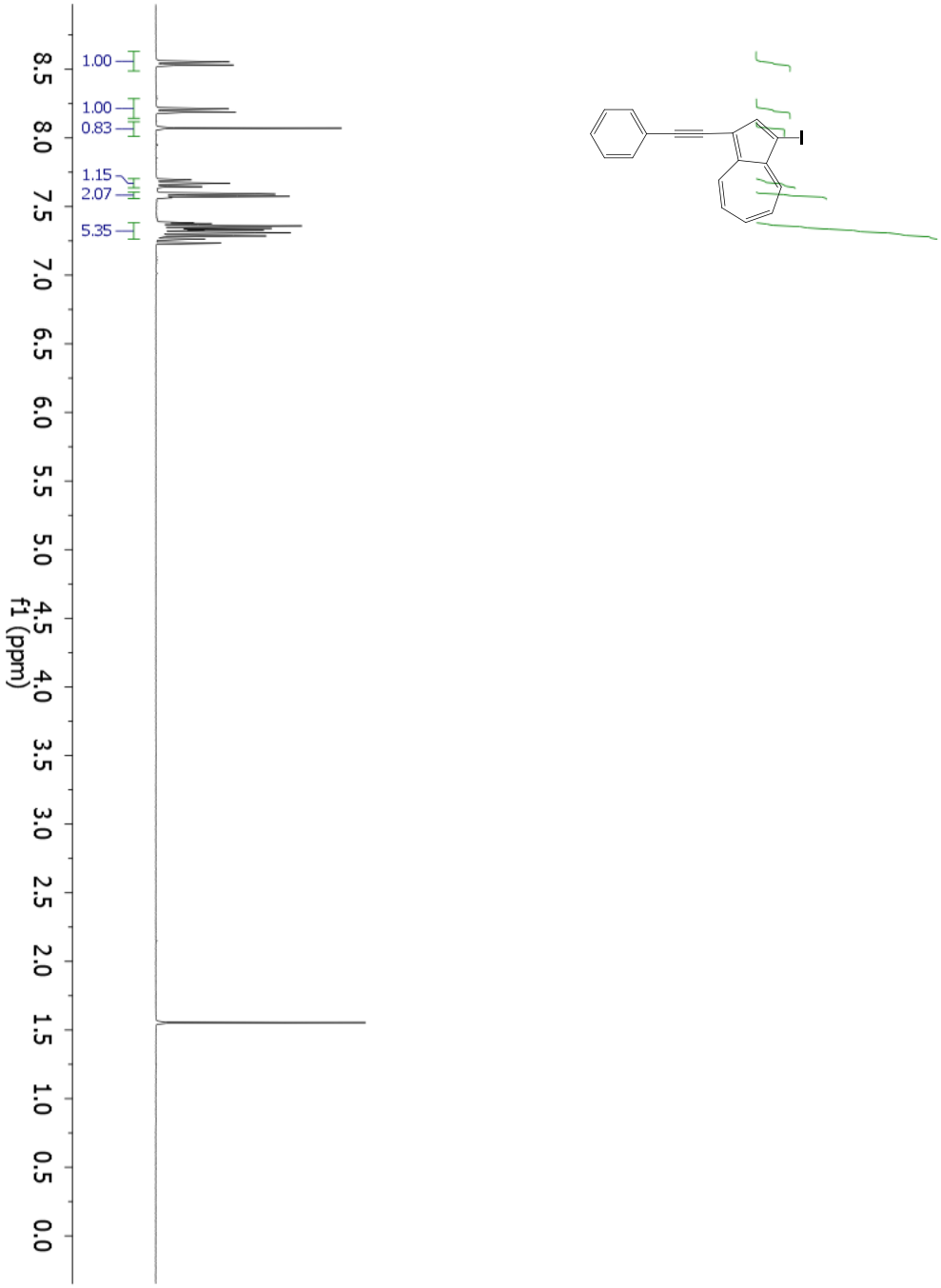

^{13}C NMR spectrum of compound (**22)**

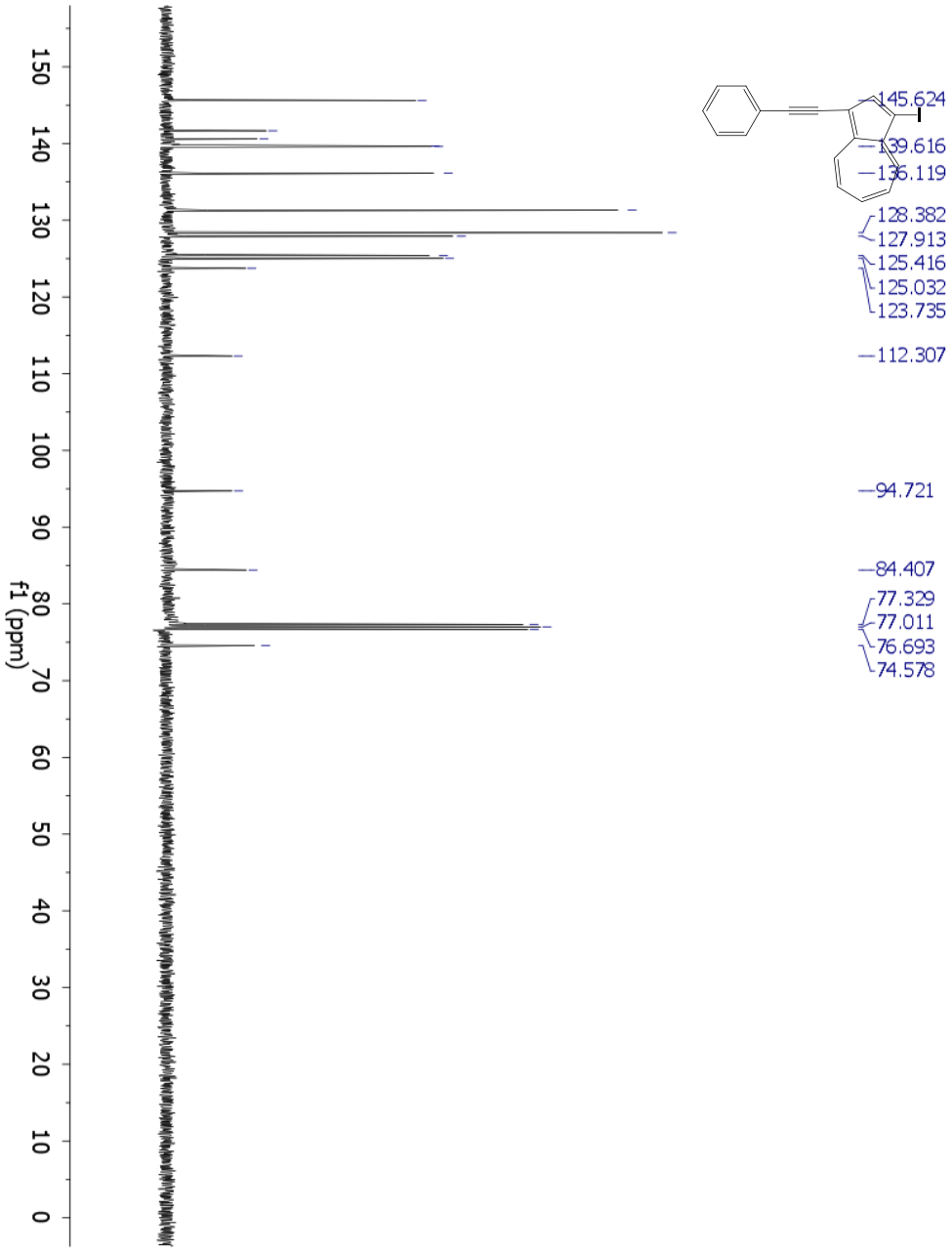

^{1}H NMR spectrum of compound (**23)**

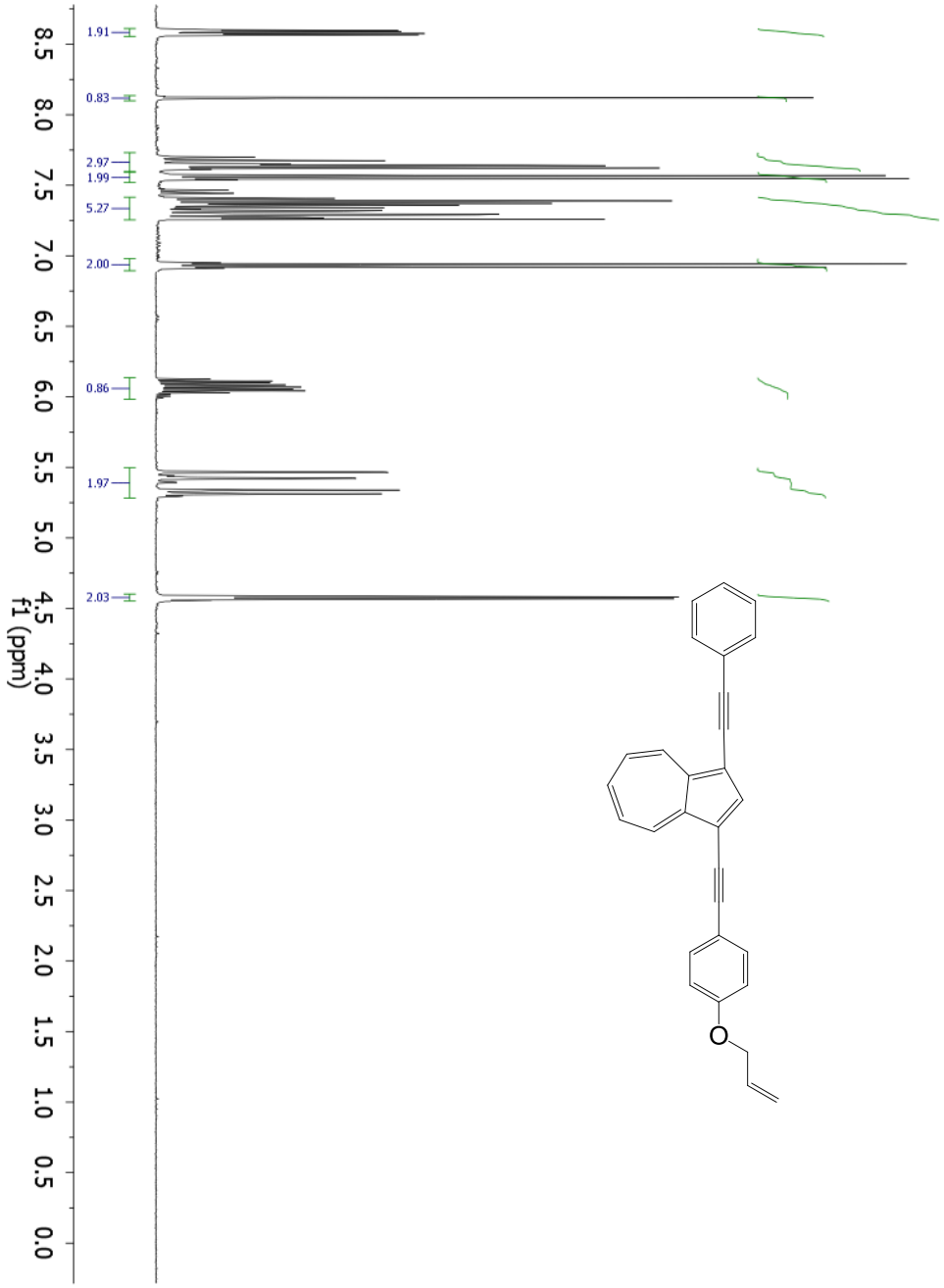

^{13}C NMR spectrum of compound (**23)**

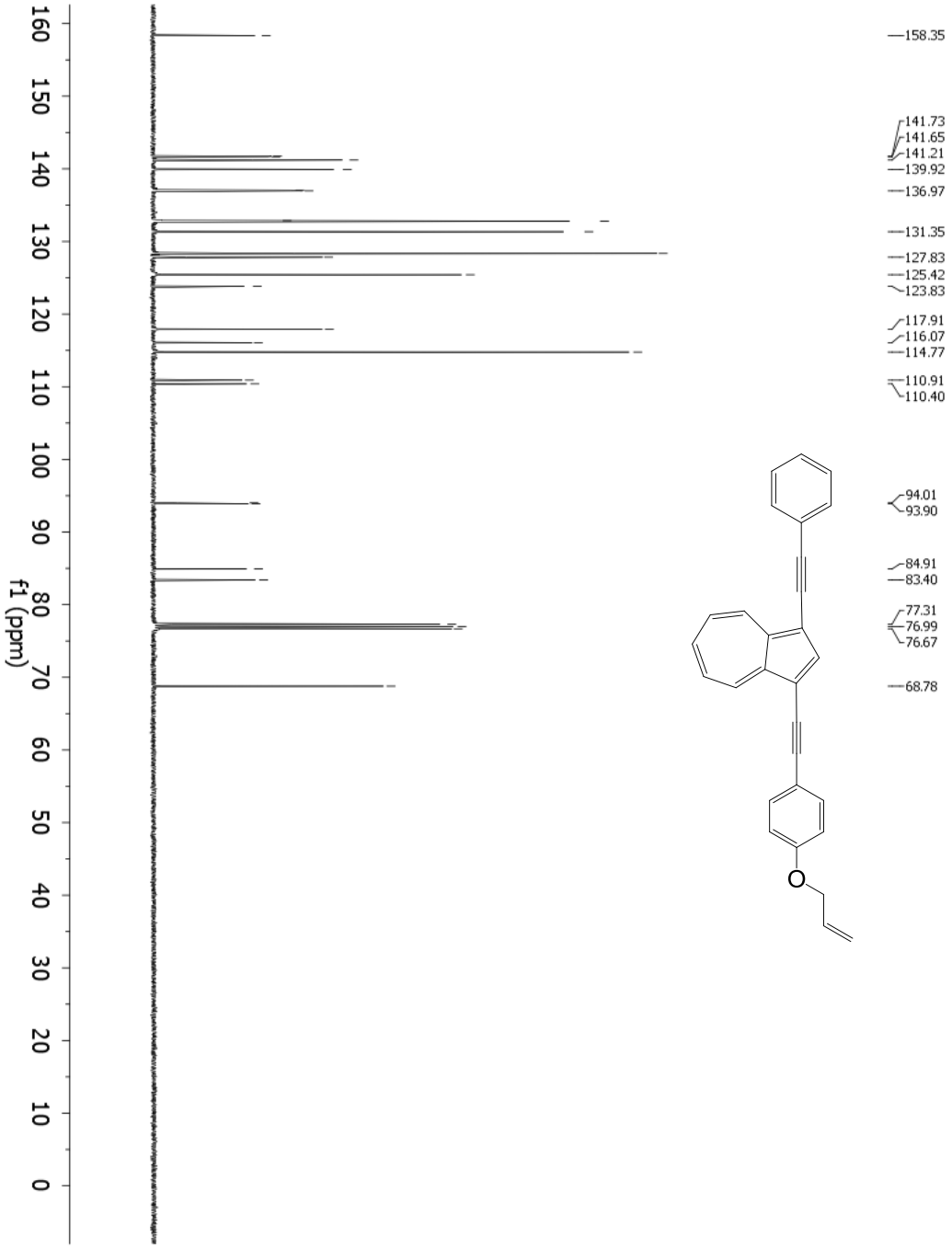

REFERENCES

(1) (a) Jegou, G.; Jenekhe, S. A. "Synthesis and Characterization of Poly (5, 8-quinoxaline ethynylene)s" *Macromolecules*, **2001**, *34*, 7926. (b) Beck, B. J.; Kokil, A.; Ray, D.; Rowan, S. J.; Weder, C.; "Facile Reduction of Poly(2,5-dialkoxy-p-phenylene ethynylene)s — An Efficient Route for the Synthesis of Poly(2,5-dialkoxyl-p-xylenes)s" *Macromolecules*, **2002**, *35*, 590. (c) Venkataramana, G.; Dongare, P.; Dawe, L. N.; Thompson, D.W.; Zhao, Y.; Bodwell. G. J. "1,8-Pyrenylene−Ethynylene Macrocycles" *Org. Lett*. **2011**, *13*, 2240. (d) Guo, X.; Watson, M. D. "Pyromellitic Diimide-Based Donor–Acceptor Poly(phenylene ethynylene)s" *Macromolecules*, **2011**, *44*, 6711. (e) Nagai, A.; Chujo, Y. "Brilliant BODIPY_Fluorene Copolymers with Dispersed Absorption and Emission Maxima" *Macromolecules*, **2010**, *43*, 193.

(2) (a) Umnov, A.G.; Korovyanko, O. J. "Photovoltaic Effect in Poly-dioctyl-phenylene-ethynylene-C_{60} Cells upon Donor and Acceptor Excitation" *Appl. Phys. Lett.* **2005**, *87*, 113506. (b) Cremer, J.; Bäuerle, P.; Wienk, M.M.; Janssen, R.A.J. "High Open-Circuit Voltage Poly(ethynylene bithienylene):Fullerene Solar Cells" *Chem. Mater.* **2006**, *18*, 5832. (c) Valentini, L.; Marrocchi, A.; Seri, M.; Mengoni, F.; Meloni, F.; Taticchi, A.; Kenny, J.M. "[2.2]Paracyclophane-Based Molecular Systems for the Development of Organic Solar Cells" *Thin Solid Films* **2008**, *516*, 7193. (d) Valentini, L.; Bagnis, D.; Marrocchi, A.; Seri, M.; Taticchi, A.; Kenny, J.M. "Novel

Anthracene-Core Molecule for the Development of Efficient PCBM-Based Solar Cells" *Chem. Mater.* **2008**, *20*, 32. (e) Marrocchi, A.; Silvestri, F.; Seri, M.; Facchetti, A.; Taticchi, A.; Marks, T.J. "Conjugated Anthracene Derivatives as Donor Materials for Bulk Heterojunction Solar Cells: Olefinic versus Acetylenic Spacers" *Chem. Commun.* **2009**, 1380.

(3) (a) Brédas, J.; Norton, J. E.; Cornil, J.; Coropceanu, V. "Molecular Understanding of Organic Solar Cells: The Challenges"*Acc. Chem. Res.,* **2009**, *42*, 1691. (b) Facchetti, A. "Benzotrithiophene -A Planar, Electron-Rich Building Block for Organic Semiconductors" *Chem. Mater.*, **2011**, *23*, 733.

(4) (a) Li, I.; Liang,Y.; Xie, Y. "Efficient Palladium-Catalyzed Homocoupling Reaction and Sonogashira Cross-Coupling Reaction of Terminal Alkynes under Aerobic Conditions" *J. Org. Chem.*, **2005**, *70*, 4393. (b) Chinchilla, R.; Nájera, C. " The Sonogashira Reaction: A Booming Methodology in Synthetic Organic Chemistry" *Chem. Rev.*, **2007**, *107*, 874. (c) Liu, C.; Luh, T. "Combining Furan Annulation, Heck Reaction, and Sonogashira Coupling for the Synthesis of Oligoaryls" *Org. Lett.*, **2002**, *4*, 4305.

(5) (a) Liang, B.; Dai,M.; Chen, J.; Yang, Z. "Copper-Free Sonogashira Coupling Reaction with $PdCl_2$ in Water under Aerobic Conditions" *J. Org. Chem.*, **2005**, *70*, 391. (b) Bag, S. S.; Kundu, R.; Das, M. "Click-Reagent Version of Sonogashira Coupling Protocol to Conjugated Fluorescent Alkynes with No or Reduced Homocoupling" *J. Org. Chem.*, **2011**, *76*, 2332. (c) Soheili, A.; Albaneze-Walker, J.;

Murry, J.A.; Dormer, P. G.; Hughes.D. L. "Efficient and General Protocol for the Copper-Free Sonogashira Coupling of Aryl Bromides at Room Temperature" *Org. Lett.*, **2003**, *5*, 4191. (d) Thorand , S.; Krause, N. "Improved Procedures for the Palladium-Catalyzed Coupling of Terminal Alkynes with Aryl Bromides (Sonogashira Coupling)" *J. Org. Chem.*, **1998**, *63*, 8551. (e) Liang, Y.; Xie, Y.; Li, J. "Modified Palladium-Catalyzed Sonogashira Cross-Coupling Reactions under Copper-, Amine-, and Solvent-Free Conditions" *J. Org. Chem.*, **2006**, *71*, 379. (f) Huang, H.; Liu, H.; Jiang, H.; Chen. K. "Note Rapid and Efficient Pd-Catalyzed Sonogashira Coupling of Aryl Chlorides" *J. Org. Chem.*, **2008**, *73*, 6037.

(6) Chen, X.; Barnes, C.; Jerry R. Dias, J. R.; Sandreczki, T.C. "Investigation of sp2-sp Coupling for Electron-Enriched Aryl Dihalides Under Oxygen-Free Sonogashira Coupling Reaction Conditions Using a Two-Chamber Reaction System" *Chem. Eur. J.* **2009**, *15*.2041.

(7) James M. Tour, J. M.; Rawlett, A. M.; Kozaki, M.; Yao, Y.; Jagessar, R. C.; Dirk, S. M.; Price, D. W.; Reed, M. A.; Zhou, C.; Chen, J.; Wang, W.; Campbell, I. "Synthesis and Preliminary Testing of Molecular Wires and Devices" *Chem. Eur. J.* **2001**, *7,* 5118.

(8) Dri, C.; Peters, M. V.; Schwarz, J.; Hecht, S.; Grill, L. "Spatial Periodicity in Molecular Switching" *nature nanotechnology* **2008**, *3*, 649.

(9) Elangovan, A.; Wang, Y.; Ho, T. "Sonogashira Coupling Reaction with Diminished Homocoupling" *Org. Lett.*, **2003**, *5*, 1841.

(10) Chen, X.; Barnes, C.; Bai, X.; Sandreczki, T. C.; Peng, Z.; Kadnikova, E. N.; Dias, J. R. "Synthesis and Structural Analysis of a Novel Iodinated Cyclopentadienone *via* Ring-Contraction Iodination and Its Application in Synthesis of Alkyne-Functionalized Cyclopentadienones " *Chem. Comm*. **2010**, *46*, 8171.

(11) Seminario, J. M.; Zacarias, A. G.; Tour, J. M. "Molecular Scale Electronics: A Synthetic/Computational Approach to Digital Computing" *J. Am. Chem. Soc*. **1998**,*120*, 3970.

VITA

Xinyan Bai was born on September 2, 1977 in Manasi, Xinjiang, China. She obtained her bachelor's degree in Polymer Science and Engineering from Qingdao University of Science and Technology, in 2000. She obtained her Master's degree in Chemistry from East China Normal University in 2003. After two years serving in industry as a research chemist, she began to pursue her Ph.D degree in Organic Chemistry at the University of Missouri-Kansas City (UMKC) in 2005, with a co-discipline of Pharmaceutical Sciences. She worked on the synthesis of novel bile acid based derivatives in Dr. Dias's group. During her work in UMKC Chemistry department, Xinyan Bai synthesized and characterized cage-like molecular architectures derived from chenodeoxycholic acid. She also participates on the synthesis of π-conjugated arylene ethynylene oligomers as blue-light-emitting materials.

Selected Peer-reviewed Publications:

[1]. Bai, X.; Barnes, C.; Pascal, R. A. Jr., Chen, X.; Dias, J. R. "Bile acid-based cage compounds with lipophilic outer shells and innercavities," *Org. Lett*. **2011**, *13*, 3064.

[2]. Chen, X; Barnes, C.; Bai, X.; Sandreczki, T. C.; Peng, Z; Kadnikova, E.N.; Dias, J. R. "Synthesis and structural analysis of a novel iodinated cyclopentadienone via ring-contraction iodination and its application in synthesis of alkyne-functionalized cyclopentadienones," *Chem.Comm*. **2010**, *46*, 8171.

[3]. Chen, X.; Bai, X.; Sandreczki, T. C.; Dias, J. R.; Ouyang, L.; Liu, Y. "Reversible self-assembly of 2,5-bis-(dodecycloxy)-1,4-phenylene)bis (ethyne-2,1-diyl) differrocene by H-π interactions. Physically linked ferrocene containing polymer," *Polymer Preprints* **2010**, *51*, 463.

[4]. Bai, X.; Barnes, C.; Dias, J. R. "Synthesis and comparative spectroscopic analysis of two chenodeoxycholic acid (CDCA) derivatives with closely related 7alpha-ester moieties," *Tetrahedron Letters* **2009**, *50*, 503.

[5]. Bai, X.; Liu, B.; Yan, J. "Adsorption behavior of water-wettable hydrophobic porous resins based on divinylbenzene and methyl acrylate," *Reactive & Functional Polymers* **2005**, *63*, 43.

[6]. Wei, J.; Bai, X.; Yan, J. "Water-Swellable Hydrophobic Porous Copolymers Based on Divinylbenzene and Methyl Acrylate: Preparation and Water-Swelling Behavior," *Macromolecules* **2003**, *36*, 4960.

[7].Bai, X.; Tang, X.; Zhao, X.; Yan, J. Swelling behavior of solvent-modified pH-sensitive gels based on diethylaminoethyl methacrylate and alkyl methacrylate esters. *Lizi Jiaohuan Yu Xifu* **2003**, *19*, 193.